ENGINEERING SOILS TO ACT AS CARBON SINKS

A DETAILED STUDY INTO THE POTENTIAL FOR SOIL ENGINEERING AS A MEANS OF SEQUESTERING ATMOSPHERIC CO_2

CARLA-LEANNE WASHBOURNE

A thesis submitted to the University of Newcastle for the degree of Doctor of Philosophy in the Faculty of Science

Department of Civil Engineering and Geosciences
University of Newcastle upon Tyne
Newcastle upon Tyne
Cassie Building
NE1 7RU

April 2014

TABLE OF CONTENTS

LIST OF TABLES

LIST OF FIGURES

Chapter 5

Appendix D

DECLARATION

I hereby certify that this work is my own, except where otherwise acknowledged, and that it has not been submitted previously for a degree at this, or any other, university

.....

Carla-Leanne Washbourne

20/12/2013

PREFACE

The author gained a BSc in Natural Sciences (Earth Sciences and Archaeology) from the University of Durham in 2006 and an MSc in Engineering Geology from Newcastle University in 2009. Since this point she has undertaken the doctoral research contained in this thesis.

The author is currently based within the Department of Science, Technology, Engineering and Public Policy at University College London, undertaking a long-term secondment as a Physical Sciences Adviser in the Parliamentary Office of Science and Technology. Her research focuses on the technical and policy aspects of ecosystem services in urban areas, working at the interface between science and public policy.

DEDICATION

This thesis is dedicated to all of the people who have been a help and an inspiration through what has been a very rewarding but very challenging time in my life.

Underneath our feet
Crystals grow like plants

Björk Guðmundsdóttir

ACKNOWLEDGEMENTS

I would like to thank Professor David Manning for his guidance and insight in this project. Thanks to Dr Phil Renforth for his unfailing enthusiasm and unwavering support, Dr Elisa Lopez-Capel for her advice and energy and all of the wonderful project students who were part of the research group: Joe Taylder, Caitlin Stalker and Sam Thompson. My deepest thanks to the Natural Environment Research Council for sponsoring the work contained in this thesis.

For their support during my time at Newcastle University I would like to thank Dr Colin Davie, Dr Martin Cooke, Dr Bryn Jones and Dr Gail de Blaquiere. For their invaluable help in my lab and field work I thank Philip Green, Stuart Patterson, Bill Cragie, Fred Beadle, Martin Robertson, Bernard Bowler, Maggie White, Pauline Carrick and Dr Cristina Dueso-Villalba.

I would like to acknowledge the staff at Tata Scunthorpe who went above and beyond to help me with my research: Paul Whitby, Mandy Talbot, Phil Togwell, Louise Payne, and to Jonathan Robinson at Tarmac. Input from John Martin and Nigel Robinson at TerraConsult was also very helpful in directing my fieldwork at Tata Scunthorpe.

I would like to thank the University of Oxford's Department of Earth Sciences for allowing me the use of their IRMS equipment; special thanks to Professor Gideon Henderson and Dr Norman Charnley. Thanks to Nick Marsh at the University of Leicester for XRF analysis, Mike Hall at Edinburgh University for thin section preparation and Dr Philippa Ascough at SUERC for ^{14}C dating.

I would also like to thank Peter Barraclough, Dr Jason Blackstock, Adam James Cooper, Dr Luke Handley, Luke Harrison, Stephanie Henderson, Patrick Lawrence and Dr Pete Manning. And last, but by no means least, my long-suffering family, who by now must be experts-by-proxy in soil carbon dynamics!

ABSTRACT

Soils containing calcium (Ca) and magnesium (Mg) bearing waste silicate minerals may be intentionally engineered to capture and store atmospheric carbon (C). Within the soil environment these minerals can capture and store atmospheric C through the process of weathering that releases Ca and Mg which then precipitate as carbonate minerals. Like natural silicates, silicate 'wastes' and artificial silicates sequester C through carbonation of calcium (Ca^{2+}) and magnesium (Mg^{2+}). Terrestrial CO_2 sequestration may be promoted by the inclusion of these reactive mineral substrates in soils, and many waste sites and urban and anthropogenic soils already contain quantities of these materials.

The UK Government is currently committed to reducing carbon emissions by 80% in 2050 (against a 1990 baseline) and soils have a role to play, acting as sinks for carbon. It is proposed that soil engineering measures could harness the high C turnover of the global pedologic system, ~120Pg C a^{-1}, to develop an efficient method of enhanced weathering. Artificial silicates have the potential to capture 192-333 Mt C a^{-1}, representing 2.0-3.7% of contemporary global C emissions; natural silicates present a carbon capture potential many orders of magnitude greater. Mineral carbonation in an artificial soil setting has the potential to capture inorganic carbon comparable to organic carbon accumulation. Soils of this type can accumulate 20-30 kg C m^2 as carbonates (≥ organic carbon content in natural soils, ~17.5 kg C m^2 for rural soils in the UK).

Laboratory investigations were carried out on a number of experimental scales, from meso-scale flow-through reactors to micro-scale batch experiments, to determine the rate at which Ca and Mg could be supplied from suitable materials in engineered soil systems to perform a carbon capture function. Environmental factors were controlled for each in order to constrain their contribution to the overall process. Batch experiments were carried out at standard temperature and pressure (STP) to investigate effects of changes in solute concentration, water chemistry, agitation and particle size. pH controlled experiments were run at STP from pH 3-8, to determine the effects of pH changes on the weathering of wollastonite. Flow-through weathering experiments at STP investigated the effects of time, water chemistry, hydrogeological conditions and addition of CO_2 on the weathering of steel slag. Analytical results demonstrate that Ca leaches rapidly from a number of Ca-rich artificial minerals providing great potential for carbon capture to occur on human-relevant timescales. Steel slag was shown to weather

at a $\log_{10}$ rate of -9.39 to -11.88 mol Ca m^{-2} sec^{-1} in laboratory settings and -7.11 to -7.56 mol Ca m^{-2} sec^{-1} under ambient environmental conditions in the field over 975 days.

Anthropogenic soils, known to contain substantial quantities of Ca and Mg-rich minerals derived from industrial and demolition activity (including iron and steel slag, cement and concrete), were systematically sampled across two field sites. Analysis illustrated mean soil carbonate values of 21.8 ± 4.7% wt to 41.16 ± 9.89 wt % demonstrating that a large quantity of soil carbonate forms and persists in these environments, formed at a rate of 18kg CO_2 t^{-1} a^{-1}. Stable isotope data ($\delta^{13}C$, $\delta^{18}O$) confirm that up to 81% of C in these pedogenic carbonates is atmospherically derived. ^{14}C data also suggest that a significant proportion of the C present in carbonates analysed is 'modern'. Applying a current CO_2 trading cost of £8-£12 t^{-1} CO_2, the potential value of CO_2 sequestration at a study site was calculated to be £51,843 – £77,765 ha^{-1} after 58% of its carbonation potential had been exploited.

The studies contained in this thesis add to a growing body of evidence for the formation of carbonate minerals in soil settings where Ca/Mg-bearing silicate minerals occur. They also support the idea that engineered soils could be effectively utilised for carbon sequestration. Soil engineering for carbon capture provides a comparatively cheap, easy and attractive way of beginning to offset the environmental impact of certain industrial processes. Carbonation of waste silicates is a useful exercise in 'closing the loop' on C emissions produced in their manufacture. Carbon capture taking place on sites containing industrial waste materials is of interest to a variety of stakeholders: site owners, third sector bodies and local and national legislative bodies. Effective, low-energy field-scale implementation of mineral carbonation through soil engineering could assuage current constraints on economic performance of enhanced weathering technologies and highlight the importance of soil carbon storage.

ABBREVIATIONS

Abbreviation	Meaning
BGL	Below Ground Level
CCS	Carbon Capture and Storage
ESEM	Environmental Scanning Electron Microscope
GHG	Greenhouse Gas
IPCC	Intergovernmental Panel on Climate Change
IRMS	Isotopic Ratio Mass Spectrometry
MCCS	Mineral Carbon Capture and Storage
PDB	Pee Dee Belemnite
PSD	Particle Size Distribution
QMS	Quadrupole Mass Spectrometer
SEM	Scanning Electron Microscope
STP	Standard Temperature and Pressure
TG	Thermo-gravimetric
V-PDB	Vienna Pee Dee Belemnite
XRD	X-Ray Diffraction
XRF	X-Ray Fluorescence

CHAPTER 1 – Introduction

Chapter Summary

- Context
- Purpose and scope
    - Aims and objectives
    - Geochemical efficacy
    - Field-scale feasibility
- Major findings of technical work
    - Dissemination
- Thesis outline

1.1 Context

Climate change is one of the most pressing scientific concerns of the modern age, with public awareness increasing in recent years due to its potential to influence the global environment, with significant implications for society, policy and economic development. This thesis presents technical data supporting the utilisation of carbon capture processes taking place in soils to assist in mitigating the effects of climate change.

The theoretical premise behind climate change (or global warming as it is also frequently termed), exacerbated by anthropogenic greenhouse gas emissions, has existed for many years (Arrhenius 1896, 1897; Callendar, 1938). Contemporary acknowledgement of the potential global impacts of climate change has been buoyed by consensus publications from the IPCC (Intergovernmental Panel on Climate Change) (1990, 1995, 2001, 2007, 2013) UNFCCC (United Nations Framework Convention on Climate Change) (1992-2009), ECCP (European Climate Change Programme) (2001-2009) and UKCIP (United Kingdom Climate Impacts Programme) (2002).

Currently global annual CO_2 emissions account for approximately ~8,900 Mt C a^{-1} (EIA 2011). UNFCC (2007) proceedings, most recently COP19 (UNFCCC, 2013), have marked out general targets for global climate stabilisation, roughly equivalent to the maintenance of an atmospheric CO_2 concentration below 350ppm, making it necessary to implement measures to reduce emissions significantly in the near to mid-term. (It

should be noted that whilst CO_2 is not the sole culprit for climate change, it is the most abundantly produced anthropogenic forcing factor and is generally used as an equivalency measure for the effects of other greenhouse gases.) Whilst significant political focus regarding the mitigation of climate change is directed towards a socio-economic paradigm shift to low carbon technologies, it is believed that direct CO_2 mitigation strategies may play an important part in the short to medium-term reduction of greenhouse gases. It is increasingly agreed that whilst the rapid shift from high CO_2 to low CO_2 technologies, encompassing changes in energy production, industry, transport and land management, is of paramount importance, these reactivist measures will have limited effect on ameliorating the near-term effects of climate change.

Geoengineering is a term used to describe a number of technologies which aim to alter the Earth's climate through interventions to its environmental systems (Royal Society, 2009). Carbon capture and storage (CCS) describes one category of geoengineering techniques, all of which aim to prevent CO_2 emission to, or to increase CO_2 removal from, the atmosphere. Contemporarily proposed CCS technologies include storage in the ocean (direct injection of carbon dioxide in to the oceans), deep saline aquifers, geologic reservoirs (direct injection of carbon dioxide in to subterranean voids) and via mineral 'neutralisation' of carbon dioxide to form bicarbonates or carbonates. The term 'carbon capture and storage' (CCS) is currently most synonymous with geologic 'underground' carbon storage, with a small number of projects already operating around the globe. Carbon capture and storage is presented by many researchers and public bodies (DECC, 2013) as the only, currently feasible, means by which we are able to effectively cap our emissions in the short to mid-term. December 2009 saw the meeting of UNFCC Global Policy Makers in Copenhagen, Denmark, where, amongst fuel and transport reforms, research in to carbon capture and storage (CCS) was recommended as a complimentary mitigation technology. 2009 also saw the U.K. unveiling of the 'world's first carbon budget' (UK Climate Change Act (2008); The Guardian, 2009), including positive legislative action by the UK government to propose direct investment in to CCS as a viable mitigation commodity.

Mineral carbon capture and storage (MCCS), through chemical capture and binding of CO_2, is still frequently seen as immature in the current field of CCS technology. It is a naturally-occurring process, which acts to sequester CO_2 from the environment over geologic timescales. MCCS is a process that has been theoretically validated through

experiment and observation as a possible mitigation technology, encompassing a suite of chemical reactions occurring in alkaline earth compounds within natural and synthetic minerals. During silicate weathering, Ca and Mg silicate minerals naturally react with dissolved carbon dioxide (CO_2) to form carbonates (Berner et al., 1983; Lackner et al., 1995; Seifritz, 1990) effectively capturing and fixing atmospheric carbon. Weathering involves leaching and transport of Ca^{2+} and Mg^{2+} in solution and these react with carbonate anions formed by CO_2 dissolution in soil pore waters (depending on system pH, as H_2CO_3, HCO_3^- and CO_3^{2-}) to precipitate solid carbonates. This process contributes to the stabilisation of atmospheric CO_2 over geological time periods (Berner et al., 1983; Berner and Lasaga, 1989) and also contributes to the formation of pedogenic carbonates in natural soils (Nettleton, 1991) and artificial soils (Manning, 2008 and Manning et al., 2013a; Renforth et al., 2009). A simplified version of this reaction is given in Equation 1.1. This reaction (1.1) acts to sequester carbon from the local environment.

Equation 1.1:

$$(Ca, Mg)SiO_3 + CO_2 + 2H_2O \leftrightarrow (Ca, Mg)CO_3 + H_4SiO_4$$

Feasibility studies to date have regularly concluded that MCCS does not presently provide an economic or practical equivalent to alternative existing CCS technologies. Much of the preliminary work on MCCS has focussed on the use of suitable minerals as feedstocks for carbon capture reactions taking place in industrial reactors (Huijgen et al, 2005, 2006, 2007). These processes have frequently employed the use of elevated temperature or pressure conditions and material pre-treatment in order to achieve large quantities of carbon capture over short timescales. In order to prove its utility, future work on MCCS must focus upon balancing efficacy and economy, reducing the need for additional energy input, which has proven a limiting factor for adoption in many contemporary settings.

A number of recent studies (Harrison et al., 2013; Manning, 2008; Manning et al., 2013a,b; Power et al., 2009; Renforth et al., 2009, 2011a; Thom et al., 2013; Wilson et al., 2009, 2011) have addressed the potential for silicate weathering in the ambient environment as an effective means of overcoming the resource and environmental issues associated with the use of industrial reactors for MCCS. It has been proposed that through artificial addition of calcium and magnesium-rich silicates to soils it may be

possible to promote the accelerated draw-down and storage of CO_2 from the atmosphere as geologically stable carbonate minerals (Manning, 2008; Schuiling and Krijgsman, 2006). Recent research (Renforth et al., 2009) has identified this process occurring in urban brownfield soils where Ca-rich demolition waste derived from cement mortar is mixed into the soil profile. Isotopic analysis of secondary carbonate minerals forming under ambient soil conditions (Renforth et al, 2009; Wilson et al., 2010) confirms that a significant proportion of the carbonate carbon has been sequestered from the atmosphere. This thesis draws upon these studies to further elucidate the manner in which MCCS could be effectively engineered in to soil systems.

An increasing number of studies (Manning, 2008 and Manning et al., 2013b; Power et al., 2009; Renforth et al., 2009, 2011a; Wilson et al., 2009, 2011) have focussed on the carbonation of artificial and waste minerals in this context, due to their abundance and ability to provide a readily available and accessible analogue for natural processes. The weathering rates of artificial silicates may also be swifter than the natural silicates in similar environmental settings (Renforth, 2011b). Urban brownfield sites, waste landfills and ex-industrial sites may demonstrate MCCS phenomena, as construction activities in urban soils usually involve incidental or intentional addition of Ca/Mg-rich artificial substrates. If included in such soils, construction and demolition (C&D) waste, fly ashes, iron and steel slag etc. are therefore able to act as carbon sequestration tools in the urban environment (Morales-Flórez, 2011; Renforth et al., 2011a,b). This property imparts an inherent environmental value to materials which may otherwise be regarded as 'wastes' to be disposed of without regard to their potential environmental benefits. The overall mitigation potential of waste silicates is 190-332 Mt C a^{-1} (Renforth et al, 2011c) representing 2.1 – 3.7% of global carbon emissions (8,900 MtC a^{-1} (EIA, 2011)). This is an overall potential and does not consider emissions from the processes which produce these materials, but in principle carbonation could be used to offset a portion of the carbon emissions associated with their production.

There is potential for carbon sequestration through MCCS to be a design consideration in anthropogenic soils, with minimal additional energy input, little change in current management practise and minimal translocation of materials. This thesis investigates a number of critical parameters to assess the feasibility of implementing the approach suggested above at field-scale.

1.2 Purpose and scope

This project set out to investigate the process by which *in situ* mineral carbon capture, using industrial residues in soil settings, could be implemented at field scale with specific focus on characterising reaction rates and limiting factors. An understanding of this process in lab and field settings was sought. Preliminary research aimed to characterise geochemical processes in a selection of waste silicates through small and large-scale lab-based work. Results from this initial phase were used as a basis for fieldwork, to elucidate how any observed process manifested in field-scale systems. Opportunistic, intrusive fieldwork was planned in support of this core data to provide cross-references across multiple study sites. Through a close synthesis of all aspects of this research a conceptual model, for the implementation of this form of carbon capture and storage (CCS) in the context of current technical knowledge was to be produced. The feasibility of the process was also to be assessed within a range of economic and legislative settings.

The work contained in this thesis contributes to knowledge across a number of physical science, engineering and policy fields. It has implications for the interpretation of other studies looking to understand MCCS in natural and artificial systems, including the weathering processes affecting man-made infrastructure (concrete structures, geotechnical aspects of construction on sites underlain by artificial silicate minerals), carbonate formation following CO_2 injection in deep geological reservoirs, weathering of natural silicates and in the study of pedogenic carbonate formation.

1.3 Aims and objectives

Detailed aims and objectives are outlined in the following section. These 5 aims cover a range of aspects related to the effective field-scale implementation of MCCS. They are presented as 'geochemical aspects' and 'field-scale aspects'. This project aimed to tie together geochemical knowledge of mineral carbonation reactions with new laboratory data looking specifically at these reactions in artificial minerals derived from anthropogenic wastes, and analyses from field sites. By understanding the mineral carbonation process on a variety of scales it is hoped that proposals can be made for how soil engineering through these methods might be used as a viable carbon capture technology.

In particular this project aimed to address a number of outstanding questions pertaining to the use of mineral carbon capture and storage in soil settings which had not been addressed by previous studies documented in the peer-reviewed literature.

1.3.1 Geochemical efficacy

Aim 1: Identify suitable materials for further research and determine their potential in MCCS

Suitable materials for MCCS were identified, to provide a direct comparison between the potential efficacies of different types of compositionally appropriate material in carbon capture applications

Chapter 2

- An extensive review of existing literature was completed

Aim 2: Determine weathering rates in Ca/Mg-rich industrial residues

A selection of natural and artificial silicate minerals were subjected to controlled batch-weathering experiments to determine the comparative rate parameters relevant to MCCS. Additional data regarding 'real time' mineral weathering / carbon sequestration data in *in* situ field settings was acquired

Chapter 3

- Batch weathering experiments were carried out at standard temperature and pressure (STP) under a variety of simulated environmental conditions
- Single mineral weathering experiments were carried out using wollastonite ($CaSiO_3$) at a range of pH values

- Weathering rates were determined in materials weathering under ambient conditions over controlled time periods

1.3.2 Field-scale feasibility

Aim 1: Determine the rate of carbon capture using landfill cell engineering / soil admixing through investigation of existing sites

Field-scale studies were carried out to investigate the weathering of residues in diffuse soil and waste landfill settings. Stratigraphic analysis was also carried out where possible.

Chapters 4 and 5

- Analogue field sites were selected and subjected to analysis to determine the efficacy of the proposed methods
- Field sites were analysed at a variety of time points to determine field-scale weathering rates

Aim 2: Quantify field-scale efficacy of carbon capture using industrial residues

Quantification of carbon already captured by field sites, and the potential for future capture was estimated from multiple lines of evidence

Chapter 5

- Multiple geochemical properties from laboratory analysis were used to estimate the carbon capture potential of field sites

Aim 3: Determine efficacy and capacity of carbon capture using industrial residues at commercial scales and in current legislative and regulatory settings

Overall capacity of the MCCS process was determined and its potential for use as a climate change mitigation strategy was considered under current economic and legislative settings.

Chapters 2-6

- Capacity across single field sites and on larger scales was calculated from data attained in Chapters 2-5
- Commercial and policy potential for roll-out of technology was considered in the context of relevant contemporary legislation in Chapter 6

Table 1.1 summarises the original research questions, from earlier work (Washbourne, 2009 (MSc thesis)) and literature review, which were used to shape the aims and objectives of this study.

Table 1.1 – Study questions used in the shaping of aims and objectives

Geochemical efficacy	**Field-Scale Feasibility**
• ***Which artificial silicate minerals are effective as study materials in carbon sequestration?*** – How many artificial silicate minerals could be effective in soil engineering for carbon capture? – Are all of these materials realistically suitable for ongoing research? – What are their comparative benefits and limitations for carbon sink engineering?	• ***Which soil manipulation contexts offer the greatest potential for passive carbon capture and storage?*** – What is the efficacy of engineered landfill cells and soil admixing to achieve carbon capture? How does this compare to un-engineered sites? – With respect to transport, construction, emplacement and maintenance costs, which approaches present the greatest potential for real-world implementation?
• ***What are the weathering properties and geochemical constraints affecting the sequestration reactions occurring in artificial silicate minerals?*** – What are the innate structural and chemical constraints of these processes? – How do climatic, geological, geological and hydrological factors affect the sequestration reaction? – Can laboratory weathering experiments demonstrate the time dependant nature of *in situ* carbon capture? – To what extent do biomass interactions influence the sequestration reaction? – What proportions of calcium carbonate are formed by hydroxylation?	• ***Can carbon capture through soil engineering be used in emissions mitigation to a locally or globally significant extent?*** – What is the cumulative quantitative carbon capture potential presented by engineered soils? – What are the additional environmental implications of carbon capture and storage using passive mineral sequestration? Do the reaction products have beneficial and / or harmful properties?
	• ***How could carbon capture through soil engineering be economically incentivised to encourage the construction of passive carbon sinks?*** – What are the commercial and political constraints upon the application of ground engineering for carbon capture? – What are the alterative uses for the substrate materials? – Is it possible to construct a field-scale conceptual model for the implementation of carbon capture using passive mineral sequestration?

1.4 Major findings of technical work

Through the fulfilment of the aims and objectives outlined in Section 1.3 of this chapter the technical work contained in this thesis contributes new insights to the field of mineral carbon capture in soil settings. It confirms and defines a number of reaction and precipitation rates under ambient conditions for a variety of minerals and contributes new work to the field observation of mineral carbon capture in soils, delineating spatial and temporal implications. These findings are also collated with contemporary economic, technical and legislative factors to provide a background assessment of the feasibility of this approach.

Batch weathering experiments on artificial and natural minerals allowed the comparison of calcium leaching data as a weathering proxy for these materials in a variety of previously unreported physical-chemical settings. Rate reconstructions for the weathering of wollastonite ($CaSiO_3$) (also via Ca leaching) under standard temperature and pressure under three different pH conditions confirmed the findings of similar studies, and illustrated the potential for this approach to be used to determine weathering rates for minerals under ambient environmental conditions. An investigation of artificial minerals weathering in the ambient environment provided novel, and well-constrained, time-point data to illustrate the rate of short to medium-term *in situ* weathering processes.

Field investigations at sites where suitable materials for carbon capture had been emplaced allowed the determination of, previously poorly studied, temporal and spatial (surface and profile) constraints on the MCCS process. A novel, spatially accurate chronosequence is presented for geochemical change over a study site. A broad spectrum of geochemical analyses were carried out, allowing new comparisons to be made between observed parameters on these sites where MCCS has been occurring, without intervention, at a significant and testable rate. A method of estimating carbon capture potential for a field site was developed from the data.

Larger scale weathering experiments, and field-scale observation of the geochemistry of an engineered landfill site, demonstrated the complexity of scaling the geochemical processes occurring between laboratory and field scale. Flow-through weathering experiments using glass columns had not previously been applied to determine weathering rates of the materials under the conditions used here. Initial results are also

reported from a study which set out to clarify the influence of vegetation on sites where MCCS was occurring; an early attempt to determine the contribution of vegetation to the observed difference between laboratory and field-scale mineral weathering rates on study sites.

Contemporary economic and policy aspects of the MCCS process in soils are framed in the context of lifecycle assessment, current economics and legislative mechanisms. The quantification methods used in this work are reinforced as critical to the ability to attribute environmental effects of the MCCS process.

1.5 Dissemination

A number of publications have already come from this work, and others are in preparation:

- Washbourne C-L, Renforth, P., Manning, D.A.C., (2012). Investigating carbonate formation in urban soils as a method for capture and storage of atmospheric carbon, Science of the Total Environment, 2012, 431, pp 166-175 DOI: 10.1016/j.scitotenv.2012.05.037
- Renforth, P., Washbourne, C-L., Taylder J., Manning, D. A. C. (2011). Silicate production and availability for mineral carbonation. Environmental Science and Technology, 45, (6) pp 2035-2041 DOI: 10.1021/es103241w
- Washbourne, C-L., Renforth, P., Manning, D.A.C. (2011) Carbonation of artificial silicate minerals: Passive removal of atmospheric CO_2. Mineralogical Magazine: Goldschmidt Conference Abstracts. 75, (3) pp. 2106-2187
- Washbourne, C-L., Renforth, P., Manning, D.A.C. (2010) Carbonation of Artificial Silicate Minerals in Soils: Passive Removal of Atmospheric CO_2. AGU Fall Meeting Abstracts

Other modes of dissemination have also been carried out during this project, with findings from this work presented at a number of international conferences (American Geophysical Union Fall Meeting, Goldschmidt). Engagement with possible industry and policy stakeholder groups has also been carried out, with data from this project used as part of oral and written reports produced as part of the activities carried out in fulfilment of two EPSRC Impact Award grants.

1.6 Thesis outline

This research project was conducted between September 2009 and September 2013, with the thesis component submitted in December 2013. This thesis has 8 Chapters and an Appendix consisting of 5 sections.

Chapter 1 - Introduction - sets out the background to the research undertaken and describes the aims and objectives of the work presented in the thesis.

Chapter 2 - Engineering soils as carbon sinks through mineral carbonation - reviews contemporary literature to outline current understanding of the carbon cycle, geoengineering approaches to addressing climate change, the use of mineral carbonation as a geoengineering technology, and the use of artificial silicate materials in soil engineering for carbon capture and storage.

Chapter 3 - Geochemical processes behind mineral carbon capture in soils – investigates the efficacy of carbon capture and storage through mineral sequestration as a geoengineering technology determined by a range of operational parameters. As discussed in the last section of Chapter 2 a number of materials and settings allow carbon capture and storage through mineral carbonation to occur. This Chapter focuses on the laboratory determination of geochemical processes which dictate the rate and capacity of mineral carbon capture, specifically investigating the rates at which a selection of suitable minerals weather and carbonate in small-scale controlled settings.

Chapter 4 - Mineral carbon capture in the field: analogues - presents data from investigations on field sites (Yarborough Landfill, Scunthorpe and Science Central, Newcastle upon Tyne) where artificial silicate minerals have been emplaced, in order to develop an understanding of the ways in which these minerals weather under ambient conditions and provide a comparison to laboratory analyses presented in Chapter 3.

Chapter 5 - Mineral carbon capture in ‘engineered’ systems - investigates the phenomenon of carbonate formation in field settings to explore whether parameters could be developed by which mineral carbon capture could be engineered and quantitatively measured in soil settings. The results of flow-through weathering experiments are presented, along with geochemical modelling and interpretation of data from field-scale settings.

Chapter 6 - Economic and policy implications of mineral carbon capture in soils – considers the technical aspects of treating, transporting, emplacing and managing these materials, exploring the possible applications of the data presented in the preceding Chapters and relating this work more directly to real world settings. Chapter 6 directly links the proposed benefits of MCCS in soil settings with the technical and legislative issues which would surround its implementation.

Chapter 7 – Discussion - collating all data presented in the preceding chapters and discussing the broader implications with respect to the context, purpose and aims and objectives of the project presented earlier in this section. Chapter 7 summarises the key discussion points surrounding each novel contribution of the work contained in this thesis.

Chapter 8 – Conclusions and future work – presents conclusions distilled from the summary discussions presented at the end of Chapters 3-6 and proposes areas where future work could contribute to a deeper understanding of the contextual issues surrounding the project, or provide additional insights which were beyond the technical or temporal scope of this work.

Chapter 9 – Appendices – collates summaries of methods and data relevant to the work presented. Appendix A – Methods, Appendix B – Data (Chapter 3), Appendix C – Data (Chapter 4), Appendix D – Data (Chapter 5), Appendix E – Formulae

CHAPTER 2 - Engineering soils as carbon sinks through carbonation of artificial silicate minerals

In order to understand the context of the research undertaken in this thesis, it is necessary first to understand in detail the natural and engineered systems within which it proposes to operate. Recent climate change is largely the result of anthropogenic perturbations in the Earth system (IPCC, 2013; AGU, 2013) caused by the emission of greenhouse gases; mineral carbon capture and storage is an engineering method which aims to counteract this, to assist in bringing the climate system back to an equilibrium point closer to its 'natural' state. This chapter reviews contemporary literature to outline current understanding of the carbon cycle, geoengineering approaches to addressing climate change, the use of mineral carbonation as a geoengineering technology, and the use of artificial silicate materials in soil engineering for carbon capture and storage.

Engineering of soils to create carbon sinks proposes to use a number of naturally occurring geochemical processes in mitigating increasing carbon dioxide emissions, with resultant climatic effects, by developing an effective, low energy method of capturing and storing these emissions. The geochemical processes must be understood and observed in a range of settings in order to determine the parameters required for effective soil engineering. This chapter presents a literature review carried out to identify where further data was required; most notable was a lack of lab-scale data relevant to these processes conducted under ambient environmental conditions and a lack of field-scale, high-resolution data.

Chapter Summary:

- The carbon cycle in global and local context
- Factors affecting the contemporary carbon cycle
- Geoengineering and climate: mineral carbonation as a geoengineering method
- Soils as sites for mineral carbonation: principles and work to date
- Suitable materials for engineering soils for carbon capture (sourcing, quantities, production, preparation)

2.1 The carbon cycle in global and local context

2.1.1 The carbon cycle and climate system

The carbon cycle is one of the best-known and most intensively studied planetary elemental cycles. It plays an important role in regulating both organic and inorganic processes, contributing to the maintenance of integrated planetary equilibrium states (Berner, 2001; Lovelock and Watson, 1982). Contemporary concerns relating to the damaging effects of carbon-based anthropogenic emissions released to the atmosphere can only be truly understood in their full environmental context 'that is, the global cycle of carbon' (Bolin et al. 1979). Knowledge of the carbon cycle is required to fully comprehend the potential impacts of gases such as carbon dioxide (CO_2) in changing the global climate, and it is inherently important in the construction of effective legislative and technological responses.

Figure 2.1 illustrates the natural components of the global carbon cycle (IPCC, 2001), demonstrating the co-dependency of stores and fluxes and illustrating the relative magnitude of fluxes between the ocean-atmosphere-land-geological stores. Climate change represents an increase in the atmospheric store caused by a significantly increased carbon flux from fossil carbon (fossil fuel burning), rock carbonate (mineral processing) and land use change (IPCC, 2001, 2007).

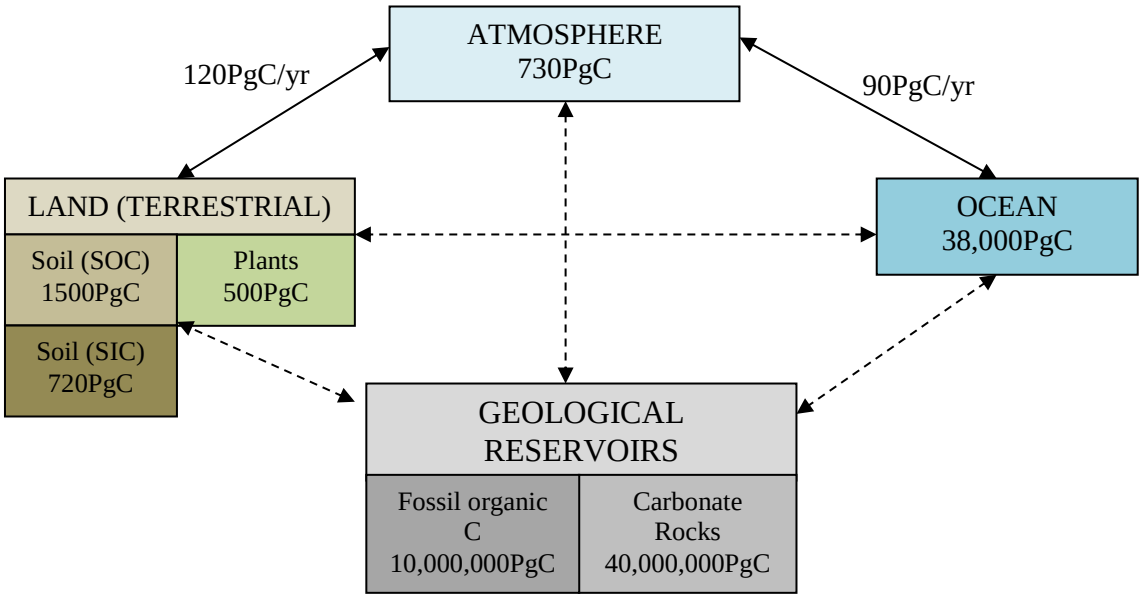

Figure 2.1 - After IPCC (2001). Schematic of the global carbon cycle: major stores and fluxes (Kump et al 2004).

2.1.2 Atmospheric carbon

The atmospheric store is relatively small in comparison to other stores in the system, but receives large, dynamic fluxes from both the oceanic and terrestrial stores. Early studies linking atmospheric carbon (C) to climate change were published by Arrhenius (1896, 1897) and Callendar (1938). These works extrapolated the incidental observation that molecular CO_2 possessed a potentially unfavourable physical ability, through its bonding structure, to absorb long-wave Infra-Red but not shortwave radiation. Arrhenius theorised that, when applied to the Earth's atmosphere, this phenomenon would mean that increases in atmospheric CO_2 would lead to a decreased release of radiant heat from the Earth's surface, creating a gradual global warming effect. A number of other gases also exhibit this property (water vapour, methane), but as carbon dioxide is the most commonly produced by human activity, most reportage represents warming potential of these gases as 'CO_2' and converts the effects of non-CO_2 gases to a 'CO_2 equivalent' value (CO_2e). The carbon cycle is intrinsically linked to global atmospheric composition and, therefore, global temperature regulation.

2.1.3 Oceanic carbon

The oceanic store is a large, dynamic store, around 50 times larger than the atmospheric store and 14 times larger than the combined terrestrial stores. C flux to the ocean is relatively small from the geological, atmospheric and terrestrial stores. C is removed from the oceanic store through nutrient cycling effects, and returned via a number of complex chemical processes. Phenomena linked to ocean acidification are closely correlated with rising atmospheric CO_2; increased dissolution of CO_2 in to the surface layers of the ocean produces carbonic acid which ultimately dissociates lowering the pH of the ocean water and affecting geochemical and biological processes such as the formation of carbonate shells (Doney et al., 2009). In the oceanic store, most carbon exists as dissolved inorganic carbon (DIC).

2.1.4 Geological carbon

The geological store is by far the largest of the stores in the cycle, but C flux to the geological carbon store is relatively small from the oceanic, atmospheric and terrestrial stores. C is removed from the geological store through fossil C exploitation (fossil fuels) and mineral processing, such as the calcining of carbonate rocks, and returned via the natural weathering processes of silicate and carbonate rocks, which are able to sequester large quantities of CO_2 (Lackner, 2003; Berner et al, 1983). While changes in

global climate are unlikely to significantly destabilise the geological carbon store over short periods, increased oceanic and hydrological acidity has the potential to alter the rates of rock (silicate) weathering, which in turn could lead to increased rates of carbon sequestration.

For many years, the geological store of the carbon cycle was considered relatively inert. The premise of rock weathering playing a large part in regulating global systems was first strongly considered in the early-20th Century, referred to as the 'geochemical carbon cycle' (Berner et al., 1983). One of the most significant academic developments in this field was made by Harold C. Urey, in his dictation of the Urey Reaction (Urey 1952), Equation 2.1, which describes the weathering of silicate rocks in the presence of carbon dioxide gas to form carbonate minerals:

Equation 2.1:

$$CO_2 + CaSiO_3 = CaCO_3 + SiO_2$$

More recently these ideas have been consolidated and developed in to the BLAG model (named for its creators Berner, Lasaga and Garrels) (Berner et al, 1983, 1985, 2002) and GEOCARB I (Berner, 1991), II (Berner, 1994) III and III (Berner et al, 2001) models. These propose that large-scale carbonate formation is part of a dynamic global cycle, by which carbon is cycled through a sequence of chemical sequestration and weathering reactions. Figure 2.2 demonstrates the simplified interaction of global geochemical stores and fluxes, as proposed in the BLAG model. This model illustrates the significance of geological calcium carbonate (calcite, $CaCO_3$) as a global carbon store. It was from this clarified understanding of the role of mineral weathering in the regulation of global cycles that the ideas behind mineral carbon capture and storage evolved, with the realisation that the intentional manipulation of this system could have large impacts on the global climate.

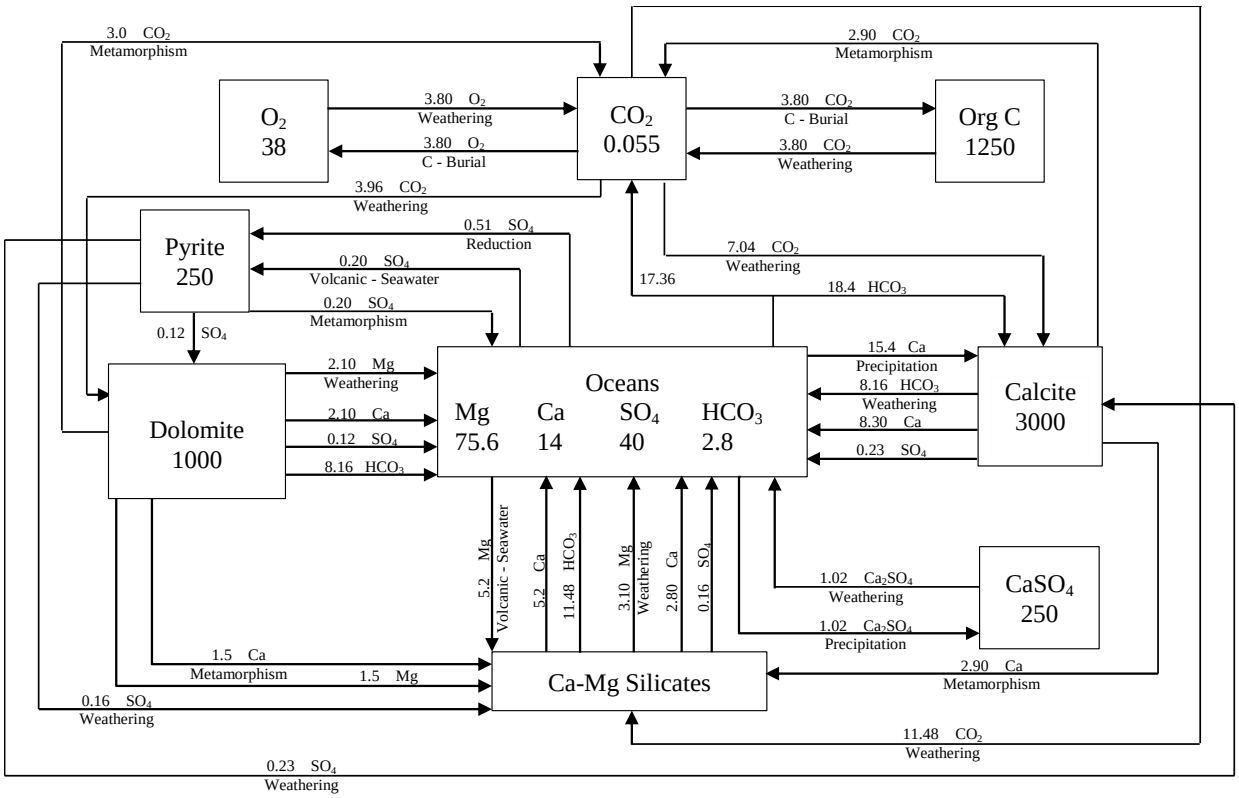

Figure 2.2 - The BLAG geochemical model. From Lasaga, Berner, and Garrels (in Sudquist and Broecker, 1985) in The Carbon Cycle and Atmospheric CO_2: Natural Variations Archean to Present (Source: Parrish, 1998)

2.1.5 Terrestrial carbon

The terrestrial store is moderately sized, in comparison with the other global stores, with a combined magnitude of approximately 2720PgC. As presented in Figure 2.3, the terrestrial store is comprised of a number of subsidiary stores, segregating organic and inorganic soil processes from biotic processes (plant growth). C flux to the terrestrial store is comparatively large and dynamic. Being the store in which human activity is immediately concentrated, through agriculture and land-use, the terrestrial carbon store is readily affected by numerous anthropogenic processes.

The terrestrial store is composed of biomass and soil components, and groundwater-carried carbon can also be included (as in Figure 2.3). Biomass carbon is characterised by living and recently deceased organic matter. Terrestrial biomass commonly includes plant biomass as a major component, with microbial and animal biomass. C can be removed from the terrestrial biomass store through anthropogenic processes including deforestation and other land clearance processes. Total carbon content in soil is a combination of organic compounds and inorganic carbonate minerals. Organic carbon in soils is functionally characterised into labile and recalcitrant pools, with differing

chemical reactivity and residence times, ultimately derived from living biomass (Sohi et al., 2001). Inorganic carbon storage in soils is dominated by calcium and magnesium carbonates (Schlesinger, 1982). There is a wide acceptance that the preservation of soil organic matter is critical in maintaining and increasing soil carbon stores (Kyoto Protocol, 1997; EU Soil Framework Directive, 2006), especially in agricultural soils, many of which are net CO_2 emitters (Paustian et al, 2000) due to intensive cropping and tillage practises.

The potential for soils to store carbon has long been recognised (IPCC 1997a, b ,c; Lal, 2004), however, the magnitude and significance of this store has only recently been quantified (Smith et al., 1997; Smith, 2004). In a global context, soils are now recognised as an important buffer for chemical and physical processes in the environment and as a potential tool for mitigation or reduction of rising atmospheric CO_2 concentrations. The 1997 Kyoto Protocol highlighted soils as a 'major carbon store' and recognised that processes underlying soil function should be considered in CO_2 emissions accounting. In the UK, DEFRA's Soil Strategy documents (2009) highlighted a pressing need to 'develop a better understanding of steps that can be taken to protect or enhance levels of soil carbon'.

Continuing research explores the potential impact of preserving or increasing the inorganic carbon pool. Scarce data has been an issue in assessing the geographical significance of soil carbonate in temperate climates (Rawlins et al., 2011). The significance of soil inorganic carbon storage may have been historically underestimated due to the belief that pedogenic (soil-formed) carbonates, formed by mineral carbonation, were not widespread phenomena, tending to be a feature of arid soils (Jenny, 1980). However, recent work has identified carbonates in temperate regions (Boguckyi et al., 2006; Łacka et al., 2008). In both 'natural' and anthropogenic soils carbonates appear to form readily in the presence of Ca/Mg source materials (Figure 2.4). This is discussed further in following sections.

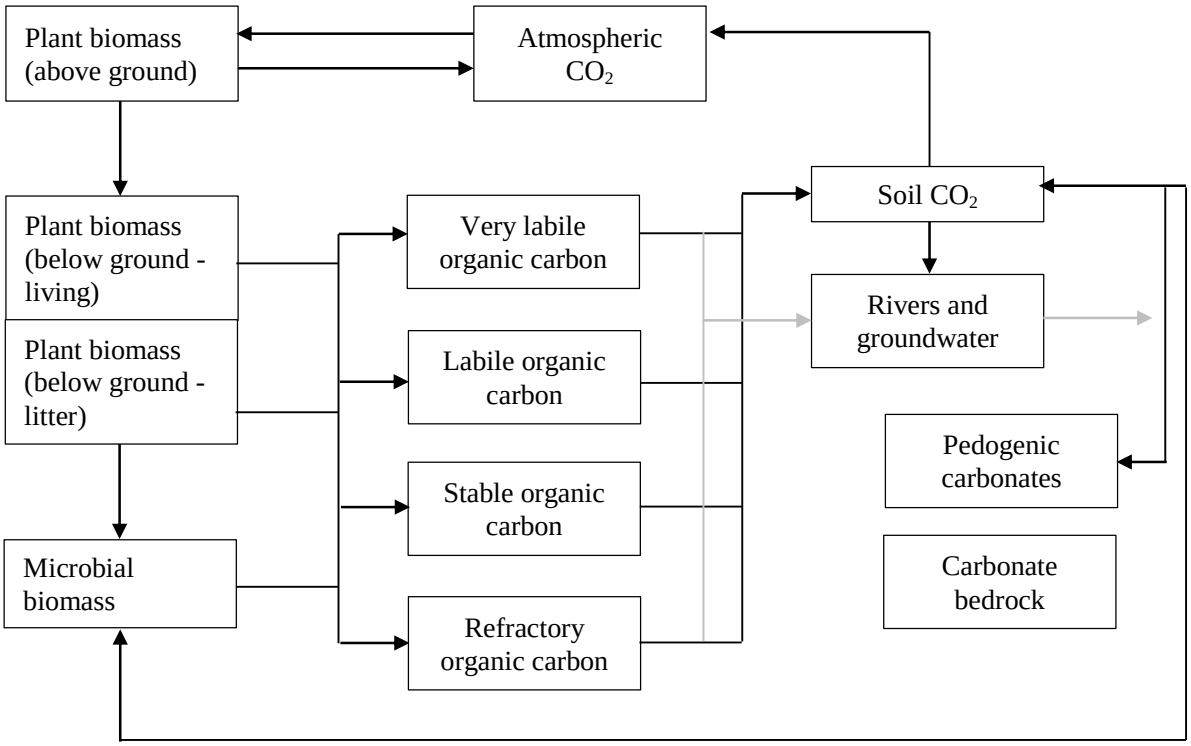

Figure 2.3 - Soil carbon stores and fluxes (after Renforth, 2011 (PhD thesis))

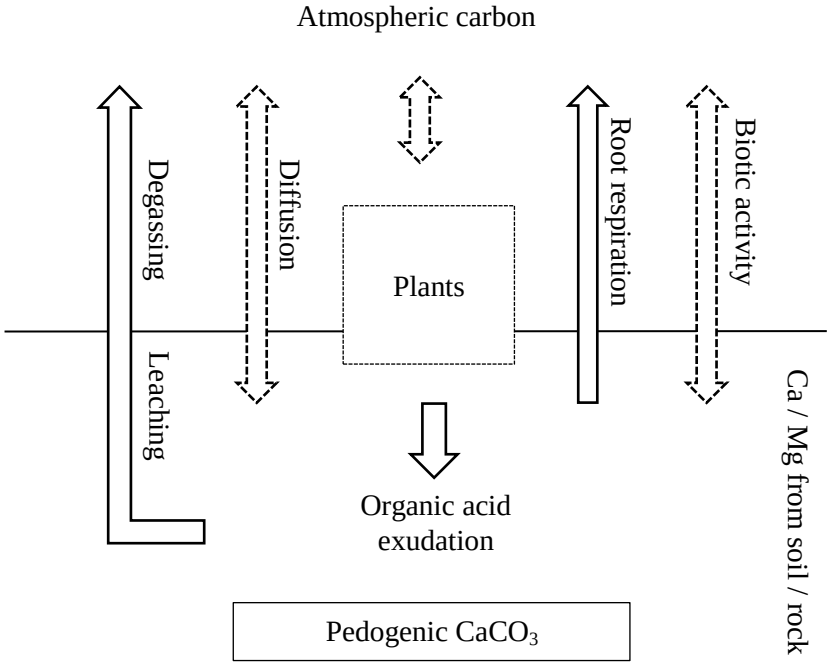

Figure 2.4 - Routes of pedogenic carbonate formation in soils. Arrows indicate carbon fluxes.

2.2 Factors affecting the contemporary carbon cycle

The carbon cycle is affected by factors which alter, or perturb, any of the elements illustrated in the previous section. Alterations to these stores and fluxes can occur on a variety of timescales, with long term changes occurring throughout Earth history, playing a role in the moderation of the Earth's climate over geological timescales. In the context of contemporary climate change discussions, changes in the global carbon cycle over the last few hundred years are most frequently referenced (figures are generally quoted to a 1750 baseline in IPCC physical science reports (IPCC 2001, 2007)).

In the long term (100s-1000s years), the rise of agriculture and increased land use change has contributed to changes in global climate; Ruddiman (2003, 2005) shows that anthropogenically driven changes may have been a significant driver of increased carbon emissions to the atmosphere. Over shorter periods, since 1750's and the start of the industrial revolution, fossil fuels have been burnt at an increasing rate to generate power for industry and society. Increases in the global levels of industrialisation occurred over 19^{th} and 20^{th} centuries, with recent but significant expansion with the rise of BRIC economies (Brazil, Russia, India, China) in the 2000's (Pao, 2010). Fossil fuel derived emissions are now a major contributor to increases in the concentration of carbon dioxide and other greenhouse gases in the Earth's atmosphere (IPCC, 2007).

Figure 2.5 shows anthropogenic emissions of greenhouse gases in 2007, including breakdown by composition and emission sector. Increase in the emission of fossil fuel C is also shown (Figure 2.6), demonstrating that these emissions are a significant and growing concern. Global emissions are currently reported at ~8,900 Mt C a^{-1} (EIA, 2011).

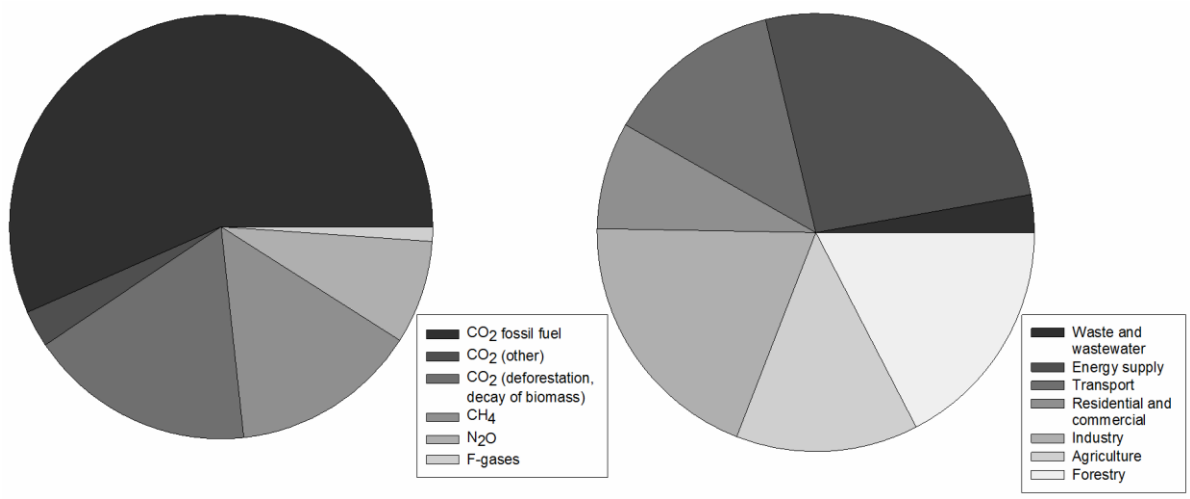

Figure 2.5 - Global greenhouse gas production by type and CO_2 production by sector

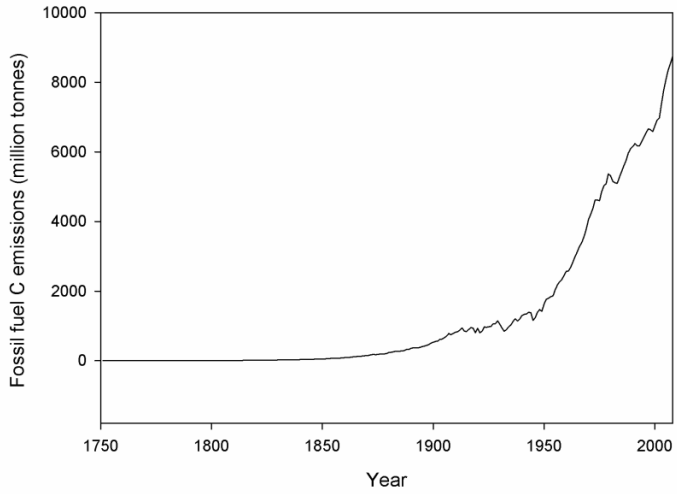

Figure 2.6 - Increased contribution of fossil fuels to atmospheric carbon since 1750 (IPCC, 2007; IEA, 2012)

In order to monitor any resultant effects on global levels of atmospheric carbon, it is necessary to directly measure the concentration of these gases; these measured changes in atmospheric chemistry clearly illustrate an increase in atmospheric carbon dioxide over the last 50 years. The now famous Keeling curve illustrates the measured concentration of atmospheric CO_2 since the 1960's (Keeling and Whorf, 2004). Detailed readings have been taken from the Mauna Loa Observatory in Hawaii, which proves useful high-resolution data for monitoring these changes. Figure 2.7 shows the data plotted in graphical format, demonstrating a significant upward trend in the concentration of atmospheric CO_2 measured at this station (small scale variability reflects seasonal changes in CO_2 uptake).

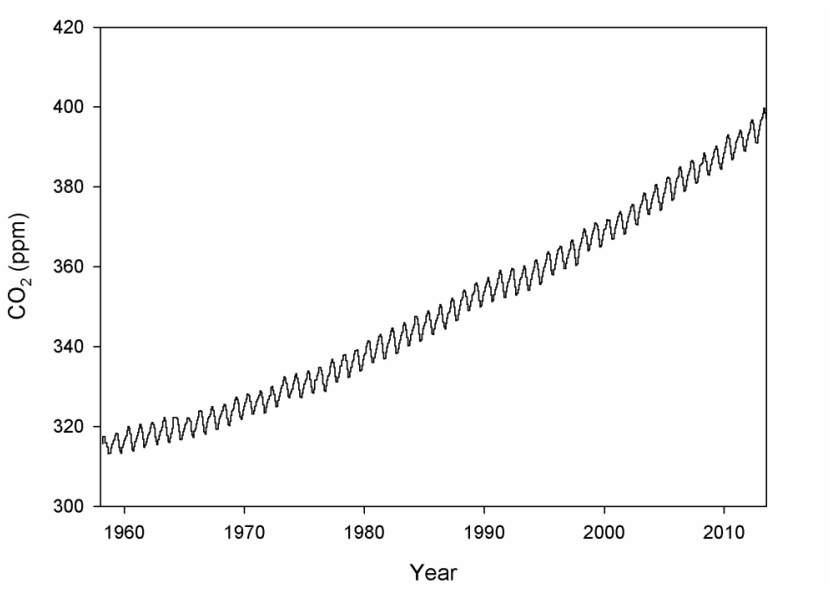

Figure 2.7 – Measured atmospheric CO_2 concentrations at the Mauna Loa Observatory, Hawaii, since 1960. (Keeling and Whorf, 2004)

Absolute recordings can be made, but assessing the likely response of the climate system is much more challenging. 'Scenario models' of emissions have been created by bodies like the IPCC (IPCC, 2000) in order to determine what could happen to the climate over the following decades. These range from optimistic to highly pessimistic with respect to the quantity of technological change, population growth and emissions mitigation implemented. In the IPCC cases these are divided in to a number of 'families' which assume the variation in different parameters which have the potential to affect the climate system. These are presented in Table 2.1 and Figure 2.8.

Table 2.1 - Storylines summarized (IPCC, 2000)

A1 storyline and scenario family	A future world of very rapid economic growth, global population that peaks in mid-century and declines thereafter, and rapid introduction of new and more efficient technologies.
A2 storyline and scenario family	A very heterogeneous world with continuously increasing global population and regionally oriented economic growth that is more fragmented and slower than in other storylines.
B1 storyline and scenario family	A convergent world with the same global population as in the A1 storyline but with rapid changes in economic structures toward a service and information economy, with reductions in material intensity, and the introduction of clean and resource-efficient technologies.
B2 storyline and scenario family	A world in which the emphasis is on local solutions to economic, social, and environmental sustainability, with continuously increasing population (lower than A2) and intermediate economic development.

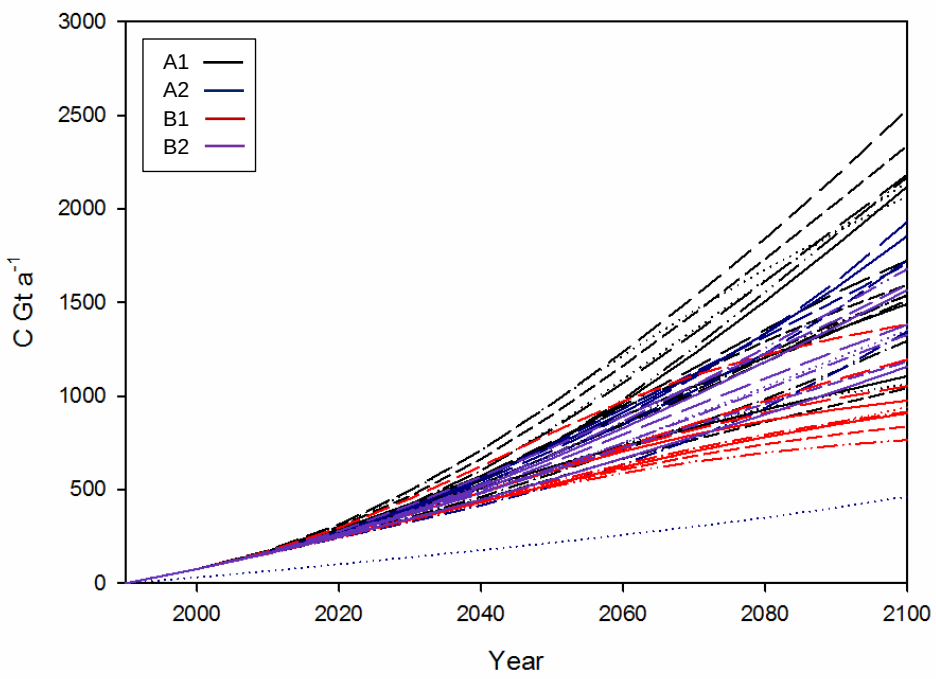

Figure 2.8 – Cumulative Gt C produced, estimated by IPCC SRES emissions scenarios. Source IPCC (2000) Colours relate to the 'storylines' in Table 2.1.

These scenarios illustrate clearly that all of the projected outcomes, even the most optimistic, suggest an increase in annual CO_2 production in the period up to 2100. Whilst the scenarios presented above consider factors such as population and carbon intensity of societies, there is no explicit reference made in their descriptions to the potential for actively reducing these emissions using technical solutions.

The effects of this increase in emissions on climate change are still poorly constrained, although contemporary well-supported observations suggest a likely increase in extreme weather events: droughts, floods, driving more widespread environmental change (IPCC, 2007). Some of the apparent difficulty in modelling the likely effects to this system is caused by the lack of knowledge around the sensitivity of different components of the carbon cycle.

The Stern Review (2007) looked in detail at the economic aspects of climate change, assessing how more 'responsible' approaches might be applied in the real world. Mitigation and reducing emissions are considered to be the first critical steps in reducing emissions overall. 'Geoengineering' technologies are briefly mentioned in the review under several guises, and present ways in which the Earth system could be manipulated in order to reduce the effects of warming, or reduce the amount of CO_2 in the air by actively removing it through capture and storage.

2.3 Geoengineering and global climate: mineral carbonation as a geoengineering method

2.3.1 Principles of geoengineering

Although the original usage of the term 'geoengineering' was in reference to a proposal to collect CO_2 at power plants and inject it into deep ocean waters (Marchetti, 1976), the concept of geoengineering has now come to describe a variety of techniques which aim to engineer the Earth's climate system by large-scale manipulation of the global carbon or energy balance. The Royal Society's 2009 report 'Geoengineering the climate: science, governance and uncertainty' still provides the most comprehensive summary of academic approaches to the idea of climate change mitigation through geoengineering (a summary of the technologies covered by the review can be seen in Figure 2.9). The report divides contemporary geoengineering methods in to carbon dioxide removal (CDR) techniques and solar radiation management (SRM) techniques. Solar radiation management techniques seek to reduce warming effects of climate change by reducing the quantity of solar radiation entering the Earth system, or increasing the quantity going out. The following section focuses upon CDR techniques, those which aim to directly remove CO_2 from the atmosphere reducing cumulative global concentration, and specifically carbon capture and storage (CCS).

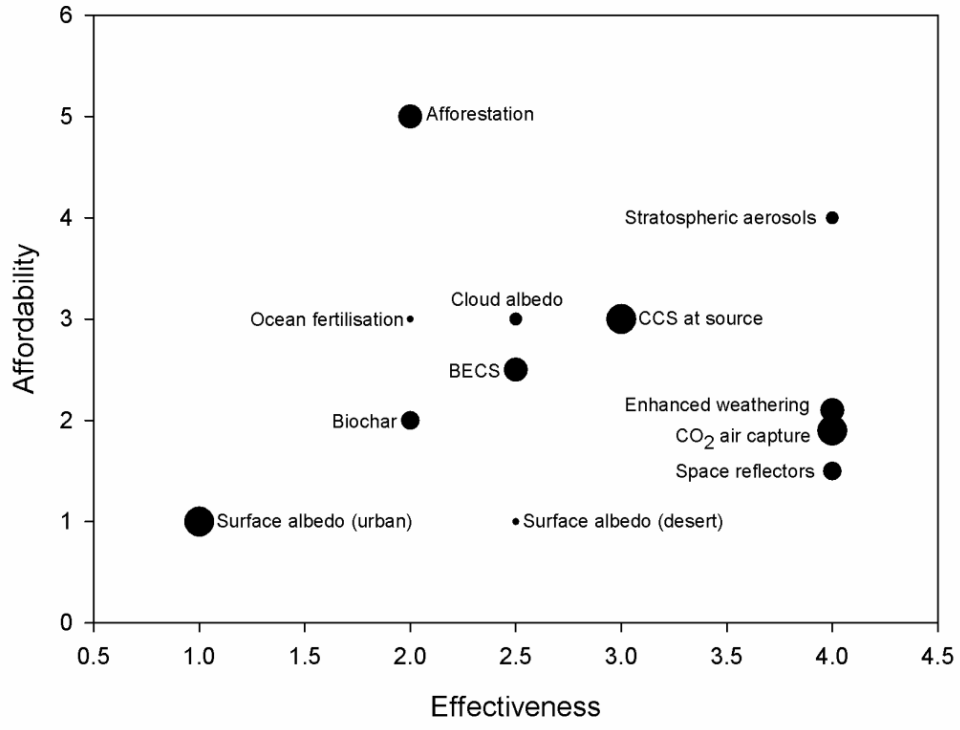

Figure 2.9 – Economic and technical assessment of various geoengineering technologies (Royal Society, 2009). The size of the bubble is relative safety of the method determined (large=safe, where safety includes predictability and verifiability of intended effects, and adverse side-effects and environmental impacts).CCS – carbon capture and storage, BECS – bioenergy with CO_2 capture and sequestration

Keith (2001) emphasizes that it is "the deliberateness that distinguishes geo-engineering from other large-scale, human impacts on the global environment; impacts such as those that result from large-scale agriculture, global forestry activities, or fossil fuel combustion." Geoengineering technologies are developed with the full intention to engineer the Earth system along a desired trajectory.

2.3.2 Carbon capture and storage

The IPCC produced a special report in its early 'Climate Change Reports' series addressing 'Mitigation' (IPCC, 2001), alleviation of climate change drivers, which includes references to carbon capture and storage. The IPCC (2005) Carbon Dioxide Capture and Storage report summarised technical and economic assessments of CCS technologies. Lackner (2003) effectively describes the spectrum of contemporarily available CCS technologies contained within this report: oceanic (direct injection of carbon dioxide in to the oceans), deep saline aquifers, geologic (direct injection of carbon dioxide in to subterranean voids) and mineral 'neutralisation' of carbon dioxide to form bicarbonates or carbonates. Contemporarily, the term 'carbon capture and storage' (CCS) is most synonymous with geologic 'underground' carbon storage, with a small number of projects already operating around the globe, mostly undertaking injection of CO_2 streams in to depleted gas reserves, oil reserves and deep saline aquifers. The first, and one if the best-known, pilot scale project for geologic CCS is Sleipner, Norway (Statoil, 1996). Since 1996 the Sleipner project has injected more than 10 million tonnes of CO_2 in to the Utsira Reservoir under the North Sea (Statoil, 2013).

At present a number of geologic CCS plants are active around the world, as shown in Table 2.2. Many of these projects are associated with CO_2 point sources, or are part of a large industrial process such as Enhanced Oil Recovery (EOR). The UK Carbon Capture and Storage Consortium (UKCCSC) continue to roll out geologic CCS as an industrially feasible method and provide technical and academic expertise (UKCCSC, 2013). In April 2012 the Department for Energy and Climate Change's UK CCS Commercialisation Competition made available "£1 billion capital funding, together with additional support through the UK Electricity Market Reforms, to support the practical experience in the design, construction and operation of commercial-scale". This project incentivised the planning of pilot scale CCS facilities in the UK – the two selected sites, Ferrybridge and White Rose, will come online around 2015-16.

Table 2.2 – Active or planned CCS plants (Olajire, 2013) showing planned capacity or current operational capacity where data is available

Project	**Location**	**Planned capacity / current rate of injection**	**Start up**
Sleipner CO_2 injection	Norway		1996
In Salah CO_2 injection	Algeria	17 Mt CO_2	2005
Weyburn-Midale CO_2 Monitoring and storage project	Canada / United States	20 Mt CO_2	2000
Snohvit CO_2 injection	Norway	0.7 Mt CO_2 a^{-1}	2006
Gorgon CO_2 injection	Australia	3.4 – 4 Mt CO_2 a^{-1}	2015
Rangely Weber Sand Unit CO_2 injection project	United States	23-25 Mt CO_2 (since 1986)	1986
Salt Creek Enhanced Oil Recovery (EOR)	United States	-	2004
Enid Fertilizer	United States	0.7 Mt CO_2 a^{-1}	2003
Appalachian Basin R.E. Burger Plant	United States	-	2008
Cincinnati Arch East Bend Station	United States	-	2009
Michigan Basin State-Charlton 30/31	United States	-	2008
Basalt formation of North Western India	India	-	Planning
Moxa Arch in south western Wyoming	United States	-	Planning
BP Peterhead-DF1	UK	-	2015
Don Valley power project	UK	-	2015
Plant Barry Project	US	0.15 Mt CO_2 a^{-1}	2011
Ordos project	China	0.3 Mt CO_2 (by 2014)	2011
Boundary Dam Project	Canada	-	2014
Carson-DF2	USA	-	2012

Other forms of carbon capture and storage have not been major considerations to date in the commercial setting, and present stances towards technologies such as mineral CCS (trapping atmospheric CO_2 through chemical reactions with minerals, usually to form carbonates) are less certain. For the purposes of contemporary feasibility, point source capture and processing is overwhelmingly favoured, due to the perceived and mechanical difficulties involved in the sequestration of dispersed CO_2 from ambient air. Geologic CCS is based upon the concept of removing CO_2 at point source (Huijgen et al ,2005). Mineral CCS may also be used at point source, but also has the potential to achieve direct sequestration of the gas from ambient atmosphere (Keith et al., 2006). As shown in Figure 2.10, Mineral CCS (shown here as 'Mineral carbonates') has a long characteristic storage time as a CCS technology and a larger capacity than 'underground injection' of CO_2. There are a number of reasons surrounding the reticence to roll out mineral CCS as a commercial technology, which are discussed further in Chapter 6.

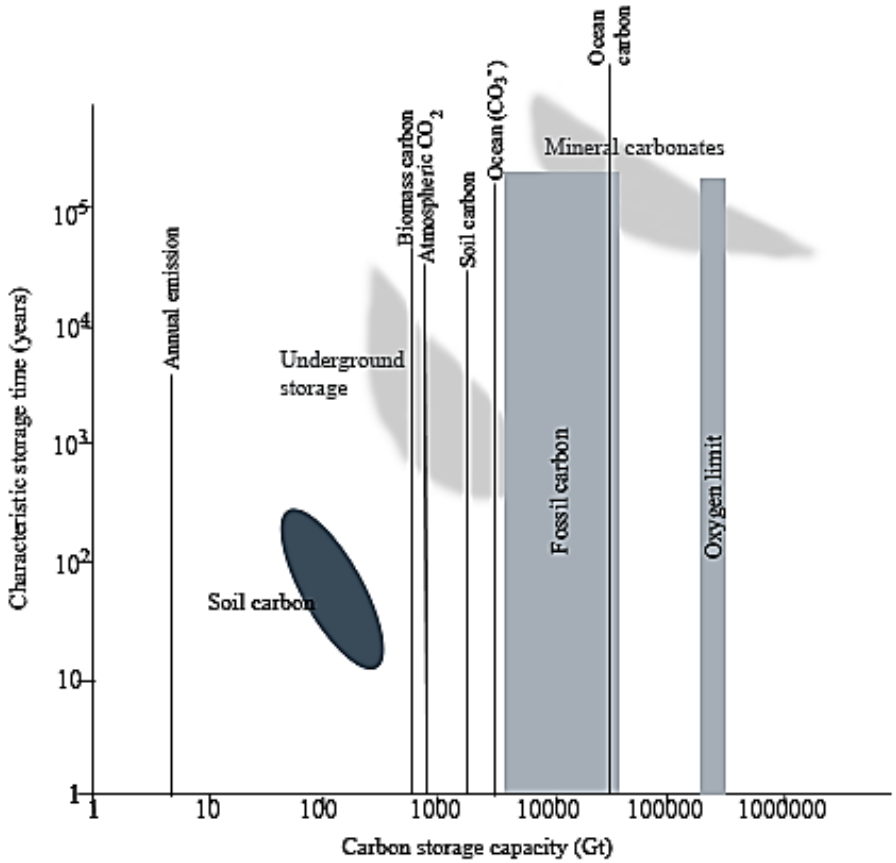

Figure 2.10 – Estimated storage capacities and times for selected sequestration methods (after Lackner, 2003). Shaded areas relate to estimated current stores, while lines indicate the theoretical limits of these stores.

2.3.3 Mineral sequestration for carbon capture and storage

Mineral sequestration as a CCS approach is considered to be an 'enhanced weathering' technique (Royal Society, 2009); taking its premise from the natural carbonation of Ca-/Mg-rich materials weathered from rocks in the geochemical carbon cycle (Berner et al, 1983) and implementing measures to accelerate this process beyond its present background level. Whilst it is widely accepted (Lackner, 2003; Huijgen et al., 2005, 2006) that CCS through mineral carbonation is empirically viable, experimental work has frequently concluded that this viability is limited by excessive running costs; imposed either by the mineral extraction costs of reserves required to provide necessary reactive material, or due to excessive energy requirements for processing or maintenance of industrially coupled CCS programmes. It is noted that enhanced mineral weathering schemes propose to produce stable, natural products which are already abundant in the environment, do not require monitoring and 'may therefore be regarded as benign in principle' (Royal Society, 2009).

Mineral CCS is far from being a new theory. Discussion of the potential for carbon capture and storage through mineral sequestration is originally attributed to Seifritz (1990) who discussed the feasibility for atmospheric CO_2 to be 'bound chemically via an exothermic reaction to form a stable, permanent substance'. Carbon sequestration is able to occur through the reaction of gaseous or aqueous CO_2 with mineral compounds, especially those containing alkaline earth metals, specifically calcium and magnesium. For purposes of carbon capture, magnesium silicate rocks such as serpentinite and peridotite and calcium silicate minerals such as wollastonite have been proposed as effective research routes. The use of artificial mineral substrates as an alternative to natural minerals in carbon capture and storage has also been proposed only recently and is not considered in the Royal Society Geoengineering Report 2009, but is mentioned briefly in the IPCC Special Report on Carbon Capture and Storage 2005.

Contemporary studies tend to fall in to two groups, which take their broad philosophies from the fields of mechanical / chemical engineering (process-based) or environmental science / geosciences (field-based) respectively:

A process-based approach

Process-based projects to date have focussed on both natural (Lackner et al., 1997) and artificial minerals (Geerlings et al, 2004; Huijgen et al, 2005, 2006; Rawlins et al., 2008) as reactive substrates. These approaches tends to focus upon the reaction of finely crushed mineral substrates as the feedstock in a reactor or fluidised bed setting, under high temperature and pressure to produce potentially salvageable calcium carbonate as an industrial by-product.

Seifritz (1990), Lackner (1997) and Butt (1997) concentrate on a process based approach to carbon capture using silicate minerals, coupling a mechanical reaction chamber with carbon dioxide point sources. Seifritz (1990) claims that, assuming the use of a quarried silicate mineral feedstock, '100million tonnes C' could be bound by silicate weathering each year. Huijgen et al (2005, 2006) concentrate on a similar process-based method using Ca-rich iron and steel slag. Each paper has independently concluded through cost-benefit analysis that the mineral CCS process is unfeasible prior to the introduction of further economic incentives for carbon capture, due to the excessive costs involved in extracting, processing and reacting the minerals.

A field-scale approach

Field scale projects focus upon the potential for acceleration of natural carbonation in certain silicate rock formations by the injection of fluids (Kelemen et al., 2008, 2011), supercritical CO_2 (Lin et al. 2008) or other geochemical fluids in order to elicit the forced carbonation of Ca and Mg rich minerals by the physical and chemical exploitation of mapped formations.

Observations of weathering processes acting at field scale provide a useful precedent for the way in which field scale weathering might be used as a mineral sequestration technology. Carbonation of natural silicates in the field is well observed, with many recent studies focussing on the carbonation of ophiolite complexes and estimating the time over which this occurs (Kelemen et al., 2011). There are suggestions that the process could be accelerated through shallow injection of fluids and gas into the rock formations, and feasibility studies are currently being carried out as part of the CarbFix project in Hellisheiði, Iceland (CarbFix, 2013). Studies focussing on mineral CCS at the Earth's surface include (Schuilling and Krijgsman, 2006; Wilson et al, 2009) assessing the potential for carbonation of crushed silicate intentionally spread on to land, and the carbonation of materials such as quarry fines through sub-aerial or accelerated weathering.

Stolaroff et al. (2005) provide a mixed approach, assessing how ambient air capture of CO_2 using Ca and Mg-rich minerals could be promoted with the use of large-scale, open-air bed reactors, in a system which is semi-process-based and semi-field-scale. This approach was deemed to be feasible and low cost, due to the limited energy input for processing. Section 2.4 examines in more detail the potential for inducing low-cost ambient air capture of CO_2 though an approach which integrates the benefits of a number of these process ideas – the use of soil systems to promote mineral CCS.

2.4 Soils as sites for mineral carbonation: principles and work to date

Soil systems provide a large number of positive conditions to promote the weathering of parent material and facilitate reactions with atmospheric CO_2. In this thesis they are considered as an alternative setting to the process-based approaches for enhanced weathering described in the previous section. This work aims to determine the potential for soil systems containing suitable materials to contribute to carbon sequestration processes.

2.4.1 The importance of SIC

The atmosphere-soil carbon flux equates to approximately 120Pg C a^{-1} (Figure 2.1, Manning, 2008), larger than the flux between all other stores noted in Section 2.1. Soil carbon therefore acts as a significant buffer reservoir for atmospheric carbon dioxide. Mineral carbonates, formed through many of the same chemical routes as described in Section 2.3.3, represent the main component of the inorganic part of this reservoir; Ryskov et al (2008) state that soil carbonates sequester CO_2 from the atmosphere and so serve as an 'additional' sink in the carbon cycle.

Pedogenic carbonates are found across large parts of the arid and semi-arid land areas of the Earth, formed following the weathering of Ca and Mg-rich host materials. They persist across much of North Africa and the Middle East, South Africa, Central Asia, Southern Australia and parts of the western seaboard of North America and Canada where the annual mean net precipitation is exceeded by evapotranspiration. Many of these areas experience marked 'wet' and 'dry' seasons, allowing supersaturation of minerals in soil solution. Recently a growing body of evidence has developed for pedogenic carbonate formation in temperate soils (Kovda, 2006; Mikhailova, 2006) and even monsoonal settings (Sinha, 2006), recorded in locations where Ca/Mg-rich conditions persist due to inputs from parent rock or translocated material.

Carbonate horizons are well documented in the literature concerning soil formation; Jenny (1980) describes the 'pedocal process' by which Aridosols are emplaced with carbonate horizons, mainly in the form of calcite although some dolomite and magnesite may be present, through a process of precipitation and crystallisation. It was historically believed that these horizons were formed by the downward migration of carbonates in rainwater, which then re-ascended to the vadose zone to precipitate at the soil moisture

boundary. It was observed that whilst pedocals were understandably common in regions where carbonates dominated the parent rock (e.g. limestone) they also formed in areas where Ca-rich parent rocks (e.g. basalt) persist (Chiquet, 1999; Durand, 2006). It is known that calcite horizon intensity in pedocals can also be increased by carbonate inputs from aeolian and marine sources (Anand, 1997; Dart, 2007; Quade, 1995). The theoretical basis behind precipitation occurrence is summarised by Mumm et al (2007); carbonate precipitation may occur due to changes in the physical environment (e.g. pressure or temperature change) or in the chemical environment: P_{CO_2}, pH and related variation in ionic concentration. This equilibrium relationship is shown in Equation 2.2.

Equation 2.2:

$$CaCO_3 + CO_2 + H_2O = Ca^{2+} + 2HCO_3^-$$

The formation of pedogenic carbonates is directly related to the standard factors of soil formation referred to by Jenny (1980): climate, biotic factors, topography, parent material and time or age. Specific factors within these general conditions may also be identified; Cerling (1991) notes that soils which freeze can have an increased atmospheric concentration of CO_2 and where precipitation > 100cm a^{-1}., freezing of the soil solution may be an additional carbonate formation mechanism. These factors are referred to in Figure 2.11, which also demonstrates the basic carbon fluxes between the atmospheric and soil carbon pools as described in section 3.1.

- Soil chemistry
- Vegetation cover / type
- Biotic activity
- Precipitation
- Ambient temperature
- Time / age
- pCO_2

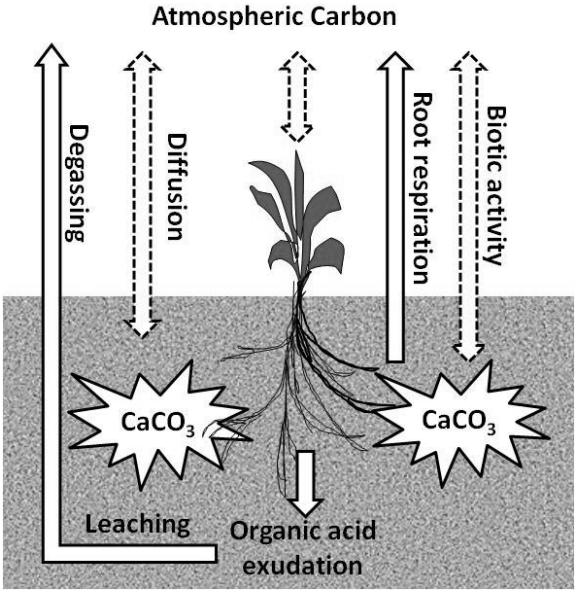

Figure 2.11 – Diagram illustrating the main components of soil carbon cycling with respect to carbon sequestration

As documented by Wright and Tucker (1991), truly pedogenic (vadose) carbonate forms in the vadose zone during pedogenesis (soil formation). Deposition may also occur in temporarily phreatic conditions, however, carbonates cannot easily form in situations where water-logging persists. Calcretes forming in association with groundwater, at or near groundwater level are known as 'phreatic' carbonates and are controlled by different geochemical processes than their pedogenic counterparts.

Anecdotal evidence has culminated in the demonstration of the occurrence of *in situ* carbon sequestration reactions occurring at post-industrial and urban sites, confirmed by recent studies (Krishnamurthy et al, 2003), where calcium-rich residues are present or have been emplaced. Mayes (2008) notes that the hydration of lime (CaO) in slag to portlandite ($Ca(OH)_2$) and dissolution produces the hydroxyl ion (OH^-) which elevates solution pH. "For the CO_2-$CaCO_3$-H_2O system, a rise in pH (increasing CO_2) and addition of Ca" "will force precipitation of calcite when saturation is reached" (Kalin et al, 1997). Geochemical behaviour here may be controlled by factors which relate directly to those in natural pedogenic carbonate systems, including physical-chemical composition, age, co-deposited wastes, native ground and surface water geochemistry and hydrogeological setting.

Manning (2008) notes that 'soils have a role to play as passive agents in the removal of atmospheric CO_2'; being the largest terrestrial carbon sink, carbon capture through soil engineering is able to harness the associated rapid turnover of C promoting fixation in stable minerals at a faster rate than in natural systems. Recent work by Renforth et al (2009), building upon analytical field studies such as Krishnamurthy et al (2003), has proven the potential for urban soil engineering for carbon capture using Ca/Mg-rich wastes, with specific reference to cement, construction and demolition wastes and iron and steel industry wastes. Other suitable sources include quarry waste and mine tailings (Power et al, 2013; Wilson et al, 2009). The use of industrial and construction residues is promising; with the potential for dual considerations of waste recycling and CCS to be aligned in a single project as discussed further in Section 2.5.

Calcium and magnesium-bearing waste silicate minerals within the soil environment can capture and store atmospheric carbon through the process of weathering and secondary carbonate mineral precipitation in much the same manner as pedogenic carbonates are formed (Renforth et al, 2009; Washbourne et al, 2012). This presents the

potential for engineered urban soils to capture and store atmospheric carbon. Many urban soils contain Ca/Mg-rich 'wastes' (Manning et al., 2013a), constituting an important part of the urban engineered environment and providing carbon capture as an important ecosystem service.

Extensive urban areas are now an international phenomenon, with the world's urban population increasing by 1.76% a^{-1} between 2009 and 2025 (UN, 2009), reaching 6.3 billion people by 2050, and then representing ~69% of the world's population. As urban areas grow in magnitude and complexity, a deep understanding of the environment which supports them becomes critical to ensuring sustainable growth and maintenance of ecosystem services, benefits provided by the natural environment. Urban soils are the basal component of built and green infrastructure within cities and are a critical element of the urban ecosystem. As noted by Lehmann and Stahr (2007), they can be seen as a fundamental ecological asset for land-use planning and are critical in urban landscaping.

2.5 Suitable materials for soil mineral carbon capture and storage (MCCS) (sourcing, quantities, production, preparation)

The use of Ca/Mg-rich wastes for carbon capture has been extensively considered (e.g. Gunning at al., 2010; Huijgen et al., 2005; Huntzinger et al., 2009; Rawlins, 2008; Rawlins et al., 2008). As mentioned in the previous section magnesium silicate minerals such as serpentine (in serpentinite), olivine (in peridotite) and calcium silicate minerals such as wollastonite are possible candidates for mineral CCS, as are a number of artificial mineral substrates. Natural silicates are ubiquitous and widely available but their exploitation requires energy investment in quarrying, processing and transport. Artificial silicates are significantly less abundant, but are potentially readily available at specific production centres as they frequently form a component of industrial waste streams, they also regularly occur close to large industrial CO_2 point sources.

As there has been a large focus on carbonation in batch reactors, where elevated pressure and/or temperature are applied to accelerate the carbon sequestration reaction (Huijgen et al., 2006; Lackner et al., 1995), much of the experimental literature also involves pre-treatment of the material (grinding, heat treatment etc.) to accelerate dissolution and application of heat or pressure. Acceleration of sequestration by wastes in passive *in situ* settings, soils and open-air stockpiles, is an alternative low energy process which has been considered by a small number of studies (Renforth et al., 2009; Stolaroff et al., 2005; Washbourne et al., 2012; Wilson et al., 2009). Figure 2.12 demonstrates how this process might occur. Iron and steel slag is referenced here, but the basic process applies to most materials composed of calcium, magnesium and iron minerals.

Globally 7-17 billion tonnes of waste silicate suitable for this purpose are produced each year (Renforth et al., 2011c) and so there appears to be a considerable incentive to develop and assess procedures that harness this potential. At present there is insufficient available information concerning the accounting statistics for material fluxes to permit quantitative assessment of global carbon capture potential through ambient air capture by weathering of artificial minerals. An estimate of slag, construction and demolition waste, pulverised fuel ash and quarry fines production since the 18^{th} century is provided in Renforth et al. (2011c); overall these materials are estimated to have the potential to collectively capture 190-332 Mt C a^{-1}. Further understanding of the settings in which

the carbonation reaction is promoted must be developed through an understanding of soil carbon storage processes (Figure 2.12).

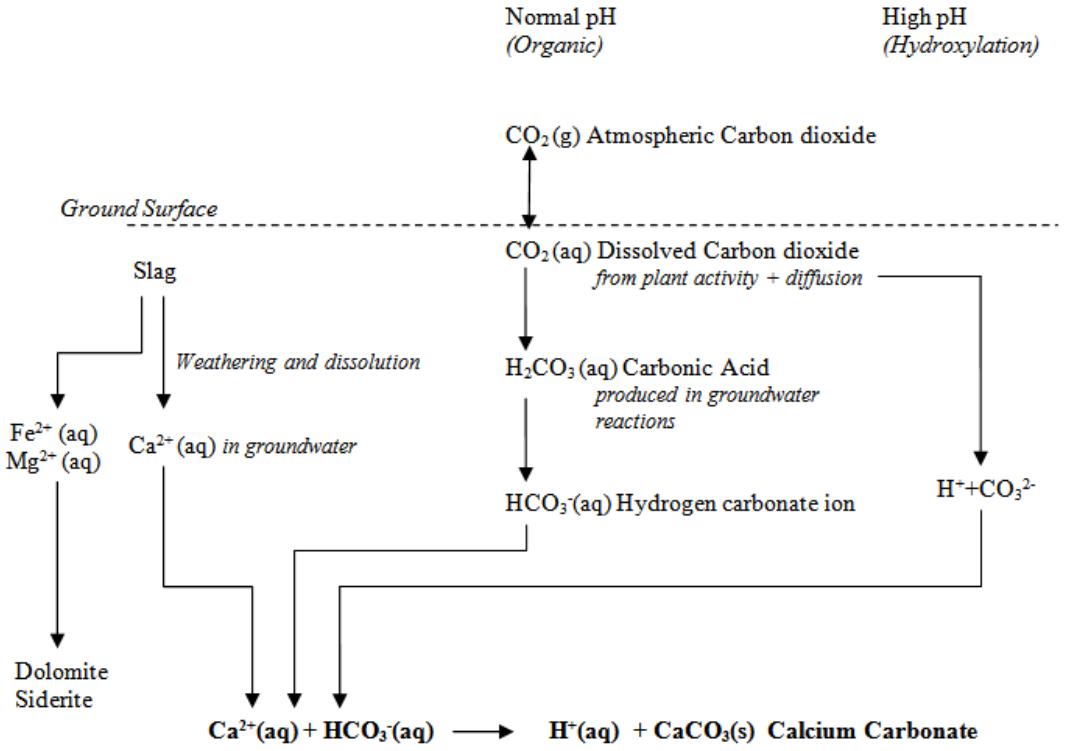

Figure 2.12 - Simplified slag sequestration mechanism (After Huijen et al, 2005)

Mineral CCS using artificial minerals in soil settings provides an interesting means of re-purposing waste products, which may otherwise be disposed of in a less sustainable manner, for an environmental benefit. It can also be viewed as assisting in 'closing the loop' on CO_2 and solid wastes from certain industrial processes (Figure 2.13). It should be noted that mineral sequestration using waste minerals is thermodynamically unable to capture more CO_2 than was emitted in the original production of the waste. Whilst this is not innately a limitation to use, due to the high residual potential exhibited in aforementioned studies, it must be appreciated that conventional mineral sequestration is unable to render an industry 'carbon neutral' and there will always be a small to moderate net surplus of CO_2.

A number of artificial materials are suitable for mineral CCS, as shown in Table 2.3. The 'suitability' in this case is determined by the significant presence of divalent cations which have a known ability to take part in mineral carbon capture reactions. For the purposes of this work, two classes of artificial mineral have been selected: iron and steel slag and construction and demolition waste. These have been chosen as analogue materials for further field and lab work, being widely produced, readily available and

not previously widely studied in the specific contexts proposed – as soil amendments for promoting carbon sequestration.

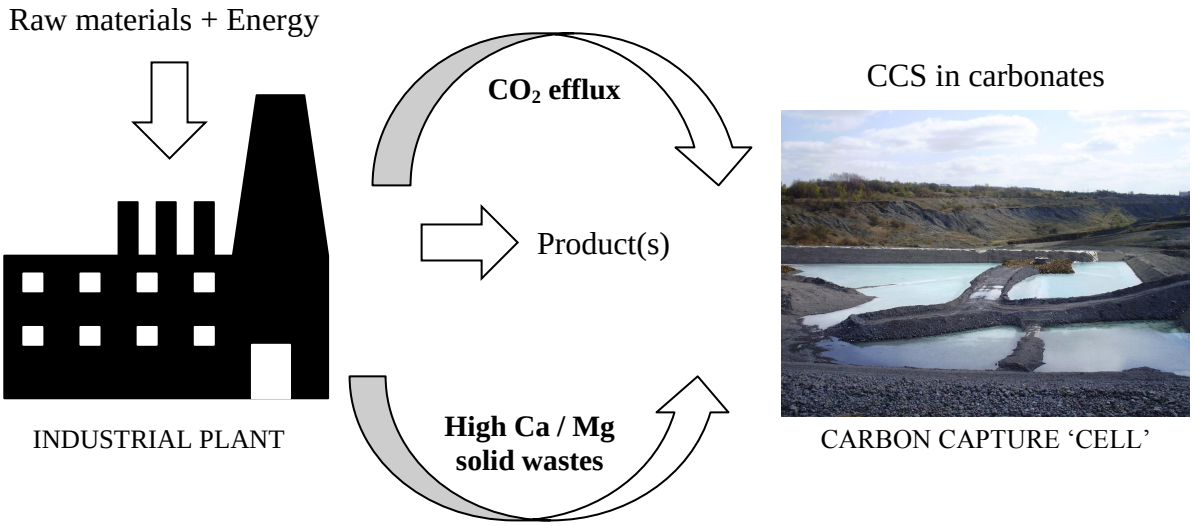

Figure 2.13 - Simplified schematic of 'field-scale' carbon capture and storage

Table 2.3 - Carbon capture potential of silicate minerals (Renforth et al., 2011c)

Material	**Approximate Ca and Mg content**	**Global production (Mt a^{-1})**	**Carbon capture potential (MtC a^{-1})**	**Historically produced (Mt)**
Fines from aggregate production	3% CaO 3% MgO nominal	3,300	130	
Mine waste	unknown	2000-6500	unknown	
Cement kiln dust	65% CaO	420-568	59-79	9,000-12,000
Construction waste	14% CaO	294-1,239	9-37	Maximum limited by cement production around 60 Gt
Demolition waste	10% CaO	1,106-4,661	24-100	
Blast furnace slag	38% CaO 12% MgO	250-300	53-64	7,900-9,500 (since 1875 - 80% potentially reused)
Steel making slag	45% CaO 7% MgO	130-200	23-35	4,200-6,400 (since 1875)
Stainless steel slag	46% CaO 6% MgO	6.5	0.6	
Blast furnace flue dust / sludge	4.9% CaO	30	0.3	
Lignite ash	20% CaO 1% MgO	57-73	3-4	7,700-14,600 (since 1927)
Anthracite ash	3% CaO 1% MgO	36-46	<1	
Bituminous ash	3% CaO 1% MgO	257-331	4-6	
Red mud	40% CaO 1%MgO	70	6	
Total			192-333	

2.5.1 Cement, construction and demolition waste

Cement is one of the predominant global construction materials, produced by heating calcium carbonate (from mined limestone), silica and alumina (both from clay or fly ash), to high temperatures (between 1300-1500°C). A range of calcium silicate minerals are formed depending upon the Ca/Si ratio of the raw materials, usually di and tri-calcium silicates as well as readily weathered free lime (CaO). Construction and demolition (C&D) waste is the term used to describe the wastes derived from construction and demolition activities. This waste is a complex mixture of concrete, brick, block and aggregate, with residues of other construction materials including metals, plaster and paper (a detailed description in given in Table 2.4).

Table 2.4 - Construction and demolition waste properties (Renforth et al., 2011c)

Material Type	**% wt**	**Likely material composition**	**CaO %**
Construction waste			
Concrete, bricks, blocks, aggregate	7.4	Calcium silicates (hydrated and un-hydrated), Free lime CaO, $CaCO_3$ and gypsum in concrete. Calcium aluminium silicates and Fe oxides in masonry. Silica in sand and gravel.	28.6[1]
Metals	5.9	Predominantly Fe from steel and Cr from stainless steel. Cu and Zn from plumbing. Potentially trace Pb from roofing materials.	N/A
Excess mortar/concrete	2.6	Similar to concrete above	25.0[2]
Timer products	1.7	Organic carbon including lignin and cellulose	N/A
Plastics	1.9	Petroleum products	N/A
Plasterboard and plaster	0.6	Mainly gypsum	32.6[3]
Paper and cardboard	0.4	Organic carbon similar to timber products	N/A
Vegetation	0.2	Organic carbon	N/A
Soil	0.2	Silica in sand and gravel, clay, organic carbon	N/A
Demolition Waste			
Concrete	25.5	Similar to concrete above	28.6[1]
Masonry	15.3	Aluminium silicates, Fe oxides and quartz, with small quantities of free lime	2.6[4]
Paper, cardboard and plastics	12.1	Organic carbon and petroleum products	N/A
Asphalt	9.6	Petroleum products, silicates in aggregate	N/A
Wood based	2.1	Similar to timber products above	N/A
Road planings	14.0	Similar to asphalt	N/A
Total	99.5	**CaO content as a % of total material**	**10.7**

The CaO content of construction waste varies from 10 to 20% (Renforth et al 2011c), providing a small but significant potential for providing Ca to be used in mineral CCS. Cement-based products form the largest component of the waste stream at 35.5% but in some cases could actually reach up to 67%, providing a much higher sequestration potential and highlighting the heterogeneous nature of the material.

Approximately 2.8 Gt of cement are produced annually and it is estimated that nearly 60 Gt of cement have been manufactured since the mid-1920s (Figure 2.14) when it was first used as a widespread construction material. The production of 1 t of cement uses approximately 1.7 t of raw material and produces 150-200 kg of waste as 'kiln dust' (van Oss and Padovani, 2003) which suggests that approximately 9-12 Gt of kiln dust may have been produced globally.

Worrell et al. (2001) calculate the emissions from cement manufacture to be approximately 244 kg C t^{-1}, but this can vary depending on processes used and does not take in to account the emissions associated with mineral extraction and transport involved in its original production. A crude estimation of global C&D waste production is 1.4-5.9 Gt a^{-1} (21% from construction and 79% demolition) although this material is poorly accounted for, therefore this estimate is derived from construction industry proxy data (Renforth et al., 2011c)

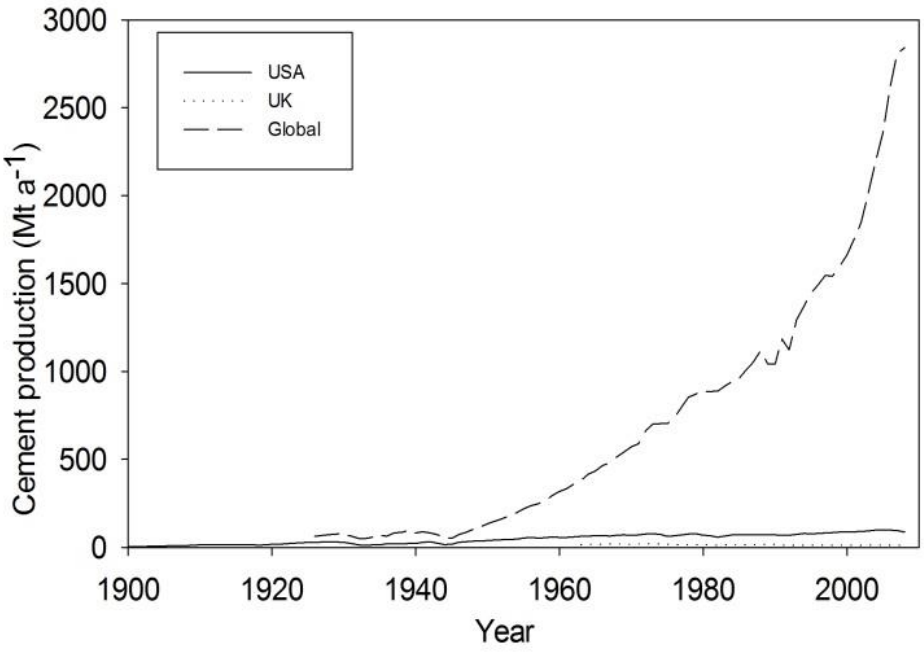

Figure 2.14 - Global cement production (Renforth et al., 2011c)

C&D waste is frequently reused as a 'secondary aggregate' and can be processed to form a raw material for brick manufacturing. Use as a structural material is limited by the possible presence of low strength or high expansion materials listed in Table 2.4 (bitumen, gypsum, organic matter, etc.). Waste which is not reused has been historically sent to landfill, with 40-45 Mt a^{-1} of C&D waste either spread on registered sites or disposed in landfill representing approximately 51% of the total UK production of C&D waste.

9-12 Gt of kiln dust may have been produced globally, with a carbon capture potential of 1.2-1.7 Gt C (based on a CaO content of 65%). Although the fate within the environment of this material is unknown it is likely to have partially or fully carbonated. Most of the 60 Gt of cement produced globally has been used for construction.

Cement kiln dust has an average carbon capture potential of 1.2-1.7 Gt C (based on a CaO content of 65%). Combining the production statistics (Figure 2.13) with the typical composition (Table 2.4), it is estimated that construction and demolition wastes have carbon capture potentials of 9-37 and 24-100 Mt C a^{-1} respectively assuming the full carbonation of all CaO present. In context, this represents an offset of 6-97% to annual global cement production (103-139 Mt C a^{-1}) (Renforth et al, 2011c; Worrell et al, 2001)

2.5.2 Iron and steel making slag

Slag is the name given to a specific portion of the solid wastes created during the production of iron and steel. It may be subdivided in to two major classes: blast-furnace slag and steel slag. Oxides of iron, silica and alumina (from iron ore) are mixed with $CaCO_3$ and $CaMg(CO_3)_2$ (from limestone and dolomite) and heated in a blast furnace (at 1300-1600°C) to form pig iron and iron slag. Steel is manufactured by refining pig iron or scrap steel using oxygen and $CaCO_3$/$CaMg(CO_3)_2$ as a flux in a basic oxygen (BOS) furnace to produce steel and steel slag (Lee, 1974).

The chemical composition of slag varies considerably (Table 2.5), but is typically between 38-46% CaO and 6-12% MgO (Poh et al., 2006; Proctor et al., 2000). The major chemical components of iron and steel slag are calcium oxide, silica and aluminium oxides, in varying proportions. The most common minerals associated with slag are melilite ($(Ca,Na)_2(Al,Mg,Fe(II))(Si,Al)_2O_7$) and anorthite ($CaAl_2Si_2O_8$) (Lee,

1974), and amorphous calcium magnesium alumina silicate glasses are also common (Fredericci et al., 2000).

Table 2.5 – Average composition of iron and steel slag values in wt %

	Blast furnace slag (Proctor et al., 2000)	**Steel slag (Poh et al., 2006)**	**Stainless steel slag (Shen and Forssberg, 2003)**
SiO_2	36.44	12.67	28.39
Al_2O_3	7.79	2.84	4.33
CaO	38.34	44.87	46.20
MgO	11.67	6.87	6.08
FeO	-	15.73	4.22 (total Fe)
Fe_2O_3	2.48	9.81	-
TiO_2	-	0.62	0.33
P_2O_6	-	1.11	-
MnO	0.71	3.81	1.69
Na_2O	-	0.11	0.06
K_2O	-	0.57	0.05
SO_2	2.57	0.00	-
Cr_2O_3	-	-	5.12
Total	100.00	99.01	96.47

3 Mt of blast furnace slag and 1 Mt of steel slag are produced annually in the UK (EA, 2007; Poh et al., 2006). In 1992 China became the largest manufacturer of iron (and steel in 1996) and produces around 970 Mt a^{-1} today (500 Mt steel and 470 Mt iron in 2008) (BGS, United Kingdom Minerals Yearbook up to 2008). It is estimated that global slag production is 250-300 Mt a^{-1} for iron slag and between 130-200 Mt a^{-1} for steel slag. Approximately 12,200-15,900 Mt of slag have been created since the 1870s (Table 2.6 and Figure 2.15).

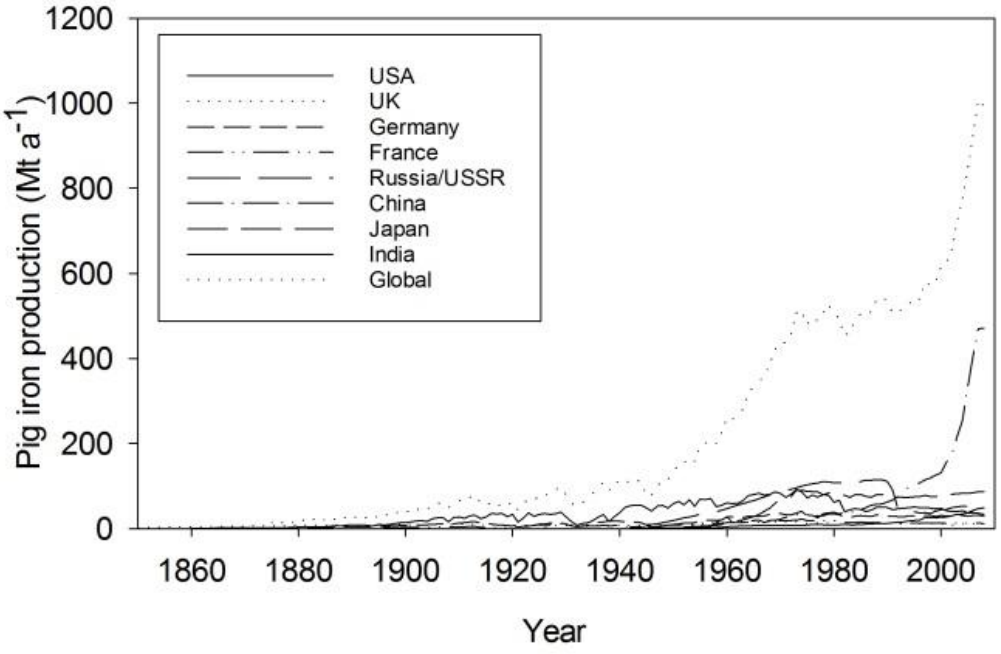

Figure 2.15 - Global production of pig iron (Renforth et al., 2011c)

Table 2.6 - Global slag production, *includes figures from the former USSR (Renforth et al., 2011c)

Country	Current pig iron production (Mt a^{-1})	Current steel production (Mt a^{-1})	Total pig iron production (Mt)	Total Steel production (Mt)	Total historic pig iron slag produced (Mt)	Total historic steel slag produced (Mt)
UK	10	14	1,500	1,600	400	200
USA	35	95	5,200	7,900	1,400	990
Germany	30	45	2,260	3,000	620	370
Japan	85	120	3,500	4,700	960	580
Russia*	50	70	4,100	5,600	1,100	700
China	471	500	4,550	4,570	1,252	571
India	49	55	801	807	220	101
Global Total	1,000	1,300	32,000	43,000	8,700	5,300

Blast furnace slag is not classified as a waste and is often reused as secondary aggregate in concrete, as filler in road construction (Mahieux et al., 2009), or used in soil stabilisation processes (Poh et al., 2006). Blast-furnace slag is a relatively porous material with a variable, but generally low, bulk density. Significant instability in blast-furnace slag occurs only in relatively rare instances where high lime or iron and sulphur contents are encountered. It is likely that a large proportion of this slag, particularly from pig iron, has been sold and reused for these purposes. Steel slag is a non-porous material with relatively high bulk density and is more physically unstable than blast furnace slag. Steel slag is relatively enriched in free lime and is usually left to 'weather' prior to use. Approximately 10% of steel slag is used in the UK (Poh et al., 2006), the remainder being stockpiled or sent to landfill.

Recorded sales of iron slag in the USA since 2001 vary between 75 and 100% of total production (USGS, 2009) and slag from old stockpiles is also extracted and sold (USGS, 2008). Assuming the majority of steel slag and around 20% of iron slag remains stockpiled, it can be estimated that 5.8-8.3 Gt of slag has been stockpiled, spread on land, or disposed in landfill globally since the mid-19th century, with a total carbon capture potential of 0.5-1.1 GtC.

Assuming CaO and MgO contents of 38-46% and 6-12% the carbon capture potential for slag is 99-135 kg C t^{-1}, current global production of slag is estimated to have a maximum carbon capture potential of 44 - 59 Mt C a^{-1}. CaO / MgO contents may be lower than reported due to pre-carbonation, although figures for this are not available.

In context, this represents an offset of 10-14% to global steel production (410-440 Mt C) (Renforth et al, 2011c; IPCC, 2007).

2.5.3 Combined potential

Iron and steel slag and construction and demolition waste have a combined carbon capture potential of 109-236 Mt Ca^{-1}, as shown in Table 2.7. This is an overall potential and does not include an offset against emissions during the production of the materials. This represents a mitigation of 1.2 – 2.7% of global carbon emissions (8.900 MtC a^{-1} (EIA, 2011))

Table 2.7 – Carbon capture potential of selected artificial silicate minerals (Renforth et al., 2011c)

Material	**Approximate divalent cation content**	**Carbon capture potential (MtC a^{-1})**
Construction waste	14% CaO	9-37
Demolition waste	10% CaO	24-100
Blast furnace slag	38% CaO 12% MgO	53-64
Steel making slag	45% CaO 7% MgO	23-35
TOTAL		109-236

2.6 Summary and relevance to this research

The global carbon cycle consists of a number of interlinked components, all ultimately providing feedbacks, on different timescales and magnitudes, to the global climate. Carbon dioxide emission to the atmosphere from anthropogenic sources is a major driver of contemporary climate change, with emissions currently ~8,900 Mt C a^{-1} (EIA, 2011).

A number of measures can be taken to reduce contemporary carbon emissions, however Carbon Dioxide Removal (CDR) methods of geoengineering may be able to mitigate further, and even play a part in actively reducing carbon dioxide concentration in the atmosphere. Mineral carbon capture and storage is one geoengineering route by which carbon dioxide can be captured and stored.

Mineral carbon capture and storage, through the weathering of suitable materials and precipitation of secondary soil-formed (pedogenic) carbonate minerals is a process which occurs naturally in a number of global soil systems and acts to capture carbon dioxide from the atmosphere. The soil system has a high rate of C turnover, and pedogenic carbonate has been identified in young, anthropogenically influenced soils in a number of studies.

Many artificial and ‘waste’ silicate materials have the appropriate composition to act as substrates for mineral carbon capture and storage. The overall carbon capture potential of the materials included in this study (C&D waste, iron and steel slag) is 109-236 Mt C a^{-1}. Globally, waste silicate minerals have the potential to capture 192-333 Mt C a^{-1}, representing 2.0-3.7% of global emissions (EIA, 2011). Studying the means by which easily accessible, and readily available, artificial and waste silicate minerals can be used in soil engineering for carbon capture provides an insight in to the possible use of natural silicate minerals for the same purpose.

In summary, this chapter collates relevant information surrounding the use of artificial silicate minerals in promoting carbon capture and storage in soil systems. It provides the technical background to demonstrating how mineral carbon capture could be promoted through the application and management of iron and steel slag and construction and demolition waste as sources of Ca and Mg for mineral carbonation. Research in the following chapters has been conducted with consideration to the critical interface that soils occupy in the global carbon cycle, how natural factors can be utilised to promote soil carbon sequestration, and the technical, legislative and economic setting in which this type of research is likely to operate.

CHAPTER 3 - Geochemical processes behind mineral carbon capture in soils

The efficacy of carbon capture and storage through mineral sequestration as a geoengineering technology will be determined by a range of parameters. As discussed in the last section of Chapter 2, a number of materials and settings allow carbon capture and storage through mineral carbonation to occur. This chapter focuses on the geochemical processes which dictate the rate and capacity of mineral carbon capture in a selected group of materials, specifically investigating the rates at which suitable minerals weather and carbonate in small-scale controlled settings. These results were used to inform larger-scale studies presented in the following chapters.

Results contained in this chapter contribute additional data to a large base of peer-reviewed literature regarding the weathering rate of specific silicate minerals under a number of geochemical conditions. Experimental work in this case focused on a selection of materials as analogues for the weathering of basic calcium silicate minerals, artificial: steel slag, construction and demolition waste, and natural: wollastonite ($CaSiO_3$) and dolerite. Weathering rates and geochemical behaviour of these materials were calculated in each case in order to comment on their potential applicability in engineering soils for carbon capture.

The complexity of the geochemistry surrounding carbon capture and storage in real-world settings is briefly discussed, summarising the challenges of applying laboratory derived weathering rates to field scale settings. The use of stable isotope geochemistry of carbon and oxygen in secondary carbonate minerals to estimate provenance and formation routes is also discussed, an approach which is applied in subsequent chapters.

Chapter Summary:

Weathering experiments on artificial and natural minerals allowed the comparison of Ca leaching data for these materials, as a proxy for their potential to perform MCCS, in a variety of previously unreported physical-chemical settings.

- Comparative weathering rates determined through the analysis of Ca leaching data for artificial silicate minerals in a variety of physical-chemical settings
- Rate reconstruction for the weathering of wollastonite $CaSiO_3$ (Ca leaching) under STP under three different pH conditions
- Time-point data for *in situ* weathering of steel slag under ambient environmental conditions

3.1 The geochemistry of mineral carbon capture

Mineral carbon capture and storage schemes have been proposed to utilise the carbonation potential of a number of materials, outlined in detail in Chapter 2. All of these materials have some physical-chemical components in common, most being silicate minerals of varying structure and complexity, natural and artificial. Silicate minerals weather naturally in the ambient environment, associated with the flow and chemistry of water at the Earth's surface (White and Brantley, 1995), and can act to draw down atmospheric carbon dioxide, capturing and storing it in stable minerals in the process. The geochemistry of silicate weathering can be complex, and significant experimental work has been carried out (White and Brantley, 2003 and references therein) in order to further elucidate the rates and mechanisms by which these processes occur under a variety of conditions (temperature, pressure and variations in chemistry).

3.1.1 Mineral weathering: structural and chemical characteristics

Structural

The structure of silicates in natural and artificial minerals is very varied. An exhaustive coverage of the diversity of silicate mineral structures is beyond the scope of this work, but comprehensive summaries can be found in White and Brantley, 1995 and Palandri and Kharaka 2004. Natural silicate mineral structures are based on a number of crystalline forms, from isolated tetrahedra to large sheets or chains comprised of these more structurally simple units. The crystal structures of silicate minerals have a strong influence over their physical properties. In combination with variations in chemistry this provides an explanation for the large range of weathering rates observed in silicate minerals. Shibata et al (2006) note that weathering rates of rare earth elements (which were comparable to those of Mg and Ca (Shibata et al, 2006)) depend mostly on the compatibility of each element with crystal structure of the mineral. Curtis (1976) notes that the influence of physical (crystal) structure on weathering is not as readily understood as chemical processes of weathering which can be tied to particular, known atomic, molecular or ionic properties.

Artificial silicate minerals frequently exhibit a variety of textures which may differ from natural silicates. A number of artificial silicate materials also show a tendency to form amorphous gels and glasses, and poorly crystalline phases characteristic of material produced through high-temperature processes and specific chemical conditions

(Tossavainen et al, 2007). Cement in particular, a large component of construction and demolition waste, is frequently composed mostly of calcium-silicate-hydrate gels which can be described as ‘tobermorite-like’ or ‘jennite-like’ (Chen et al., 2004; Renforth et al., 2011b). Solubility in these materials is considered a function of the Ca/Si ratio in the solid (a chemical factor), which is related to mean chain length in a silicate (a structural factor) (Renforth et al, 2011b). Gels and glasses weather differently from their crystalline forms (Hamilton et al., 2000) appearing to exhibit more rapid leaching behaviour which is discussed in more detail in the following sections.

Chemical

All of the materials considered to date for carbon sequestration through mineral weathering have a number of chemical factors in common: almost all are silicates (with silicon as major component) (Hartmann et al., 2013) or are derived from silicate parent material, and most contain the divalent cations calcium and / or magnesium which must be weathered out into solution to react with ions formed from dissolved CO_2, ultimately forming carbonates.

Cement is composed of poorly crystalline calcium-silicate-hydrate gels (Powers, 1958), portlandite and a small number of other minerals including gypsum and ettringite (Renforth 2011b) These materials may also include iron, aluminium and magnesium, incorporated into the silicate framework, as is also frequently the case with steel slag Proctor et al., 2000, Poh et al., 2006). A comprehensive study of the solubility of a range of cement minerals is presented in Matschei et al. (2007) and Renforth (2011b).

As well as in crystalline silicates, gels and glasses, readily weathered cations may also be found in other mineral forms within the materials of interest, some of which occur as intermediate weathering products derived from the original silicates (especially hydrated forms), and some of which are formed during mineral production or processing. With respect to construction and demolition waste and iron and steel slag, free lime (CaO) and portlandite ($Ca(OH)_2$) are common constituents. Gypsum may also be present. These materials are highly unstable and readily weather and carbonate in the presence of dissolved CO_2.

Macro- and micro-scale processes

Physical and chemical properties of the material as shown above have significant influence over its weathering behaviour. Macro and micro-scale properties of the environment also significantly influence the way in which materials weather. Figure 3.1 illustrates a conceptual model of the weathering of idealised spherical particles in an air-water system, highlighting some of the factors affecting the movement of fluids in relation to solids and solutes. From observing simplified systems of this type a number of possible controlling factors can be proposed to influence the rate of weathering:

- Particle size / surface area
- Flow conditions in fluids
- Saturation / unsaturation
- pH range and chemistry of the soil pore water
- The proximity of the material to the soil surface / weathering margins

Carbonate formation will also depend upon:

- Rate of leaching of Ca from the material / the relative solubility of the different materials
- CO_2 partial pressure / diffusion of CO_2(g) in to pore fluids

These factors are discussed in greater detail in the following sections, specifically section 3.2 of this chapter.

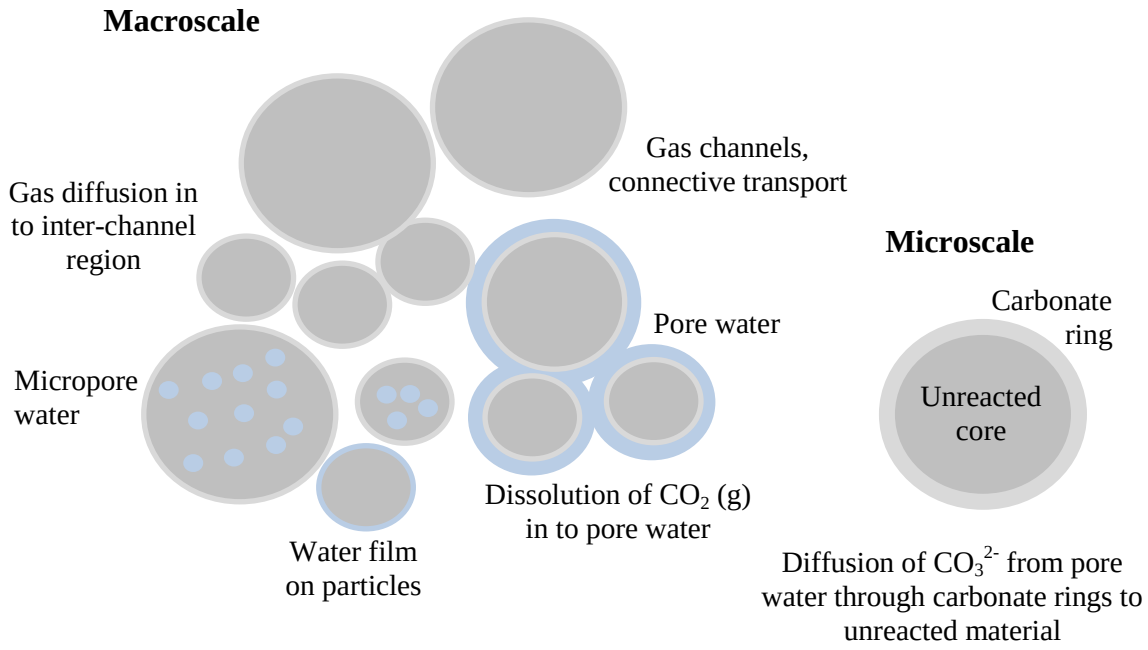

Figure 3.1 - Huntzinger (2006 (PhD thesis)) Microscale to macroscale processes

3.1.2 Silicate weathering: mechanism and rates

The rates and mechanisms of silicate mineral weathering are well studied, due to their importance in understanding the Earth surface system. Studying the behaviour of silicate minerals has enabled a deeper understanding of the global environment due to their wide influence over weathering processes, soil formation, plant nutrition and global biogeochemical cycles. They are also some of the most abundant and widely used materials in human activity.

Weathering as a physical and chemical process has been proposed since the very early days of geology as a science in the mid 19th century. Chemical weathering is recognised as a result of the change in thermodynamic conditions between mineral formation conditions and the ambient environment at the Earth's surface (White and Brantley, 1995). Theories of the mechanisms by which minerals weather have evolved a great deal, however as early as 1833 (Fournet, 1833) it was proposed that this could be linked to the action of 'water containing carbonic acid'. This idea was extended throughout the 19th Century, adding the potential action of organic acids and other environmental factors to the theory. The first controlled weathering experiments were carried out in 1848 (Rodgers and Rodgers, 1848) providing some of the first evidence of mineral weathering rates (White and Brantley, 1995).

Throughout the 20th century, theories of weathering processes have been expanded and refined to include knowledge of the macro and micro-scale processes at work in weathering environments. Advances in analytical techniques, surface chemistry and physics and kinetic theory have allowed a greater understanding of how processes at different scales contribute to the overall observed geochemical behaviour of weathering materials. Interactions with biology, hydrology and climate have also been clarified and emphasised (Berner et al., 2001). By the late 19th Century (White and Brantley, 1995 and references therein) the potential contribution of chemical weathering to the global carbon cycle and effects on global temperature was well recognised.

The mechanisms behind silicate weathering from a chemical perspective are well understood, recognising that a number of sequential mechanisms contribute to the overall weathering process. Chemical weathering of silicates takes place through hydrolysis of surface species. Activity at the mineral surface is critical to the weathering process, with studies (Gerard et al., 2003) claiming that surface-mediated dissolution

strongly affects weathering under laboratory conditions. Field-scale weathering appears to be subject to other rate-limiting properties, which will be discussed further in the following sections. Some studies (Nugent et al, 1998; White et al, 1996) have questioned whether observed rate differences are due to a lack of ability to characterise the complexity of the dissolution mechanisms operating in natural systems, or whether the basic dissolution mechanisms differ fundamentally between field and laboratory.

Under laboratory conditions it can be seen that over certain ranges pH strongly influences weathering rates (Palandri and Kharaka, 2004). At pH 5 and below, silicate dissolution is strongly linked to pH which is interpreted as the observed result of proton-promoted dissolution, as the mineral surface becomes highly protonated with increasing concentration of H^+. Above pH ~5 the weathering rate is almost independent of pH (Brady and Walther, 1989). At high pH, dissolution rate increases for Al-bearing minerals as seen in the dissolution rate for albite in Figure 3.2. The molecular weight of the acids present in reacting solutions can influence the weathering rate in either direction (Drever and Stillings, 1997; Renforth et al., 2011b). Presence of dissolved organic carbon is able to promote dissolution under acidic conditions.

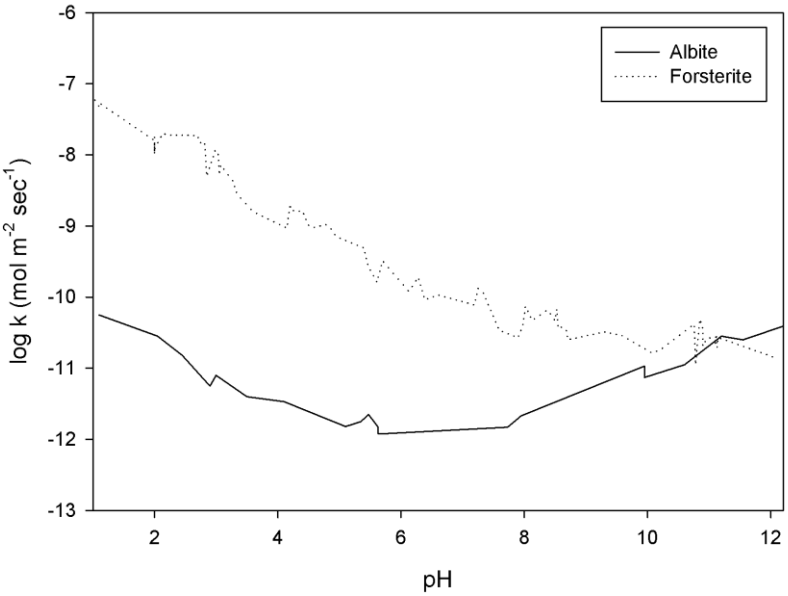

Figure 3.2 –Dissolution rate vs pH for selected silicate minerals: Albite ($NaAlSi_3O_8$ Amelia albite (Chou and Wollast 1985)) and Forsterite ($Mg_2(SiO_4)$ natural forsterite fo91 (Pokrovsky and Schott 2000, Oelkers 2001))

Mineral surfaces change over time, influencing weathering rates by affecting the available reactive surface through the formation of secondary mineral coatings or leached layers (Figure 3.3). This is likely to be one of the factors which causes disparities between laboratory and field-scale weathering rates.

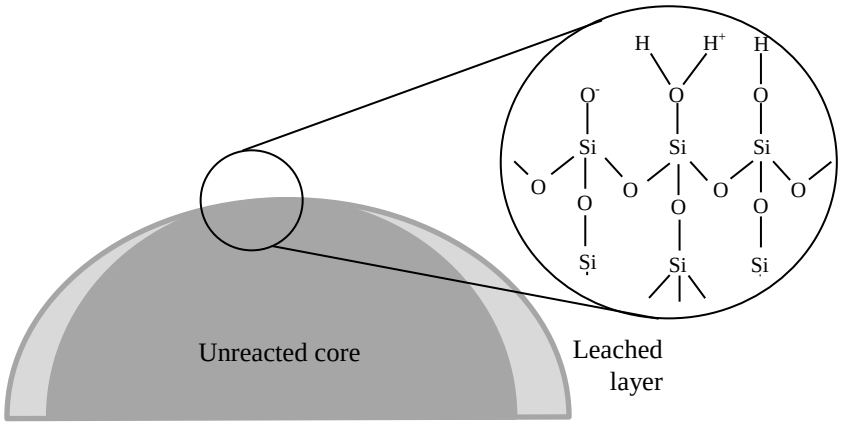

Figure 3.3 – Schematic of the surface mechanisms controlling silicate weathering – a quartz surface (SiO_4) showing adsorbed hydroxyl groups and protons (Brady and Walther, 1989)

The Goldich series (Figure 3.4) remains one of the most concise empirically-derived frameworks for defining the relative reactivity of silicate minerals. In this scheme, minerals forming at higher temperature and pressure are less stable and more readily weathered, dependent on physical and chemical properties described in the preceding section. The magnitude of the difference between the T/P conditions under which minerals were formed and the ones to which they are exposed determines their relative stability or instability – the larger the difference, the larger the instability. Composition also plays a vital role, with sodium-rich plagioclase feldspars weathering more slowly than calcium-rich feldspars. There are, however a number of exceptions to this scheme, discussed by Curtis (1979), which limits its application.

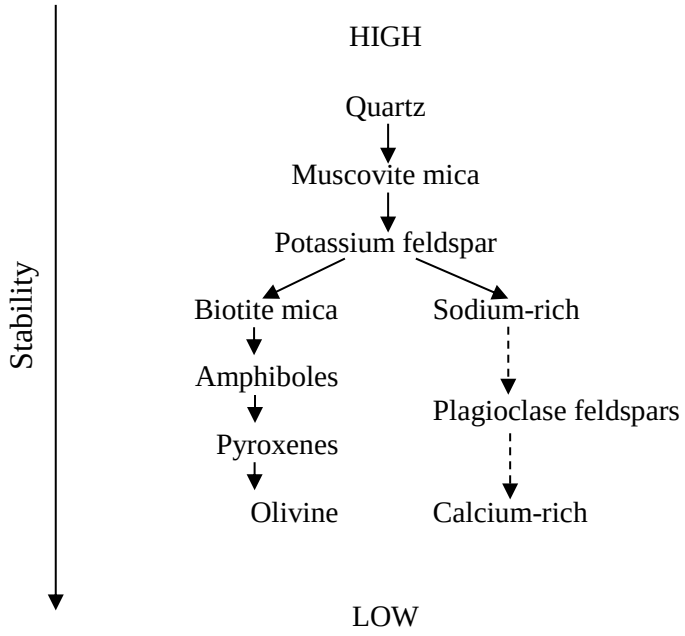

Figure 3.4 – Goldich stability series (simplified) (Goldich 1938)

The rate at which minerals carbonate can be empirically and theoretically linked to parameters such as the 'free energy of reaction' (ΔG_r) of a given reaction (Lasaga, 1994), a thermodynamic quantity that is related to equilibrium. Table 3.2 (Renforth et al, 2011c) illustrates the associated free energy changes of carbonation reactions in a variety of minerals. The majority of widely occurring calcium silicate minerals (and portlandite) are predicted to undergo carbonation reactions under ambient conditions (Renforth et al, 2011c).

Reaction kinetics which determine the rate at which a reaction approaches equilibrium are also important in this context, and the rate of reaction for a number of silicate minerals weathering under controlled conditions is presented in the following sections. Table 3.1 illustrates example rates for four selected silicate minerals under different pH and weathering conditions Together these factors help to determine the nature of a reaction occurring under given conditions.

Table 3.1 - Weathering rates of selected silicate minerals reported from laboratory-based weathering experiments at STP using data from White et al. 2003

Mineral	**Rate, log R (mol m^{-2} s^{-1})**	**Log (years)**	**pH**	**Weathering environment**	**Reference**
Albite	-12.1	-0.86	5	Flow-through reactor	Knauss and Wolery, 1988
Albite	-11.9	-1.74	5.6	Fluidized bed reactor	Chou and Wollast, 1984
Albite	-12.5	-2	5.6	Flow-through reactor	Hamilton et al., 2000
Albite	-11.3	-0.64	6	Flow-through reactor	Holdren and Speyer, 1987
Albite	-11.3	-1.86	6	Fluidized bed reactor	Welch and Ullman, 1996
Bytownite	-10.6	-1.29	6.1	Fluidized bed reactor, fresh mineral	Welch and Ullman, 1993
Labradorite	-10.7	-0.24	3.2	Fluidized bed reactor	Taylor et al., 2000a
Labradorite	-11.3	-0.68	4	Batch reactor	Siegal and Pfannkuch, 1984
Labradorite	-11.6	-0.32	5	Flow-through cell	van Hees et al., 2002
Oligoclase	-11.4	-0.86	5	Fluidized bed reactor	Mast and Drever, 1987
Oligoclase	-11.6	-0.86	5	Batch reactor	Busenberg and Clemency, 1976
Oligoclase	-12	-0.69	5	Fluidized bed reactor	Oxburgh et al., 1994

Table 3.2 - Carbonation reactions and their associated free energy changes (ΔG_r) at STP, including products stable in the weathering environment, overall and expressed normalized to the number of moles of carbonate mineral product. Using data from [Lothenbach et al 2008, Robie and Hemingway 1995].[1]

Mineral/ material	Formula	Occurrence	ΔG_f, kJ/mol	Carbonation reaction	ΔG_r, kJ/mol	ΔG_r, kJ/mol carbonate
Portlandite	$Ca(OH)_2$	Portland cement	-898.0	$Ca(OH)_2 + H_2CO_3 = CaCO_3 + 2H_2O$	-81.50	-81.50
Larnite	Ca_2SiO_4	Cement clinker	-2191.2	$Ca_2SiO_4 + 2H_2CO_3 = 2CaCO_3 + H_4SiO_4$	-127.20	-63.60
Anorthite	$CaAl_2Si_2O_8$	Basic rocks	-4007.9	$CaAl_2Si_2O_8 + H_2CO_3 + H_2O = CaCO_3 + Al_2Si_2(OH)_4$	-57.80	-57.80
Jennite	$Ca_9Si_6O_{16}(OH)_2.6H_2O$	Hydrated cement	-2480.8	$Ca_{1.67}SiO_{1.57}(OH)_{4.2} + 1.67H_2CO_3 = 1.67CaCO_3 + H_4SiO_4 + 1.77H_2O$	-90.51	-54.20
Rankinite	$Ca_3Si_2O_7$	Cement clinker/slag	-3748.1	$Ca_3Si_2O_7 + 3H_2CO_3 + H_2O = 3CaCO_3 + 2H_4SiO_4$	-146.30	-48.77
Akermanite	$Ca_2MgSi_2O_7$	Slag	-3667.5	$Ca_2MgSi_2O_7 + 3H_2CO_3 + H_2O = 2CaCO_3 + MgCO_3 + 2H_4SiO_4$	-127.90	-42.63
Forsterite	Mg_2SiO_4	Basic rocks; slag	-2053.6	$Mg_2SiO_4 + 2H_2CO_3 = 2MgCO_3 + H_4SiO_4$	-66.80	-33.40
Wollastonite	$CaSiO_3$	Metamorphic rocks	-1549.0	$CaSiO_3 + H_2CO_3 + H_2O = CaCO_3 + H_4SiO_4$	-27.00	-27.00
Tobermorite	$Ca_5Si_6O_{16}(OH)_2.4H_2O$	Metamorphic rocks	-1744.4	$Ca_{0.83}SiO_{1.53}(OH)_{2.6} + 0.83H_2CO_3 = 0.83CaCO_3 + H_4SiO_4 + 0.13H_2O$	-13.66	-16.46
Diopside	$CaMgSi_2O_6$	Basic rocks	-3026.8	$CaMgSi_2O_6 + 2H_2CO_3 + 2H_2O = CaCO_3 + MgCO_3 + 2H_4SiO_4$	-26.20	-13.10
Chrysotile	$Mg_3Si_2O_5(OH)_4$	Metamorphic rocks	-4032.4	$Mg_3Si_2O_5(OH)_4 + 3H_2CO_3 = 3MgCO_3 + 2H_4SiO_4 + H_2O$	-39.20	-13.07
Tremolite	$Ca_2Mg_5Si_8O_{22}(OH)_2$	Metamorphic rocks	-11574.6	$Ca_2Mg_5Si_8O_{22}(OH)_2 + 7H_2CO_3 + 8H_2O = 2CaCO_3 + 5MgCO_3 + 8H_4SiO_4$	-33.10	-4.73
Enstatite	$MgSiO_3$	Basic rocks	-1458.3	$MgSiO_3 + H_2CO_3 + H_2O = MgCO_3 + H_4SiO_4$	0.14	0.14
Laumontite	$CaAl_2Si_4O_{12}.4H_2O$	Metamorphic rocks	-6772.0	$CaAl_2Si_4O_{12}.4H_2O + H_2CO_3 + H_2O = CaCO_3 + Al_2Si_2(OH)_4 + 2H_4SiO_4$	90.70	90.70
Water	H_2O		-237.1			
Kaolinite	$Al_2Si_2(OH)_4$		-3797.5			
Calcite	$CaCO_3$		-1128.5			
Magnesite	$MgCO_3$		-1029.5			
$(carbonate)_{aq}$	H_2CO_3		-623.2			
$(silica)_{aq}$	H_4SiO_4		-1307.8			

[1] *NB: reactions for jennite and tobermorite use mineral formulae corresponding to those cited in [Lothenbach et al 2008], the source of the data for ΔG_f. Formulae and values for ΔG_f for other reactants, including dissolved carbonic acid, and products, including dissolved silica, are also given. For internal consistency, all thermodynamic data except ΔG_f for jennite and tobermorite, are from [Robie and Hemingway 1995].*

3.2 Laboratory weathering (batch weathering experiments and pH stat experiments)

A suite of laboratory weathering experiments was carried out to determine whether the materials of interest in this study (with a focus on construction and demolition waste and steel slag) behaved in the way predicted by single-mineral experiments and large-scale data from the academic literature. In the first instance batches of material were allowed to weather under a variety of conditions to elucidate their comparative weathering rates. In the second case a number of experiments were carried out on wollastonite in a batch reactor where pH could be continuously buffered (pH stat), to determine the rate of dissolution of this this material and assess whether it could act as an analogue for a understanding more complex silicate dissolution in field settings. Existing data for wollastonite dissolution under conditions close to the natural environment was scarce.

3.2.1 Batch experiments

Batch experiments were carried out on a selection of natural and artificial silicate minerals, in order to compare their behaviour in a simple weathering system over short time periods. This work was carried out in order to allow direct comparisons to be made between the materials under controlled conditions.

Method

Materials used:

- Dolerite (from Great Whin Sill at Barrasford Quarry, supplied by Lafarge Tarmac)
- Crushed concrete (from Trinity Square, Gateshead, supplied by Thompsons of Prudhoe)
- Steel slag (from Tata Steel, Scunthorpe)
- Wollastonite (commercial ‘Wollastonite 90’, supplied via MIRO; 90% wollastonite)

All materials were air dried and crushed on receipt using a Tema laboratory disc mill, then sieved to <63μm or <2mm (2mm – 1.18mm) respectively (as noted in Table 3.3). Samples were then dried overnight, or to constant mass in an oven at 80°C and stored in airtight containers.

The experimental matrices, detailing the separate treatments given to the materials can be seen in Appendix B. A summary is included in Table 3.4.

Table 3.3 – Material characteristics including BET Data (surface characterisation) and carbonate content

Material	**Particle size**	**SA (m^2 g^{-1})**	**$CaCO_3$ (initial) wt % (±0.19)**
C&D waste	<63µm	8.304	22.73
C&D waste	<2mm	-	12.53
Dolerite	<63µm	4.150	2.67
Steel slag	<63µm	1.862	8.15
Steel slag	<2mm	-	8.92
Wollastonite	<63µm	0.7086	3.71

Table 3.4 – Summary of batch experiment conditions

	Materials	**Particle size**	**Duration**	**Conditions**
Batch 1	Steel slag, C&D waste, Wollastonite, Dolerite	<63µm	144hrs	Deionised water, variation in particle density
Batch 2	Steel slag, C&D waste	<2mm	144hrs	Variation in particle size
Batch 3	Steel slag, C&D waste	<63µm	144hrs	Variation in solution chemistry and particle density
Batch 4	Steel slag, C&D waste	<63µm	144hrs	Agitation by orbital shaker and variation in particle density

Quantity of material varied between batches, with all batches receiving ~2mg (Batch 1, Batch 2) or ~20mg (Batch 3, Batch 4).

Evian water was used in Batch 3 as a means of supplying dissolved inorganic carbon in the form of bicarbonate ions, in order to determine whether the supply of carbonate species was a limiting factor in this system. Commercially reported analysis of the water at source can be seen in Table 3.5. A number of other species, including Ca were also added as a result of using this reagent, which is elaborated on in the discussion section.

Table 3.5 - Evian water composition as used in Batch 3 as a reagent (reported) (pH = 7.2)

Cations	**Conc (mg l^{-1})**	**Anions**	**Conc (mg l^{-1})**
Calcium (Ca^{2+})	80	Bicarbonate (HCO_3^-)	360
Magnesium (Mg^{2+})	26	Sulphate (SO_4^{2-})	12.6
Sodium (Na^+)	6.5	Chloride (Cl^-)	6.8
Potassium (K^+)	1	Nitrate (NO_3^-)	3.7
		-	
		Silica	15

Agitation was applied to Batch 4 using an orbital shaker, running continuously over the period of the experiment.

A small quantity of each material was weighed into a 30ml Sterilin polystyrene / polypropylene sample tube as detailed in Appendix B. At the start of each experimental run 20ml of appropriate reagent fluid was dispensed in to each tube using an adjustable bottle-top dispenser, recording the time at which this occurred. Samples were mixed, sealed and then left to stand at constant temperature (ambient room temperature ~25°C) (with the exception of Batch 4 as described in Table 3.4) for an allotted period of time.

At specified times after the start of the experiment (between 1 and 144 hours) the reaction in each tube was halted by immediate filtering of a 10ml portion through a 0.2μm PTFE syringe filter. Fluid samples were immediately acidified to <pH 3 with nitric acid (Analar reagent grade) and refrigerated prior to chemical analysis.

All samples were analysed for calcium content using AAS (Atomic Absorption Spectrometry) (method in Appendix A). Prior to analysis 5ml of each sample was decanted into a fresh 30ml Sterilin tube and spiked with 0.5ml 1% lanthanum chloride. Samples were analysed using a Varian SpectrAA 400 with reproducibility 0.04 ± mg l^{-1} (including dilution factor).

Any samples exceeding the detection limits of the apparatus for Ca (~25 mg l^{-1}) were diluted by a factor of 5. 1ml of sample diluted in 30ml Sterilin tubes with 3.5ml deionised water, spiked with 0.5ml 1% lanthanum chloride and analysed as before.

Results

Figure 3.5 illustrates the quantity of Ca present in solution after cumulative reaction time (in seconds) as detected by AAS, normalised to the initial mass of sample. Figures 3.5a and b compile the data from all of the experiments run, with additional figures in Appendix B showing batches 2, 3 and 4 on separate plots for improved clarity.

From this figure is can be seen that there was a large degree of variation in Ca concentration produced by the different materials as the experiment progressed. The highest values of Ca were seen in the batch with the highest starting concentration of material; however between the remaining samples, where initial concentration was

similar, variation still persists. This is partially due to variation in the surface area of the materials which can have a significant effect on the rate at which the material weathers (as discussed in section 3.1 of this chapter).

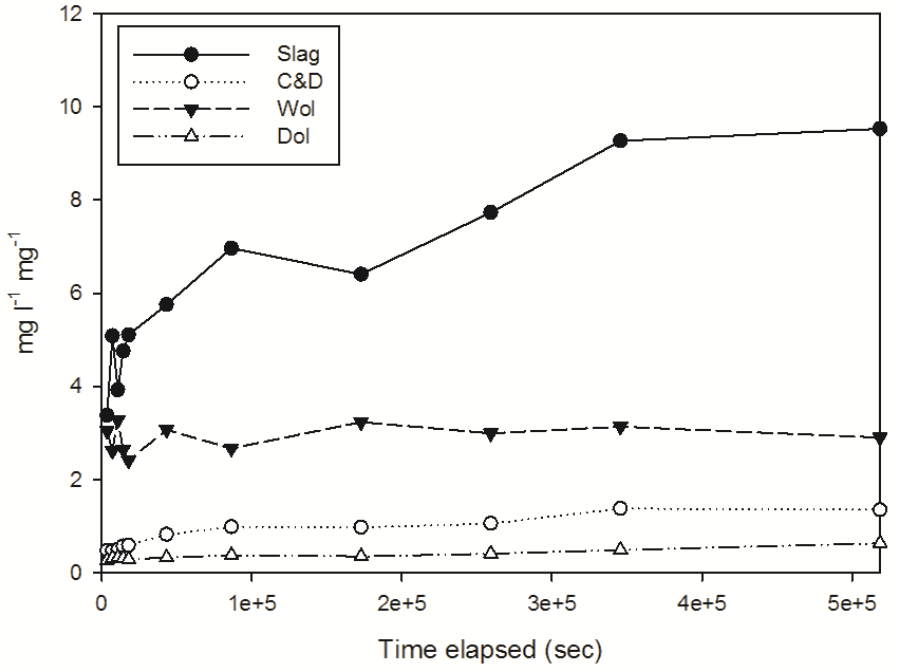

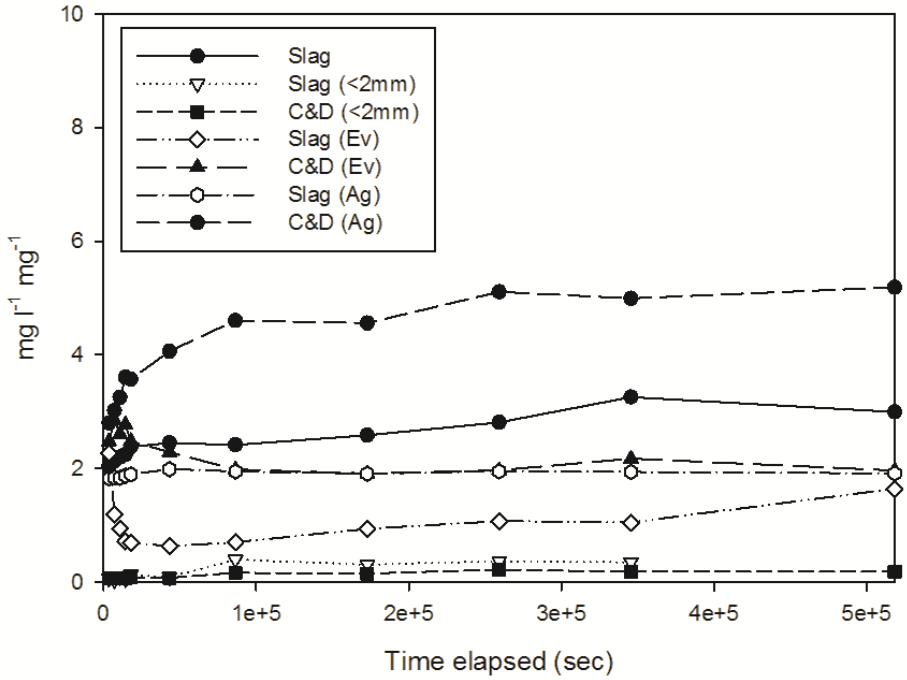

Figures 3.5a and b – Calcium leached from solids at given times. Starting mass of sample ~2mg in 5a and ~20mg in 5b (raw data from AAS) In 5b, Slag = 0.63um in deionised water (<2mm) = particle size 1.18-2mm, (Ev) = with Evian water, (Ag) = with agitation. Analytical error bars are within diameter of point.

Figures 3.6 – 3.8 show the calculated rate at which Ca is being leached from the weathering material (Velbel 1993; Siegel and Pfannkuch 1984), assuming that all Ca in solution is derived from weathering, normalised by mass and surface area (using data from Table 3.3 and Appendix B). These curves show distinct variation in weathering rates between the different materials, and between the different conditions applied, per unit area. Rates at each time point are calculated using Equation 3.1.

Equation 3.1 (adapted from White et al 2003):

$$R = \frac{Q}{St}$$

Where R (mol Ca m^{-2} s^{-1}) is the weathering rate of a silicate mineral with respect to Ca, where Q (mol) is the moles of Ca in solution, S (m^2) is the surface area and t (s) is time elapsed in seconds. Cumulative rates of Ca leaching are plotted in Figures 3.6 - 3.10. 'Cumulative' here refers to the average value of Ca in solution at each sampled time step.

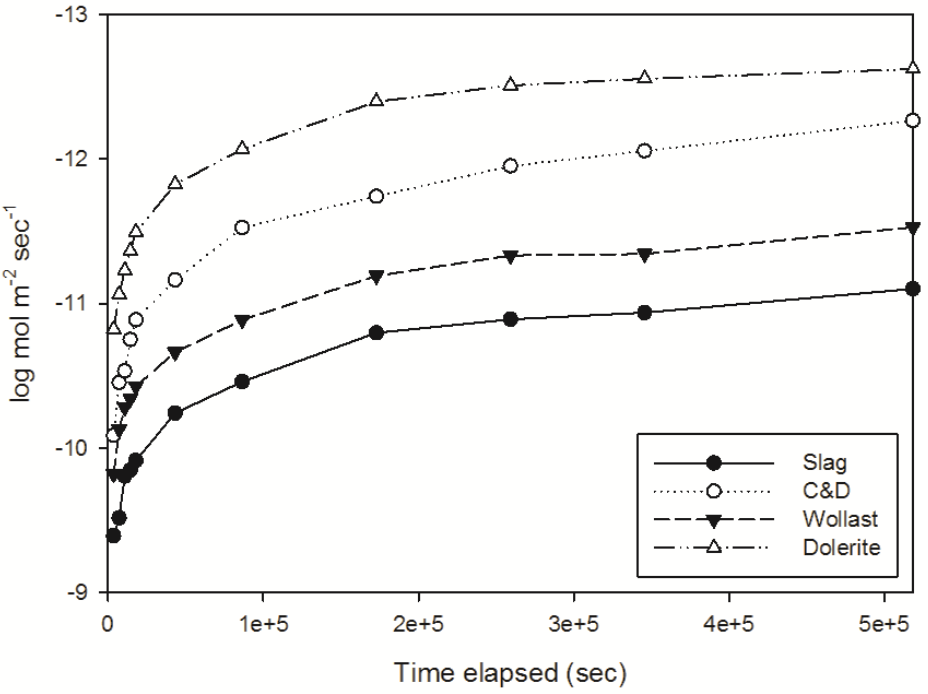

Figure 3.6 – Batch 1 rate of Ca leaching in to solution, normalised to mass and surface area when dissolved in deionised water. Starting mass of sample ~2mg. Analytical error bars are within diameter of point.

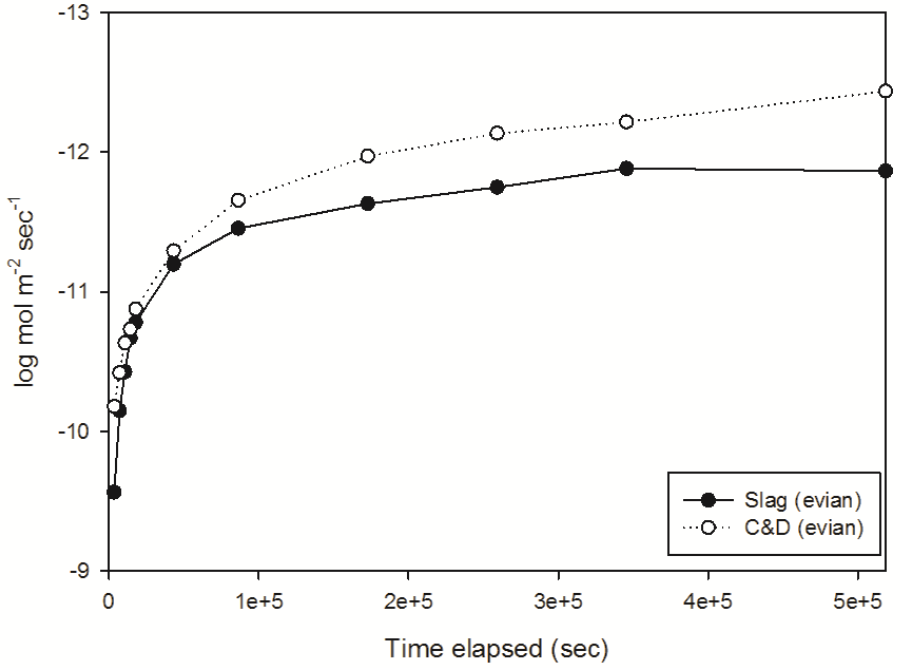

Figure 3.7 – Batch 3 rate of Ca leaching in to solution, normalised to mass and surface area when treated with Evian water (as a source of carbonate). Starting mass of sample ~20mg. Analytical error bars are within diameter of point.

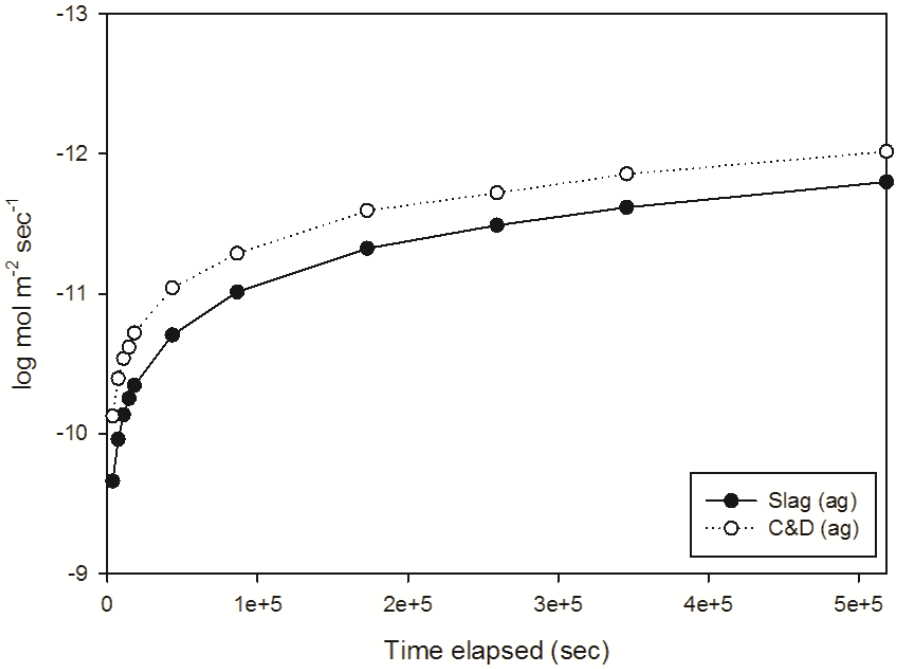

Figure 3.8 - Batch 4 rate of Ca leaching in to solution, normalised to mass and surface area when treated by constant agitation on an orbital shaker. Starting mass of sample ~20mg. Analytical error bars are within diameter of point.

Figures 3.9 and 3.10 illustrate the variation in weathering rate for steel slag and C&D waste respectively, where the conditions, other than those noted in Table 3.4, remain

constant. They represent the effects that changes in solution chemistry (addition of bicarbonate) and agitation have on the rate of Ca leaching.

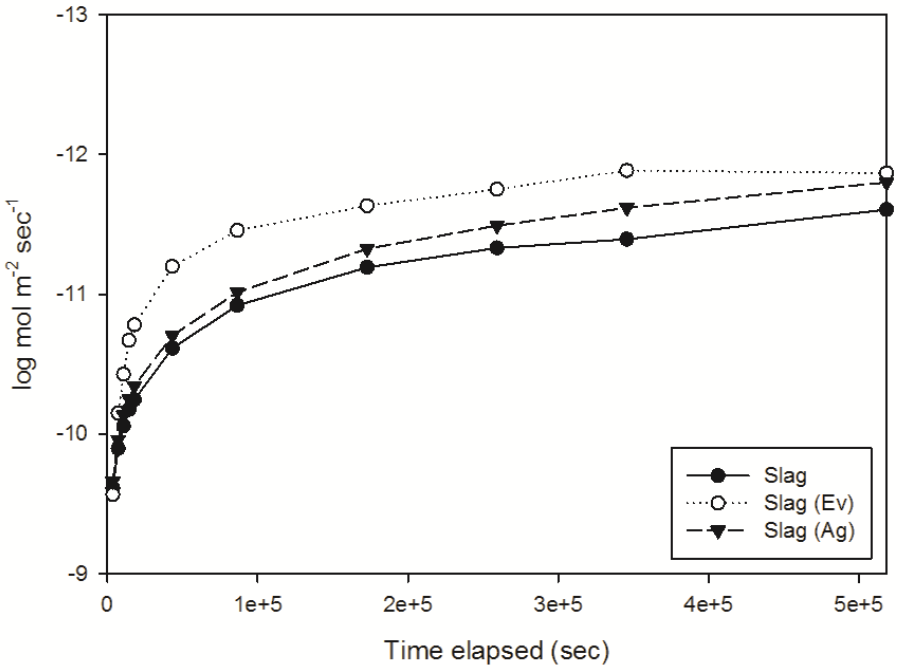

Figure 3.9 –Rate of Ca leaching from steel slag in to solution under different conditions, normalised to mass and surface area. (Ev) = with Evian water, (Ag) = with agitation. Starting mass of sample ~20mg. Analytical error bars are within diameter of point.

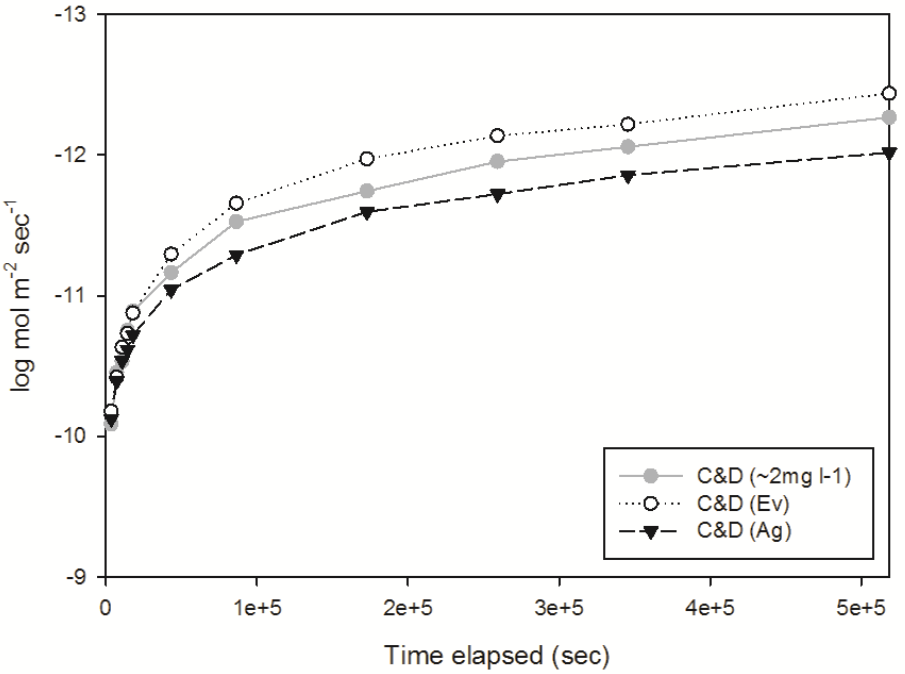

Figure 3.10 - Rate of Ca leaching from C&D waste in to solution under different conditions, normalised to mass and surface area. (Ev) = with Evian water, (Ag) = with agitation. Starting mass of sample ~20mg. Analytical error bars are within diameter of point.

From Figures 3.6-3.10 it can be seen that in the case of steel slag, agitation and variation in solution chemistry (bicarbonate) led to a decreased rate of leaching when compared to the baseline value in deionised water. An experiment run with a lower initial concentration of solids in deionised water produced a more rapid apparent weathering rate than the baseline shown in Figure 3.9; this may be due in part to the formation and precipitation of solid calcium carbonate removing Ca from solution at higher concentration (discussed in the following section). This may be supported by data showing the addition of bicarbonate most strongly retarded the apparent rate of dissolution of Ca in to solution, especially at early stages of the reaction. This may also be linked to the CO_2 dynamics in this small, closed system where CO_2(g) may be depleted over the period of the experiment.

For C&D waste agitation produced a more rapid leaching rate than the addition of bicarbonate. C&D waste at ambient conditions, with low initial sample mass, provides an intermediate weathering rate. Further data is unavailable, but it is assumed that, as in the case of steel slag, at high initial concentration a reduced rate of leaching may also have been observed for C&D waste.

Table 3.6 – Weathering rates determined in this section

	Weathering rate (log mol Ca m^{-2} sec^{-1})	**Estimation method**
Steel slag	-9.39 to -11.88	Leaching of Ca
C&D waste	-10.10 to -12.40	Leaching of Ca
Wollastonite	-9.82 to -11.53	Leaching of Ca
Dolerite	-10.82 to -12.62	Leaching of Ca

A summary of the rate data calculated using Equation 3.1 is shown in Table 3.6. It should be noted that the rates reported here are 'apparent' leaching rates – derived only from the quantity of Ca in solution. The presence of Ca in solution is a good indicator of leaching, but does not take in to account the possibility that Ca has been dissolved preferentially. It also does not account for Ca added to the batches in other forms, which is particularly likely to be the case with B3 samples, where bicarbonate was intentionally added in the leaching solution with a number of other chemical species.

Discussion

Figure 3.11 illustrates a number of weathering rates determined in the batch experiments (Ca weathering rates) compared with those reported in the literature. The

reported values are all for single-mineral weathering experiments, and although some of the batch materials were mixtures or composites, they remain comparable. A range of weathering rates is indicated for each material, representing the rates calculated across the range of different conditions the batches were subjected to. It should be noted that precipitation of solids could not be quantified in the experiments conducted. The formation and precipitation of solid calcium carbonate, and its possible removal during the filtering stage of sample preparation, would lead to an underestimation of rates due to the reduction of Ca in solution.

All of the materials tested exhibit apparent weathering rates which correlate well with those determined for other silicates (Figure 3.11). Steel slag and wollastonite weather particularly rapidly, with C&D waste and dolerite exhibiting slightly slower values across all tested parameters. In all cases it is assumed that initial composition was homogenous throughout a sample, and although efforts were made to ensure that all samples were homogenised some variation is likely to remain.

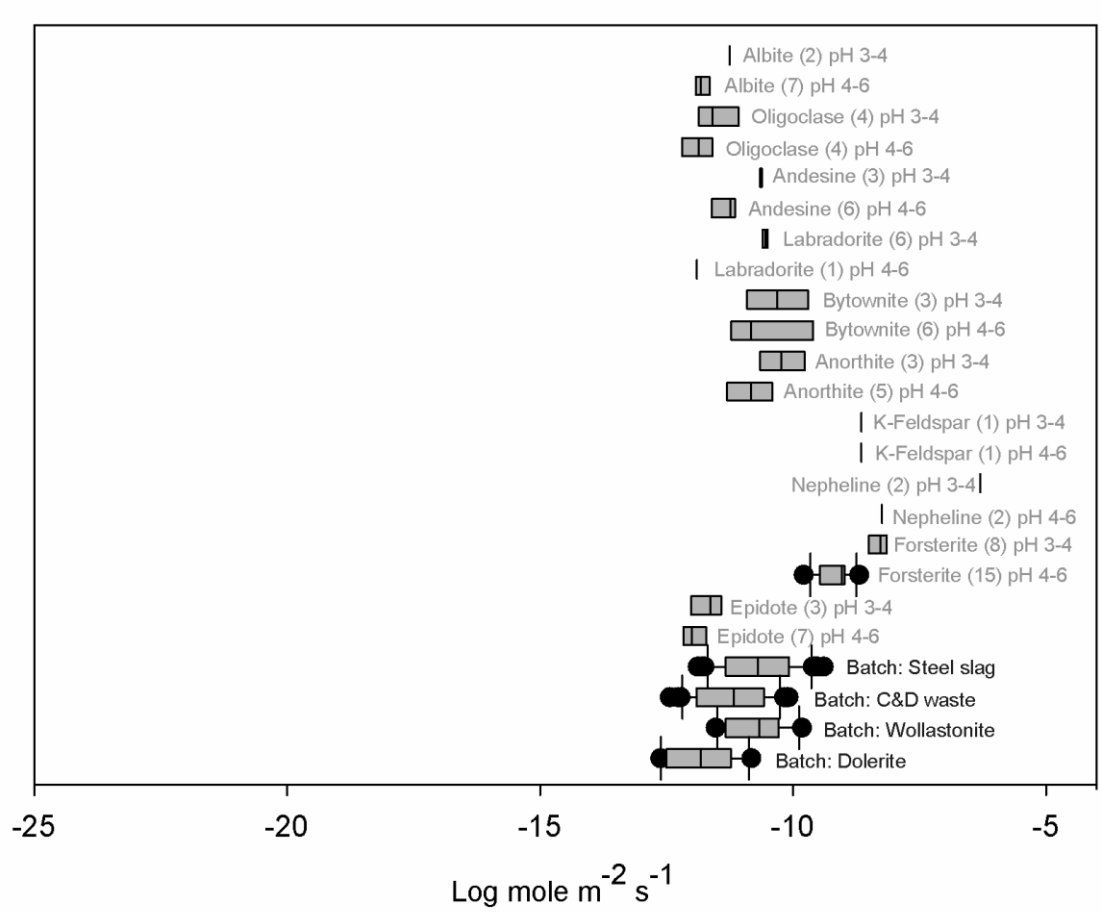

Figure 3.11 –Relative rate of weathering of various silicate materials and batch experiment data, presented in as values inferred from Ca leaching rate, adapted from Hartmann et al, 2013)

Analysis of the samples treated with Evian water illustrates the possible limitations of using Ca in solution as a weathering proxy. Reported analysis of the water assumes a starting concentration for Ca of 80mg l^{-1}, however the analysed batch samples show much lower concentrations between 60.6 and 13.3 mg l^{-1}. This highlights the potential for removal of Ca into minerals which are filtered out during preparation and not detected by AAS analysis. This is supported by the values of Ca which begin high, rapidly drop for the first 1-5 hours, most notably in the batch with steel slag, before increasing over the remaining experimental period showing that Ca is being removed from solution, before continuing to leach. This may be due to the depletion of Ca from surface layers.

Agitation appeared to have little effect on the observed leaching rate of the materials. In the case of steel slag the rate of Ca leaching decreased, but in the case of C&D waste it increased. Agitation has the potential to increase the rate of leaching by avoiding the formation of localised regions of saturation, and may influence the manner in which coatings of secondary minerals form on particle surfaces.

The overall rate of Ca weathering, determined using Equation 3.1, decreases with time in all batches, which may be due to proximity to equilibrium of species in solution (especially as gas diffusion to the batches is limited by carrying out the reaction in sealed containers), formation of solids which may limit the rate of leaching if deposited on mineral surfaces (as in Figures 3.1 and 3.5) and relative depletion of Ca in the solid phase.

Summary

- Variation in the rate of Ca leaching from a selection of natural and artificial silicates can be observed at standard temperature and pressure over 144 hours
- Steel slag exhibited high rates of leaching, up to -9.39 log mol Ca m^{-2} sec^{-1}
- Wollastonite exhibited rates of leaching, up to -9.82 log mol Ca m^{-2} sec^{-1}
- Construction and Demolition waste exhibited rates of leaching, up to -10.10 log mol Ca m^{-2} sec^{-1}
- Dolerite exhibited rates of leaching, up to -10.82 log mol Ca m^{-2} sec^{-1}
- Observed rates of Ca leaching are in agreement with reported rates for silicate mineral dissolution under laboratory conditions

3.2.2 pH-stat experiments

Batch experiments were carried out using wollastonite ($CaSiO_3$), as an example of a simple calcium silicate mineral, to determine whether the weathering rates under a variety of pH conditions compared to those from the peer-reviewed literature. Wollastonite weathering and dissolution has been well-studied, but many of the conditions reported within the literature are inappropriate for direct application to the field-scale weathering of silicates under ambient conditions (i.e. elevated temperature).

This work was carried out using a Radiometer Analytical Potentiometric Titration Workstation (856) in auto-titration mode, which allowed the pH of experimental solutions to be kept at constant pH for long time-periods, to a high degree of accuracy (up to ±0.001 pH units), in order to determine critical parameters for the weathering rate.

Method

Materials used:

- Wollastonite (Wollastonite 90, supplied via MIRO)

Preparation of the material was as described in section 3.2.1 Properties of the material used were as reported in Table 3.3.

Thermo-gravimetric analysis was carried out using a Netzsch Jupiter STA449C TG-DSC system connected to a Netzsch Aeolos 403C QMS for the mass spectral analysis of evolved gas (method as described in Appendix A) in order to determine the composition of the material and assess the presence of any hydrated phases. As seen in Figure 3.12, this analysis determined the presence of a small quantity of carbonate indicated by mass change around 650-700°C (corroborated by the evolution of CO_2 gas at the same point, as measured by Quadrupole Mass Spectrometer (QMS)). The QMS trace for H_2O (not shown) does not suggest the presence of loosely bound water or hydrated phases.

Two short trials were carried out in order to determine the parameters of the apparatus used. The four data-producing trials reported below summarise the final data sets attained for the weathering of wollastonite at pH 3, 5 and ~8. These pH values were selected to reflect the likely pH range in a number of realistic environmental settings,

and also allow direct comparison with conditions reported by previous studies. pH~8 reflects the 'native' pH of the weathering material, when allowed to react with deionised water without intentional pH manipulation or buffering.

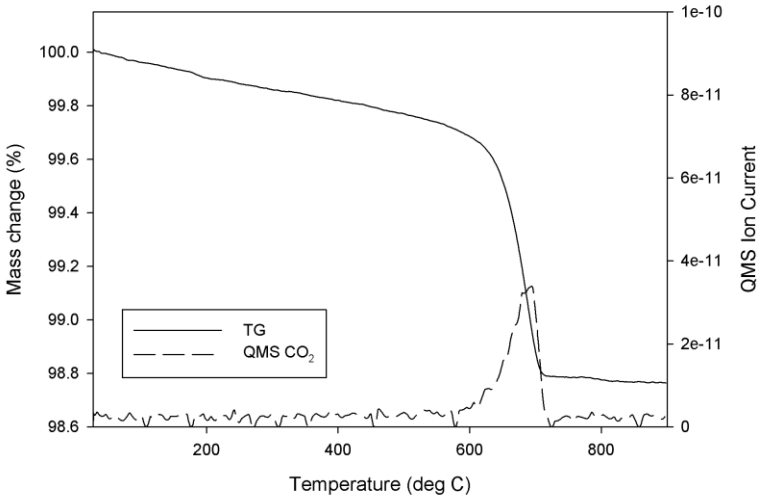

Figure 3.12 – TG / QMS data for Wollastonite 90

Reaction solutions were made up to pH 3 and pH 5 using deionised water and Analar reagent grade hydrochloric acid. The reaction solution for ~pH 8 used only deionised water, allowing pH within the system to self-regulate on addition of solid reagents. During the experiments pH was maintained at pH 3 (±0.27), pH 5 (±0.87), pH 8 (unregulated) (±0.60).

Approximately 0.15 to 1.5g wollastonite was added to a 1.5 l glass reactor vessel, as noted in Appendix B, with adapted glass cap to allow easy mounting of pH stat titration apparatus to permit constant monitoring and adjustment of pH. 1 l of reaction solution was added and electronic titration apparatus started. Solutions were stirred throughout using magnetic bar-stirrers. All experimental runs were carried out at a constant temperature of 25°C, moderated by the use of a water bath. All experiments were allowed to run for between 7 and 48 hours. All experiments were carried out in at atmospheric pressure, with gases allowed to diffuse freely through the reactor vessel cap.

Aliquots of 5ml of solution were taken at time intervals throughout the experiment (as recorded in Appendix B), and immediately filtered through a 0.2μm PTFE syringe filter. Samples were immediately acidified to <pH 3 with nitric acid (Analar reagent grade) and refrigerated prior to chemical analysis.

All samples were analysed for calcium content using AAS (Atomic Absorption Spectrometry) to identify the presence of Ca in solution. Prior to analysis 1ml of each sample was decanted in to fresh 30ml Sterilin tubes, diluted 10 x with deionised water and spiked with 0.1ml 10% lanthanum chloride. Samples were analysed using a Varian SpectrAA 400 with reproducibility 0.15 ± mg l^{-1} (including dilution factor).

Results

Figures 3.13 and 3.14 show the measured concentration of Ca in solution over time for each pH regime tested, and the dissolution rate for wollastonite (based on Ca) that this is likely to represent assuming the leaching of Ca as a weathering proxy. As in section 3.2.1 the weathering rate has been derived from the Ca concentration in solution normalised to initial mass and surface area (Table 3.2) of the sample.

Figure 3.13 illustrates a number of pertinent observations; most notably that calcium concentration in solution at any given time is progressively higher at lower pH values. Where initial mass is increased by 10 times, the concentration of Ca in solution increases by a factor of approximately 10 (observed in this case only over short timescales).

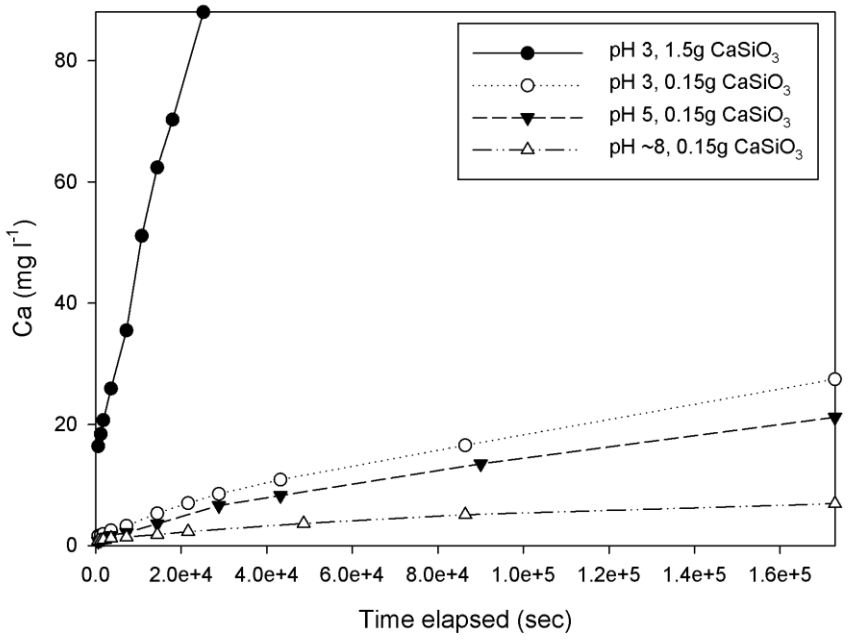

Figure 3.13 – Calcium in solution over time as detected by AAS, starting conditions for each experiment are summarised in legend (error bars for analysis are within diameter of point)

Figure 3.14 shows the predicted weathering rates with respect to Ca leaching, calculated using Equation 3.1. The highest weathering log rate -6.19 mol Ca m^{-2} sec^{-1} was recorded

after 600 seconds of weathering at pH 3. The slowest log rate -8.03 mol Ca m^{-2} sec^{-1} was recorded after 172800 seconds of weathering at pH 8. These findings are summarised in Table 3.7. Figure 3.14 illustrates that the observed leaching rate of Ca occurs at approximately the same rate at pH 3 at different starting quantities which illustrates that both starting masses represent a concentration of Ca far below the level at which a number of kinetic or chemical factors become limiting (i.e. the solution is far from equilibrium). It confirms that the fastest rates of leaching occur at pH 3, with a progressive decrease at higher pH values.

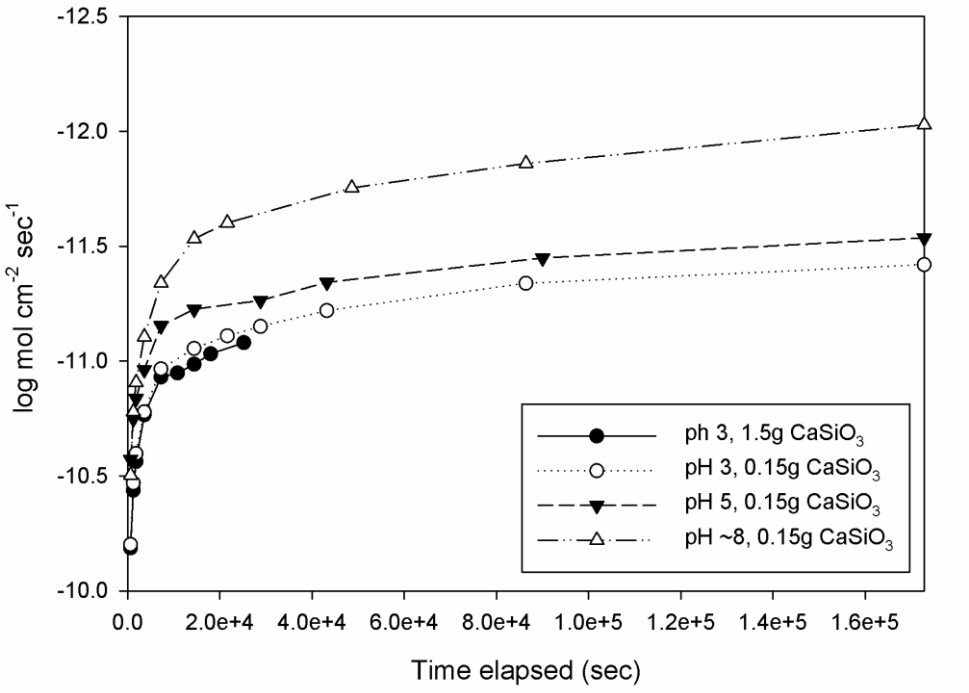

Figure 3.14 – Weathering rate determined using Ca in solution over time as detected by AAS as a proxy for mineral weathering

Table 3.7 – Weathering rates determined in this section

Initial mass	**pH**	**Weathering rate (log mol Ca m^{-2} sec^{-1})**	**Estimation method**
1.5g	3	-6.2 to -7.1	Leaching of Ca
0.15g	3	-6.2 to -7.4	Leaching of Ca
0.15g	5	-6.6 to -7.5	Leaching of Ca
0.15g	8	-6.5 to -8.0	Leaching of Ca

Mechanism	**Rate constant (log mol m^{-2} sec^{-1})**	**Source**
Acid	-5.37	Murphy and Helgeson (1987; 1989) and Rimstidt and Dove (1986)
Neutral	-8.88	Murphy and Helgeson (1987; 1989) and Rimstidt and Dove (1986)

Discussion

When compared with reported data for weathering of silicate minerals (Table 3.6) (as in the previous section) under a variety of conditions, it can be seen that the weathering rates derived for wollastonite during this set of experiments are all very rapid, as highlighted in Figure 3.15. While higher pH values seem to reduce the overall weathering rate over the time periods observed, all of the experimental data exhibits weathering rates more rapid that those of the natural silicate minerals listed. The range of weathering log rates determined at different pH conditions (-6.19 to -8.08 mol Ca m^{-2} sec^{-1}) are more rapid than the rates observed for almost all of the suite of silicate minerals shown in Figure 3.15.

When considered with the batch experiment data in the preceding section (summarised in Figure 3.11), it can be seen that the rate of weathering (Ca leaching) for wollastonite in the pH stat experiments is significantly faster. This is due in part to the pH conditions, although the sample at pH~8 still shows a faster rate than its close counterparts in the batch experiments. This is likely to be due to a number of other factors including improved diffusion of gases in to the reactor and may be due to variations in stirring rate. The initial concentration of material is similar in the two experiments (0.15-1.50g l^{-1} in pH stat compared to 0.10-1.00g l^{-1}in batches). As agitation was not seen to have a significant effect on weathering rates in the batch weathering experiments, this suggests that it is likely that difference in the weathering rate observed in this case is due to an increased rate of CO_2 exchange with the surroundings.

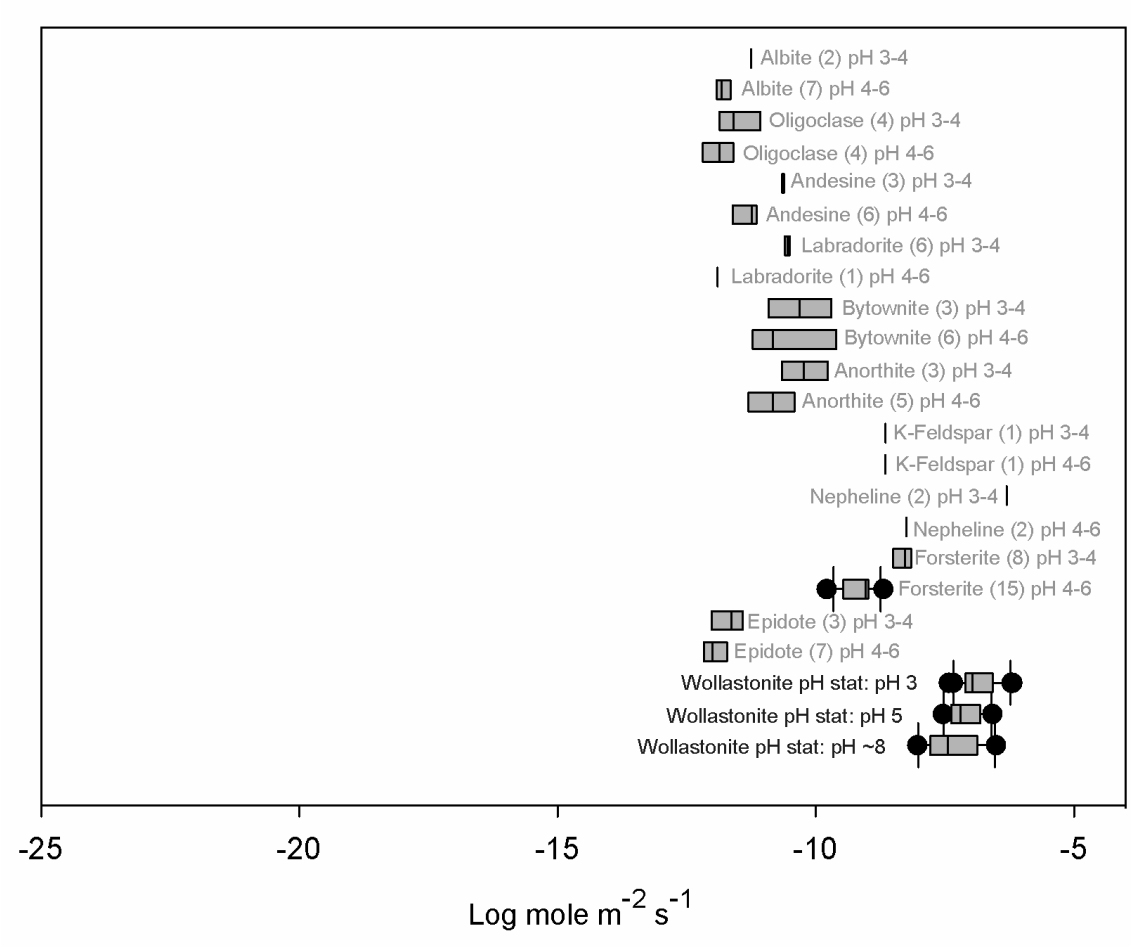

Figure 3.15 –Relative rate of reaction of wollastonite in pH stat experiments in relation to other values, adapted from Hartmann et al, 2013)

Equation 3.1 is useful in quantifying the overall cumulative accumulation of Ca in solution during weathering, but does not provide detailed information regarding other parameters such as the equilibrium conditions. A different approach is applied to experimental data from section 3.2.2 to determine additional weathering parameters. This technique was used by Rimstidt and Barnes (1980) to model a reaction approaching equilibrium concentration (K) over time assuming first order reaction kinetics, as is assumed to be the case in the dissolution of wollastonite under the conditions specified. An 'N' value (the weathering rate, or rate of mass transfer of the dissolving material in to solution) is determined through iterative substitution of values of K (the equilibrium concentration) to attain the highest r^2 value for the straight line fit to the experimental data. The value for -N is taken as the slope of the line of the notation shown overleaf plotted against time for various time-points throughout the experiment. The relationship between parameters determining the dissolution of the material in to solution is defined in Equation 3.2.

Plot of $\left(1-\frac{c}{K}\right) vs. t$ to find slope = -N

Equation 3.2

$$N = ka(K - c)$$

(Where N = rate of dissolution (m s^{-1}), c = observed concentration at time t (mol m^{-3}), K = equilibrium concentration (mol m^{-3}), a = area (m^2) and k = the coefficient of mass transfer of the dissolving material in to solution (m/s))

Full calculations can be seen in Appendix B.19. Table 3.8 shows that this approach highlights the variation in weathering behaviour between the experimental runs carried out at different pH values. As in section 3.2.2, the rate of dissolution is seen to be higher under low pH conditions, reducing as pH increases. The equilibrium concentration at pH 3 is notably higher than that at pH 5 or 8, illustrating a strong pH dependency.

Table 3.8 – Weathering rate values calculated using method described in Rimstidt and Barnes (1980)

Initial mass	**pH**	**Equilibrium concentration (K) (mol m^{-3})**	**Rate of dissolution (N) (s^{-1})**
0.15g	3	1.1 x10^{-3}	0.52 x 10^{-7}
0.15g	5	0.8 x10^{-3}	0.61 x 10^{-7}
0.15g	8	0.2 x10^{-3}	1.08 x 10^{-7}

The pH stat method presented a number of limitations including the duration over which experiments could be run and associated issues with some elements of the pH stat hardware, including malfunction of magnetic stirring bars leading to solution not being equally mixed at some points during the tests. The pH stat method using only a single titre (HCl) was reliable at lower pH, but more difficult to control with a single solution titration when close to acid inflection points causing more significant variation in pH at pH 5.

Summary

- Variation in the rate of Ca leaching from wollastonite can be seen across a range of pH values at standard temperature and pressure
- Between pH 3 and pH 8, over a period of 48 hours, Ca weathers at a rate of -6.2 to -8.0 log mol Ca m^{-2} sec^{-1}
- Observed rates of Ca leaching are more rapid than many reported rates for silicate mineral dissolution under laboratory conditions

3.3 Field-scale weathering (stockpile analysis date from Tata Scunthorpe)

Data from analysis of steel slag solids weathering in stockpiles on an inert waste disposal site in Scunthorpe, UK (described further in Chapter 4) is presented, to illustrate the weathering behaviour of this material at ambient environmental conditions over well-constrained time periods. As all steel slag waste at this site is logged on production and a large amount of information is available relating to its handling and fate, analysis could be carried out with the assurance of known production and approximate emplacement dates for each of the samples.

An experiment was carried out to estimate field scale weathering rates in materials of known age, by way of analysis of basic oxygen steel (BOS) slag from current and historic stockpiles managed by Tarmac Ltd, adjacent to the Yarborough Landfill site, Tata, Scunthorpe. This material had been produced, stockpiled and stored in much the same manner over the time period analysed, therefore the duration of exposure was considered the only significant variable.

Method

Materials:

10 samples of stockpiled slag material (approx. 15kg each) pre-screened to 10-6mm, were supplied by Tarmac, via Tata Steel, received on 27/05/10.

Samples were received bagged, with detailed labels documenting material type, location and production date (-3yrs to contemporary). Sample references were allocated as delivered samples were logged in order to reduce biasing during preparation and analysis (Additional data in Appendix B) as shown in Table 3.9.

Table 3.9 – Log of samples received, description and age

Sample Ref.	Description	Production Date	Age (Days)
YAR/TAR/1	6/10 Slag 3 Months	01/03/10	89
YAR/TAR/2	6/10 Slag 3 Months	01/03/10	89
YAR/TAR/3	6/10 Slag Fresh	15/05/10	16
YAR/TAR/4	6/10 Slag Fresh	15/05/10	16
YAR/TAR/5	6/10 Slag 12 Months	29/04/09	395
YAR/TAR/6	6/10 Slag 12 Months	29/04/09	395
YAR/TAR/7	6/10 Slag 6 Months	27/10/09	214
YAR/TAR/8	6/10 Slag 6 Months	27/10/09	214
YAR/TAR/9	6/10 Slag Oldest	10/09/07	991
YAR/TAR/10	6/10 Slag Oldest	10/09/07	991

All material was air dried and riffled to produce representative sub-samples, approximately 150g. Representative samples were ground using a Tema laboratory disc mill, sieved to <63μm and oven dried before being stored in airtight containers.

Material was analysed by acid digestion to determine calcium carbonate content using an Eijelkamp Calcimeter (full method in Appendix A), which had been calibrated immediately prior to analysis, operated to BS 7755-3.10:1995 ISO 10693:1995. Samples were reacted with 0.4M HCl and $CaCO_3$ content inferred from volumetric measurement of CO_2 gas evolved

Material was analysed for pH using an aqueous methodology (full method in Appendix A): 10ml material shaken on an orbital shaker with distilled water, and allowed to stand for 24hrs. pH was analysed using a Jenway electronic pH probe, which had been calibrated immediately prior to analysis.

A subset of samples were also analysed to determine the stable isotope content of the carbon and oxygen present in any carbonates they contained. This is discussed in detail in section 3.5 of this chapter.

Results

Figures 3.16 and 3.17 show the results of pH and acid digestion analysis, presented as variation over time assuming an approximately equal initial composition for all of the materials analysed.

pH values are high, 12.46-12.64, and demonstrate a very slight decrease in pH with increasing production age of material, though this is insignificant within the analytical precision. pH remains high over time, with materials which have been weathering in the environment for 991 days still producing significantly elevated pH values of 12.46-12.48.

Acid Digestion shows a minimum calcium carbonate content of 6.35 % wt $CaCO_3$ at 16 days post-production and a maximum calcium carbonate content 16.96 % wt $CaCO_3$ at 89 days post-production. The samples taken at 89 days illustrate very high carbonate contents with respect to the other samples tested, and may be an artefact of an undisclosed variation in composition or treatment on-site. Excluding these samples, there is a general progressive increase with time of carbonate content, as would be expected as the material progressively weathers.

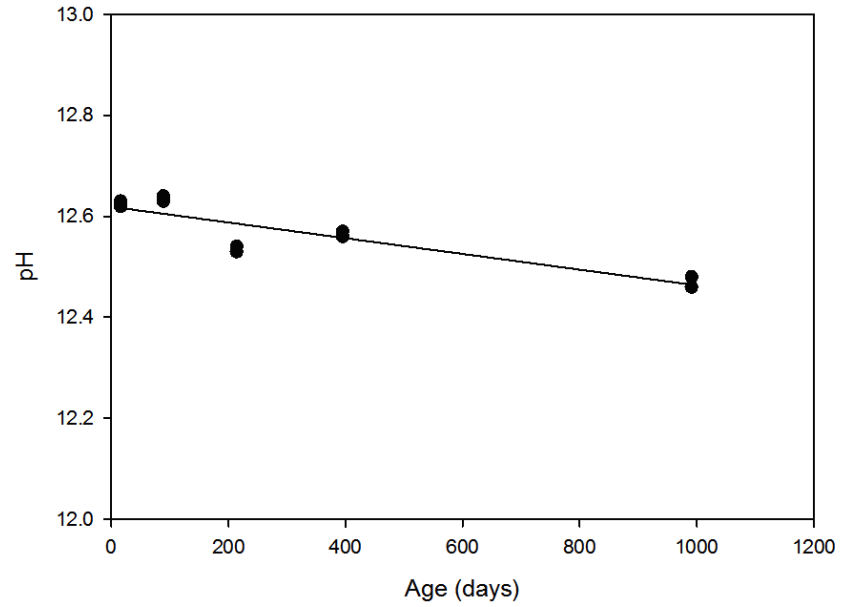

Figure 3.16 – Variation of pH with respect to production age of sample (analytical error bars are within diameter of point)

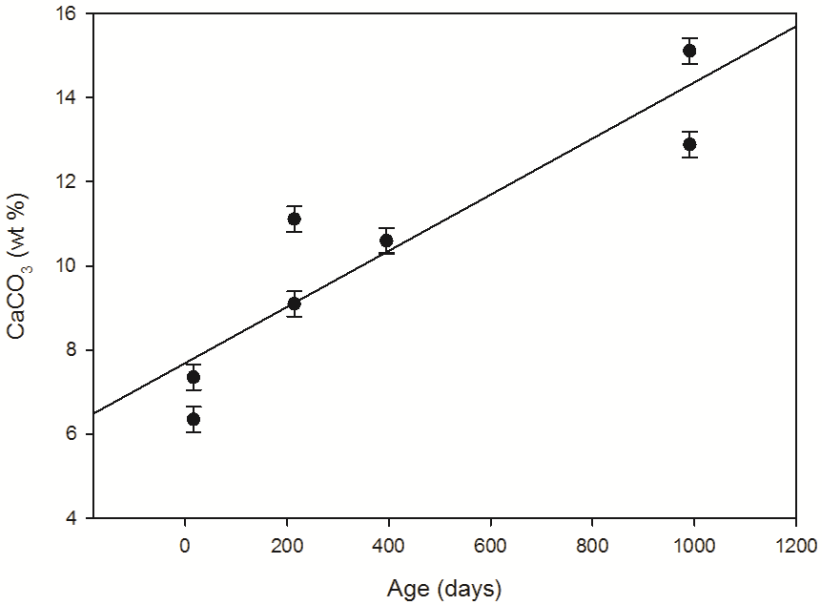

Figure 3.17 – Variation of % wt $CaCO_3$ with respect to production age of sample (sample at 395 days encompasses two points, but data values so close it appears as one. Outlier at 89 days excluded) r^2 = 0.8388

A carbonation rate can be determined from Figure 3.17, as a minimum estimate. This translates to a formation rate of 0.0073 g $CaCO_3$ 100g $slag^{-1}$ day^{-1}, or ~2.7 g $CaCO_3$ 100g $slag^{-1}$ a^{-1}.

Table 3.10 – Weathering rates determined in this section

	Weathering rate (log mol Ca m^{-2} sec^{-1})	**Estimation method**
Steel slag	Field -7.11 to -7.56	Formation of $CaCO_3$

The calculations in Table 3.10 assume 1 tonne of material (this may take any value as all calculations are made as a wt % of $CaCO_3$ and are therefore scalable), and an arithmetic spherical surface area for each particle (6-10mm) of 0.00011 – 0.00031 m^2. Ca contained in carbonates has been leached from the stockpiled material, between 19 and 991 days, at a cumulative rate of -7.11 to -7.56 log mol m^{-2} sec^{-1}, summarised in Table 3.10.

Discussion

All stockpile samples were found to contain significant quantities of calcium carbonate. This material has formed over a relatively short time period (days to months), with no obvious C contribution other than that from atmospheric / environmental sources. Samples analysed at 16 days post-production exhibited moderately high carbonate concentrations (6.9 % wt $CaCO_3$) suggesting a significant quantity of slag carbonation is achieved rapidly during, or soon after, production.

The weathering rate of -7.11 to -7.56 log mol Ca m^{-2} sec^{-1} over 975 days is rapid in comparison to laboratory data for similar material, such as the steel slag in batch experiments in section 3.2.1. As 16 days is taken as the start point, when a large quantity of carbonate formation has already occurred, this calculation implies the formation of 7.15 wt % $CaCO_3$ over 975 days. This may illustrate that the weathering rates attained for batch experiments and pH stat experiments are slower than would be the case if secondary mineral formation was used as a proxy, rather than solution chemistry. This suggests that the leaching of Ca^{2+} and precipitation of $CaCO_3$ is directly affected by other limiting factors within the system, discussed further in section 3.4.

This is encouraging in the assessment of steel slag with respect to the dynamics of its use in carbon sink engineering, particularly the evidence that significant carbonation of the slag material occurs rapidly during and after production. As this data was taken from an open system, although many of the conditions are constrained it is possible that the rate of leaching may appear artificially reduced, as some of the Ca leached may have been transported out of the system, possibly precipitating in other areas of the stockpile.

It may conversely may appear artificially accelerated as Ca may have leached in to the samples from other parts of the stockpile to be deposited as secondary minerals depending upon local drainage regimes.

Summary

- $CaCO_3$ was observed, forming as a result of Ca leaching from steel slag, at a rate of 0.0073 g $CaCO_3$ 100g $slag^{-1}$ day^{-1}, or ~2.7 g $CaCO_3$ 100g $slag^{-1}$ a^{-1} under ambient environmental conditions
- Ca was estimated to leach at a rate of -7.11 to -7.56 log mol Ca m^{-2} sec^{-1} over 975 days

3.4 Complex reactions in real-world environments

The complexity of the weathering reaction in laboratory studies is amplified in large-scale and field settings. Studies trying to scale field scale processes up from lab scale and meso-scale often face difficulties in fully accounting for the observed discrepancies. Difficulty in linking these studies is caused by the large number of complex, interacting factors which dictate the rates of mineral weathering in large-scale real world settings. These are discussed further in Chapter 4.

Some important observations have been made with respect to the weathering of artificial silicate minerals for carbon capture in 'process based' approaches, which have a significance for field-scale activities carried out in this area. Huijgen et al (2005) assessed the weathering rate of steel slag, as a carbon capture analogue material, in large batch reactors with specific focus given to the effects of:

- Particle size
- Reaction temperature
- Reaction time
- CO_2 pressure

Whilst this work was carried out in batch reactors at elevated temperature and pressure, these factors are critical to weathering and mineral formation under any conditions. The carbonation reaction was observed to occur in two process steps, which were defined as the leaching of calcium from steel slag into solution (the weathering step, including issues with the creation of weathered layers) and the precipitation of secondary minerals on the surface of the reactive particles (calcium carbonate and others). Either of these

steps could prove to be rate limiting depending on the contribution they make to the equilibrium geochemistry of the system. In the batch weathering experiments presented in the previous section the analytical focus was upon determining the rate of Ca leaching in to solution due to the limitations of the experimental design in quantifying precipitates, and in the field-analogue stockpile analysis the focus was upon precipitated minerals due to the lack of hydrogeological data. These studies showed that observing either as a proxy for weathering rates provides useful information, however data regarding both steps allow a concise picture of a complex weathering environment to be constructed. Flow-through weathering experiments in Chapter 5 (section 5.2.1) consider both of these aspects in greater detail.

Huijgen et al (2006) also defined five consecutive steps in their process-based approach, one or more of which may be rate limiting: the diffusion of Ca towards the particle surface (from within the mineral structure), the leaching of Ca from particle surface to liquid (in to porewater – which depends on pH), the dissolution of $CO_{2(g)}$ in the liquid (into porewater), the conversion of dissolved CO_2 (partial-pressure dependent) into the (bi-)carbonate ion (temperature dependent) and the precipitation of $CaCO_3$ (on to material surface as shown in Figure 3.1 – which ultimately acts to limit the first step, diffusion from the surface, and reduces the rate of weathering). The batch weathering experiments presented in the previous section set out to investigate a number of these parameters: rate of Ca leaching, variations in dissolved inorganic carbon and processes which could act against the formation of surface precipitates. It was shown that these factors were complex, and materials did not always behave in a predicted manner to variations in these conditions, although consideration of surface and equilibrium chemistry provided clarification.

From these data, it is logical to conclude that the geochemical processes instigated by the weathering of the slag material and the physical aspects, including availability of precipitation nuclei, both have the potential to govern the rate of this reaction. Weathering of *in situ* material depends upon the proximity of the material to the weathering agents, the presence of any impermeable boundaries between the reacting solid and fluids and the pH range of the soil pore water. As mentioned in section 3.1 this can affect the weathering rate in a number of ways, and the rate of leaching of Ca from the material / the relative solubility of the different materials which is controlled by innate physical and chemical properties of the material and environment.

The precipitation of calcium carbonate depends upon the availability of Ca^{2+} in solution (which is both quantitatively and rate limiting), diffusion of $CO_{2(g)}$ in the liquid or the supply of carbonate species from other sources and the availability of a free precipitation surface on which the secondary mineral can be deposited, which under experimental conditions with crushed slag appeared to be a limiting factor (Huijgen et al, 2005, 2006). Calcium carbonate is sparingly soluble in water and precipitation of solids is promoted in many environments where saturation occurs. It may be the case that the presence of other solid matter in association with slag material could act to provide an additional surface for reaction or nucleation.

Mineral sequestration possesses a number of methodological and physical limitations. It is subject to both chemical and physical-chemical limits; sequestration of this type can be quantified in terms of a 'sequestration potential', which generally refers to the overall stoichiometric chemical relationship between the reacting species. As has been discovered by many previous studies (Huijgen, 2006), this concept of 'sequestration potential' is not always the best approach to estimating a realistic quantitative ability for CO_2 capture. Maximum sequestration capacity is rarely attained in a real-world setting due to limiting factors such as temperature, pCO_2, leachate saturation, unavailability of reaction surfaces. The effects of these factors on real-world study sites are discussed further in the next chapter.

3.5 Elucidating the atmospheric carbon capture reaction: stable isotope geochemistry

The following section discusses one of the approaches which can be used to determine the proportion of carbon bound in carbonates derived from the atmosphere during carbonation reactions. This is a useful tool for determining the amount of sequestration which has already occurred at a setting where initial conditions are unknown. Data presented is based upon stable isotope analysis of samples discussed in section 3.3.

Stable isotope analysis has long been championed as a method for determining provenance of particular elements within mineral structures. 'Stable isotopes' are atoms of an element which possess nuclei that contain the same number of protons but different numbers of neutrons, but retain nuclear stability. Oxygen and carbon have stable isotopes (^{12}C = 98.89%, ^{13}C = 1.11% (Nier, 1950) and ^{16}O = 99.763%, ^{17}O = 0.0375% and ^{18}O = 0.1995% (Garlick, 1969)) and are amongst the large suite of elements which exhibit stable isotope variations due to inherent kinetic effects during the chemical reactions in which they participate. Stable isotopes are reported as an enrichment (+) or depletion (-) from a reference value, defined by a geological standard such as Pee Dee Belemnite, or the more recently developed proxy Vienna Pee Dee Belemnite (V-PDB) which is used in all stable isotope data reported in this work. For oxygen the value is defined as the ratio of O^{18} to O^{16} ($\delta^{18}O$), and for carbon the value is based on the ratio of C^{13} to C^{12} ($\delta^{13}C$).

Fractionation of carbon and oxygen isotopes during carbonate formation in soils is a complex process which is influenced by kinetic processes related to inorganic carbonate formation and biogenic processes related to the contribution of organic acids, other photosynthetic products and respired CO_2 in the shallow surface (Cerling, 1984, 1989).

'Isotope equilibrium exchange reactions' occur in the inorganic carbon system where inorganic carbonates form through an "atmospheric CO_2 – dissolved bicarbonate – solid carbonate" process leading to an enrichment of ^{13}C in lithogenic carbonates (Hoeffs, 1997). An isotopic fractionation effect is present between all of the equilibria in this system (seen in Equation(s) 3.3). At low temperatures the largest fractionation effect occurs between dissolved CO_2 and bicarbonate. Isotope signatures for these carbonates tend to fall around -2 ‰ and -10 ‰ for $\delta^{13}C$ and 0 ‰ and -5 ‰ for $\delta^{18}O$.

Equation(s) 3.3a, b, c, d:

$$CO_{2\,(aq)} + H_2O = H_2CO_3$$

$$H_2CO_3 = H^+ + HCO_3^-$$

$$HCO_3^- = H^+ + CO_3^{2-}$$

$$Ca^{2+} + CO_3^{2-} = CaCO_3$$

Kinetic isotope effects during photosynthesis concentrate ^{12}C in organic materials (Hoeffs, 1997), which may affect the stable isotope signature of soil carbonates which have formed following interactions with plant-derived exudates. The influence of organic interactions on the isotope signature of carbonates is beyond the scope of this study, as the samples reported are mostly taken from settings where biological processes are minimal (un-vegetated sites and newly produced artificial minerals).

$\delta^{18}O$ and $\delta^{13}C$ values have been consistently used in environmental, ecological and palaeoclimatic studies to determine the relative contributions of plants with different (C_3 and C_4) metabolic pathways to soil carbonate formation, as an important indicator of climatic zone mapping. C_3 versus C_4 isotopic effects were noted by Cerling (1984) and Hoeffs (1997), with the consensus that C_3 pathways tended to produce a more depleted isotopic signature and C_4 pathways produced a less depleted isotopic signature (Salomons and Mook, 1976), $\delta^{13}C$ -27 ‰ for C_3 plants, -13 ‰ for C_4 plants (Cerling, 1984). Figure 3.18 illustrates some of the factors affecting the formation of pedogenic carbonates, which have the potential to influence the isotopic signature of the carbonates formed.

Numerous studies of natural pedogenic calcite (caliche) formation have employed stable isotope analysis as palaeoclimatic indicators. Knauth et al (2003) note that the oxygen isotopes are fixed at the time of (caliche) formation and reflect the temperature and composition of local meteoric waters and atmospheric CO_2 composition, while carbon isotope composition is generally determined with respect to the relative contributions by atmospheric CO_2, organic processes (including respiration) and re-worked rock (lithogenic) material. For this reason, $\delta^{13}C$ data are able to shed light upon the provenance of C found in soil-formed carbonates, demonstrating the presence of atmospherically derived CO_2 in their structure (Renforth et al, 2009; Wang et al., 1994).

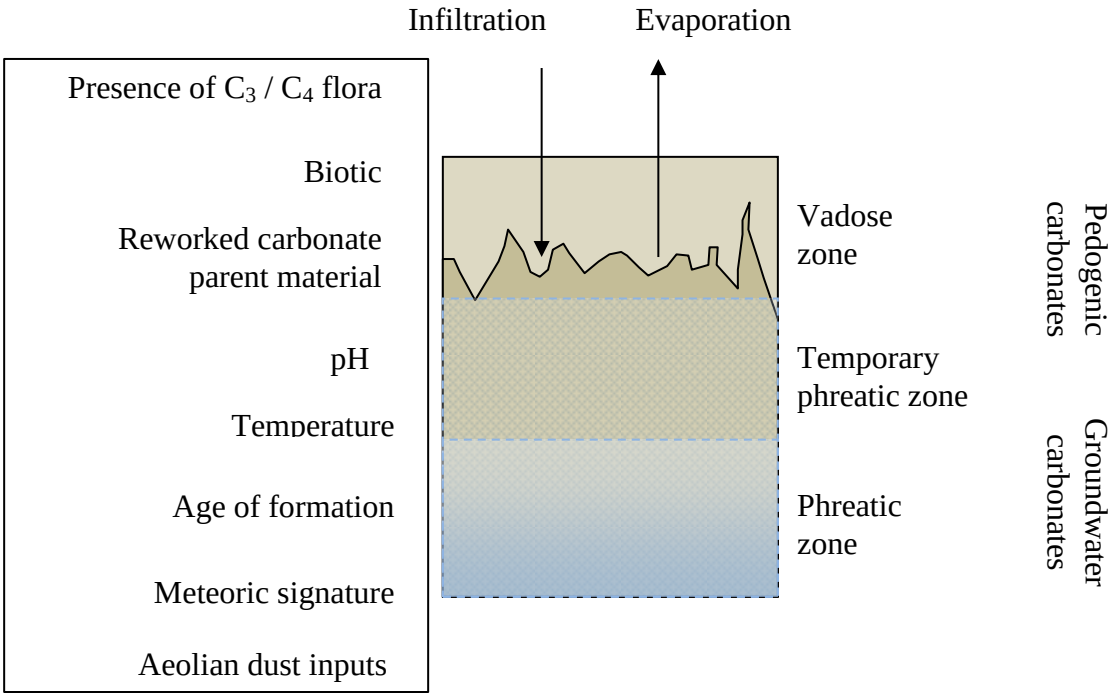

Figure 3.18 – A summary of influences to the formation of secondary soil carbonates (Jenny, 1980; Cerling, 1984)

Hydroxylation occurs at high pH, in environments like those dominated by the weathering of artificial silicate minerals (section 3.3 demonstrates that these may commonly reach values ~ pH 12). Equation 3.4 illustrates the reaction, which involves hydroxide ions (OH^-) produced through the weathering of portlandite ($Ca(OH)_2$), a component of cement and steel slag and a common 'intermediate' weathering product. The isotope signature is governed by diffusion of CO_2 in to aqueous solution and formation of $CaCO_3$. The rate of hydroxylation exerts the greatest influence on the isotope signature of high pH solutions (pH > 11.5) (Dietzel et al., 1992) and can be assigned a large role in determining the isotopic composition of carbonates formed from the weathering of artificial minerals in soil settings.

Equation 3.4:

$$Ca(OH)_2 + CO_2 \leftrightarrow Ca^{2+} + 2OH^- + CO_{2\,(aq)} \leftrightarrow CaCO_3 + H_2O$$

Contemporary studies (Dietzel et al., 1992; Krishnamurthy et al., 2003, and Andrews et al., 1997) have illustrated that the stable isotope signatures of C and O can be used to assess sequestration of CO_2 in pedogenic inorganic carbonates. These studies have mostly been carried out on temperate or sparsely vegetated soils, therefore the influence of C_3 / C_4 pathways should be minimised, due to the overwhelming dominance of C_3

species or lack of vegetation in general. In these cases, variation in C isotopic signatures is deemed to be caused solely by the discrepancy between C fixed through inorganic processes driven by CO_2 dissolved in soil pore water attained through simple atmospheric diffusion and those present in lithogenic materials. The potential to identify carbonate formed through organic processes mediated by plants and other organisms has been suggested by some studies (Cerling, 1984, (in Swart, 1993); Renforth et al, 2009) although difficulties may arise in quantifying the relative contributions if the analysis is based on a mixing line (Figure 3.19) with defined end-members which overlap, as described in the sections below.

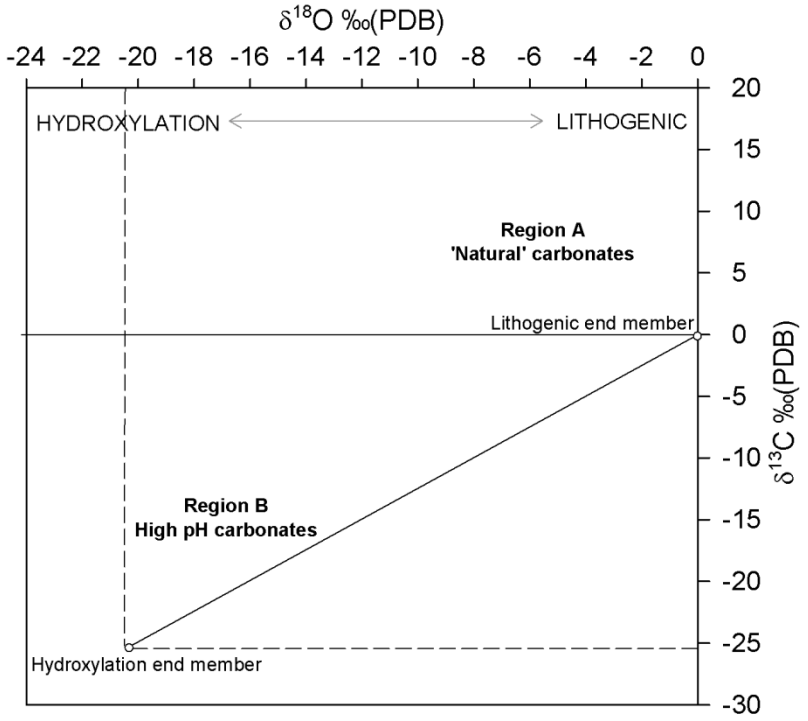

Figure 3.19 – Mixing line for determination of carbonate provenance using C and O isotopes (adapted from Washbourne et al, 2012)

This hypothesis relates the kinetic principles behind stable isotope fractionation to the real-world observations likely to be made for lithogenic and high pH carbonates. The end members used in Figure 3.19 are: lithogenic end member $\delta^{18}O$=−0.0‰, $\delta^{13}C$=−0.0‰ (Andrews, 2006; Renforth et al., 2009), hydroxylation (high pH) end member $\delta^{18}O$=−20.5‰ (Dietzel et al., 1992; Usdowski and Hoefs, 1986); assuming meteoric water $\delta^{18}O$=−7.8‰ vs SMOW (Darling et al., 2003), $\delta^{13}C$=−25.3‰ (Washbourne et al 2012). Other studies (Cerling, 1984; Renforth et al., 2009) have reported a 'biogenic' end member, which could be characteristic of a carbonate formed with a contribution from organic processes: $\delta^{18}O$ = -6.75‰, $\delta^{13}C$ = -8‰ (Cerling, 1984; Renforth et al

2009). This end member has not been used in calculations shown in the following sections of this report as so little organic matter is identified in all contexts that it is unlikely that a large contribution would be present, and the insertion of this intermediate point may mask the relative contribution of the other end members. Renforth (2011 PhD thesis) notes that work by Wilson et al. (2010) demonstrate that more negative values of $\delta^{13}C$ could be produced through the presence of diffusional carbonates; precipitated in a system limited by CO_2 diffusion (Wilson et al., 2010) to estimated values up to $\delta^{13}C$ = -47‰. These are not included on the end-member plot for hydroxylation and lithogenic materials, but may be invoked to explain deviations with respect to $\delta^{13}C$ from this mixing line in some contexts.

Results of stable isotope analysis ($\delta^{13}C$, $\delta^{18}O$) of steel slag from the Yarborough Landfill site, Scunthorpe, from contemporary and historic stockpiles are presented in the next section to illustrate the ways in which these data can be analysed and interpreted. Other examples will be presented in later chapters.

Method

Materials:

Samples were supplied and prepared as in section 3.2.1. Representative samples (Table 3.11) were ground using Tema laboratory disc mill and sieved to <63μm. 3 samples (of differing ages) were packed and sent to Iso-Analytical Ltd., Cheshire for C and O stable isotope analysis using the methodology supplied below (also Appendix A).

Table 3.11 – Log of samples sent for IRMS analysis, description and age

Sample Ref.	Description	Production Date	Age (Days)
YAR/TAR/4	6/10 Slag Fresh	15/05/10	16
YAR/TAR/2	6/10 Slag 3 Months	01/03/10	89
YAR/TAR/9	6/10 Slag Oldest	10/09/07	991

Samples were weighed into clean Exetainer™ tubes and the tubes placed in a drying oven for 24 hours to remove moisture. Once the samples were dry septum caps were fitted to the tubes.

The tubes were then flushed with 99.995 % helium and 0.5 mL of phosphoric acid, which had been prepared for isotopic analysis in accordance with Coplen et al. (1983), was injected through the septum into the vials.

The vials were mixed and left for 24 hours at room temperature for the acid to react with the samples. After 24 hours vials were heated to 65°C for 2 hours to ensure all available carbonate was converted to carbon dioxide

The CO_2 gas liberated from samples was then analysed by Continuous Flow-Isotope Ratio Mass Spectrometry (CF-IRMS). Carbon dioxide was sampled from the Exetainer^{TM} tubes into a continuously flowing helium stream using a double holed needle.

The CO_2 was resolved on a packed column gas chromatograph and the resultant chromatographic peak carried forward into the ion source of a Europa Scientific 20-20 IRMS where it is ionised and accelerated. Gas species of different mass are separated in a magnetic field then simultaneously measured using a Faraday cup collector array to measure the isotopomers of CO_2 at m/z 44, 45, and 46.

Results

Figure 3.20 shows the values for carbon $\delta^{13}C_{V\text{-}PBD}$ (‰) and oxygen $\delta^{18}O_{V\text{-}PBD}$ (‰) determined through IRMS analysis (included in Appendix A). The stockpile samples demonstrated $\delta^{13}C_{V\text{-}PBD}$ (‰) values between -14.93 and -20.45 and $\delta^{18}O_{V\text{-}PBD}$ (‰) values between -12.25 and -16.95. These values showed some evidence of higher depletion in $\delta^{13}C$ with increasing age: 16 days = -17.73‰, 89 days = -19.54‰, 991 days = -20.45‰.

Comparative data, shown here in white circles, is taken from Renforth et al (2009) and represents values attained for slag material weathering at a former steelworks (age is not constrained in this study, but > 30 years). A mixing line is superimposed, taken from Washbourne et al (2012) which assumes end-members of $\delta^{18}O$=−0.0‰, $\delta^{13}C$=−0.0‰ (lithogenic) and $\delta^{18}O$=−20.5‰, $\delta^{13}C$=−25.3‰ (hydroxylation) as stated in the previous section. All points fall some distance below the proposed line with respect to $\delta^{13}C$, suggesting that another fractionation process may be involved in their formation. It may also be due to variations in $\delta^{18}O$ due to water contributions from different sources. An estimated trend line for hydroxylation and diffusion (Renforth, 2011 (PhD thesis)) is overlaid (assumed end-members $\delta^{18}O$=−0.0‰, $\delta^{13}C$=−0.0‰ (lithogenic) and $\delta^{18}O$=−20.3‰, $\delta^{13}C$=−34‰ (hydroxylation and diffusion)) to illustrate the potential contribution from this additional process in this setting.

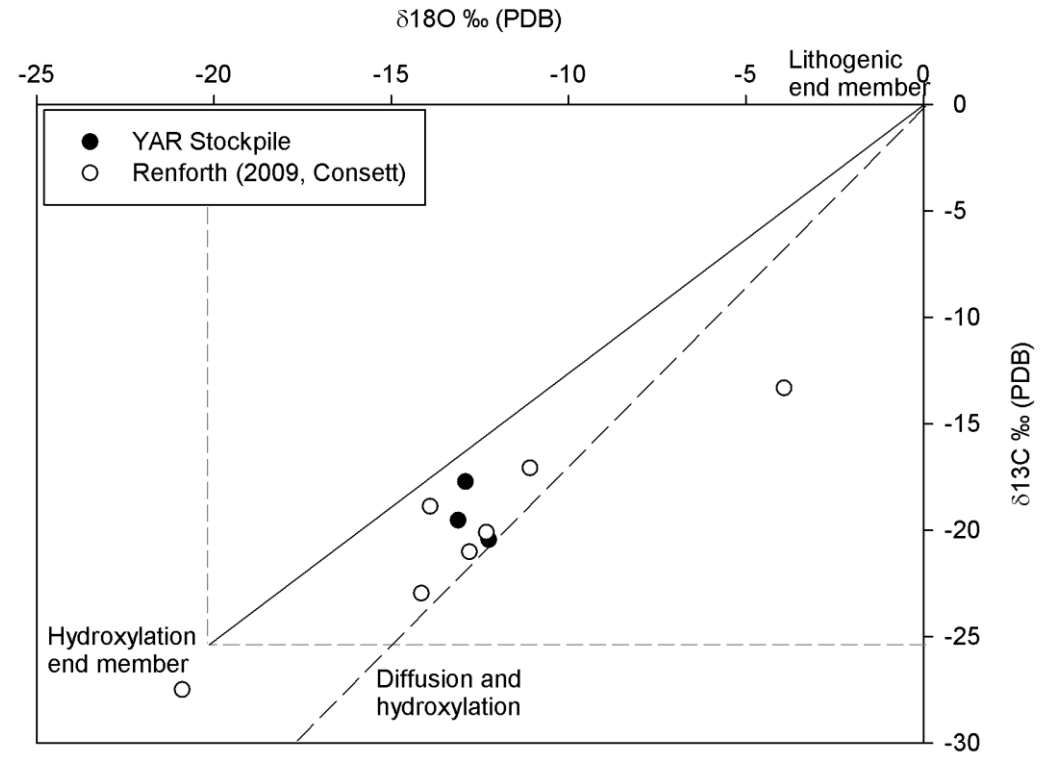

Figure 3.20 – Stable isotope values for carbon $\delta^{13}C_{V\text{-}PBD}$ (‰) and oxygen $\delta^{18}O_{V\text{-}PBD}$ (‰) determined by IRMS, with mixing line from Figure 3.19 superimposed and additional data from Renforth et al 2009, 2011 (thesis)

Figure 3.21 shows the relative proportion of carbonate present in the 3 stockpile samples which is likely to have been formed through a hydroxylation / atmospheric capture route on the basis of the carbon isotope data. These proportions were determined through the use of the end members reported earlier in this section – $\delta^{18}O$=−0.0‰, $\delta^{13}C$=−0.0‰ and $\delta^{18}O$=−20.5‰, $\delta^{13}C$=−25.3‰. The contribution of each member to the values observed is calculated relative to its position with respect to each point along a mixing line. It can be seen that most of the carbonate present in these samples appears to have formed through hydroxylation (70-81%), with the proportion of hydroxylated material increasing with the age of the sample.

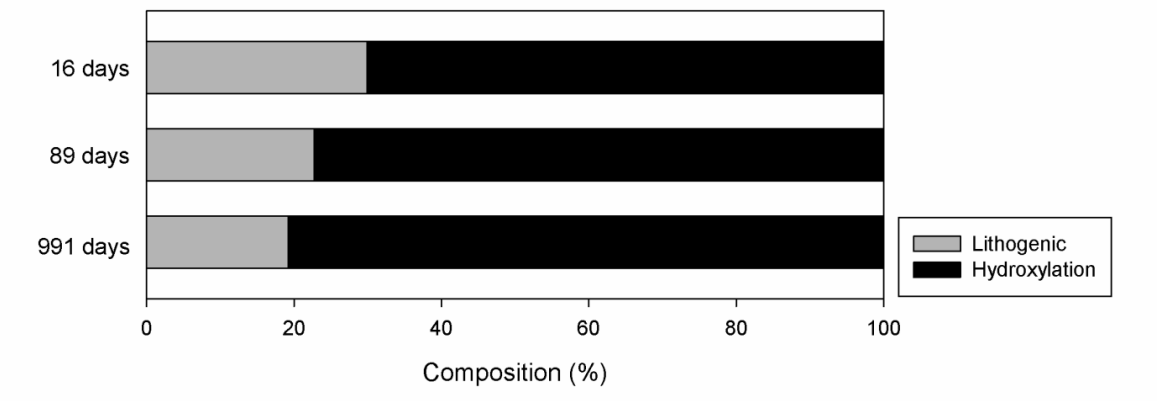

Figure 3.21 – Relative proportions of carbonate from lithogenic sources or formed through hydroxylation processes determined by end-member analysis

Discussion

All samples analysed were found to contain C sequestered from atmospheric CO_2. Very negative values for $\delta^{13}C$ observed are characteristic of carbonate formed in high-pH environments and through diffusion of atmospheric CO_2. These data indicate a strong atmospheric influence on the provenance of stable isotopes in the carbonates forming in the Yarbrough landfill, suggesting significant quantities of atmospheric CO_2 have been sequestered in their formation. None of the carbonate present in the landfill or stockpiled samples was found to contain large quantities of lithogenically derived material. This is promising with respect to soil engineering for carbon capture, exhibiting the preponderance of atmospheric carbon sequestration under these ambient conditions.

These findings illustrate the value of stable isotope analysis as a means of determining the provenance of C and O in pedogenic carbonates, and assigning an estimate of proportional contribution of different formation routes. The observed increase in hydroxylated material over time illustrates the progression of the reaction contributing to the formation of carbonate.

Summary

- Stable isotopes of C and O can be used to estimate the provenance of C and O in carbonates formed in natural weathering environments
- Using end-member analysis it was determined that 70-81% of the carbonate present in steel slag samples weathering under ambient environmental conditions appeared to have formed through hydroxylation / atmospheric capture of carbon
- $\delta^{13}C_{V\text{-}PBD}$ (‰) values were shown to decrease over time with the cumulative deposition of carbonates containing atmospherically derived C

3.6 Summary

The data presented in this chapter support the proposition that artificial minerals could effectively be used for carbon capture and storage in the ambient environment. Table 3.12 compares the weathering rates derived for a selection of different silicate minerals from the experimental work contained in this chapter. In all cases these were found to be comparable to, or more rapid than many weathering rates for silicate minerals reported in previous studies.

Table 3.12 – Comparative weathering rates of materials reported in this chapter

	Weathering rate (log mol Ca m^{-2} sec^{-1})	**Estimation method**
Steel slag	Batch -9.39 to -11.88 Field -7.11 to -7.56	Leaching of Ca Formation of $CaCO_3$
C&D waste	-10.10 to -12.40	Leaching of Ca
Wollastonite	Batch -9.82 to -11.53 pH stat -6.19 to -8.03	Leaching of Ca Leaching of Ca
Dolerite	-10.82 to -12.62	Leaching of Ca

At laboratory scale the estimated weathering rates demonstrate that artificial silicate minerals break down rapidly under ambient environmental conditions experienced in weathering at the Earth's surface. At field-scale, the weathering rate of -7.11 to -7.56 log mol Ca m^{-2} sec^{-1} over 975 days observed in stockpiled steel slag is exceptionally rapid in comparison to the weathering of other silicate minerals at laboratory scale. Acid digestion analysis showed a minimum calcium carbonate content of 6.35 % wt $CaCO_3$ at 16 days post-production and a maximum calcium carbonate content 16.96 % wt $CaCO_3$ at 89 days. High pH values (12.46-12.64) which persisted over time, presented the potential for carbonates to form through hydroxylation processes which were confirmed by IRMS analysis (included in Appendix B). The stockpile samples demonstrated $\delta^{13}C_{V\text{-}PBD}$ (‰) values between -14.93 and -20.45 and $\delta^{18}O_{V\text{-}PBD}$ (‰) values between -12.25 and -16.95. These values showed some evidence of higher depletion in $\delta^{13}C$ with increasing age: 16 days = -17.73‰, 89 days = -19.54‰, 991 days = -20.45‰ showing the increasing dominance of hydroxylation as a carbonate formation route.

The following chapters aim to investigate how these findings translate to field-scale settings, through an intrusive investigation of carbonate formation at a number of selected field sites.

CHAPTER 4 - Mineral carbon capture in the field: analogues

Progressing from understanding the geochemical factors involved in mineral carbon capture using artificial silicate minerals as discussed in the preceding chapter, Chapter 4 assesses how these factors manifest in observations made at field scale. The overarching aim of this work is to assess the potential for developing mineral carbon capture processes in soils; therefore investigations were undertaken in suitable field-scale settings in order to determine the applicability and scalability of the basic parameters.

As discussed in Chapter 2, soil systems have the ability to capture and store carbon, playing a vital role in regulating the climate through their impacts on the global carbon cycle. Total carbon content in soil includes organic compounds and inorganic carbonate minerals, both of which can be managed to promote carbon storage. Inorganic carbon storage in soils is dominated by calcium and magnesium carbonates (Schlesinger, 1982). This pool can be managed through 'enhanced weathering', increasing the draw-down of CO_2 from the atmosphere through chemical reactions with cations produced by the weathering of natural or artificial silicate minerals to form soil carbonates.

This chapter presents data from a number of investigations on field sites where artificial silicate minerals have been emplaced, in order to develop an understanding of the ways in which these minerals weather under ambient conditions and provide a comparison to laboratory analyses presented in the preceding chapter.

Chapter summary:

Field investigations at sites where suitable materials for carbon capture had been emplaced allowed the determination of, previously poorly studied, temporal and spatial (surface and profile) constraints on the MCCS process.

- Broad spectrum geochemical analysis of sites where MCCS has been occurring without intervention at a significant and testable rate
- Novel, spatially accurate chronosequence presented for geochemical change over a selected field site
- New method of estimating carbon capture potential for a field site developed from the data

4.1 Factors in soil formation / calcium carbonate formation in soils

As previously noted, during weathering Ca and Mg silicate minerals naturally react with dissolved carbon dioxide (CO_2) to increase local alkalinity and form secondary carbonates (Berner et al., 1983; Seifritz 1990; Lackner et al., 1995). In soil settings, when this process occurs through direct weathering of silicates it provides a means of effectively capturing and fixing atmospheric carbon. Weathering involves leaching (discussed in Chapter 3) and transport of cations (Ca^{2+} and Mg^{2+}) in solution, which react with carbonate anions formed by CO_2 dissolution in soil pore waters to precipitate solid carbonates. A simplified version of this reaction is shown in Equation 4.1.

Equation 4.1:

$$(Ca, Mg)SiO_3 + CO_2 + 2H_2O \leftrightarrow (Ca, Mg)CO_3 + H_4SiO_4 \qquad (1)$$

Durand et al (2007) claim that conditions for weathering and precipitation of carbonates in natural soils are 'best fulfilled' by semi-arid conditions and marked seasonal variations in rainfall and temperature. These climatic settings promote the cyclic formation of complex clay minerals such as sepiolite by weathering during the dry season, from which materials can be progressively leached and re-distributed in the wet season. Carbonate deposition tends to be inhibited by very high rainfall due to increased removal in solution of products; Goudie (1983) notes that the 'ideal' precipitation scenario for pedogenic carbonate formation is 400-600mm a^{-1} (additional information regarding morphology and depth is not given), but that formation may still occur in regions where rainfall exceeds 1000-1500mm a^{-1}. Other studies (Jenny, 1980; Royer, 1999) have observed that calcium carbonate formation is not only affected by precipitation in a quantitative sense, but that the depth of carbonate horizons can be affected by variation in mean average rainfall, with higher rates of precipitation leading to deeper carbonate formation (recorded up to 3m by Jenny, 1980), potentially due to the variation in position of the transient phreatic zone in these conditions. Table 4.1 summarises some formation conditions.

As mentioned in Chapter 2, a number of studies identify carbonates in temperate regions (Boguckyi et al, 2006; Łacka et al., 2008). Studies have also provided evidence that pedogenic carbonates are able to form under temperate soil conditions in natural and artificial soils. Renforth et al. (2009) investigated the formation of pedogenic carbonates in artificial soils created by rubble and fines after demolition of concrete

structures. These sites were deemed to have little to no contribution of calcium (or calcium containing minerals such as $CaCO_3$) from local geological materials and revealed an average C content of 30 ± 15.3 Kg C m^{-2} in the form of calcium carbonate. It was previously considered that the low temperature, high rainfall climatic conditions were unsuitable for carbonate formation, however, field studies on Ca-silicate parent rocks in the north east U.K. have yielded pedogenic carbonates (Manning et al, 2013b; Renforth et al, 2009; Washbourne, 2008 (MSc thesis)). Work completed at the former site of Consett Iron and Steel works demonstrated that *in situ* carbonation of iron and steel slag in a temperate soil setting occurs even without intervention, predicting potential carbon capture figures of up to 2.4t km^{-2}. This work focussed on the chemical characterisation of the field site, but did not address the mechanisms by which carbon sequestration was occurring or quantify reaction rate. Limited information is available for the formation of pedogenic carbonates in UK soils, with Rawlins (2011) estimating the total IC stock of soil (0–30 cm depth) in this region to be 186 MtC, around 5.5% of the estimated total soil carbon stock (OC plus IC) across the UK.

Table 4.1 – Schematic representation of the formation of pedogenic carbonates in generalised soil profiles

Rainfall ⟶

	Arid (e.g. Goudie 1996)	**Stepp (e.g. Mikhailova et al. 2006)**	**Temperate (e.g. Kalin 1997)**
Topsoil	Visible carbonate formation at surface		
Soil profile		Carbonate formation in the soil profile	
Parent material			Carbonate precipitation in the joints of the parent material
Bedrock			

Depth (m): 0 — 1 m (Typical soil analysis depth) — 2 m ▼

Relatively little is known about the *in situ* weathering and carbonation behaviour of minerals in artificial soils, although a number of studies have contributed to the evidence for pedogenic carbonate formation on artificial mineral substrates. Krishnamurthy et al (2003) and Dietzel et al. (1992) explored the effects of mineral leaching from concrete structures on the formation of calcium carbonate in surrounding environs. As discussed in more detail at the end of the preceding chapter, stable isotope analysis was used in these studies to confirm the atmospheric provenance of C in the

calcium carbonate precipitates, confirming that they had formed under the influence of hydroxylation reactions, combination with carbonic acid produced through direct atmospheric CO_2 dissolution and a possible contribution from plant root respiration and exudates. Renforth et al. (2009) showed that urban soils potentially capture 12.5 $kgCO_2$ $tonne^{-1}$ soil yr^{-1} by this process and that formation of carbonate minerals in urban soils may be a significant and exploitable storage route for soil carbon.

A summary of factors likely to affect the precipitation of carbonate in soils is listed in Table 4.2. These factors may be divided in to physical and chemical (properties related to the material itself), environmental (climate-related) and biological aspects. A brief discussion of the influence of these factors in presented in the following sections.

Table 4.2 – Factors affecting the formation and precipitation of carbonate in soils

Increased carbonate precipitation	Decreased carbonate precipitation
+ High Ca availability	- High net H_2O input
+ Low to moderate net water input	- High soil gas pressure
+ Marked alternation of wet / dry periods	- Low pH
+ Low pressure of CO_2 (pCO_2)	
+ Varied pH / buffering activity	
+ High temperature	

4.1.1 Physical-chemical properties

Cation availability heavily affects carbonate formation in soils. As carbonate formation is dependent upon the weathering and on-going reaction of divalent cations, the total Ca/Mg available will play a large role, as will the overall weathering rate. There is an 'ideal' point for Ca/Mg concentration to promote secondary carbonate formation, relating to the reaction equilibrium (Eq. 1). Once a soil solution has become saturated with Ca/Mg any further cation contribution above the rate at which it is removed from solution is not beneficial to the formation of carbonate which will become limited by other factors.

pH affects carbonate precipitation by altering the equilibrium position with respect to soil carbonate formation (see Equation 3.1 Chapter 3). As discussed in Chapter 3 Ca leaching is promoted by low pH (<5), however when pH decreases dissolution of carbonate minerals is promoted. Elevated pCO_2 and the presence of acids increase the concentration of H^+ ions through the formation of carbonic acid and other complex acid

species. This increases the solubility of $CaCO_3$ by leading to the formation of calcium bicarbonate $Ca(HCO_3)_2$. Increased alkalinity promotes the precipitation of carbonates, by creating supersaturated conditions in soil water – but this reaction must be buffered by a weak acid solution in order to promote on-going precipitation. It is, therefore, known that variation in pH / buffering activity would have a complex effect on soil carbonate formation.

Low pCO_2 conditions promote the formation of carbonate; whilst a steady supply of CO_2 is required to ensure the carbonation reaction is not limited in this respect, as mentioned in the previous section high pCO_2 increases the solubility of carbonate minerals, promoting the formation of bicarbonate.

4.1.2 Environmental

Climate (temperature and precipitation) can have a significant impact on the rate at which carbonate formation occurs, and as noted in the previous section can also affect the depth and geometry of the carbonate formations.

In regions which undergo marked alternation of wet / dry periods, carbonate formation is frequently promoted if suitable source materials are present (onsite or imported). An overall low-to-moderate net H_2O input is also useful in predicting where carbonate formation will occur most readily and extensively, which provides a useful basis for designing site investigation programmes intended to assess carbonate formation.

Temperature may also have an effect on carbonate formation, although the temperature range provided by typical soil settings is limited. White and Brantley (1995) propose a link between climatic conditions, noting that precipitation has a more significant impact on silicate weathering rates in warmer climates and may have a more limited impact in temperate regions.

4.1.3 Biological

Organic products from biological processes including respiration may influence the formation of pedogenic carbonates. Renforth (2011 (thesis)) investigated the effects of organic acids on the formation of carbonate in artificial soil analogues by exposing cement minerals to citric acid, finding that the presence of an organic acid enhances the weathering rate by half an order of magnitude, though possibly with the contribution

from the buffering effects provided by another part of the experimental design. Other studies (Drever and Stillings, 1997; Huang et al, 1972) have also concluded that exposure to organic acids can promote or inhibit the leaching of Ca from source materials, which may in turn promote or inhibit the formation of carbonates.

Physical factors caused by biological agents may also play a part in influencing the rate of soil carbonate formation, including physical breakdown of minerals through burrowing or dissolution by biological agents; this may be linked to factors including root networks and fungal hyphae, where extensive biological systems provide extended influence upon the local geochemistry of their environments (Breemen et al., 2000; Berner et al., 2001). Biological factors including soil respiration are able to elevate levels of pCO_2, which therefore has the potential to promote cation leaching but hinder carbonate formation.

4.1.4 Rate effects

The aforementioned factors have the potential not just to affect the total quantity of carbonate formed at a site, but also assist in constraining the rate at which minerals form within the soil system. There is a large disparity between many of the leaching / weathering rates observed during field studies and those attained through laboratory work. The reconciliation of these rates is strongly dependent on the effects of soil formation factors being accounted for in laboratory studies. White and Brantley (1995) explain much of this discrepancy as being part of a range of factors including soil age, saturation, hydrological heterogeneity and climate. All of these factors can act to reduce the weathering rate at field scale compared with rates suggested by theory and laboratory investigation. Discrepancies also exist over factors linked to surface area determination and other empirical parameters which can provide a large amount of apparent variation.

The findings reported in the following sections are expected to be subject to the factors described in sections 4.1.1 to 4.1.3 which influence carbonate formation in soils at field scale while being less apparent in the laboratory scale investigations detailed in Chapter 3. In this study the sites can be envisaged as un-vegetated soil chronosequences, assuming that most of the conditions onsite (climate, source material, slope and topography) are consistent over the study period (taking in to account seasonal variation) with the exception of the additional time elapsed.

4.2 Pedogenic carbonate formation in artificial soils

Artificial soils are soils which have been significantly affected or wholly changed through human interaction (Rossiter, 2007). Many contemporary soils can be considered to be 'artificial' to a greater or lesser extent. For the purpose of the field sites discussed later in this chapter, the soils emplaced are wholly artificial, derived from industrial waste products. Urban soils and 'waste' sites are a useful setting for observing the formation of pedogenic carbonates in soil settings which are partly or wholly artificial. They provide an opportunity for *in situ* manipulation and monitoring of properties over well-constrained, easily observable geographic areas. Wholly artificial soils can be found in a limited number of places, for the purposes of this study the sites selected were inert waste landfills and recent urban demolition sites where the input materials were monitored and well-constrained.

Physical and chemical development of artificial soils often differs from their natural counterparts and may include extensive excavation, emplacement, compaction or translocation (Rosenbaum et al., 2003). It may also include the addition of anthropogenic or technogenic materials some of which may be considered contaminants or pollutants (Lorenz and Lal, 2009). Artificial soils, however, are also subject to many of the same pedogenic influences as 'natural' soils (described in section 4.1). Soil forming processes in urban soils may occur at accelerated rates and be mediated by agents which are not present in 'natural' settings (Effland and Pouyat, 1997). These complex formation histories create 'manipulated' soils which function differently from soils in the 'natural' landscape (Craul, 1992).

Much research on urban and anthropogenic soils to date has been 'comparative', focussing upon disparities in physical properties and the respective enhancement or depletion in nutrient cycling when compared to 'natural' counterparts (Yaalon and Yaron, 1966). Scharenbroch et al. (2005) highlights the detrimental effects that preparation and management of urban soils have on nutrient availability and organic C content. Pouyat et al. (2006) demonstrate the potential for soil organic carbon (SOC) to be significantly depleted through soil degradation in temperate urban settings, though it is proposed that urban soils under 'effective' management regimes (with water and nutrient supplies) may actually act as effective C stores, possessing higher SOC than natural analogues (Kaye et al., 2005). Few studies have focussed on the potential for

inorganic carbon sequestration by mineral carbonation in these settings (Manning 2008; Renforth et al., 2009).

4.3 Field sites as analogues for mineral carbon capture

Data relating to carbon storage in urban and artificial soils is currently limited to large scale assessment of organic carbon concentration (Poyuat et al., 2006; Lorenz and Lal, 2009) and small scale opportunistic determination of inorganic carbon (Renforth et al, 2009). Large-scale spatial investigation of inorganic carbon storage has not been undertaken previously. The following sections present data from field-scale investigations of inorganic C storage in artificial soils in the UK, with specific reference to the ability of artificial silicate minerals to form stable carbonates under the influence of short-term (months to years) weathering processes.

Study Sites

The study sites presented are Yarborough Landfill, an inert waste landfill on Tata Steel's operational site in Scunthorpe, UK, and Science Central, a development site overlain at the time of investigation by a thick layer of 'made ground' composed of demolition derived material, in Newcastle upon Tyne, UK (Figure 4.1).

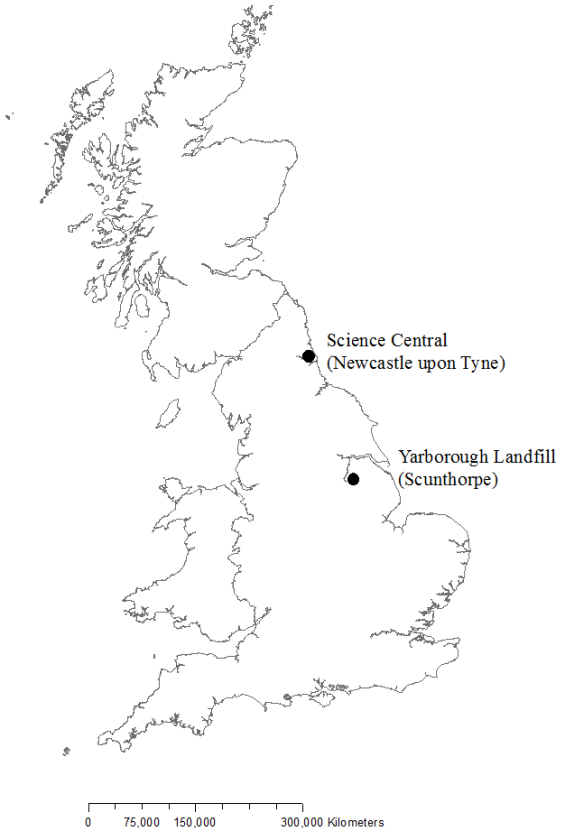

Figure 4.1 – Location of field sites described in Chapter 4

The following sections illustrate:

- Opportunistic intrusive sampling at an inert waste landfill, and high-resolution field-scale coverage of a 10 ha demolition site: to address spatial significance of carbonate formation processes and address heterogeneity
- Broad spectrum geochemical analysis of materials to determine the linkages between soil geochemistry and carbonate formation and to investigate the active geochemical processes

These studies have been reported in part in Washbourne et al., (2012) and Washbourne et al (in preparation), and are timely in light of increasing interest in urban and anthropogenic soils (Rawlins, 2008; Renforth et al., 2011a and references therein).

Yarborough Landfill, Scunthorpe

This work aimed to investigate the formation of carbonate minerals in artificial soils over time, determining changes over depth in soil profiles which have been established for a number of years. Intrusive sampling was carried out in 2010 and 2012. Fresh cut slag blocks were also suspended in leachate sampling wells onsite in order to determine the geochemical effects of exposure on this fresh material from a known time point. This approach addresses the depth constraint of many previous surveys, seeking to determine whether variations in carbonate formation occur below the depth to which soils are commonly surveyed (~1m).

4.3.1 Yarborough Landfill, Scunthorpe: Excavation

Yarborough and its environs form a 140 ha site to the east of Scunthorpe (UK National Grid Reference for the centre of the site is SE 915 127). The complex is bound to the west by the A1029 road, which is the main access to the works. The quarry area is bound to the north and east by agricultural land and to the south and west by the works. The site is currently occupied by structures and operations belonging to Tata Steel (formerly Corus Steel, British Steel). Yarborough landfill is located in the eastern part of the site. The site has been occupied by steelworks and quarrying operations since the mid-19th Century. Data presented in ground investigation reports (Terraconsult Factual Report on 2004/2005 Ground Investigation April 2005) confirms that made ground exists to significant depth across the site.

Geologically, the site is underlain by Quaternary and Recent windblown sands with interstitial silt and clay. These deposits occur sparsely around the study site, having mostly been disturbed during its long history of quarrying and industrial exploitation. The solid geology includes lower Jurassic formations comprised of three units: Coleby Mudstone Formation overlying Frodingham Ironstone and Scunthorpe Mudstone Formation. The Frodingham Ironstone was historically exploited commercially by a number of ironworks in the area. The hydrogeology of the site is complex, mostly influenced by the infilling of the formerly quarried areas. Some parts of the site are free-draining, while surface water is present in others. Bottesford Beck runs South-North along the landfill, and is culverted under the southern part of the current steelworks complex.

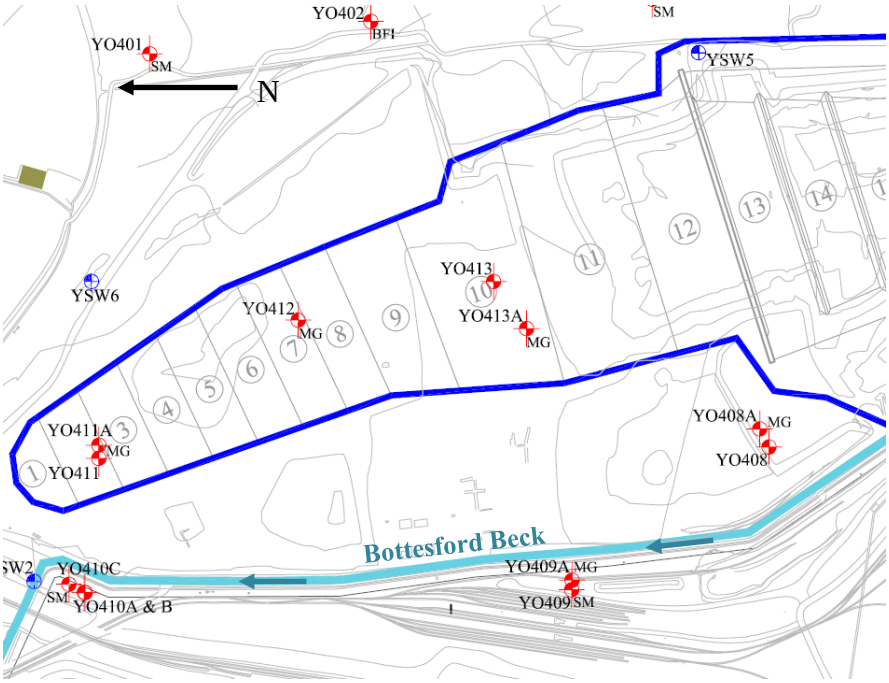

Figure 4.2 – Yarborough landfill map (TerraConsult Factual Report on 2004/2005 Ground Investigation), location of landfill cells ('YO…' labelled points indicate sampling wells. Numbered circles are cell references)

The site has been modified extensively over the life of the steelworks. The cells of Yarborough Landfill are built within the former site of the ironstone quarry which supplied the original works. Cell 1 construction began in 1989 and was completed in 1991, representing a potential site for carbonation of material over 19 to 21 years, measured to the survey dates of 2010 and 2012. The site has developed progressively over this time, spreading south as each landfill cell is filled and completed (Figures 4.2 and 4.3). The cells themselves are filled in 'lifts', layers of material of varying depth,

which are levelled out across the site in a regular stratigraphy. The surface of the site has undergone a great deal of remobilisation and it can be assumed that significant quantities of material have been removed and emplaced over time. The point of waste deposition is taken as an approximate 'time zero' for the carbonation of material onsite, therefore by knowing the dates between which material was emplaced in specific cells, some estimation can be made as to the amount of time elapsed to the current state.

Figure 4.3 – Location of trial pits in Cell 1 of Yarborough Landfill, Scunthorpe (Google Maps 2010) The square features are stacks of girders, stored periodically in this area of the site

Method

Following field reconnaissance and discussions with Tata Steel, Scunthorpe (December 2009, April 2010) and environmental consultancy firm TerraConsult, St Helens (February 2010) who oversaw recent developments on the landfill, intrusive sampling of existing waste cells was carried out to assess their temporal development. Laboratory analysis of slag material excavated from Yarborough Landfill on 4th June 2010 and 21st February 2012 is presented as a summary of field notes and analysis of bulk and depth-profile samples from the excavations.

An intrusive sampling plan was designed to examine the in *situ* behaviour of landfill material after known and incrementally increasing periods of weathering and maturation. The initial project plan aimed to carry out intrusive sampling to ≤ 6m depth, in addition to a programme of normal site operations implemented at a suitable agreed location. This was to be carried out at intervals between 2010 and 2012. In 2010 the maximum depth attained in the trial pits was 0.95m owing to unfavourable ground conditions; in 2012 the maximum depth was approximately 3.5m.

Excavation of a small portion of the surface of Cell 1, the oldest cell in the landfill complex was carried out with the use of a bucket excavator. Observations of ground conditions / mineral deposition were logged photographically and diagrammatically throughout the excavation (Appendix C). Samples of 0.5-1.0 kg were taken at regular intervals throughout the exposed profile.

Excavation of trial pits was carried out using a CAT hydraulic excavator, with four pits being dug in 2010 (YAR/TP1-4) and one pit in 2012 (YAR/TP5). Trial pits 1 and 2 were unsuccessful, failing to break the concreted surface layer in YAR/TP1 and encountering clay in YAR/TP2. Samples were collected from trial pits 3 (YAR/TP3) and 4 (YAR/TP4) across exposed depth profiles at 0.1-0.15m intervals to maximum depth 0.95m. Samples were collected at 3 depth points from YAR/TP5 to maximum depth 2.5m as allowed by restrictions imposed though working in unsupported excavations (BS 6031:2009).

Materials collected were bagged onsite and transported back to Newcastle University for air-drying. Material from TP3, TP4 and TP5 was riffled to produce representative sub-samples, approx. 150g. All loose samples were air dried, separated with pestle and mortar and sieved to 2mm prior to analysis. Samples were analysed for bulk carbonate by acid digestion using an Eikjelkamp Calcimeter (methodology detailed in methods section of Appendix A), which had been calibrated immediately prior to analysis, to BS 7755-3.10:1995 ISO 10693:1995. Samples were reacted with 0.4M HCl and $CaCO_3$ content inferred from volumetric measurement of CO_2 gas evolved

Thermo-gravimetric analysis was carried out using a Netzsch Jupiter STA449C TG-DSC system connected to a Netzsch Aeolos 403C QMS for the mass spectral analysis of evolved gas (method as described in Appendix A)

Concreted material recovered from YAR/TP 2 and 3 were sent for polished thin section preparation at Edinburgh University. Thin sections were analysed using a optical petrographic microscope and FEI/Philips XL-30 Field Emission Environmental Scanning Electron Microscope at Newcastle University Advanced Chemical and Materials Analysis unit (full method in Appendix A).

Stable isotope analysis (C and O) was carried out on 9 samples from the Yarborough landfill trial pits. Representative samples were ground using Tema laboratory disc mill and sieved to <63µm. 3 samples (of differing ages) were packed and sent to Iso-Analytical Ltd., Cheshire for C and O stable isotope analysis using the methodology supplied in Chapter 3 (Appendix A).

Table 4.3 – Summary trial pit log

Trial Pit	Description	Depth
YAR/TP1 (2010)	Central trial pit located in south-central area of the site. Difficulty excavating compacted surface material. Hard pan encountered at approximately 0.5m. Pit terminated.	0.5m
YAR/TP2 (2010)	Central trial pit located at northern boundary of the site, to exploit areas not compacted by vehicular traffic. Slag cover present to shallow depth. Mudstone / clays, natural geology or liner, encountered at very shallow depth demarking the edge of the original cell excavation. Pit terminated.	~0.5m
YAR/TP3 (2010)	Eastern trial pit located towards the central–eastern boundary of the site (adjacent to loose spoil heap). Surface material broken through with relative ease. Pit excavated to approximately 1.0m before hard pan encountered. Hard pans / laminated deposits recovered from approx. 0.5-0.95m. Profile, point and bulk samples collected.	~1m
YAR/TP4 (2010)	Eastern trial pit located within slope of loose slag heap bounding Cell 1 to the east. Material excavated with ease. Large notch cut. Profile, point and bulk samples collected	~1m
YAR/TP5 (2012)	Later pit located in the north east of the site, adjacent to a gas inspection well. Surface material broken through with some difficulty due to presence of hard pan at 0.2-0.3m. Pit excavated to ~3.5m, breaking through levels of heavily cemented granular slag material and un-engineered clay.	~3.5m

Results

Acid digestion results from analysis of samples from YAR/TP3 and TP4 collected during site excavations show that the top ≤ 0.95m of soil across the active Yarborough Landfill provided a maximum value of 27.61 % wt $CaCO_3$ and average 11.24 ± 5% wt $CaCO_3$. TP5 yielded maximum and minimum values of 25.65 % and 6.24 % wt $CaCO_3$, with an average of 12.99 ± 7.97 % wt. Calcium carbonate concentration appears to

show several trends with depth as seen in the YAR/TP3 and 4 data shown in Figure 4.4a, and YAR/TP5 data shown in Figure 4.4b.

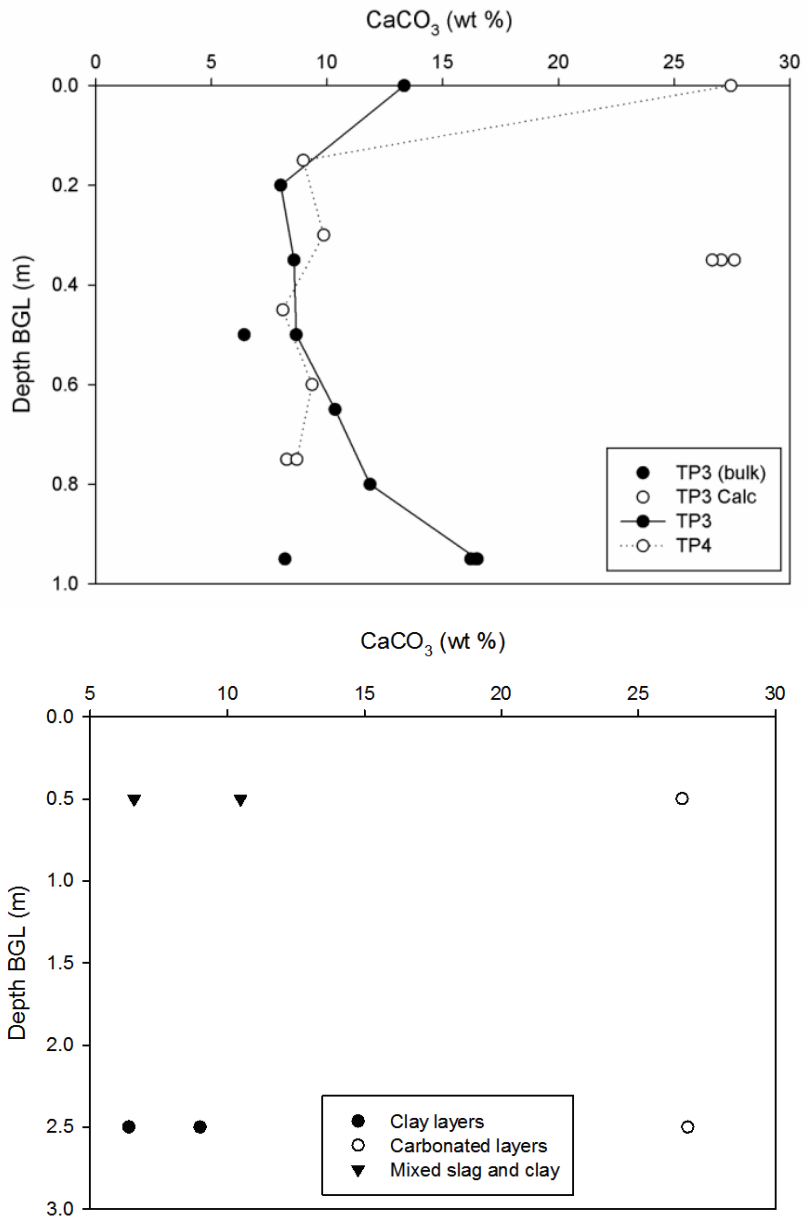

Figure 4.4a, b – a) 2010 Variation in calcium carbonate concentration with depth. 'YAR/TP' is the trial pit reference. 'Bulk' refers to bulk samples taken from excavator spoil across large depth intervals. 'Calc' refers to results taken from visible calcium carbonate 'hotspots' b) 2012 Variation in calcium carbonate concentration with depth in YAR/TP5. Open symbols indicate observed regions of carbonated slag, filled triangle indicate mixed slag and clay blocks, filled circles indicate the presence of clay layers

Both profiles in Figure 4.4a illustrate high calcium carbonate concentrations in samples taken from the near surface (≤ 0.1m), 13.33% wt $CaCO_3$ in YAR/TP3 and 27.45% wt $CaCO_3$ in YAR/TP4. From 0.15-0.8m both profiles illustrate similar calcium carbonate concentrations, between 8 and 11% wt $CaCO_3$, with little variation between the trial pit locations. At depths greater than 0.8m YAR/TP3 illustrates a trend towards increasing $CaCO_3$ concentration, reaching values of 16.49% wt $CaCO_3$. The sample log for

samples from TP5 (Figure 4.4b) shows the presence of a number of intermixed layers of slag and clay material. Where slag persists, the calcium carbonate content measured in the material does not seem to be strongly affected by depth between 0.5 and 2.5m.

Figure 4.5 presents the evolved gas data for CO_2 and H_2O evolution during TG-QMS analysis of samples taken from TP3 and TP4. A CO_2 peak is present for all samples at around 700°C indicating the presence of carbonate. A peak in the H_2O trace between 400 and 500°C indicates the likely presence of hydrated mineral phases such as portlandite.

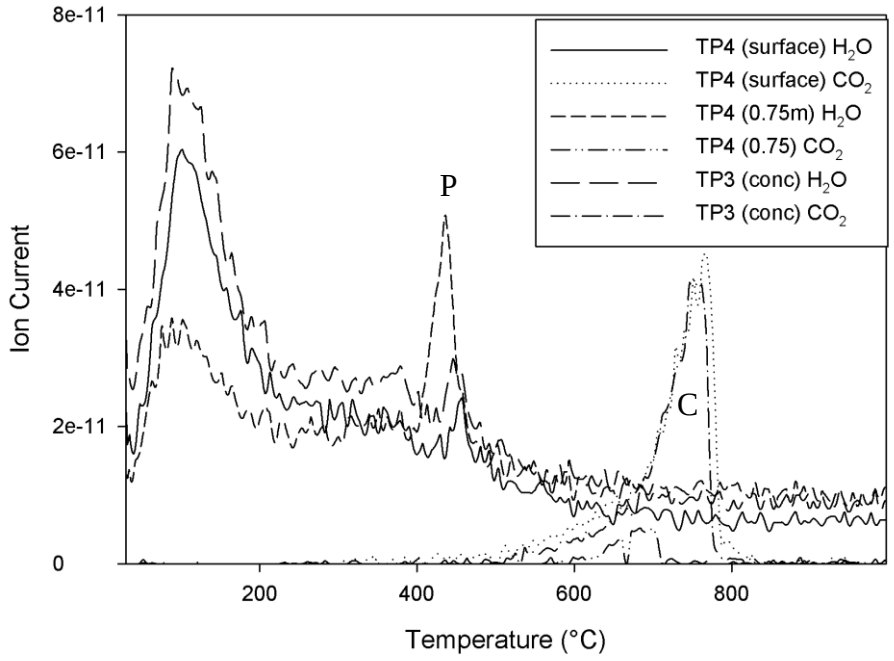

Figure 4.5 – Quadrupole mass spectrometer (QMS) traces for CO_2 and H_2O in trial pits 3 and 4. P = hydrated minerals such as portlandite, C = carbonate

Thin section analysis demonstrated the presence of significant calcium carbonate, precipitated around the margins of the material at various scales. In Figure 4.6, the white-orange material contains a significant proportion of calcite. ESEM analysis enabled these regions to be studied in greater detail, confirming that these structurally disordered regions were mixtures of calcium carbonate and weathered silicate minerals (analytical details in Appendix C) as seen in Figure 4.7.

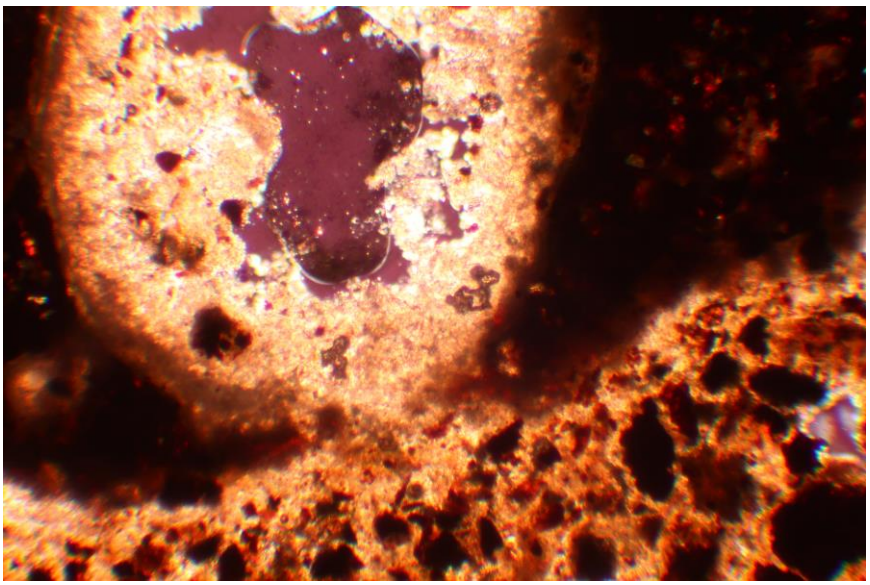

Figure 4.6 – YAR/TP3 Optical image in thin section under petrographic light microscope illustrating carbonate precipitation

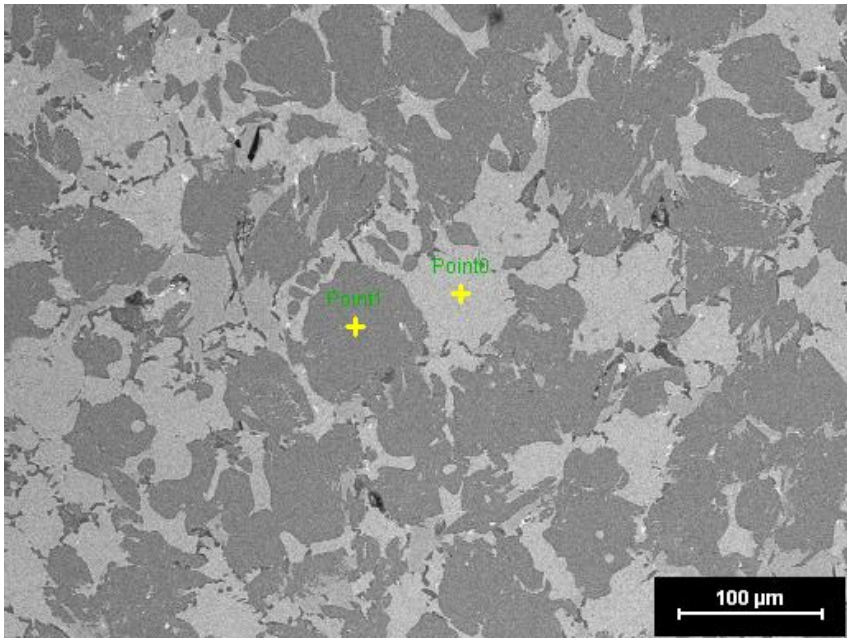

Figure 4.7 – Backscatter electron image of polished thin section. Environmental Scanning Electron Microscope image YAR/TP3 0-50 x 200 (point analysis for Point 0 and Point 1 are included in Appendix C)

Stable isotope analysis yielded $\delta^{18}O$ values between -13.46‰ and -16.95‰ and $\delta^{13}C$ values between -14.93‰ and –18.68‰ against Vienna Pee-Dee Belemnite (V-PDB). As seen in Figure 4.8, very little variation in C isotope signature with depth was observed other than at the surface of the site. All of samples collected at the site were shown to be significantly depleted with respect to both ^{18}O and ^{13}C.

End member analysis was used to determine the proportion of C present in the carbonates derived from atmospheric sources as 64.65 ± 4.16%. These were derived using the following end-member figures: lithogenic end member: $\delta^{18}O$ = -0.0‰, $\delta^{13}C$ =

-0.0‰ (Andrews, 2006; Renforth et al., 2009), hydroxylation (high pH) end member: $\delta^{18}O$ = -20.5‰ (Dietzel et al., 1992; Udowski and Hoefs, 1986; assuming meteoric water $\delta^{18}O$ = -7.8‰ vs SMOW (Darling et al 2003), $\delta^{13}C$ = -25.3‰.

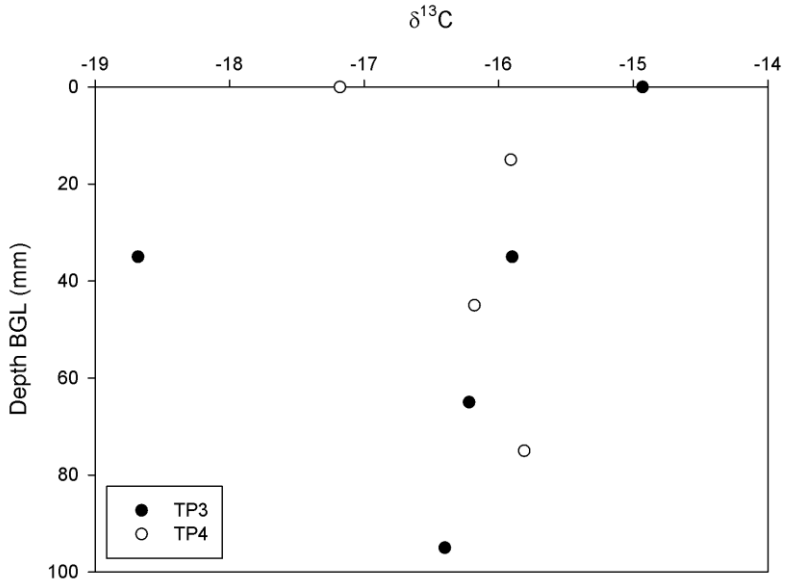

Figure 4.8 –Yarborough Landfill: IRMS data. $\delta^{13}C$ plotted against sample depth.

Discussion

Fieldwork at the Yarborough landfill site has shown that calcium carbonate formation does occur in artificial soils of appropriate parent chemistry (Ca-rich), in temperate settings. It also demonstrates the complexity of carbonate formation with depth at sites of this type, showing that a great deal of heterogeneity can arise from mixing of materials during deposition. Due to the nature and history of infilling in 'lifts', carbonate formation is shown to have occurred to significant depth (<2.5m) suggesting the possibility for large cumulative C values to be extrapolated for sites where carbonate formation is only confirmed at the surface. Whilst beyond the scope of this report, and robust data is not available for this site regarding the exact nature of infilling for Cell 1, the method for filling the cells has implications for engineering design protocols.

As the data for carbonate formation to significant depth onsite is sparse, an estimate was made of the carbon capture potential in the upper 0.95m of the site (where properties are better constrained). It can be estimated that across the in-filled Yarborough Landfill area (approx. 34 ha) to 0.95m depth there is a potential presence of 13,758 T C bound as carbonate. Assuming the completion of the study cell occurred in 1991, this implies a calcium carbonate formation rate equivalent to 21 T C ha^{-1} a^{-1}.

It is noted that the Yarborough landfill site has accumulated significant quantities of calcium carbonate during its lifespan. It can only presently be estimated whether calcium carbonate concentration at depth remains at high levels, but investigations in 2012 suggest that this may be the case to ≤2.5m. This has formed over a relatively short time period, with no obvious C contribution other than from atmospheric sources due to a scarcity of biological factors. The quantitative and formation rate data attained during this site visit match well with findings from similar field settings (Washbourne, 2009 (MSc thesis)), including the stockpile analysis from this report. This is encouraging in the assessment of BOS slag with respect to its use in carbon sink engineering.

Summary

- Average calcium carbonate content 11.24 ± 5% wt $CaCO_3$
- Maximum calcium carbonate content 27.61 % wt $CaCO_3$
- Trends in calcium carbonate content with depth observed include high concentration at surface in both TP3 and TP4, 8-10 % wt $CaCO_3$ concentration between 0.5-0.8m and some evidence of increasing $CaCO_3$ > 0.8m.
- Stable isotope analysis yielded $\delta^{18}O$ values between -13.46‰ and -16.95‰ and $\delta^{13}C$ values between -14.93‰ and –18.68‰ against Vienna Pee-Dee Belemnite (V-PDB). This suggests that the proportion of C present in the carbonates derived from atmospheric sources is 64.65 ± 4.16%.
- There is a significant presence of calcium carbonate in the artificial soils which form Yarborough Landfill. This has formed over a relatively short time period, with no obvious C contribution than from atmospheric sources. This is encouraging in the assessment of BOS slag with respect to its use in carbon sink engineering.

4.3.2 Yarborough Landfill, Scunthorpe: leachate well experiments

This study aimed to determine the effects of submersing fresh slag material in the leachate developed on the Yarborough landfill site, to better understand the contemporary geochemistry of the system and its response to perturbation. In the newer parts of the landfill the cells are fitted with monitoring wells which are routinely used to

test the quantity and composition of gaseous and liquid emissions from the landfill site. These points are mandatorily monitored at regular intervals, with the data being used to ensure compliance of the landfill with contemporary regulation (EU Landfill Directive (EEC/1999/31/EC); Landfill Regulations (England and Wales) 2002). The leachate wells in the newly developed, engineered part of the Yarborough landfill are large and accessible, therefore providing potential sites for experimental work of this type.

Method

An experiment was devised to investigate the consequences of leachate interaction with landfill material, and other substrates, in field sites where artificial silicate minerals are present in large quantities. A number of artificially machined, solid slag blocks (Appendix C) were suspended in the leachate wells in the more recent, active region of the landfill site (Cells 12 and 13). Many of the older cells do not include leachate management systems or suitable monitoring points where this work could be carried out.

6 x slag blocks (approx. 0.2 x 0.1 x 0.05 metres) were cut from a larger fragment of fresh slag material, taken from the Yarborough landfill site on an earlier occasion, and suspended in active leachate sampling points. Multiple blocks were used in order to allow for comparison between samples, and as an insurance against loss or damage of blocks during general plant operation. After an extensive site survey, 3 blocks were emplaced on the landfill (Table 4.4). The emplacement of the remaining blocks was hindered by a lack of suitable monitoring points where leachate levels were consistently high enough to ensure submersion and the blocks would not be removed or disturbed as part of normal site activities. Many of the potential sites including gas monitoring wells did not contain sufficient levels of leachate, contained obstructions or were not wide enough to allow access for the experimental apparatus, or were not sufficiently vertical to allow the block to sit unimpeded.

Figure C.6 Appendix C, illustrates the general design of leachate well trials. Slag blocks were suspended in a cage consisting of inert, and non-corrodible plastic geotextile inside the leachate well to below average leachate surface level. Suspending rope was marked out in metre lengths to ensure depth was accurately measured and that sufficient leeway was given for variation in leachate level over time.

Visual monitoring and sampling were to be carried at 6 month intervals and removal and final analysis of all remaining blocks was to be carried out after 1.5-2 yrs. However, after emplacement for 12 months, notice was given that the landfill area surrounding the blocks was due for development and all remaining blocks were pre-emptively removed. In every case the block had disintegrated, with the fragments returned contained by the geotextile mesh.

Table 4.4 –Log of slag blocks in leachate wells onsite at Yarborough Landfill

Ref	**Location**	**Date emplaced**	**Date removed**
YAR 1	Cell 13 leachate well 1	Oct 2010	April 2011
YAR 2	Cell 13 leachate well 2	Oct 2010	Oct 2011
YAR 4	Cell 12 leachate lagoon	Oct 2010	Oct 2011

3 samples (at time = 0, 6 months and 12 months) were analysed for bulk carbonate by acid digestion using an Eikjelkamp Calcimeter (methodology detailed in methods section of Appendix A), which had been calibrated immediately prior to analysis, to BS 7755-3.10:1995 ISO 10693:1995. Samples were reacted with 0.4M HCl and $CaCO_3$ content inferred from volumetric measurement of CO_2 gas evolved. The fourth recovered sample taken from a leachate lagoon setting was not analysed, as it was deemed that the sample had likely been covered by a layer of sediment throughout part of the experimental period, altering the conditions sufficiently to render the data incomparable.

3 samples were sent for polished thin section preparation at Edinburgh University. Thin sections were analysed using a FEI/Philips XL-30 Field Emission Environmental Scanning Electron Microscope at Newcastle University Advanced Chemical and Materials Analysis unit (full method in Appendix A).

Results

Acid digestion results from analysis of samples from the leachate wells provided a maximum value of 3.95 % wt $CaCO_3$ (time = 12 months), minimum value of 2.04 % wt $CaCO_3$ (time = 0 months) and average 3.04 % wt $CaCO_3$. Carbonate concentration appeared to increase with time, as shown in Figure 4.9 which compiles data from two separate blocks with approximately similar initial compositions and dimensions, from the original value to that observed after 12 months exposure.

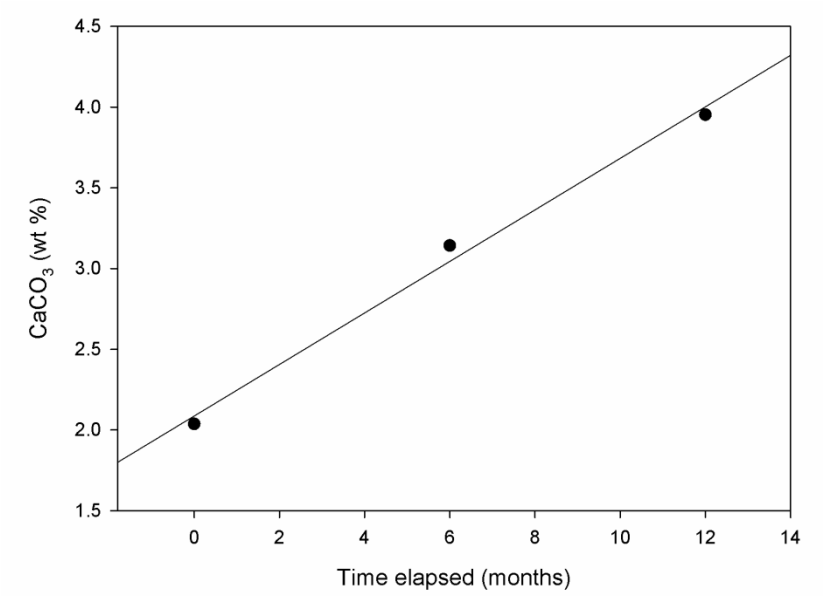

Figure 4.9 – Calcium carbonate concentration in slag block material (% wt) following suspension in leachate wells for 6 and 12-month periods – leachate lagoon sample not included due to difference in conditions

As in the previous section, thin section analysis demonstrated the presence of significant quantities of calcium carbonate, precipitated around the margins of the material at various scales. ESEM analysis allowed semi-quantitative readings to be taken around the reacting boundaries of slag fragments as shown in Figures 4.10 and 4.11. The plots in Figure 4.11 illustrate the variation in relative concentration of a number of different elements across the reacting boundary in Figure 4.10.

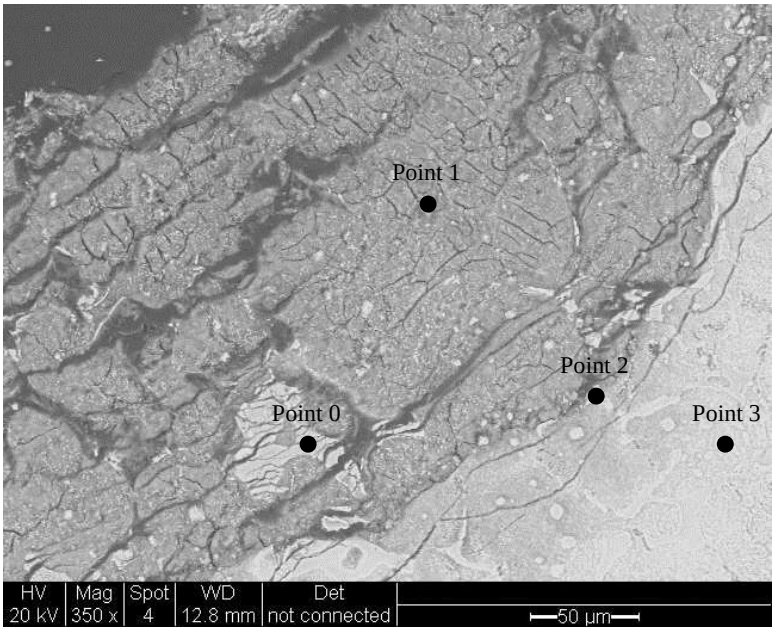

Figure 4.10 – Back scattered electron image of slag block material illustrating points at which elemental analysis was carried out

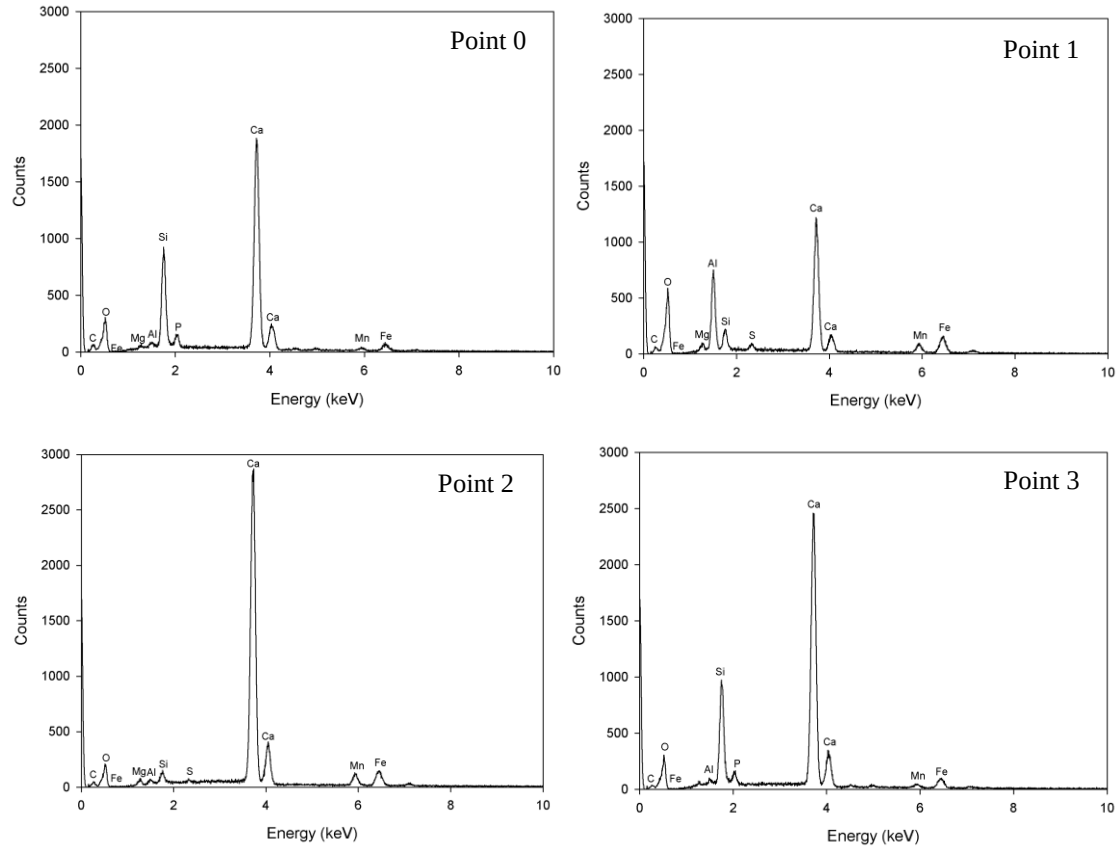

Figure 4.11- Elemental analysis points 0-3 from Figure 4.10

Discussion

Carbonate content within the blocks appeared to increase over time, indicating that carbonate materials were being precipitated within the structure of the blocks. Figure 4.9 can be interpreted as a linear plot (r^2 = 0.9922) of calcium carbonate content increasing over time, although there is insufficient data to fully verify the validity of the inferred strong linear relationship.

ESEM analysis of thin sections (Figure 4.10) showed that a number of geochemical factors were acting on the material. Calcite formation had occurred on the surface of the material, in many places forming a thick, but easily fractured layer. The region seen in Figure 4.10, viewed under ESEM, was analysed for bulk elemental data. Points 0 and 3, in the lighter grey regions, seem to represent a Si-enriched zone. At point 0 Ca and other elements appear to have been leached suggesting that this region is part of the core which has been 'rafted' away from the reacting face. Point 2 shows high concentrations of Ca, possibly illustrating the presence of the interface between reacted and unreacted materials. Point 1 illustrates significantly lower levels of Ca than the other points, but is richer in O and Al, suggesting it is likely to be evidence of secondary mineral deposition. Carbonate precipitation may also have occurred elsewhere in the system, not

associated with the surface of the block, as materials were able to move freely in and out of the reacting block.

While the geochemical data collected from the leachate wells at the Yarborough Landfill site (discussed in Chapter 5) show that much of the site is saturated or supersaturated with respect to calcite, dissolution of Ca from freshly supplied materials still occurs suggesting the movement of fluids around the site and carbonation processes occurring at depth.

Summary

- Average calcium carbonate content 3.04 % wt $CaCO_3$
- Maximum calcium carbonate content 3.95 % wt $CaCO_3$
- Calcium carbonate content increased with increasing periods of exposure to leachate well fluids, up to 12 months
- ESEM analysis demonstrated the presence of weathering rims of material around the margins of the block fragments. This demonstrates that Ca is progressively leached from the material, however a reaction rim has been evidenced which is likely to impede the rate at which this occurs.

4.3.3 Science Central Newcastle

This section presents a novel investigation of pedogenic carbonate formation in anthropogenic soils with high-resolution, spatial sampling carried out at two temporal points on a single site, September 2010 and March 2012. This approach addressed the significance of carbonate formation processes and source material heterogeneity, while allowing spatial comparison over an 18 month sampling period. Broad spectrum geochemical analysis of materials is presented, to corroborate carbonate content and formation pathways and determine and quantify the linkages between soil geochemistry and carbonate formation processes over time.

Science Central Newcastle (excavations and time point data)

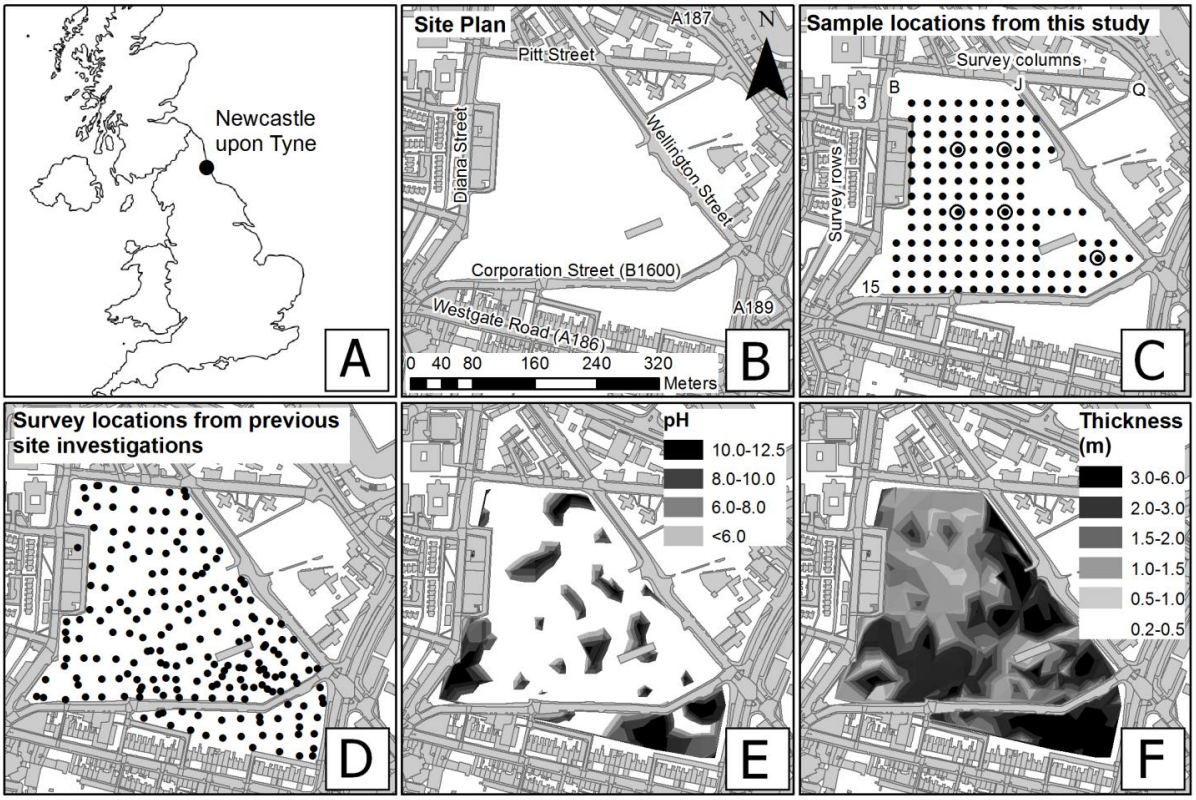

Figure 4.12 – A) Location of study site, B) site layout C) survey points used in this study, D) survey points from previous site investigations, E) soil pH findings from previous investigation and F) thickness of made ground across the site from previous investigations

The study site, "Science Central", is a 10 ha development located in the central business area of Newcastle upon Tyne (UK; National Grid Reference: NZ 2401 6404 Figure 4.1). The site was most recently occupied by structures owned and operated by Scottish and Newcastle Breweries plc, which were demolished in 2007. A large proportion of material derived from demolition was crushed and spread on the site as a layer of 'made

ground' from 0.2-6.0m in thickness. Surface elevation and depth profile information from intrusive ground investigations (Figure 4.12d) carried out by Norwest Holst Soil Engineering Ltd. (October 2005 Project No. F15481A) was used to estimate that approximately one million tonnes (Mt) of demolition-derived material is present at the site. During its long history, the site hosted numerous heavy and light industrial works (including iron and steel works, food manufacturers, the North Elswick Colliery (1805-1940's) and finally the Scottish and Newcastle Brewery, which closed in 2005. A contaminated land report compiled by Norwest Holst Soil Engineering Ltd. (July 2009 Project No. F15481B) presented a suite of soil analyses, identifying areas with elevated soil pH (Figure 4.12e) and was used to determine the possible presence of contaminants. Although generally below trigger levels, the presence of arsenic (sporadic), PAHs and other hydrocarbon species were noted.

Geologically, the site is underlain by Devensian Till, superimposed upon bedrock of Carboniferous age (High Main Post Member and Pennine Middle Coal Measures Formation) which was historically mined for coal. The hydrogeology of the site is complex; although the emplaced material is free-draining, it overlies in-filled basement construction within natural clays which reduce the permeability of the site to rain water and strongly influence groundwater behaviour (water table varies from 2.4-12.0m bgl). The site slopes significantly to the south east, with a gradient of 5%, providing a preferential drainage path for dissolved transported materials.

The site has not been significantly modified since the end of the demolition programme in 2007. Some material has been remobilised and surfaces have been compacted by vehicular movements, and it can be assumed that the physical properties of the C&D waste are as they were at the time of deposition. The point of demolition is taken as 'time zero' for carbonate formation, with all newly-formed material assumed to have developed between this point and the time of sampling (the validity of this assumption will be discussed later). Prior to demolition, carbonation would have been limited by the exposed surface area of reactive materials and their potential for exposure to the external environment. Demolition and processing of resultant material is expected to have significantly increased both parameters prior to eventual deposition.

Methods

Full methodologies are included in Appendix A, summaries of specific procedures and analytical conditions are listed below. The number of samples involved at each stage is listed in Table 4.5.

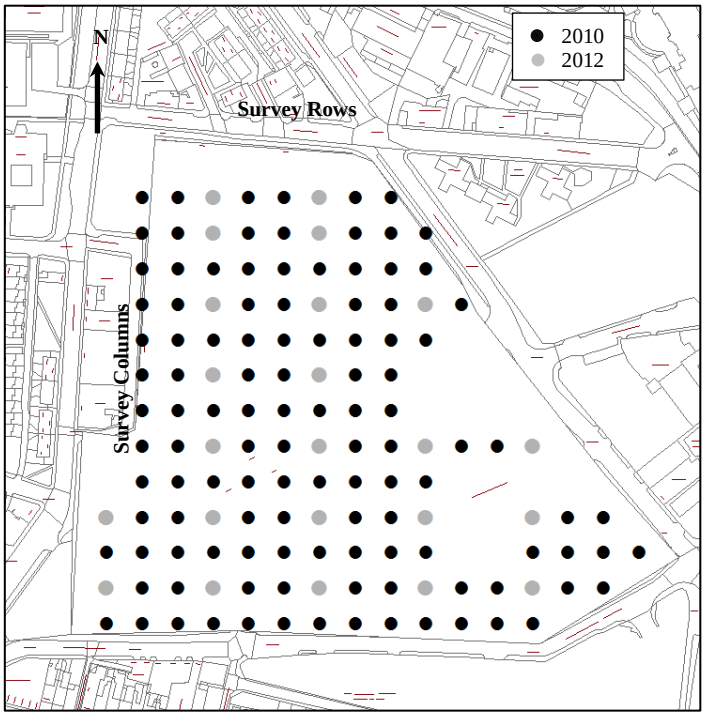

Figure 4.13 – 2010 sample points (Washbourne et al 2012) with 2012 sample points overlaid

Table 4.5 – Sample and analysis log for data presented in this chapter

	2010	**2012**
Surface samples collected	72	23
PSD samples collected	5	0
Calcimeter analysis	72	23
Leco analysis	72	23
PSD analysis	5	0
X-ray fluorescence	38 (+7 repeats in 2012)	7
X-Ray Diffraction	4	4
TG DSC QMS	6	6
IRMS	47 (+7 repeats in 2012)	7

A systematic sampling survey was constructed, dividing the site in to 72 accessible sampling points. 72 samples were taken in 2010, and 23 in 2012, resampling areas previously covered by the earlier survey (shown in Figure 4.13). Sample points were logged using Leica GPS equipment (Leica GS15 with a CS16 controller with a Smartnet RTK correction 25mm accuracy). 1-2kg of material was collected between 0-100mm depth using hand tools and wet sieved to <2mm onsite. 2 trial pits were dug to ~1m depth using a mechanical excavator with back-actor, samples were collected at 10cm

depth intervals. All samples were air dried and analysed for bulk carbonate using an Eijkelkamp calcimeter (in accordance with BS 7755-3.10:1995), and organic and inorganic carbon using a Leco CS-244 Carbon / Sulfur Determinator. In 2010 5kg of material was taken at 5 points indicated on Figure 4.12 (circled points, grid refs (I6, I10, E6, E10, O13). These samples were air dried and particle size distribution (PSD) analysis carried out to BS 1377-2:1990.

X-Ray Fluorescence (XRF) analysis was conducted by the University of Leicester Department of Geology using a PANalytical Axios Advanced XRF spectrometer. Samples were mixed with 1:5 ratio of flux (80% lithium metaborate, 20% lithium tetraborate). The samples and flux were ignited at 1100 °C and cast into fused beads. The machine was calibrated using a range of certified standards, including British Chemical Standards (BCS) BCS375 (sodium feldspar), BCS376 (potassium feldspar) and BCS372/1 (hydrated cement)

X-Ray Diffraction (XRD) analysis was carried out at Newcastle University School of Chemical Engineering and Advanced Materials. Analysis was carried out using a PANalytical X'Pert Pro Multipurpose Diffractometer fitted with an X'Celerator and a secondary monochromator, operating with a Cu anode at 40 kV and 40 mA. Spectra were acquired for Cu Kα (λ = 1.54180 Å) or Cu Kα1 (λ = 1.54060 Å) radiation over 2-70°2θ with a nominal step size of 0.0167°2θ and time per step of 100 or 150 seconds. All scans were carried out in continuous mode using the X'Celerator RTMS detector.

Thermogravimetry-differential scanning calorimetry coupled with quadrupole mass spectrometry (TG-DSC QMS) was conducted at Newcastle University. Samples were analysed using a Netzsch Jupiter STA449C TG-DSC system connected to a Netzsch Aeolos 403C QMS for the mass spectral analysis of evolved gas. Samples were heated from 30°C to 1000°C at a rate of 10°C min^{-1} in an atmosphere of 80% He + 20% O_2 (purge gas, flow rate 30 ml min^{-1}). QMS was operated in full scan mode over the range m/z 10-300, and mass spectrometric data were acquired and processed using Quadstar 422 IPI software.

Samples were analysed for $\delta^{13}C$ and $\delta^{18}O$ by Iso-Analytical Ltd (Cheshire UK) www.iso-analytical.co.uk/, using a Europa Scientific 20–20 continuous-flow isotope ratio mass spectrometer (IRMS); IA-R022, NBS-18 and NBS-19 were used as reference

materials for analysis. Replication had a standard deviation better than 0.12‰ and all of the reference material analyses were within two standard deviations of the expected results. Results were recorded relative to the Vienna Peedee Belemnite scale (V-PDB).

Results

Soil Classification

All materials encountered onsite in 2010 were classifiable as 'made ground' or anthropogenic soils (BS EN ISO 14688:2). Most samples were recorded as grey-brown (10YR 6.5 2 Munsell soil colour chart) made ground, although soil samples taken from column B of the sampling grid (Figure 4.13) differed on visual inspection, (2.5YR 7 2 Munsell soil colour chart) being yellowish and with visible carbonate formation. Following PSD analysis of the soil onsite all samples were classified by BS 1377-2:1990 as gravelly sandy soils.

Mineralogical and Elemental Analysis

XRF analysis, reported as oxides of major elements, in 2010 found SiO_2, CaO and MgO concentrations of 56.56 ± 6.27 wt %, 13.90 ± 3.00 wt%, and 1.91 ± 1.81 wt %, and in 2012 found SiO_2, CaO and MgO concentrations of 36.56 ± 5.78 wt %, 21.07 ± 3.07 wt%, and 2.64 ± 1.83 wt %, respectively (Table 4.6). This demonstrates a strong proportional depletion in the quantity of Si present in the surface soils between 2010 and 2012 (-20%). Ca and Fe show increases (+7.17 and +0.80 respectively). Eq. 4.1 predicts that this may occur due to the removal of Si in solution, however the dissolution, transport and precipitation of phases in this multi-component system is likely to be more complex. In a simple system like Eq. 4.1 a 20% decrease in Si, assuming full transport out of the system in solution, could lead to an observed enrichment in Ca of up to ~14%. When the standard deviation is taken in to account, the changes in concentration of MgO, Na_2O, K_2O and SO_3 are non-significant (71-100% of variability is within 1 standard deviation). 43-57% of the variability in TiO_2, Al_2O_3, MnO and P_2O_5 is also within 1 standard deviation of the mean.

A strong negative correlation between CaO and SiO_2 content was noted in both 2010 and 2012 data (2010 r^2 = 0.85, 2012 r^2 = 0.80; Figure 4.14) suggesting the significant presence of calcium carbonate, as opposed to silicate, minerals. The relationship between MgO and SiO_2 also suggests a large degree of partitioning in to carbonate minerals. The slope of the regression lines change between 2010 and 2012, with a

particularly marked decrease in the proportion of SiO_2 with respect to MgO. Loss on Ignition (LOI) data are consistent with the total carbon content of the samples, and have been verified in triplicate by additional thermo-gravimetric procedures, forming a 1:1 gradient when plotted graphically as %LOI vs $\%CO_2$ (not shown).

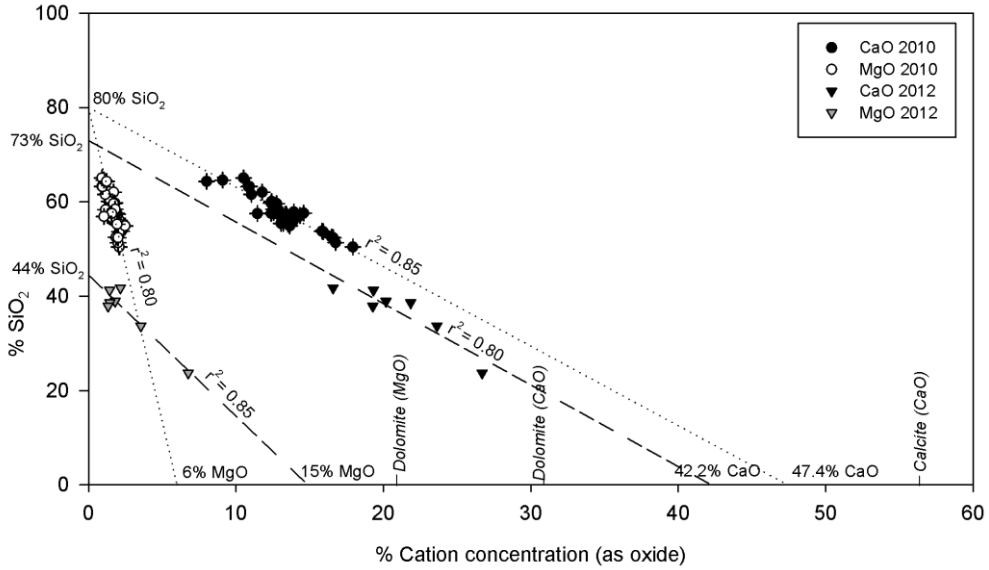

Figure 4.14 - CaO and MgO versus SiO_2 (quartz) content of samples from Science Central, illustrating likely mineral phases present

Table 4.6 - XRF Data Summary 2010 and 2012

	SiO_2	TiO_2	Al_2O_3	Fe_2O_3	MnO	MgO	CaO
Av. % 2010	56.56	0.43	6.63	3.83	0.08	1.91	13.90
St Dev	6.27	0.08	1.21	0.34	0.01	1.18	3.00
Av. % 2012	36.56	0.56	8.70	4.63	0.10	2.64	21.07
St Dev	5.78	0.12	1.91	0.53	0.01	1.83	3.07
Δ Av. %	-20.00	0.13	2.07	0.80	0.02	0.73	7.17

	Na_2O	K_2O	P_2O_5	SO_3	LOI	Total
Av. % 2010	0.41	1.16	0.09	0.22	14.95	100.1
St Dev	0.06	0.22	0.01	0.07	3.68	0.36
Av. % 2012	0.40	1.26	0.13	0.21	23.48	99.73
St Dev	0.05	0.28	0.02	0.08	3.71	0.36
Δ Av. %	-0.01	0.10	0.04	-0.01	8.53	-0.44

TG-DSC-QMS investigation of the materials has shown that all samples analysed in 2010 and 2012 exhibited similar thermo-gravimetric profiles. Peaks characteristic of hydroxyl water-loss and decarbonation reactions occur at 300-400°C and approximately 750°C respectively (Figure 4.15) indicate the presence of hydrated minerals such as portlandite ($Ca(OH)_2$) in the first instance and carbonate in the second. QMS data (Figure 4.15) show strong evolution of CO_2 at the 750°C temperature interval,

confirming the presence of carbonates. The mass loss at 750°C is consistent with the presence of carbonate attained through other methods in the following section.

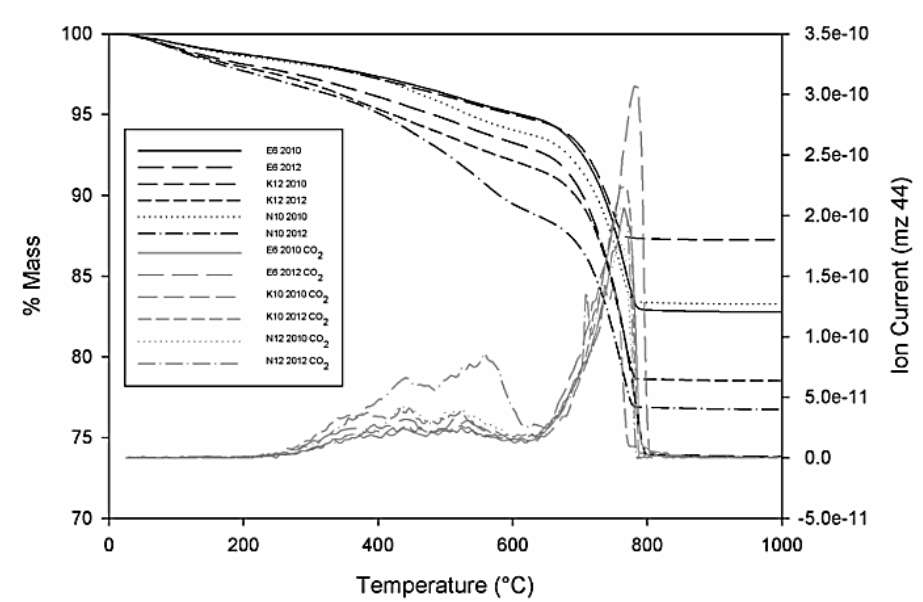

Figure 4.15 – Combined thermogravimetric curve and quadrupole mass spectrometer data for CO_2 evolution from tested samples

Mineralogical analysis by X-Ray Diffraction (XRD) demonstrated the presence of a number of mineral phases within the analysed soils (Figure 4.16; major diagnostic peaks have been labelled). The observed phases are dominated by silicate and carbonate minerals: quartz and dolomite are present, with calcium carbonate identified as calcite. Clay minerals are also likely to be present, with kaolinite identified in all samples.

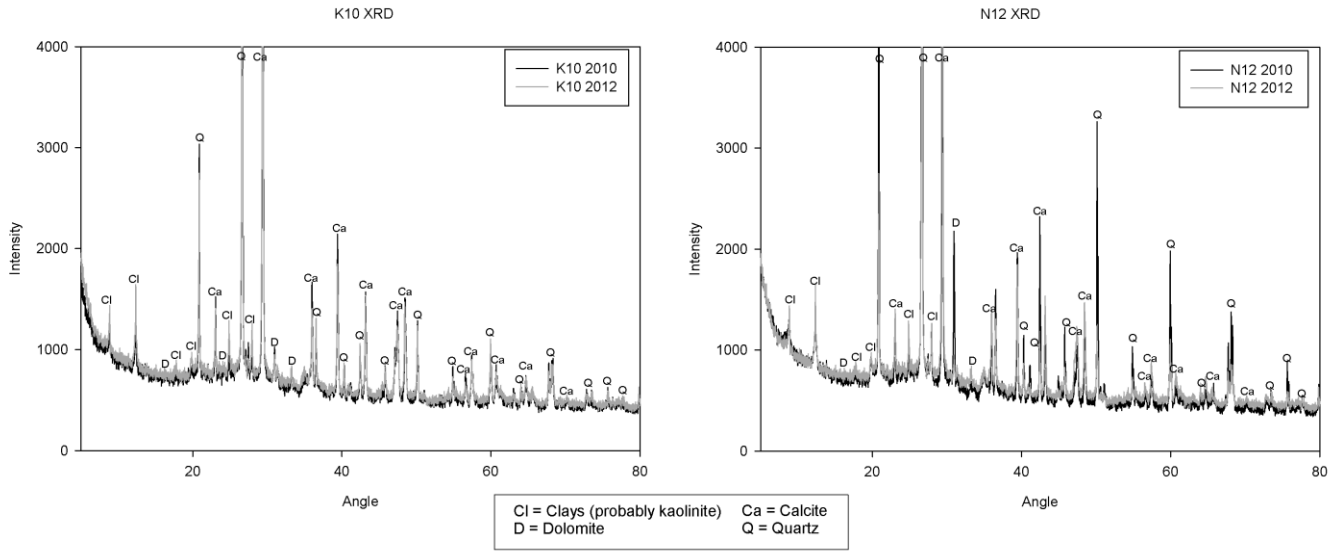

Figure 4.16 – XRD Diffractograms of samples from Science Central in 2010 and 2012 indicating characteristic peaks

Carbon Analysis

The average organic carbon content of the 2010 samples was 1.8 ± 0.6% wt, ranging from a minimum of 0.3% to a maximum of 5.7%. High organic C values of 3.3-5.7% were mainly located around the site periphery concomitant with the highest levels of vegetation cover, where the lowest inorganic carbon values of 0.6-2.4% are also found. Inorganic carbon contents in 2010 were 2.7 ± 0.7% wt (min. 0.6% max. 6.0%), corresponding to carbonate concentrations 22.5 ± 6.0 % wt (min. 5.3% max. 50.2%). In 2012 inorganic carbon content was 4.41 ± 0.96 % wt (min. 3.02 % max. 7.09 %), corresponding to an equivalent calcium carbonate concentration of 36.75 ± 7.97 % wt (min. 25.17 % max. 59.06 %). For comparison Eijkelkamp calcimeter analysis reported bulk carbonate (inorganic C) contents 21.8 ± 4.7% wt (min. 2.1% max. 44.4%) and 39.43 ± 8.14 % wt (min. 26.46 % max. 61.35 %), which correlate well within experimental error margins. This represents a mean increase of 17.28 ± 6.23 % wt in bulk carbonate content across the site. The highest values for inorganic C are found in the south west of the site where a variation in substrate colour suggests a variation in material, decreasing to a minimum of 2.1% in the south east of the site. Otherwise, minimum and maximum values for both organic and inorganic carbon are homogeneously distributed, with little statistically discernible spatial pattern.

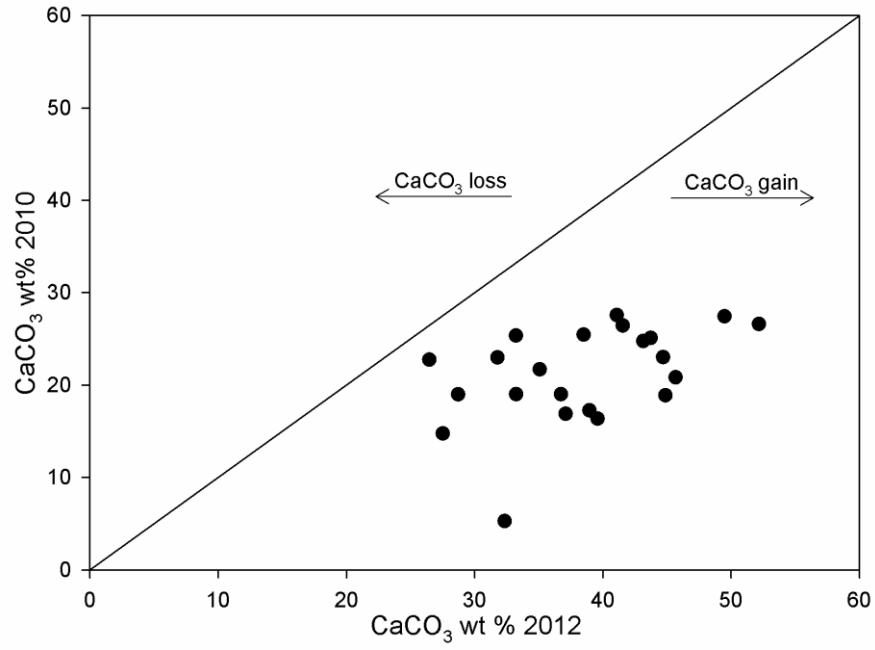

Figure 4.17 – Change in $CaCO_3$ wt % in samples analysed between 2010 and 2012

The carbonate depth profile from a similar previous site investigation (Renforth et al., 2009) found no strong correlation between sample depth (down to 2.7m) and carbonate concentration <1m depth. The Science Central data are similar to those found by Renforth et al. (2009), considering that they are limited to a depth of 0.8m (Figure

4.18). There is no systematic variation with depth at Science Central, and this is as expected given the heterogeneous nature of the ground within the top metre.

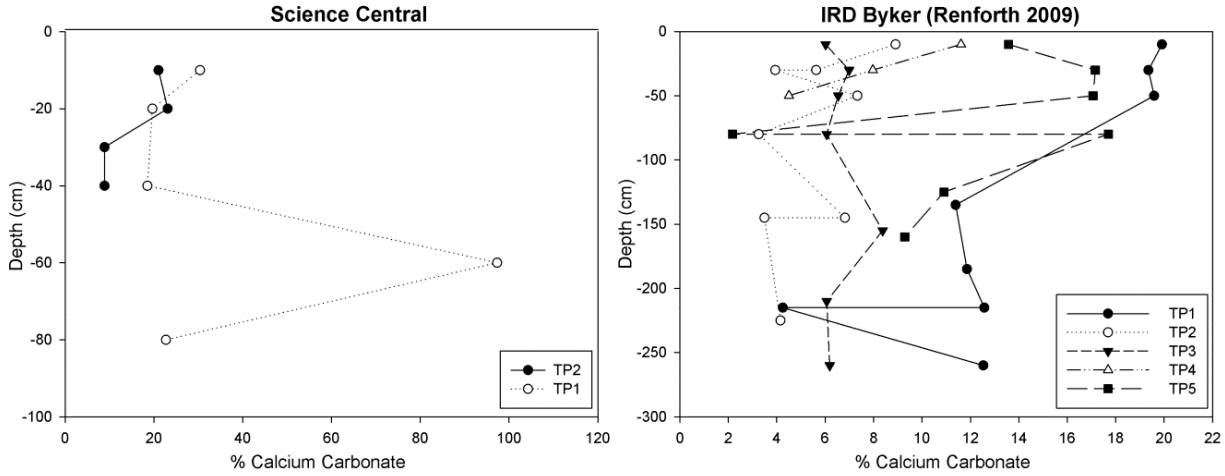

Figure 4.18 – Variation in calcium carbonate content with depth at Science Central and other comparative urban soils (Renforth et al., 2009) Note difference in y-axis scale

Stable Isotope Analysis / ^{14}C Analysis

The 2010 Science Central survey yielded $\delta^{18}O$ values between -9.4‰ and -13.3‰ and $\delta^{13}C$ values between -7.4‰ and -13.6‰. The 2012 survey yielded $\delta^{18}O$ values between -10.02‰ and -13.84‰ against Vienna Pee-Dee Belemnite (V-PDB) and $\delta^{13}C$ values between -6.53‰ and -14.57‰ (V-PDB). $\delta^{13}C$ and $\delta^{18}O$ values show a linear correlation (Figure 4.19, $r^2 = 0.73$). This represents a mean change of -2.70 ± 1.88‰ $\delta^{13}C$ and -1.82 ± 0.55‰ $\delta^{18}O$ (V-PDB). Samples appear more significantly depleted with respect to $\delta^{13}C$ than $\delta^{18}O$.

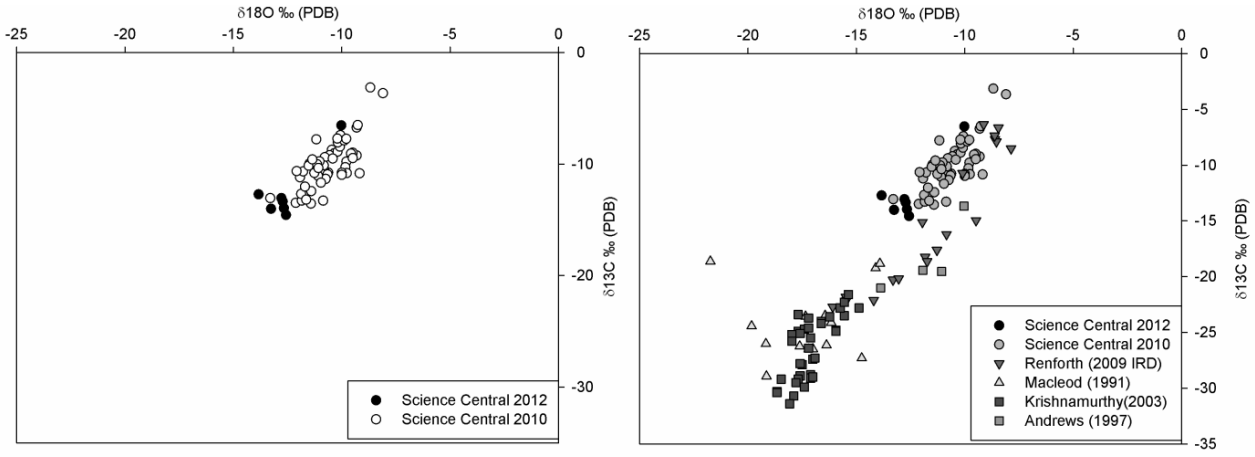

Figure 4.19 - Science Central IRMS data: $\delta^{18}O$ versus $\delta^{13}C$ ‰ (V-PDB) (repeatability error bars are within point, in comparison with IRMS values from other sites (Renforth et al., 2009; Macleod et al., 1991; Krishnamurthy et al., 2003; Andrews, 1997)

End member analysis of the 2010 data, using end member values reported in section 3.5, suggested that 39.4 ± 8.8% of the carbonate carbon had been derived from the atmosphere, the 2012 values were 49.8 ± 12.83% (Figure 4.20). Using this information, the carbon capture potential of the site, with respect to the presence of divalent cations, was calculated and is presented in Chapter 5.

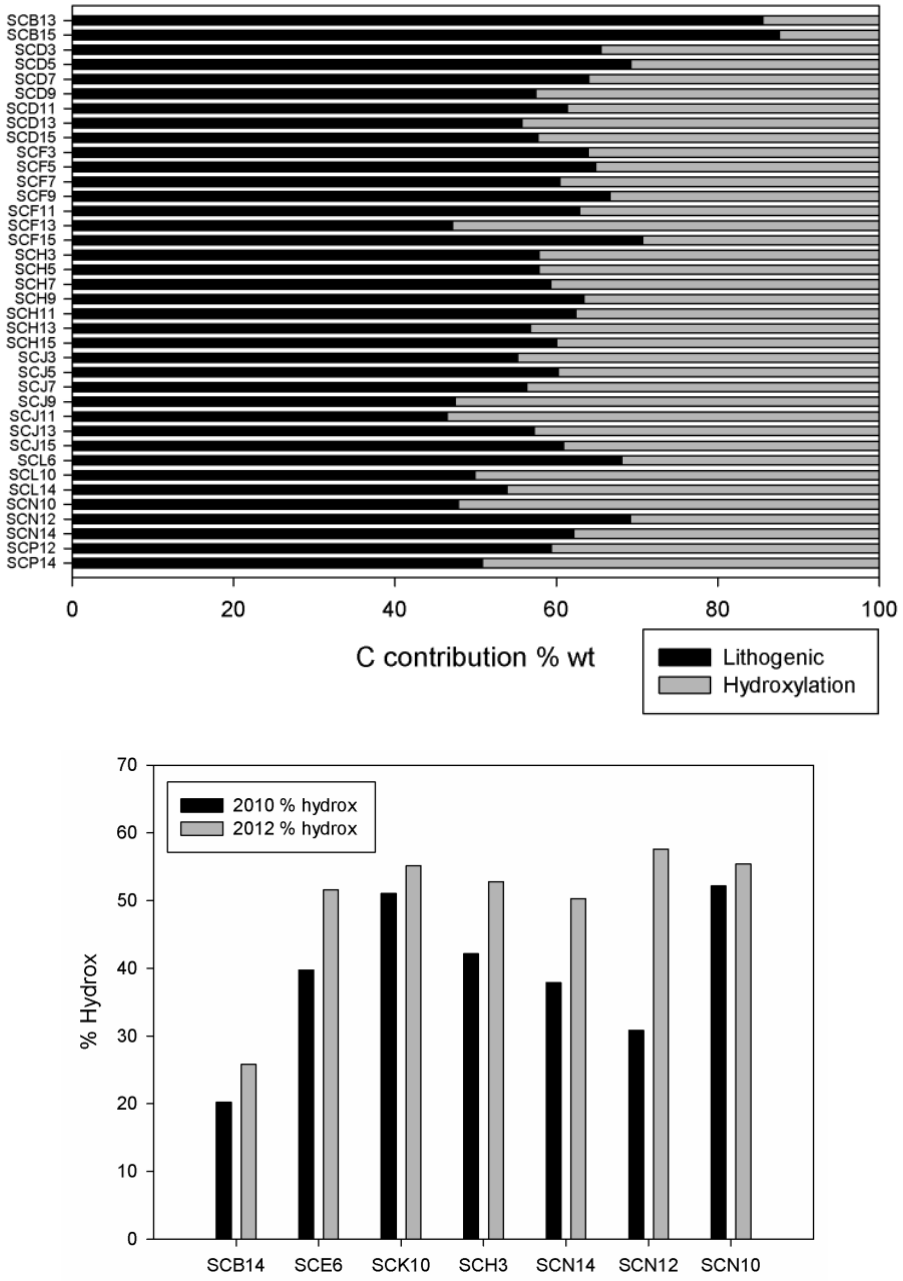

Figure 4.20 a, b - Science Central 2010 and 2012: Relative partitioning of C formation by lithogenic or hydroxylation processes

Radiocarbon (^{14}C) analysis (Appendix C) supported the interpretation that a significant proportion of the C present in carbonates was recently formed through a non-lithogenic route. 80.73 ± 0.37 % of the carbonate in a sample with a $\delta^{13}C$ value of -14.0 ± 0.5‰ was found to be 'modern'.

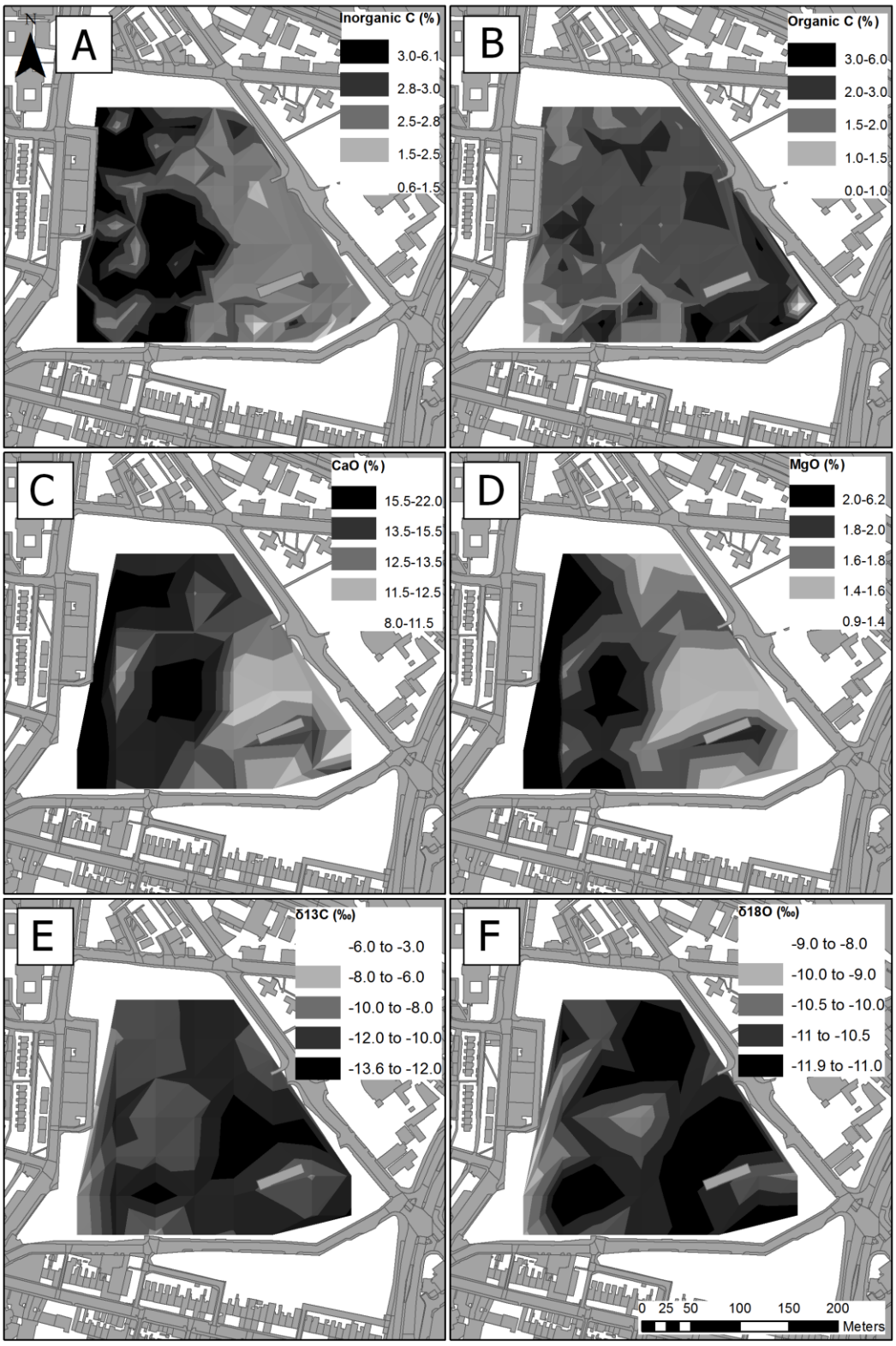

Figure 4.21 – Spatial variation in collated soil analysis data across the Science Central site: A) inorganic carbon B) organic carbon C) CaO % D) MgO % E) $\delta^{13}C$ IRMS values F) $\delta^{18}O$ IRMS values

Spatial distribution

Figure 4.21 demonstrates the spatial distribution of values across the Science Central site in 2010 for inorganic carbon, organic carbon, CaO, MgO, $\delta^{13}C$ $\delta^{18}O$.

Figure 4.22 demonstrates the spatial distribution of values across the Science Central site in 2012 for inorganic carbon, organic carbon, CaO, MgO, $\delta^{13}C$ $\delta^{18}O$.

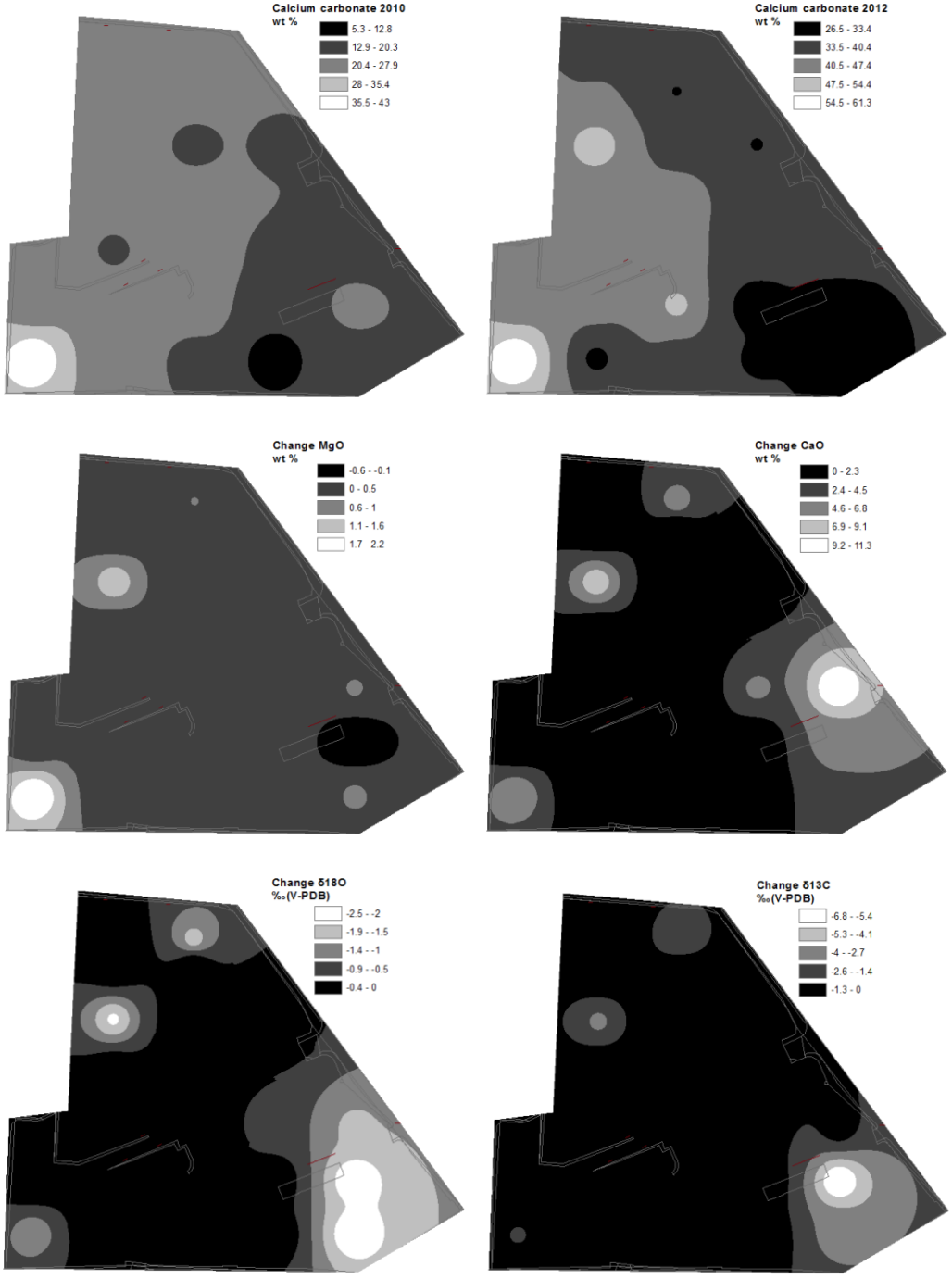

Figure 4.22 – A) $CaCO_3$ 2010 B) $CaCO_3$ 2012 C) change in MgO 2010-12 D) change in CaO 2010-12 change in $\delta^{18}O$‰ (V-PDB) 2010-12 F) change in $\delta^{13}C$‰ (V-PDB) 2010-12

Figure 4.22 summarises the changes that have occurred in key geochemical parameters between Survey 1 and 2. Inorganic carbon (carbonate), CaO, MgO $\delta^{13}C$ and $\delta^{18}O$ are shown. Carbonate content was generally elevated in the sample points along the western border of the site in 2010, and this remains the case in 2012, though points with the lowest $CaCO_3$ in 2010 do not necessarily maintain this trend in 2012. CaO and MgO are

more sparsely represented by data coverage across the site, but Figure 4.22 suggests proportionally increased CaO concentrations to the north and east of the site, and MgO to the south and west.

As in Chapter 3, Figure 4.23 compares a number of weathering rates taken from laboratory weathering experiments (Palandri and Kharaka, 2004 from Hartmann et al, 2013) and weathering rates from field studies (White and Brantley, 1995). The weathering rate at Science Central was inferred from the change in Si concentration between the two time points and is more rapid that the observed rates taken from the literature. While this figure does not show the rate of carbonate formation directly, the rate at which minerals are weathered is an important proxy for determining the availability of cations to undergo these reactions. Mass balance calculations, assuming a SiO_2 loss of 20% as suggested by XRF data, produce a log weathering rate of -12.40 to -13.30 mol cm^{-2} s^{-1} (normalised to a mineral surface area of 0.5 - 4m^2 g^{-1} (calculated from arithmetic surface area of spherical particles within the particle size distribution of the samples analysed) and assuming 1 Mt of material (Appendix C)).

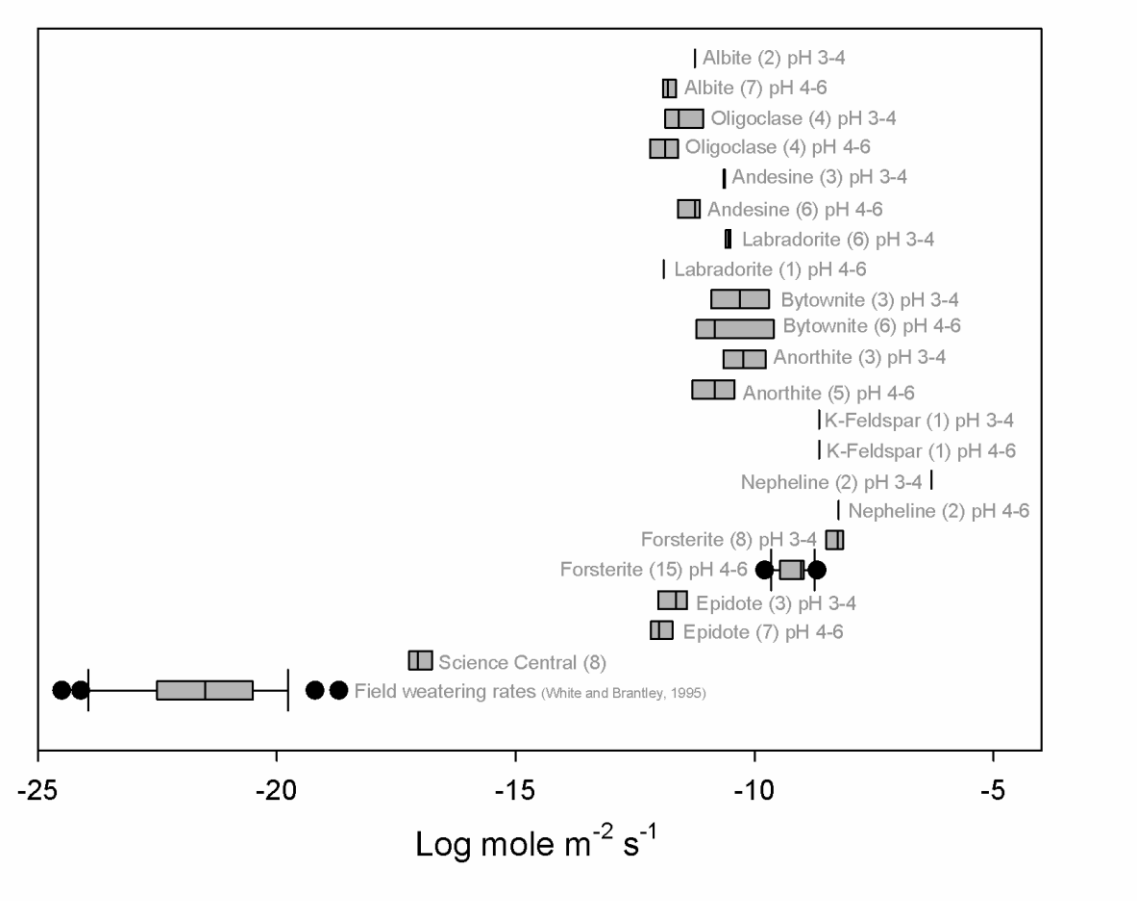

Figure 4.23 – A) adapted from Hartmann et al, 2013, indicating the weathering rate of silicates at Science Central with respect to reported laboratory and field weathering rates (Science Central data points assume surface areas 0.5, 1, 1.5, 2, 2.5, 3, 3.5, 4 m^2 g^{-1}))

Discussion

The data presented in section 4.3.3 collectively illustrate a number of changes in the soil geochemistry of the Science Central site between 2010 and 2012. Rainfall between 2010 and 2012 was around average (~960mm over study period) although spring 2010 to 2012 was described by the Met Office as being particularly dry, and spring 2011 exceptionally warm (Met Office 2011, 2012). The study period saw wetter than average summer and dryer than average winter conditions, twinned with cooler summers and warmer winters. It is assumed that the climatic conditions have not deviated enough from the average to produce significant changes to the average weathering conditions. Vegetation type and cover has changed very little throughout the study period, no major site works have occurred and there is no evidence of significant material imports or exports.

An increase in the bulk carbonate content of the soil is confirmed by acid digestion, total carbon analysis and thermo-gravimetric analysis. Considering the mean values of 21.8 ± 4.7% wt carbonate in 2010 and 41.16 ± 9.89 wt % in 2012, it can be seen that a significant quantity of soil carbonate forms in this environment. Overall carbonate values of 2.1-44.4% wt and 26.46-61.35 % wt respectively are highly variable, and serve to illustrate the inherent heterogeneity of the substrate material at Science Central. Anthropogenic soils of this type are immature, poorly mixed and composed of a number of different source materials, making the overall composition highly variable. This in turn strongly dictates the distribution and extent of soil carbonate formation. The reported standard deviation of ± 4.7% / ± 9.89 wt $CaCO_3$ for the respective datasets however illustrates that the carbonate values in this study are more closely constrained than other similar datasets (Renforth et al., 2009), indicating the value of a high-resolution sampling approach in addressing and managing heterogeneity of this type.

Data assessing the variation in calcium carbonate formation with depth in 2010 suggested potential for the localised presence of highly enriched carbonate blocks; trial pit TP1 illustrates a carbonate peak of 97.3%wt (almost pure carbonate) occurring at 60cm BGL. As compositional data with depth are limited, however, it is difficult to confirm whether this is simply due to variation in constituents of the source material throughout the profile, indicative of a more complex formation process including transport or weathering of parent material, or linked to the depth limit of permeation of CO_2 into the soil profile. There is also the potential for importation of lithogenic

carbonate materials (limestone etc.). The provenance of this additional carbonate was investigated using stable isotope methods (discussed in Chapter 3); the additional depletion in isotopic ratios for both $\delta^{13}C$ and $\delta^{18}O$ illustrates a more significant contribution of high-pH hydroxylated material, formed by reaction with dissolved CO_2 in soil solutions, in the carbonate signature (Renforth et al, 2009; Wilson et al, 2010). ^{14}C data also supports this conclusion.

SOC values vary across Science Central and spatially appear to be inversely related to the SIC values. In 2010 high SOC values of 3.3-5.7% are located around the site periphery, where the lowest SIC values of 0.6-2.4% are found. It must be noted that significantly more vegetation cover exists around the site periphery, and this would be expected to contribute to the elevated values of SOC in this region. The low values of SIC in these corresponding regions may be an artefact of the drainage regime of the site, leading to the leaching of carbonate from the material, washing from the sloped portion in the south east and its emplacement outside the site boundaries or at a greater depth than that sampled in this exercise. Considering the environmental variations noted in the available data it is not possible to conclusively determine whether the presence of high SOC or SIC are mutually incompatible phenomena, or whether one inherently limits the other. Limited literary evidence does not provide a conclusive solution, but suggests that high SOC areas in natural shallow soil / root zones are poorer in SIC which is leached to deeper levels in the profile (Wang et al, 2010).

XRF analysis of the 2012 survey data appears to show a significant depletion in SiO_2 and enrichment in CaO and Al_2O_3 between 2010 and 2012. The variability within sample sets is large, but when a 'constant oxide' calculation is carried out, to normalise the other elements to TiO_2 values assuming this to be a minimally mobile component, these figures are brought back within the bounds of variability within the dataset, with the exception of SiO_2. Silica removal from the original 'parent' material, analysed by XRF, is used as a proxy for the overall weathering rate of artificial silicates on the study site, which directly reflects the availability of Ca and Mg for carbonation reactions. Mass balance calculations, assuming a SiO_2 loss of 20% as suggested by XRF data, produce a log weathering rate of -16.40 to -17.30 mol m^{-2} s^{-1} (normalised to a mineral surface area of 0.5 - 4m^2 g^{-1} (Appendix C)) and assuming 1 Mt of material onsite). The silicate minerals at Science Central appear to weather at a much faster rate than that observed in field studies of natural silicates (Hartmann et al, 2013; Renforth et al,

2011b; White and Brantley, 1995). If we assume an 'original' SiO_2 content of the Science Central soils in 2007 of ~66% (Limbachiya et al, 2006), this produces a linear regression (r^2=0.9) with the data from 2010 and 2012 (Figure 4.24). This appears to also fit with the data for other elemental oxides from XRF analysis, with the apparent depletion in Si, mirroring their enrichment.

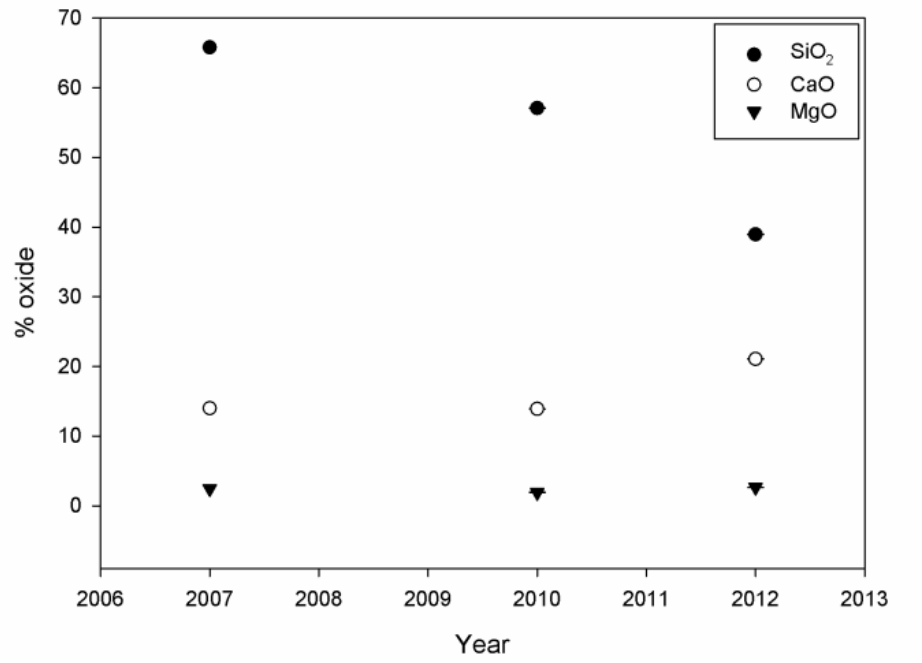

Figure 4.24 - % change in major oxides assuming an initial composition taken from Limbachiya et al, 2006, and 2010 data from Washbourne et al, 2012.

There are a number of possible explanations for a large depletion of Si, matched with minor enrichments in other minerals. At high-pH values (>9.5), which are reported for a number of location across the Science Central site (Washbourne et al, 2012), Si is rapidly weathered and leached, as the solubility of Si is greatly increased at high pH (Brady and Walther, 1989). Si could be readily transported in soil solutions vertically and horizontally on this free-draining site. Ca, Mg and many of the other elements reported by XRF are more readily retained in secondary minerals close to the soil surface including clays, especially where soil pore solutions become saturated during wetting-drying cycles. Without knowing the initial bulk composition it is difficult to predict whether the data observed is reflective of (in)congruent weathering of silicates; while Eq. 4.1 suggests that changes in Si/Ca content could be predicted, the complexity of reactions occurring in this system, combined with transport of solutes across a large spatial area make it difficult to predict whether the observed conditions are 'expected' with respect to reaction stoichiometry. Aluminium concentrations at the site are

relatively high, 8.7% wt in 2012; if these were originally present onsite in the form of aluminosilicates these may also have played a role in controlling the rate of silicate weathering. Van den Berg et al (2000), suggest that Al can be rate-limiting in the long-term dissolution of silicates at high pH, however they also suggest that their observed trend of increasing Al release rate with increasing pH qualitatively correlates with the increasing concentration of total dissolved carbon, hydrogen carbonate ion and carbonate ion, with pH for an open $CO_2(g)$-H_2O system. The dissolved carbonate ion increases the rate of Al release from the reactive surface of the silicate, therefore ultimately increasing the rate of carbonation.

The carbon and oxygen stable isotope values presented in this study agree closely with those determined in similar studies of carbonate formation on demolition waste, Renforth et al. (2009), and concrete structures, (Krishnamurthy et al., 2003; Macleod et al., 1991; Dietzel et al., 1992), which show an apparent linear relationship between high-pH carbonates (more depleted in ^{13}C and ^{18}O by kinetic fractionation) formed in pedogenic settings, and lithogenic carbonate (contiguous with $\delta^{13}C$=0‰). The majority of samples collected at the site were shown to be significantly depleted with respect to both ^{18}O and ^{13}C. The most negative (isotopically light) values for $\delta^{18}O$ and $\delta^{13}C$, indicative of high pH carbonates, predominate in the areas where inorganic carbon and CaO concentrations are lowest. Less negative values, indicating a larger lithogenic contribution to carbonate formation, predominate in central and western areas of the site. This may be due to the pattern in which materials were emplaced onsite, an artefact of overprinting by the drainage regime onsite or due to a more complex interaction between minerals in the parent material and the environment.

These values are not as depleted in ^{13}C as those from previous studies (Renforth et al., 2009; Dietzel et al., 1992), indicating a higher proportional contribution by lithogenic sources of C to the carbonates. Tendency towards less-negative values than expected from other studies may, in some areas, be due to the inclusion of lithogenic carbonates. This confirms a mixed source of carbonate in the samples analysed, a mixture of atmospheric sources with a reasonable lithogenic contribution from C+D materials. The amount of pedogenic carbonate which has formed to date can be estimated and the residual carbon sequestration potential of the site can also be determined.

Summary

- Average carbonate content 36.75 ± 7.97 % wt $CaCO_3$
- Silicate and carbonate minerals dominate: quartz and dolomite are present, with calcium carbonate identified as calcite.
- $\delta^{13}C$ values between -6.53‰ and -14.57‰ (V-PDB) and $\delta^{18}O$ values between -10.02‰ and -13.84‰ against Vienna Pee-Dee Belemnite (V-PDB) End member analysis estimates 49.8 ± 12.83% C to be from atmospheric sources
- C&D waste soils potentially capture 18 $kgCO_2\ t^{-1}\ yr^{-1}$

4.4 Summary

This study adds to a growing body of evidence for the formation of carbonate minerals in artificial soil settings where Ca/Mg-rich silicate minerals occur. The field sites reported have all undergone significant carbonation without intentional intervention, therefore this work also adds weight to the idea that specifically engineered soils could be effectively utilised for carbon sequestration. The weathering rates observed in artificial silicates are rapid with respect to observed silicate weathering rates under field conditions, suggesting that these may be effective substrates for rapid carbon capture and storage in field settings. Rates are reduced from those observed in laboratory studies (Chapter 3), illustrating that artificial silicate weathering is still constrained by a number of scaling factors from lab to field.

This work illustrates the potential for artificial soils to provide specific ecosystem services including carbon sequestration. It also supports the utilisation of materials considered to be anthropogenic 'wastes' in helping to develop and support the urban ecosystem, providing an important route for re-use. Including a carbon capture function in engineered soil design and waste management can add environmental value with little additional energy input. Ultimately if soil carbonates are included in emissions offsetting schemes, alongside management of soil organic carbon, this technology has potential to provide carbon capture credentials to urban developments, waste sites and industry stakeholders.

- The data from Yarborough Landfill and Science Central strongly support the proposition that carbonate formation is not restricted to arid soils, or unique to wholly natural soils, but can be a significant process within temperate urban and engineered soils
- Soil C sequestration can be engineered using Ca/Mg-rich material and may be significant and exploitable storage route for soil C
- Soil engineering could be an effective tool in urban ecosystems service provision (carbon capture)

CHAPTER 5 - Mineral carbon capture in 'engineered' systems

The sequestration phenomena observed at field scale in Chapter 4 all occur in settings which have not been intentionally engineered for carbon capture. This presents an opportunity for determining how the carbon capture function of these sites could be improved by intentional interventions in the manner in which materials are handled and emplaced, or alteration of the other environmental factors that they interact with. Whilst the phenomena of carbonate formation in these settings is of general scientific interest, if a methodology could be developed by which mineral carbon capture could be quantitatively engineered in soil settings there may be tangible environmental and commercial potential for applying this approach to real-world developments.

Soil engineering for carbon capture through passive sequestration of carbon dioxide by mineral weathering avoids practices which increase the material inputs or energy requirements of the process, reducing its economic cost and environmental impact. In assessing the potential for engineering soil systems for carbon capture, this report aims to assess the potential for using a soil science approach to promote mineral carbonation through the creation of favourable environmental conditions, without the need for substantial pre-treatment, transport, energy input, chemical or biological treatment.

Chapter Summary:

Flow-through weathering experiments, and field-scale observation of the geochemistry of an engineered landfill site, demonstrate the complexity of scaling the geochemical processes occurring between laboratory and field scale.

- Flow-through weathering to determine weathering rates for steel slag under a variety of physical and chemical conditions
- Geochemical data from large-scale, active, inert waste landfill, assessing MCCS in an engineered environment
- Initial results reported from a study which set out to clarify the role of vegetation in influencing the difference between laboratory and field-scale mineral weathering rates on study sites
- A method for quantification of carbon capture on a field site using geochemical data, including carbonate content and C stable isotope data.

5.1 Engineering soil systems for carbon capture

The engineering of a passive system could be taken as a contradiction in terms; any planned intervention to this system inherently increases the energy input and / or material balance of the system and is therefore not 'passive'. The aim in soil engineering for carbon capture is to minimise these inputs as much as possible, whilst still maximising capture potential. Whilst the soil system itself is dynamic, in the aforementioned field settings no specific effort has been made to activate the carbon capture properties of the emplaced materials. Building on the findings from Chapters 3 and 4, Chapter 5 'Mineral carbon capture in engineered systems' aims to investigate methods of activating this potential (rate and / or capacity) without significant material or energy input to the system.

A number of studies have proposed methods by which carbon sequestration by minerals in ambient-air settings could be utilised. This sits within the broader scope of studies which have addressed ambient air capture of carbon dioxide through spreading of silicate minerals in the open air on dedicated sites (Schuiling & Krijgsman, 2006). Manning et al. have included proposals for soil system engineering for carbon capture and storage in a number of publications (2008, 2013a, 2013b). A small number of publications put forward integrated proposals for soil carbon storage taking into account engineering practises in organic and inorganic systems and Renforth et al (2011a) produced a model of the possible interactions of these processes and how they might interact in a system where the soil carbon sink has been intentionally engineered, summarised in Figure 5.1.

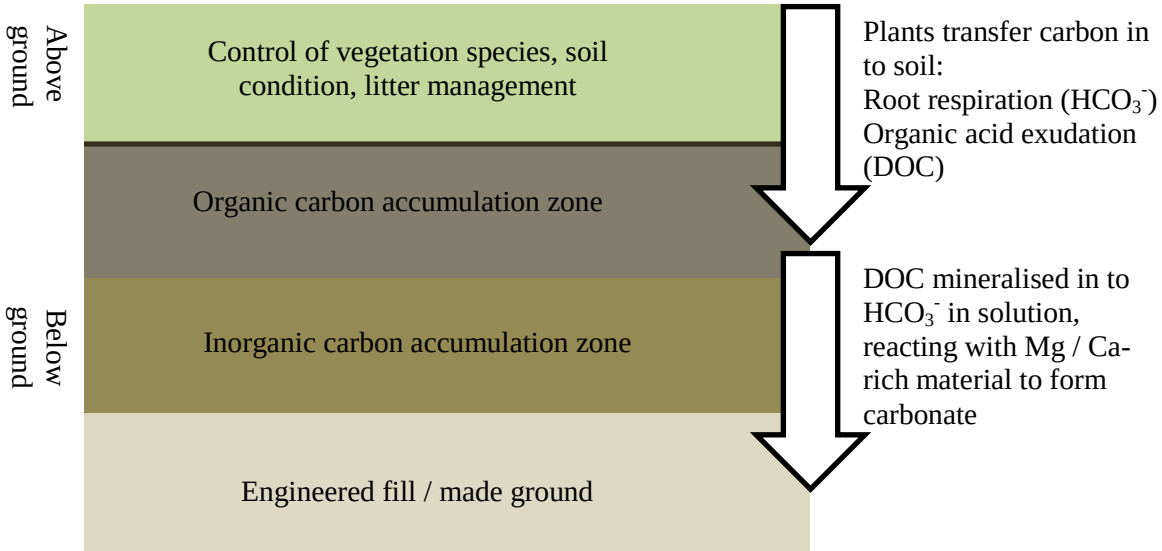

Figure 5.1 – Potential strategy for engineering the soil carbon sink (adapted from Renforth et al 2011)

5.1.1 Physical-chemical

As discussed in detail in Chapter 3, and summarised in Chapter 4, physical and chemical characteristics of the materials used for carbon sequestration play a large part in determining the rate and capacity of the overall process. It has also been noted that mechanistic and laboratory studies of these parameters do not necessarily match well with parameters taken from field data, with the frequently slower rate of the field-scale data presented suggesting that the full complexity of the system is not being accounted for in these simple simulations.

Experimental work was therefore carried out to determine the effect of a number of physical-chemical parameters on the weathering and carbonation of artificial silicate minerals at meso-scale under laboratory conditions. This employed the use of glass column reactors, packed with steel slag as a reactive substrate, with a constant flow-through of fluid applied. These columns were subjected to a variety of conditions: wetting/drying cycles, changes in ionic strength of solutions, agitation, changes in solution chemistry and supply of CO_2 in order to determine the sensitivity of the system with respect to carbonation for each of these factors. This is not intended as an exhaustive list of variables that may occur in a weathering environment, but aims to address some of the less-explored major parameters likely to control reaction rate.

Also presented is an analysis of geochemical data supplied by Tata Steel, covering the period 2006-2013 on their inert waste landfill site at Yarborough, Scunthorpe. This provides a comparison to the flow-through data, as a site with steel slag substrate with complex hydrogeological conditions. As discussed in the previous chapter the Yarborough site receives steel slag waste from the Tata Scunthorpe iron and steel plant and the data presented in this report form part of a suite of environmental monitoring undertaken by the plant on a yearly, quarterly and monthly basis, in compliance with contemporary landfill legislation (EU Landfill Directive (EEC/1999/31/EC); Landfill Regulations (England and Wales) 2002). These data allow insight into the geochemical evolution of a large scale site at which weathering of silicate minerals is occurring in a semi-controlled manner. Chemical data have been analysed using SOLMINEQ 88 (Kharaka, Yousif K., USGS 1989), a programme for modelling the geochemistry of water-rock interactions. These analyses have allowed the saturation states of minerals within the landfill site to be modelled, mapping the saturation of the landfill with respect to different materials over time to see how these conditions develop and persist.

5.2 Testing environmental parameters

5.2.1 Flow-through weathering experiments

A summary of data from flow-through weathering experiments using steel slag is presented in the following section. Detailed analyses and data can be found in Appendix D. These experiments were designed to determine the impact of a variety of chemical and physical variables on the weathering behaviour of steel slag, under conditions which were not limited by the saturation state of the surrounding fluids, through the supply of fresh fluids as a low-rate constant flow.

Results of carrying out flow-through weathering experiments on fresh (<1 months weathering) and weathered (>3yrs weathering) crushed slag in glass column reactors are presented, detailing leachate and slag chemistry. The variables for investigation were:

- Experiment duration
- Slag age / size / mobility
- Water chemistry
- Gas inputs (CO_2)
- 'Rainfall' inputs (wetting-drying cycles and effects of partial saturation)

The main aims of the experimental work were to build a model representation of *in-situ* ground conditions in soils consisting of artificial silicate minerals, with an understanding that the investigation will be constrained by the representative scale of any apparatus used. A limitation in this instance is the accuracy of modelling with respect to the inherent chemical / physical heterogeneity of most sites containing suitable materials compared to the column models presented.

It also aimed to allow a number of interventions with respect to:

- Groundwater regime (carbonate / bicarbonate content, dissolved carbon, frequency of wetting events)
- Hydrogeological setting (simulation of carbonate formation in both saturated and vadose settings, allowing analysis of formation within a dynamic groundwater setting).
- Physical factors – agitation of substrate
- Leachate formation – investigating the temporal element of leachate formation.

Method

Glass columns (Figure 5.2) were filled with 5kg of slag material, graded by the supplier to 6-10mm diameter. Fresh and weathered steel slag supplied by Tata Steel Scunthorpe, produced in the Scunthorpe plant, was used in all cases. Composition and grain size of these materials is detailed in Tables 5.1 and 5.2 in the following section.

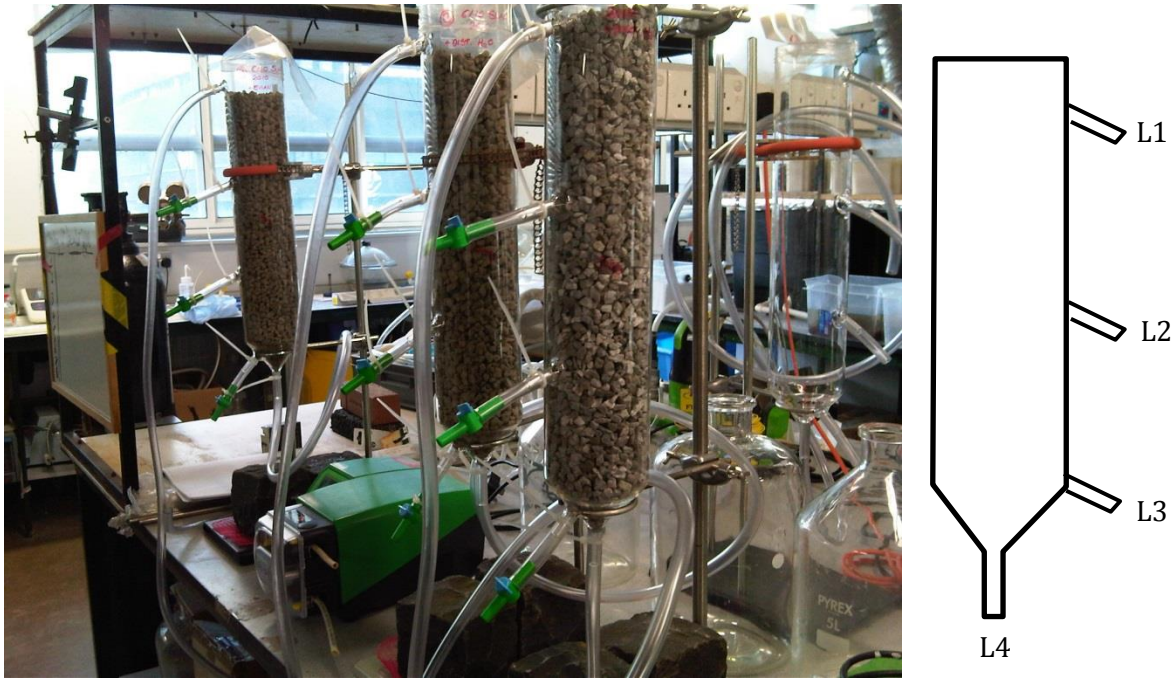

Figure 5.2 – Apparatus used during flow-through column experiments

A flow was applied to each column, with fluids supplied via a pre-calibrated peristaltic pump to the base of the column (L4) at a flow rate of ~1.15 ml min^{-1}, exiting at the top outlet (L1). All experiments were carried out at room temperature ~25°C. Periodic leachate sampling was carried out, at shorter time increments over the early part of the test and longer increments as the experiment progressed. These are detailed in Appendix D. Leachate was sampled for 15 minutes on each occasion, by applying a collecting flask to outlet L1. pH and EC were tested immediately. Samples were then acidified to <pH3 with concentrated nitric acid and refrigerated to preserve them for further analysis. All samples were filtered through a 0.2µm cellulose nitrate filter prior to analysis.

Dismantling of column apparatus took place at the end of the allocated run time for each experiment. Columns were drained and interval sampling of the substrate was applied

every 50-100mm through the column solids to determine whether variation in geochemical behaviour had occurred along the flow-length.

Analyses applied:

Leachate

Leachate analysis methods are detailed in Appendix A and summarised below.

- pH: measured using electronic Jenway 3310 pH meter
- EC (electrical conductivity): measured using VWR International EC 300 meter

pH and EC (electrical conductivity) data, collected throughout the experimental period, were collated and analysed to assess bulk geochemistry and weathering effects and the occurrence of pH buffering.

- AAS (Atomic Absorption Spectroscopy) for metals (Ca, Mg): analysis carried out using Varian SpectrAA 400 AAS
- Total Carbon analysis of leachate (inorganic carbon (IC)): carried out using Shimadzu TOC-5050A Total Carbon Analyser
- XRD (X-Ray Diffraction) for precipitated solids

Solids

Solids analysis methods are detailed in Appendix A and summarised below:

- Acid Digestion (bulk carbonate): samples analysed for bulk carbonate by acid digestion to BS 7755-3.10:1995 ISO 10693:1995 using an Eikjelkamp Calcimeter, reacted with 0.4M HCl and $CaCO_3$ content inferred from volumetric measurement of CO_2 gas evolved
- TC (Total Carbon) analysis / IC (Inorganic Carbon) / TOC (Total Organic Carbon): carried out using a Leco CS-244 Carbon / Sulfur Determinator.
- TG-DSC QMS (Thermogravimetry-Differential Scanning Calorimetry (*TG-DSC*) Quadrupole Mass Spectrometry (*QMS*)): analysis was carried out using Netzsch Jupiter STA449C TG-DSC system connected to a Netzsch Aeolos 403C quadrupole mass spectrometer
- XRD analysis was carried out using a PANalytical X'Pert Pro Multipurpose Diffractometer fitted with an X'Celerator and a secondary monochromator, operating with a Cu anode at 40 kV and 40 mA. Spectra were acquired for Cu Kα (λ = 1.54180 Å) or Cu Kα1 (λ = 1.54060 Å) radiation over 2-70°2θ with a nominal step size of 0.0167°2θ and time per step of 100 or 150 seconds. All scans were carried out in continuous mode using the X'Celerator RTMS detector.

- XRF analysis was conducted at the University of Leicester using a PANalytical Axios Advanced XRF spectrometer.
- IRMS analysis analysed carbonates for $\delta^{13}C$ and $\delta^{18}O$ and was carried out by Iso-Analytical Ltd (Cheshire UK), using a Europa Scientific 20–20 continuous-flow isotope ratio mass spectrometer. The results were recorded relative to the Vienna Peedee Belemnite scale (V-PDB).

AAS (Atomic Absorption Spectroscopy) of leachate and XRD / XRF of solids and precipitates, collected at selected points in the study, were used to assess the weathering rate of slag under flow-through conditions, and to assess the elemental variation in leachate over time.

Bulk carbonate analysis of solids, and XRF analysis taken prior to and after completion of the pilot project, were used to assess composition and extent of carbonation.

Table 5.1 – Properties of slag material used in pilot, analysed by acid digestion as described in the following section

	Date of manufacture	**Grain size**	**$CaCO_3$ (wt %)**
YAR/TAR/3	12/05/2010	6-10mm	1.65
YAR/TAR/10	10/09/2007	6-10mm	7.04

Table 5.2 – XRF average analysis of major elements in fresh slag (YAR/TAR/3) supplied by Tata Steel, Scunthorpe, analysed by the University of Leicester Department of Geology (Appendix A)

SiO_2	**TiO_2**	**Al_2O_3**	**Fe_2O_3**	**Mn_3O_4**	**MgO**	**CaO**	**P_2O_5**	**SO_3**	**V_2O_5**	**Cr_2O_3**	**LOI**	**Total**
12.21	0.65	0.78	30.06	4.69	6.13	41.52	1.33	0.19	0.51	0.17	-1.18	98.35

10 column experiments were run in total across a variety of timescales and conditions detailed in Table 5.3. Durations range from 8 to 56 days. Deionised water acted as a baseline for the analysis, ensuring that additional reactive species introduced to the system were minimised, while as in Chapter 3 Evian water was used to determine the effect of supplying carbonate-rich fluids to the system and NaCl-based simulated groundwater used to investigate the effect of variations in composition of the solutions. Wetting / drying and mobilisation regimes were also applied to the solids. CO_2 gas was introduced via a gas bottle to the column in the final experimental run (at a flow rate of 2-3 ml min^{-1}).

Table 5.3 – Matrix of experimental conditions (6/10 refers to slag graded to between 6 and 10mm in diameter)

Run #	Column	Slag	Duration	Conditions
1	1	6/10 Fresh YAR/TAR/3	8 days	Distilled water
1	2	6/10 Fresh YAR/TAR/3	8 days	Evian water (high bicarbonate content)
1	3	6/10 Weathered YAR/TAR/10	8 days	Distilled water
2	1	6/10 Fresh YAR/TAR/3	21 days	Deionised water
2	2	6/10 Fresh YAR/TAR/3	21 days	Deionised water Vadose zone
2	3	6/10 Fresh YAR/TAR/3	21 days	Deionised water Wetting-drying cycles
2	4	6/10 Fresh YAR/TAR/3	21 days	Deionised water Periodic mobilisation of materials
3	3	6/10 Fresh YAR/TAR/3	56 days	Deionised water
3	4	6/10 Fresh YAR/TAR/3	56 days	Simulated groundwater (no additional carbonate)
4	1	6/10 Fresh YAR/TAR/3	21 days	CO_2 supply

In Run (#)1 Column 2 Evian water was used as a means of supplying dissolved inorganic carbon in the form of bicarbonate ions, in order to determine whether the supply of carbonate species was a limiting factor in this system. Commercially reported analysis of the water at source can be seen in Chapter 3, Table 3.4.

In #2 C2 a vadose zone was maintained so that the leachate level never rose above L2, illustrated in Figure 5.2.

In #2 C3 the column was submitted to 24 hours of drying for every 7 days the experiment was allowed to run. #2 C4 was subjected to the same draining regime as #2 C3, after which the column was inverted, replaced and refilled with fresh solution.

The ‘simulated groundwater’ in #3 C4 comprised deionised water and reagent grade NaCl (Appendix D) to determine whether changes in the ionic strength of the supplied solution affected the observed leaching of Ca or formation of carbonate.

Results

Leachate

pH values averaged around 11-12 and varied little in the fresh slag columns (YAR/TAR/3) undergoing all treatments, with the exception of #4 C1, where CO_2 gas was continuously supplied to the system where pH averaged around 7. In column #1 C3 pre-weathered slag (YAR/TAR/10) was used as the substrate, as seen in Figure 5.3, producing a pH ~9. Almost all columns exhibited a small, but observable drop in pH over the duration of the experiment.

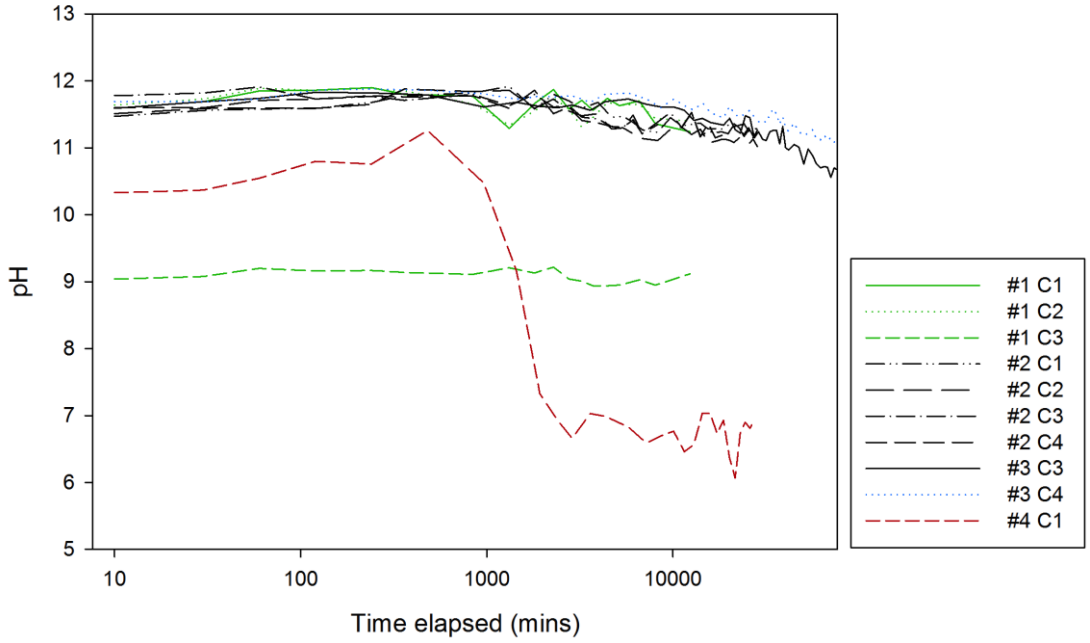

Figure 5.3 – pH in flow-through weathering columns. (Green = Distilled water, Black = Deionised water, Blue = High-NaCl water, Red = CO_2 addition) Typical error = 0.12

EC (electrical conductivity) was variable as seen in Figure 5.4. With the exclusion of #1 C3 which contained pre-weathered slag and retained a flat profile throughout, all columns exhibited an initial high EC value, within the first hour of the experiment commencing, which then dropped slowly throughout the remaining experimental period. #4 C1 showed an initial drop in EC followed by a gradual rise and fall along a similar trajectory to the other experimental columns. #3 C4 illustrates an elevated EC value due to the supply of a high-NaCl feedstock solution, but otherwise illustrates a similar EC profile.

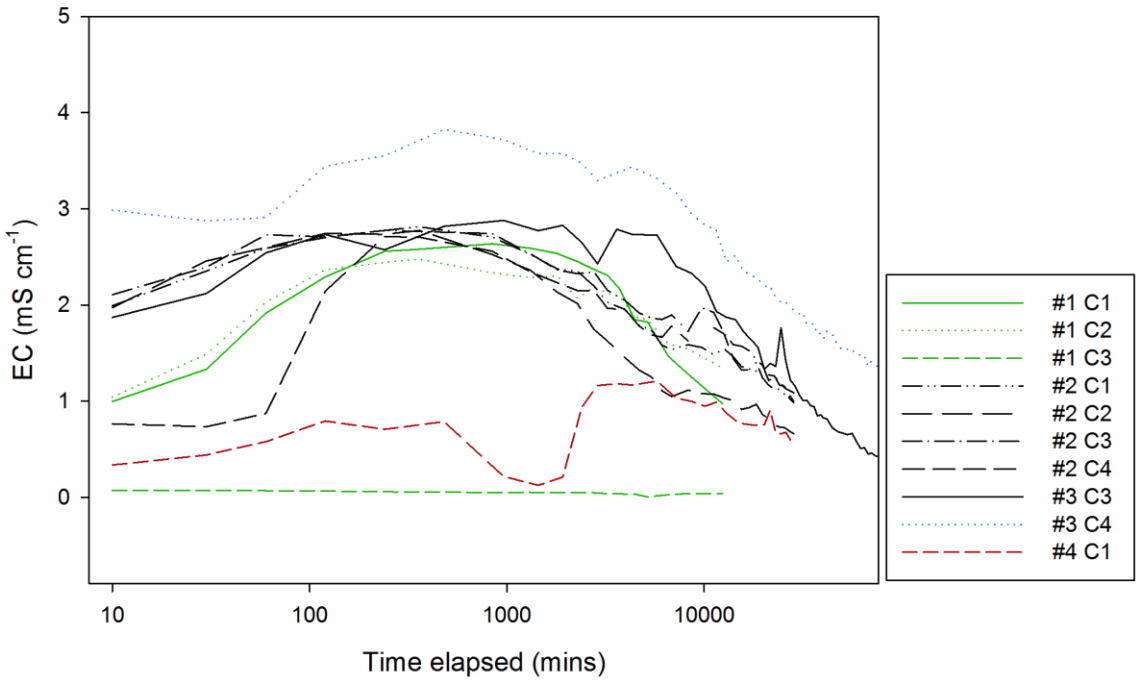

Figure 5.4 – EC (mS cm^{-1}) in flow-through weathering columns. (Green = Distilled water, Black = Deionised water, Blue = High-NaCl water, Red = CO_2 addition) Typical error = 0.28

AAS (Atomic Absorption Spectrometry) was used to determine the content of metal cations in the leachate solutions. In the first series of testing (#1, C1-3), multi-element analysis was carried out using AAS, to assess the leaching behaviour of elements other than Ca and Mg under the applied conditions. In Figure 5.5, C1 and C2 contain fresh slag material, while C3 contains weathered material. #1 C3 is the only column in this series of experiments to use pre-weathered slag as its starting substrate.

Results for Ca, Mg, K, Na and Fe are shown in Figure 5.6. Ca was seen to be the predominant cation in solution in all cases, orders of magnitude higher in concentration for fluids that reacted with the fresh slag material (note variation in y axis scales across the graphs presented). Mg, K, Na and Fe all exhibited low concentrations in solution under the leaching conditions. It can be seen that in the case of Ca, K and Na, the weathered material produced very low levels in leachate, however Mg and Fe are of a similar magnitude to the fresh slag.

As with the batch experiments described in Chapter 3, the use of Evian water in C2 produced interesting results with respect to the metal cations detected in solution; Mg, Na and Fe all appeared to be at lower concentration than in the columns treated with deionised (or distilled) water. Ca concentration was highly variable, suggesting that, as in the case of the batch experiments in Chapter 3, solute concentration may be actively

reduced at early stages of the reaction through the early precipitation of secondary minerals.

All other columns were analysed for Ca only, with the compiled data in Figure 5.5 showing that all columns with fresh slag exhibit a Ca spike in the first hour after the experiment commences, followed by a gradual reduction in the concentration of Ca in the leachate solution. Once again, #1 C3, containing weathered slag, presents a flat profile relative to the other columns.

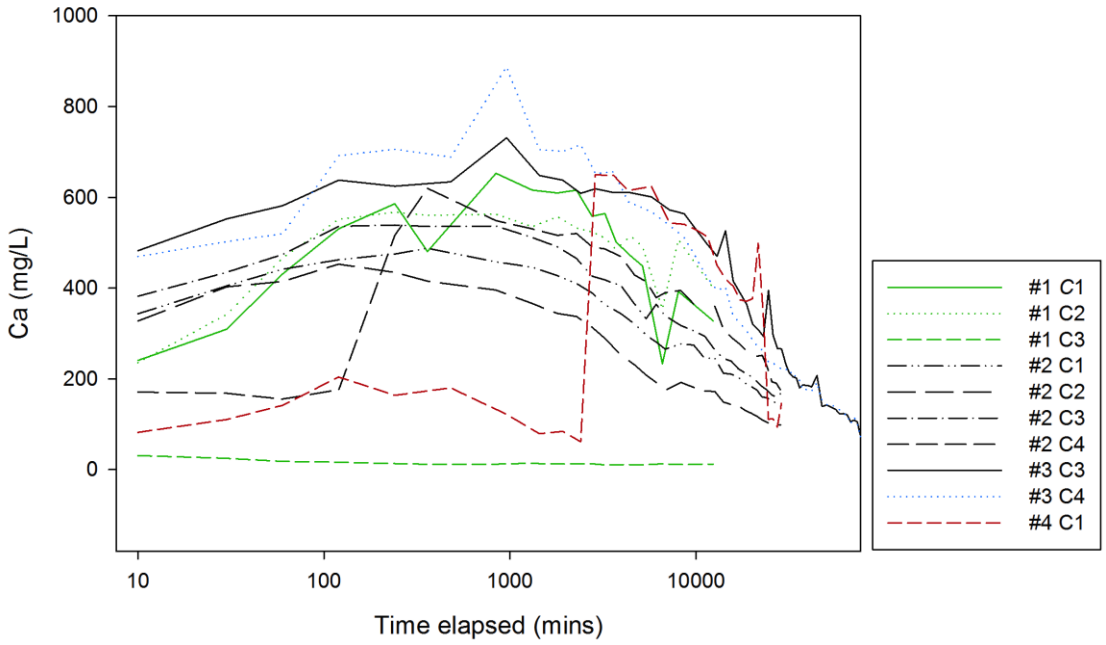

Figure 5.5 – Ca in solution, compiled data from all columns. (Green = Distilled water, Black = Deionised water, Blue = High-NaCl water, Red = CO_2 addition) Typical analytical error = 0.10

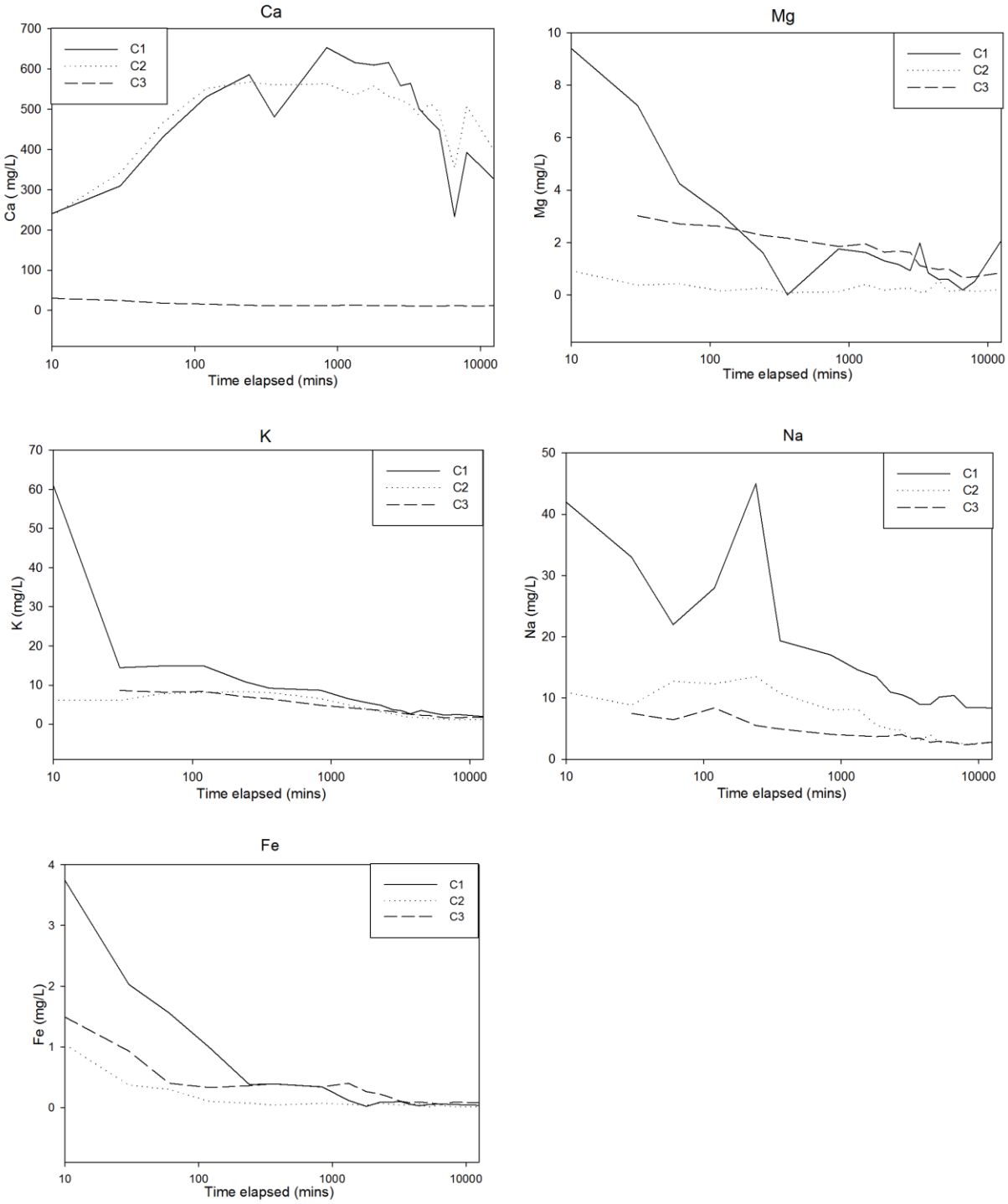

Figure 5.6 – Metals in solution in #1 Columns 1-3 (C1 = fresh slag in distilled C2 =fresh slag in Evian C3 = weathered slag in distilled) (from AAS analysis). Typical analytical error = 0.10

Total carbon analysis of leachate was carried out to determine the concentration of organic and inorganic carbon (IC) species in the leachates evolved from the columns. IC concentration was of particular interest for determining the presence of carbonate species in solution. Figure 5.7 shows an example of the inorganic carbon concentration observed in column leachate over time (Run 3, Column 3 is displayed, as an example of a typical profile) showing a gradual increase. Variation in IC over time is likely to be a

result of a number of experimental factors including variation in pumping rate, especially if clogging occurs.

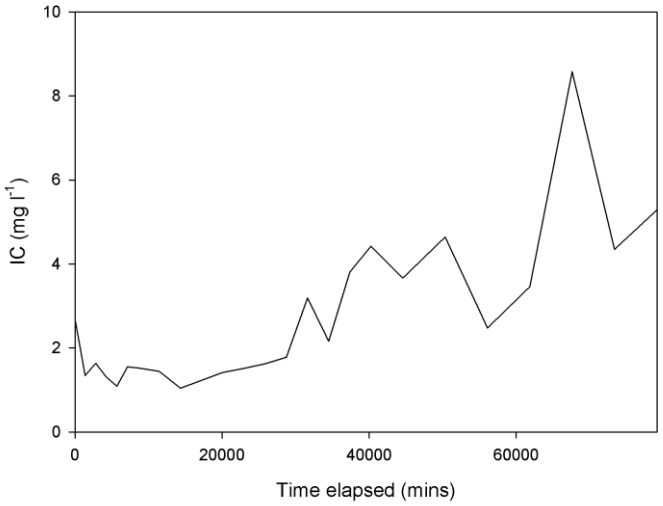

Figure 5.7 – Inorganic carbon in leachate solutions over time – #3 C3 as example. Analytical error = 0.46

Inorganic carbon in solution over time when compiled from all columns forms the complex picture seen in Figure 5.8. While the concentration of IC grows over time in solution on average, there is a large amount of variability associated with this. Figure 5.8b shows the IC values in #4 C1, where CO_2 gas was continuously supplied, as being up to two orders of magnitude higher than in other columns. Values showed little variation with depth from leachate inlet (Figure 1, Appendix D).

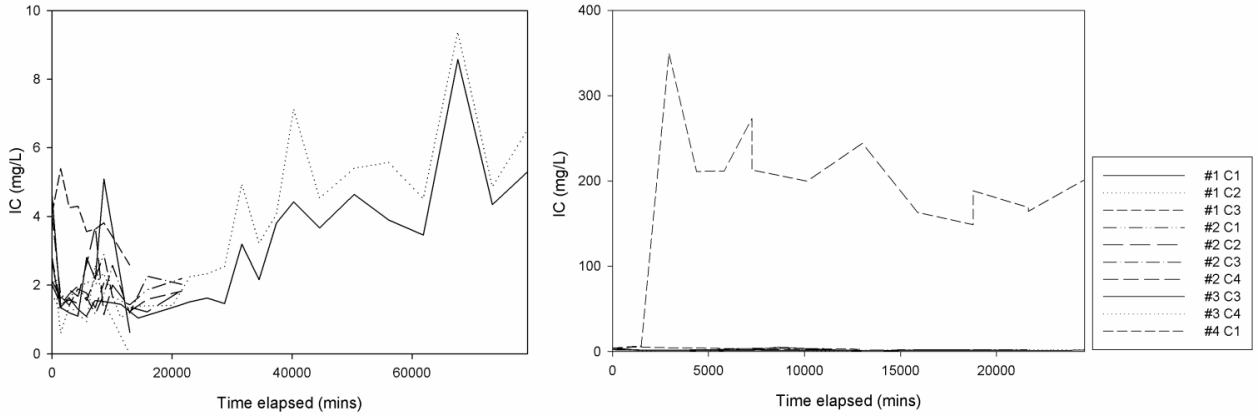

Figure 5.8a and b – Inorganic carbon in solution over time, compiled data from all columns on different 'y' axis scales. Typical analytical error = 0.46

Solids

Acid Digestion and TC (Total Carbon) analysis (IC (Inorganic Carbon) / TOC (Total Organic Carbon)) illustrated the presence of calcium carbonate minerals in the column materials (Table 5.4). While small amounts of carbonate were present in the original

materials prior to column experiments, ≤1.65 wt% $CaCO_3$ for fresh slag, 7.04 wt% $CaCO_3$ for weathered slag as in Table 5.1, all exhibited an increase in carbonate concentration over the period of the test. The largest gains were seen in #3 C3 and #3 C4, although this was not significantly higher than values seen in other columns.

Table 5.4 – Summary of analysis in experimental columns, column reference from Table 5.3 (Green = Distilled water, Black = Deionised water, Blue = High-NaCl water, Red = CO_2 addition)

#		pH	IC leachate mg/L	$CaCO_3$ % wt	TC solid % wt	IC solid % wt	TOC solid % wt
1	**C1**	11.24-11.90	0.6-4.6	1.8-4.6	0.3-1.0	0.3-0.9	0.0-0.1
1	**C2**	11.31-11.89	0.0-2.9	2.9-4.1	0.3-0.4	0.2-0.3	0.0-0.1
1	**C3**	8.94-9.22	2.5-5.4	6.8-8.3	0.6-0.9	0.6-0.8	0.0-0.2
2	**C1**	11.23-11.92	1.4-2.9	2.8-3.7	-	-	-
2	**C2**	11.02-11.88	1.1-3.7	3.0-3.6	-	-	-
2	**C3**	11.17-11.91	1.2-2.6	2.8-3.9	-	-	-
2	**C4**	11.15-11.86	1.2-4.0	2.7-3.6	-	-	-
3	**C3**	10.56-11.83	1.0-2.7	3.4-4.4	0.8	0.7	0.1
3	**C4**	11.08-11.88	1.1-2.4	3.6-4.4	1.0-1.1	0.8-1.0	0.1-0.2
4	**C1**	6.07-11.26	4-273	2.6-3.1	0.6-0.7	0.5-0.6	0.1-0.2

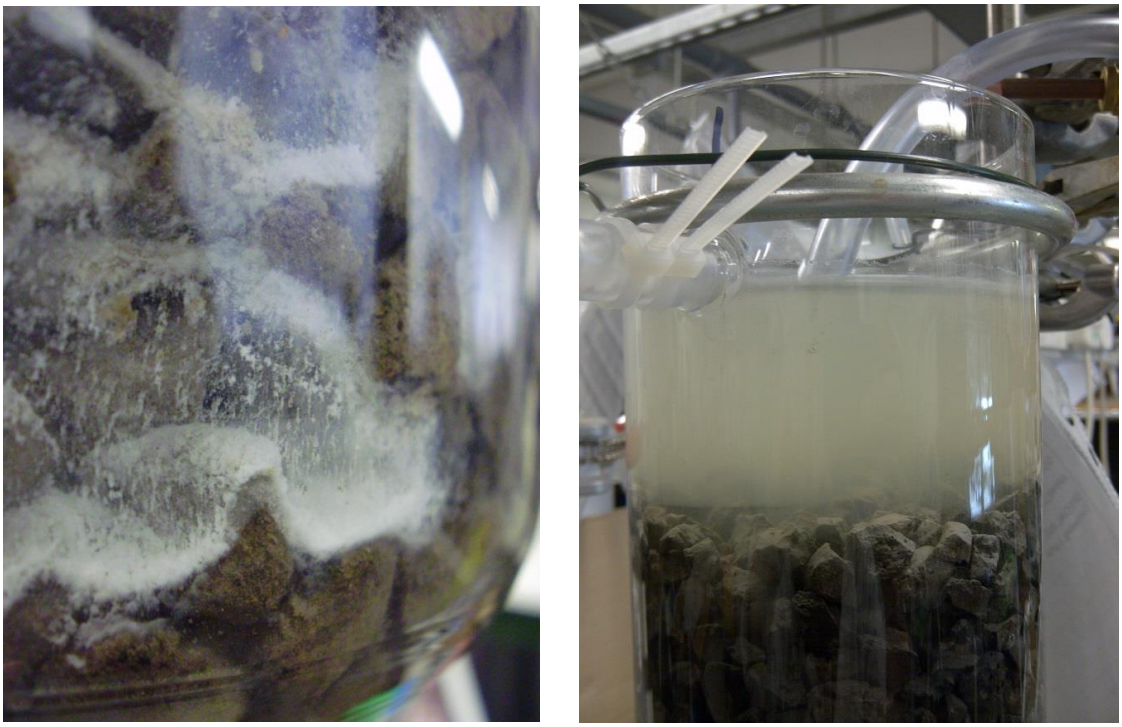

Figure 5.9a, b – Photos of columns during experimental runs (#1 C2 and #4 C1) exhibiting visible mineralisation

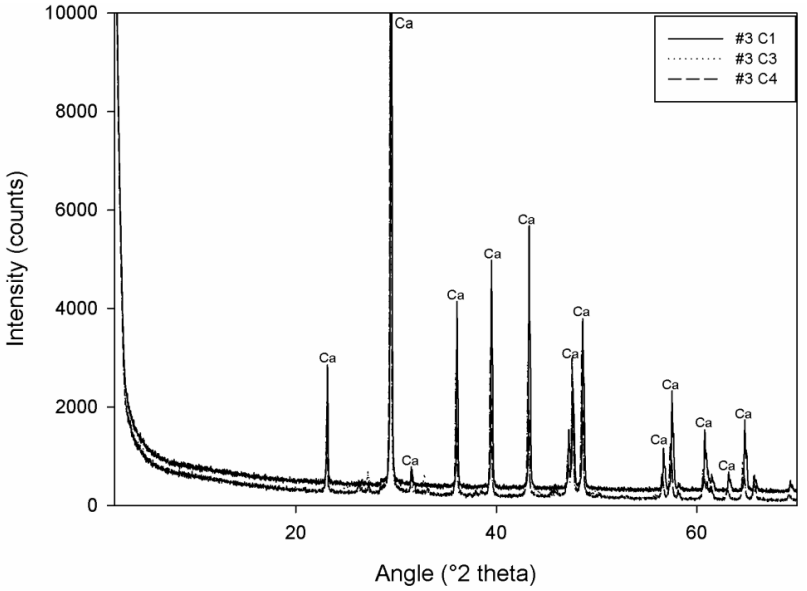

Figure 5.10 – XRD of the presence of calcite in solids recovered from evaporation of column leachates

XRD was carried out on solids from the evaporation of leachate solutions from three of the columns experiments, shown in Figure 5.10. Calcite was identified in all cases.

XRF illustrated subtle changes in the composition of solids following leaching during column experiments, but no significant departure from the parent composition.

Table 5.5 – XRF comparison data between two sets of unleached and leached material

	#3 C1 UL	**#3 CI L 450**	**#3 C3 UL**	**#3 C3 L450**
SiO_2	12.72	12.89	11.70	11.69
TiO_2	0.66	0.71	0.65	0.65
Al_2O_3	0.69	0.83	0.86	1.13
Fe_2O_3	29.12	30.00	31.01	30.14
Mn_3O_4	4.78	4.59	4.61	4.58
MgO	6.08	6.26	6.18	6.47
CaO	41.52	40.83	41.53	40.47
Na_2O	<0.011	<0.011	<0.012	<0.012
K_2O	<0.004	<0.004	<0.004	<0.004
P_2O_5	1.263	1.455	1.399	1.327
SO_3	0.169	0.150	0.20	0.262
V_2O_5	0.445	0.568	0.574	0.543
Cr_2O_3	0.201	0.132	0.130	0.139
SrO	0.044	0.047	0.049	0.047
ZrO_2	0.041	0.044	0.039	0.042
BaO	<0.008	<0.008	<0.008	<0.008
NiO	<0.003	0.022	<0.003	<0.003
CuO	<0.003	<0.003	<0.003	<0.002
ZnO	0.003	0.003	<0.002	0.004
PbO	0.014	0.019	0.017	0.019
HfO_2	<0.005	0.007	<0.005	<0.005
LOI	-2.14	-0.26	-0.23	1.37
Total	97.74	98.54	98.96	97.51

Negative LOI values indicate a mass gain, which may be due to the oxidation of materials in the sample. As the oxidation state of the iron cannot be determined by this method this may have a role in causing this observed effect. LOI increased by 1.88 and 1.60% between the unleached and leached materials reported in Table 5.5 for #3 C1 and #3 C3 respectively, suggesting a decrease in material which can be oxidised under the analytical conditions.

TG DSC QMS was carried out on solids to determine their bulk composition before and after leaching, to provide additional evidence for the presence of particular mineral phases within the leached and un-leached samples. Figure 5.11 shows the thermobalance curves and QMS curves for fresh (YAR/TAR/3) and weathered (YAR/TAR/10) slag samples, showing a small mass loss around 400°C in the fresh material, indicative of the presence of hydrated mineral phases such as portlandite, which is accompanied by a strong H_2O peak over the sample temperature range. This is less pronounced in the weathered material. Both samples show a mass loss at around 750°C, indicating the presence of carbonate minerals, supported by the evolution of CO_2 in both cases over the same temperature range. The mass loss for the weathered material is around 6.5%, compared to <1% in the fresh material.

Figure 5.12 shows the QMS curves for the solids analysed from the three columns in the first experimental run. C3 initially contained weathered slag, with C1 and C2 containing fresh material. After leaching C1 and C2 show a much lower H_2O peak around 400°C, suggesting a depletion of hydrated mineral phases, and larger CO_2 peaks around 750°C, suggesting an enrichment of carbonate phases.

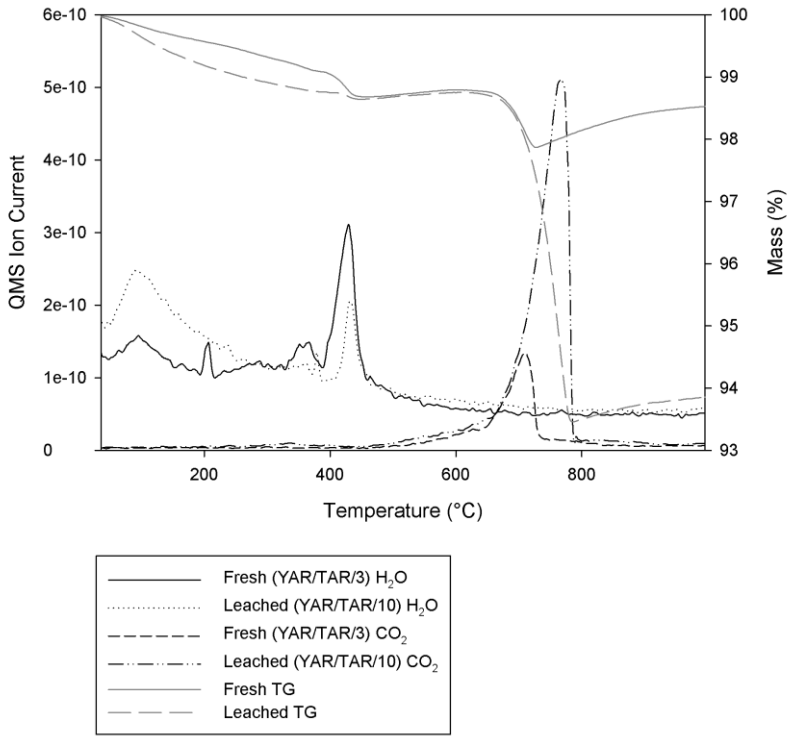

Figure 5.11 – Thermobalance curve and QMS curves for fresh and weathered material used as initial materials in column leaching experiments

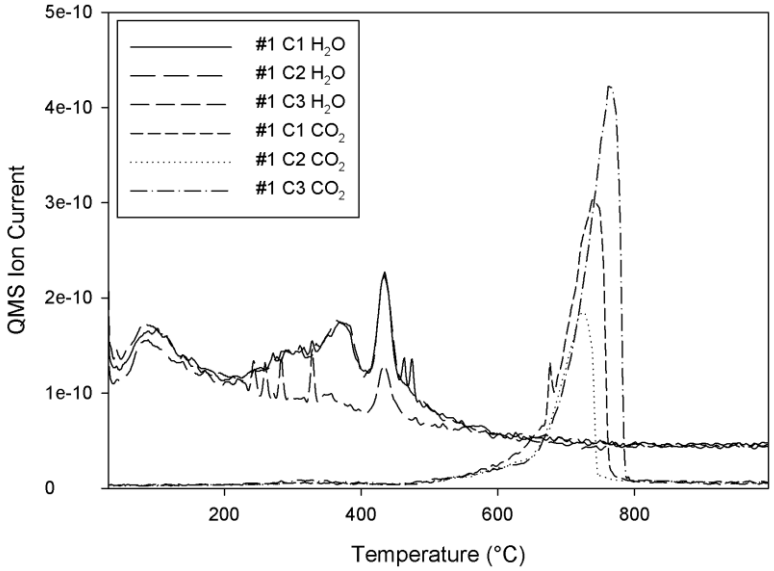

Figure 5.12 – QMS curves for materials analysed after leaching in the first run of flow-through weathering experiments

IRMS analysis of the carbonate in the residual material following flow-through weathering illustrated a number of strongly depleted signatures, up to $\delta^{13}C$ -28.55‰ and $\delta^{18}O$ -17.42‰. There is a large range around these figures, with an average composition of $\delta^{13}C$ -17.00, $\delta^{18}O$ -12.65. These data agree with the previously postulated arguments regarding the type of stable isotope signature which should be expected where high-pH carbonates have formed through a reaction with carbon dioxide. In Figure 5.11 fresh

(unleached) samples from Tata Scunthorpe (YAR/TAR/3) (filled circles) have been plotted alongside leached materials from column experiments (unfilled triangles) and leached materials sampled from stockpiles onsite (detailed in Chapter 3) (filled squares). From this graph it can be seen that all samples illustrate more negative isotope values than the fresh source material they are derived from. It can also been seen that the data acquired from calcium carbonate derived from flow-through weathering experiments is in agreement with the isotopic signatures of materials which have been weathering under ambient conditions in the field.

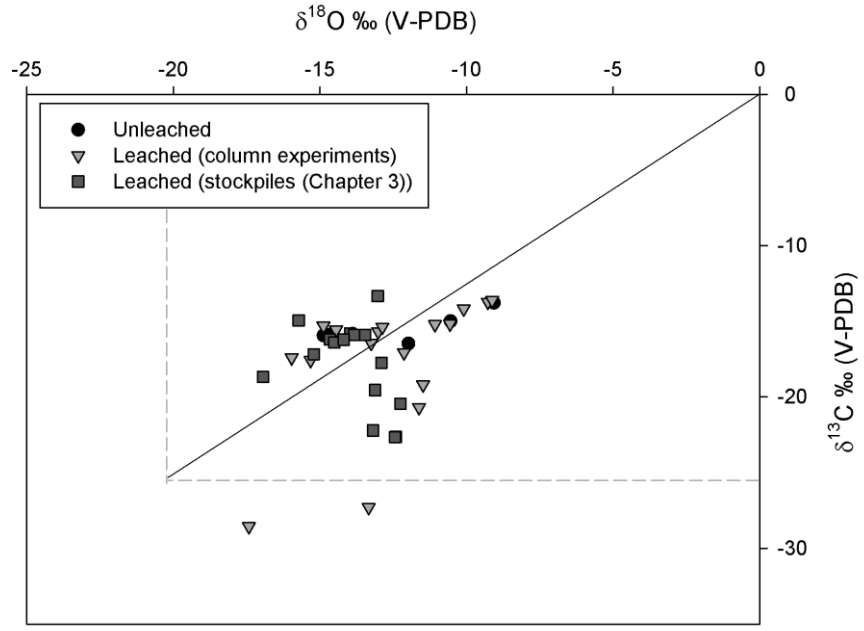

Figure 5.13 – IRMS data from column experiments in comparison with data from leached materials collected in situ on the Yarborough Landfill (detailed in Chapter 3) The straight line represents a mixing line between lithogenic (– $\delta^{18}O$=−0.0‰, $\delta^{13}C$=−0.0‰) and hydroxylation ($\delta^{18}O$=−20.5‰, $\delta^{13}C$=−25.3‰) carbonate.

Using the Ca (mg l^{-1}) in solution data from AAS analysis, and assuming a geometric surface area for the weathering particles, it has been demonstrated that in the early stages of reaction (up to 2hrs) the $\log_{10}$ values for Ca leaching vary from -8.44 to -10.9 mol cm^{-2} sec^{-1} in fresh slag (#3 C4) and weathered slag (#1 C3) respectively. A significant proportion of leaching occurs within the first 24 hrs. This is important in informing our understanding of the way in which CO_2 sequestration by slag is limited by Ca availability.

Discussion

Calcium carbonate precipitation occurred in all columns of the pilot study, confirmed by TC/IC analysis of solids and leachate, and acid digestion of solids. Strong response for

C and CO_2 in QMS supports the presence of high levels of calcium carbonate in the weathered material. $CaCO_3$ formation shows little variation with factors such as distance from fluid inflow.

Calcium carbonate precipitation in the solid phase showed little variation with respect to treatment regime. Precipitation was lowest in #4 C1 where CO_2 gas was artificially supplied to the system. pH in this column was ~6-7 for the duration of the experiment maintaining a higher concentration of C in the dissolved phase producing a high IC reading (Figure 5.8b). Wetting and drying cycles and the variation of column fluids did not significantly affect precipitation or the presence of IC in solution.

pH appears to be buffered at ~11.6 for fresh slag, which may be due to portlandite dissolution, supported by the reduction in hydrated phases after leaching observed in TG QMS analysis and at ~9.1 for weathered slag (Zomeren et al., 2011), by persistence of calcium carbonate. These flow-through weathering experiments suggest that a large amount of leaching occurs during very early stages of material weathering, due to the large elemental fluxes observed in the first hour of fresh slag weathering. It can be seen that material varying in age from 0-3 years (in this case) exhibits significant variation in 'leachate' pH, suggesting the eventual loss of a certain level of short-term buffering potential.

The weathering rate observed, based on the presence of Ca in solution, is much more rapid than natural silicates, but slower than the laboratory batch experiments carried out in Chapter 3. This may be due to factors including particle size and the mineralogy of the slag.

Summary

- $CaCO_3$ formation shows little variation with depth / distance from fluid inflow or treatment regime, with the exception of the artificial supply of CO_2 gas to the system
- A significant proportion of calcium (Ca) leaching occurs within the first 1-24 hrs of the study
- pH appears to be buffered ~11.6 for fresh slag, by portlandite dissolution, and at ~9.1 for weathered slag, by persistence of carbonate.
- The $\log_{10}$ values for Ca leaching vary from -8.44 to -10.9 mol cm^{-2} sec^{-1} in fresh slag (#3 C4) and weathered slag (#1 C3) respectively.

5.3 Observing field-scale development

A suite of data was generated from the monitoring activities completed as part of the regulatory maintenance of the Yarborough landfill, described in earlier chapters. Monitoring of a number of parameters is carried out onsite in order to ensure that the historic and contemporary landfill cells comply with contemporary legislation for air and water pollution, and the parameters set for compliance with any landfill licenses issued in compliance with contemporary landfill legislation (EU Landfill Directive (EEC/1999/31/EC); Landfill Regulations (England and Wales) 2002).

The rationale behind studying these data was to treat the inert waste landfill as a field-scale test pad, with the monitoring data showing the development of the cells over time with respect to the pH and electrical conductivity (a good indicator of solute concentration), and rate and quantity of Ca leaching where sufficient data existed. Geochemical analysis of leachate monitoring data from Yarborough inert waste landfill, Scunthorpe, was initially carried out over the period 2005-2006 with more recently acquired data providing the opportunity to add additional time points up to 2013.

At the beginning of 2009 ‘Cell 13’ was being newly developed at the Yarborough site. This cell was the first to be fully engineered, with a clay lining and leachate collection facilities – many of the earlier cells had been built to less stringent specifications as they were designed before many of the modern legislative requirements for landfill design were introduced. It was thought that this cell would provide an interesting analogue for the development of an engineered field cell, and that geochemical data could be attained over its development. Timing of the filling of the Yarborough Cell 13 was unfortunately delayed, so this work could not be completed.

Method

Data were acquired from Tata Steel in a number of stages, with detailed 2005-2006 data available early in the project and other annual data were made available after the annual review and compilation processes completed by the Yarborough landfill management team. All data points are illustrated in Figure 5.13, along with a description of the sample type detailing whether fluids have been abstracted from surface or groundwater sources (a full description of the site and its hydrogeology can be seen in section 4.3.1 Chapter 4). An example of some of the ground conditions onsite can be seen in Figure 5.12, which illustrates Cell 13 with standing surface water.

It was assumed that as noted in accompanying documentation all collated geochemical data were reliable and calculated with respect to a standardised protocol. Charge balance calculations were carried out to identify any potentially erroneous data, but otherwise corrections have not been made for potentially anomalous data. Data with charge balance between 90 and 110% were accepted.

Sample data were analysed and modelled using SOLMINEQ88: a computer programme for the geochemical modelling of water-rock interactions (Kharaka, Yousif, USGS 1989). As described relevant data were used as supplied, except:

1. Carbonate was calculated as Total Alkalinity, multiplied by 0.6 (the ratio of the relative masses of CO_3 and $CaCO_3$)
2. Total organic carbon was not included in the analysis
3. Temperature was not given in any instances, and was estimated using detailed weather records hosted by the Met Office (2008-2013)

SOLMINEQ 88 enables the calculation of saturation states for particular minerals when specific solution compositions and conditions are known, therefore enabling the determination of the presence of carbonate minerals in ground and surface waters across the Tata Yarborough Landfill as an indicator of the occurrence of mineral carbonation throughout the site.

Geochemical data were also supplied, which while unsuitable for geochemical modelling purposes could be used to demonstrate the overall geochemical behaviour of leachates onsite. pH and conductivity in particular were analysed as possible evidence of high-pH reactions occurring across the study site.

Sampling points are shown in Figure 5.14. Most are boreholes sampling groundwater on the site, but 5 surface water sampling points exist where surface water is consistently present. A subset of these sampling points is selected for routine sampling, therefore data is not reported from all of these locations on all sampling dates. Surface water can be seen in Figure 5.16. Cell 13 is the most recently developed landfill cell in the complex and throughout the duration of this work infilling activities had not yet commenced. A leachate well in the more recently developed area of the site is shown in Figure 5.15.

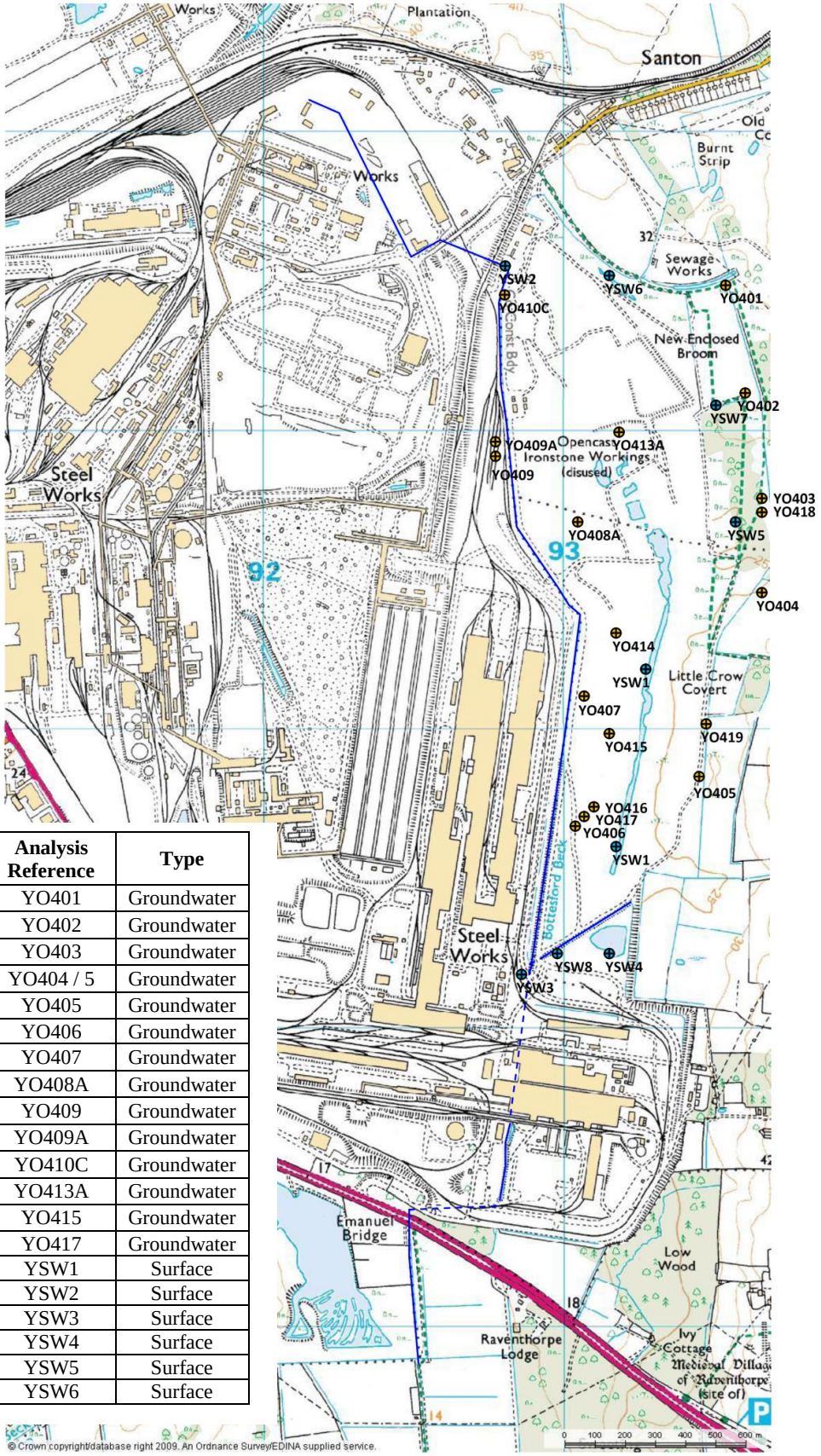

Sample Reference	Analysis Reference	Type
1	YO401	Groundwater
2	YO402	Groundwater
3	YO403	Groundwater
4	YO404 / 5	Groundwater
5	YO405	Groundwater
6	YO406	Groundwater
7	YO407	Groundwater
8	YO408A	Groundwater
9	YO409	Groundwater
10	YO409A	Groundwater
11	YO410C	Groundwater
12	YO413A	Groundwater
13	YO415	Groundwater
14	YO417	Groundwater
15	YSW1	Surface
16	YSW2	Surface
17	YSW3	Surface
18	YSW4	Surface
19	YSW5	Surface
20	YSW6	Surface

Figure 5.14 – Map of the Yarborough Landfill and surrounding area with data collection points indicated

Figure 5.15 – Leachate well at Yarborough Landfill, Tata Steel, Scunthorpe

Figure 5.16 – Cell 13, Yarborough Landfill, Tata Steel, Scunthorpe

Results

Calculated saturation indices for calcite are shown in Figures 5.17 and 5.18. In all cases, these values indicate oversaturation. Dolomite and aragonite were also predicted to be saturated.

The model also predicts possible saturation of: iron carbonate ($FeCO_3$) and manganese carbonate ($MnCO_3$) (detailed in Appendix D). This is reflected in the high levels of bicarbonate / carbonate identified in the systematic sampling programme.

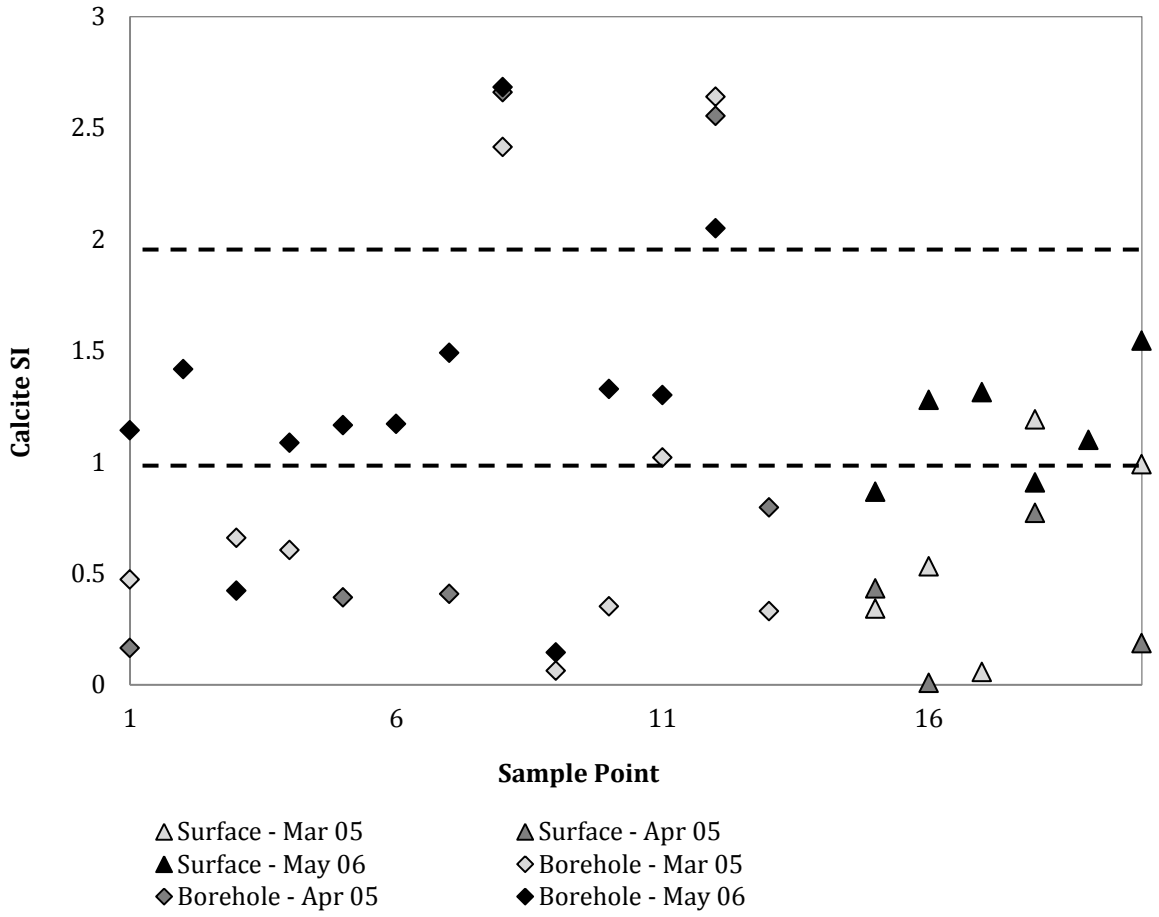

Figure 5.17 – Saturation index with respect to calcite at sample points across the Yarborough site

The relationship between pH and saturation index with respect to calcite confirms a moderately strong (r^2 = 0.6) correlation between the two parameters as should be expected, with the samples taken at very high pH showing a much higher calcite SI value.

Borehole data vary between neutral to high pH across the site, with little to no data between pH 9 and pH 11. Surface waters demonstrate pH values between neutral and

pH 10.25, with few exhibiting exceptionally elevated pH. Data can be grouped in to 2 separate 'populations' at these near-neutral or very high-pH conditions. YO408, YO413 (Figure 5.14) in the oldest part of the landfill site illustrate the highest SI values.

Variation in pH and conductivity between January 2008 and July 2013 is shown in Figures 5.18 and 5.19. All data in these figures are taken from borehole samples. pH values at the site appear to be split between near-neutral and high-pH regimes, with YO408 and YO418 demonstrating high pH values around 11-13 and all other sampling points demonstrating near-neutral pH values of 6-8. pH shows fluctuations at most sampling points, although these do not appear to be cyclically linked to consistent seasonal variations, and show no strong correlation with rainfall (Appendix D) (Met Office, 2008-2013). YO403 and YO404 show a number of high pH 'spikes'. These sampling points are located on the periphery of the site; therefore these values could correlate with movements of material or water management onsite. YO409 shows a single, significant low pH spike. This sampling point is located centrally on the works site, and at a lower gradient with respect to groundwater flow, and may illustrate the influence from other activities occurring onsite at this time.

As seen in Figure 5.19, conductivity is highly variable across the site, with YO418 (on margins of site) recording significantly elevated readings, with YO402, YO403, YO404, YO407 almost an order of magnitude lower. Two large spikes in conductivity are seen in YO404, concurrent with spikes in pH, suggesting an influx of solutes at this point which may be due to evaporation or solution mixing. A conductivity spike observed at 6 sampling points in January 2009 is not replicated in the pH signal. Figure 5.20 illustrates that there is no strong correlation between rainfall events and changes in conductivity.

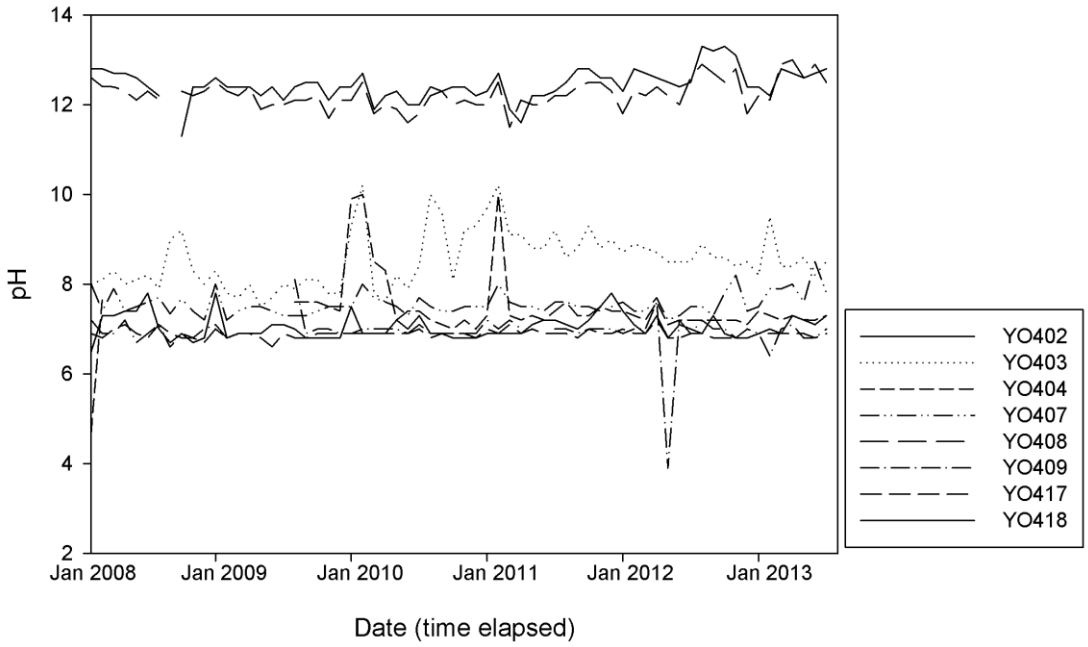

Figure 5.18 – pH variation with time across a range of sampling points on Yarborough Landfill (analytical error is not reported in the available data)

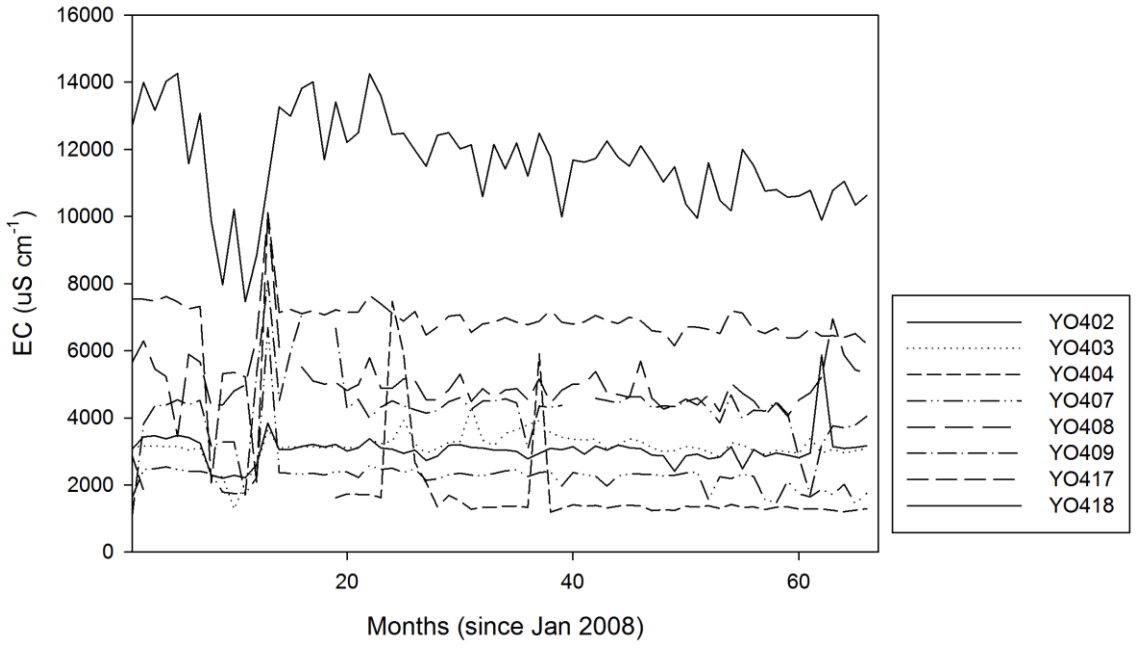

Figure 5.19 – Conductivity variation with time across a range of sampling points on Yarborough Landfill (analytical error is not reported in the available data)

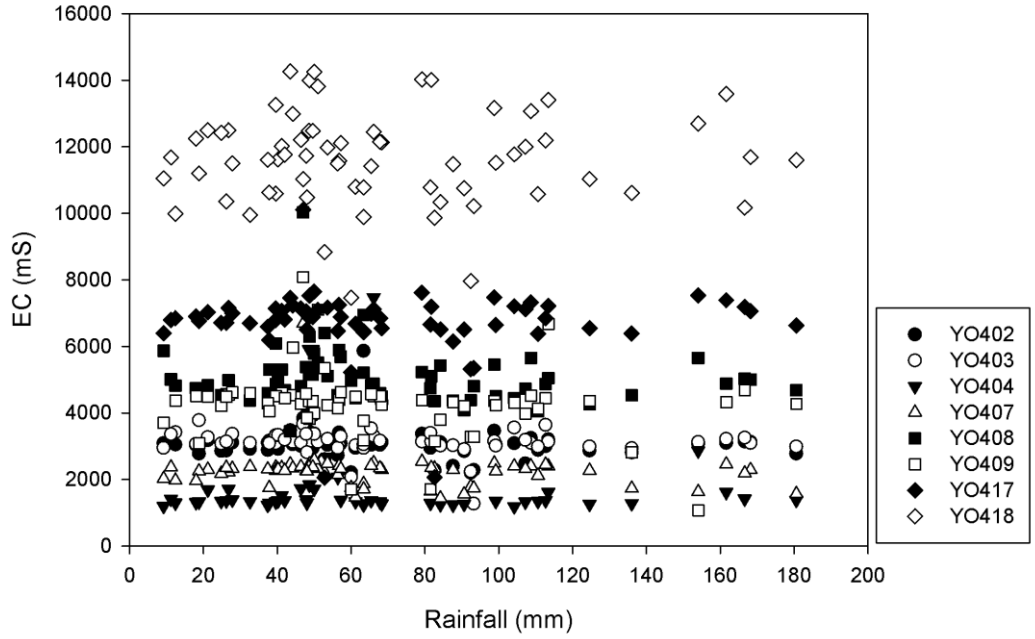

Figure 5.20 – EC variation with rainfall across a range of sampling points on Yarborough Landfill (analytical error is not reported in the available data)

Figure 5.21 illustrates the complex relationship between pH and EC onsite, combining all measured time points, showing that while the highest values for either parameter generally correspond, each borehole shows a discrete spread of values. YO418 produces significantly higher pH values than the other sample points, with elevated pH at all sampling dates. YO408 shows elevated pH values but moderate EC and YO417 shows high EC but moderate pH values. YO403 demonstrates a large pH range (7-10) while EC show little change.

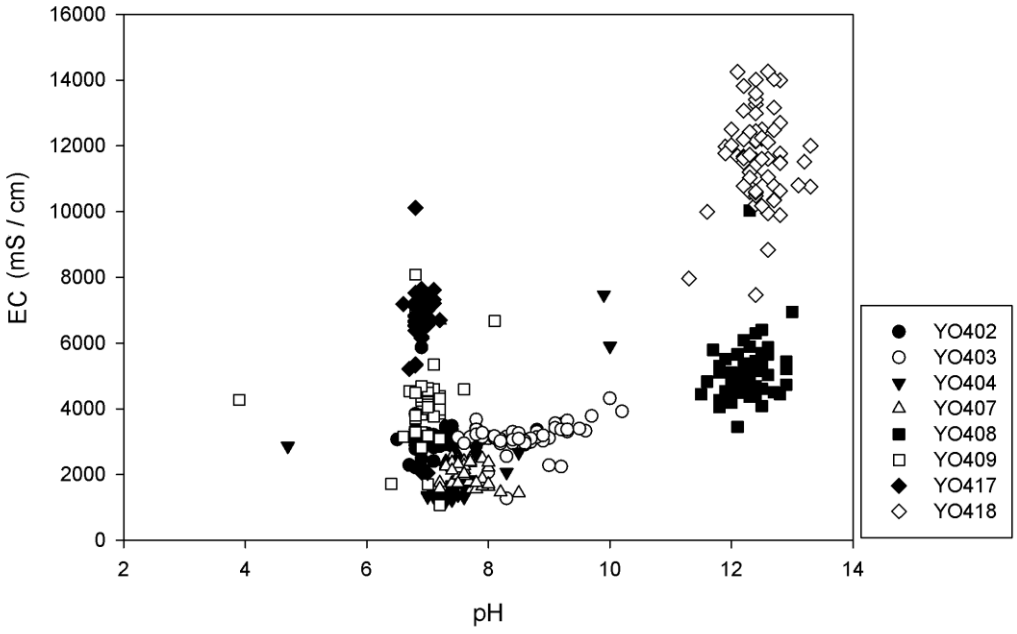

Figure 5.21 – EC variation with pH across a range of sampling points on Yarborough Landfill (analytical error is not reported in the available data)

Discussion

Further analysis of geochemical data from the Yarborough Landfill has provided an insight in to the correspondence between temporal development, local geochemistry and geography. Saturation with respect to a number of carbonate minerals is predicted by geochemical modelling, across the site. Whilst it was not modelled in SOLMINEQ 88, it is possible that as in the case of the column experiments reported in the preceding section, the lower pH population observed may be indicative of the presence of less heavily weathered material, where the local geochemistry is moderated by the dissolution of minerals such as portlandite. The higher pH population may be indicative of a region where the local geochemistry is buffered by the presence of calcite. YO408 and YO418 (Figure 5.14) in the oldest part of the landfill site where the greatest saturation with respect to calcite would be expected illustrate the highest SI values. YO403, located in the northen part of the site close to YO418, may indicate the mixing of fluids between these population.

pH and EC vary across the site, independent of rainfall patterns. Material inputs could not be mapped across the site for the study period, so a number of differences may be due to the movement of solid or liquid materials throughout the landfill. The cycling of leachate onsite was practised at a number of points throughout this study, where temporary pumps are frequently installed to redistribute leachates and surface water between different site locations. Cycled leachate is likely to be a mixture of recent and evolved material and may significantly alter the recorded geochemical parameters at a given sample point over time. The complex relationship between pH and EC suggests that there are a number of different localised geochemical conditions occurring onsite, and that the carbonate system of interest does not dominate in every case.

It is expected that the landfill will accumulate increasing amounts of solid precipitates throughout its lifespan. These preliminary results would suggest that carbonate minerals are likely to be precipitated from the landfill leachate throughout the site. It is not possible to say whether all of this material is derived from carbon sequestration, however stable isotope analysis (C, O), as discussed in Chapter 4, of stockpiled materials onsite suggests a significant contribution.

In addition to its carbon capture properties, carbonation of Ca-rich wastes in a landfill setting is also useful in the physical and chemical stabilisation of the landfill cell. Whilst

there are some notable differences in composition and management between inert and municipal sites Manning (2001) argues that carbonate formation is an essential step in the maturation of municipal landfills through carbonation of the labile Ca fraction. Calcite precipitation may also contribute strongly to the development of landfill, affecting pH balance within the material and aiding in the removal of potentially leachable hazardous materials. A study by Ettler et al (2006) has demonstrated the potential for $CaCO_3$ formation in power station fly ash to act as a factor in reducing the environmental mobility of heavy metals within the material through physical-chemical immobilisation. Reddy et al (1994) address the potential for contaminant immobilisation in alkaline solid wastes, proposing effective levels of trace element scavenging over a six-month study period dominantly occurs through a process of adsorption to the diversely polar surface of the newly formed calcite.

Summary

- Sample data from March 2005, April 2005, May 2006 were analysed using SOLMINEQ88 (Kharaka et al, 1989) illustrating saturation of carbonate minerals in waters across the site
- Modelling predicts that the Yarborough leachate samples are likely to indicate the precipitation of calcium carbonate in the landfill environment
- Investigation of variation in pH and EC showed that a significant amount of variation occurred across the site, but that single sampling points showed relatively small variations in both parameters over time

5.4 Biological

Whilst a full investigation of biological effects on soil carbon sequestration through mineral formation is beyond the scope of this study, it should be noted that this component plays a role in controlling carbonation processes in the soil system under ambient environmental conditions.

Manning et al (2013a) note that photosynthetic removal of CO_2 from the atmosphere is an important planetary carbon dioxide removal mechanism and that an amount equivalent to all atmospheric carbon passes through the coupled plant−soil system within 7 years. It is therefore possible to theorize that this may provide one means by which carbonate formation in soils can be promoted. Manning et al. (2013) also note that root-exuded carboxylic acids have the potential to supply 4−5 micromoles C $hr^{-1}g^{-1}$ fresh weight to the soil solution, and enhance silicate mineral weathering by combining with Ca liberated by mineral weathering to produce pedogenic calcium carbonate.

An earlier paper (Manning, 2008) questions whether it is possible to take a combined ecosystem service approach, to manipulate crop production to maximize carbon capture as pedogenic carbonates, assuming intentional application of calcium-rich materials to agricultural soils in order to promote carbonate formation. Promotion of calcite precipitation by plant root exudates such as malate and citrate occurs naturally on soils developed on calcium silicate regoliths, however this process has not yet been tested in soils developed on artificial silicate minerals, or intentionally engineered for carbon capture.

Renforth (2011 (PhD thesis)) notes that there is still a lack of long term field scale growth trials to understand the weathering dynamics of plant type, material, organic and inorganic carbon accumulation in the soil and the biological response. They propose that observation of plant primary succession on demolition sites can assist in this, enabling the selection of appropriate species which are likely to establish on these sites. Little work has been carried out to determine the relative benefits of particular plant species or functional types (groups of plants with a number of shared functional traits (Lavorel et al., 1997)) to the weathering and carbonate formation process, but it assumed that different species are likely to interact differently in this respect.

Figure 5.22 shows the possible dynamic routes for carbon transportation in the soil-

water system, where both plant and microbial activity may contribute to the mineralization process.

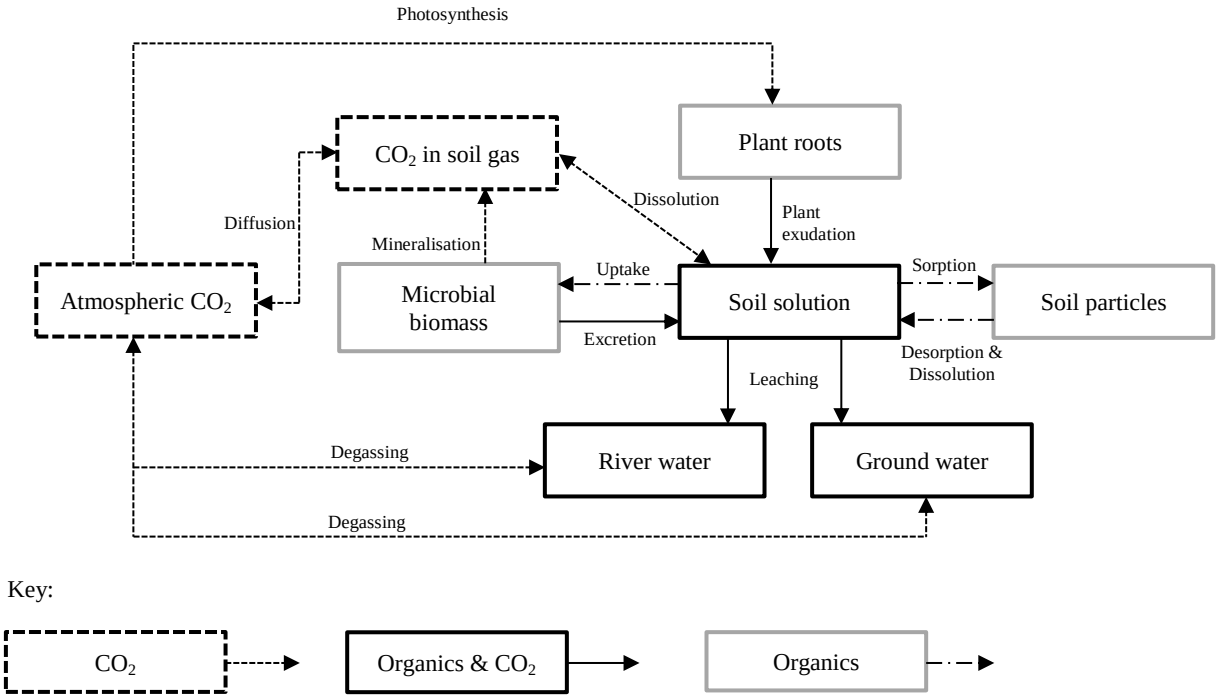

Figure 5.22 – Organic acid and CO_2 dynamics in soil (from Renforth 2011 (thesis), adapted from Jones 2003)

Testing the impact of biological factors (Carbon Capture Gardens)

Method

A 'combined ecosystem service approach' was used in the construction of the Carbon Capture Garden test site in centre of Newcastle upon Tyne. The gardens were located at Newcastle Science Central, described in detail as one of the field study sites in Chapter 4. A demolition site was selected for an in-depth trial to be carried out to determine whether the carbon storage potential of artificial soils could be increased by the addition of compost and selected plant groups. The preliminary work for this study was carried out between 2010 and 2012 and involved the creation of 24 test 'cells' (approx. 4.2 x 5m) on the site in February 2011, to which a matrix of treatments was applied (Table 5.6). Twelve of the plots were amended with 1 m^3 each of compost (a depth of approximately 10 cm), with the other twelve remaining un-amended. Compost was derived from green waste and supplied by Newcastle City Council. Species planted were known to be tolerant to the conditions expected onsite (high pH), and were planted from seed. Buddleia and birch seeds were spread at a density of 0.5g m^{-2} and wildflower mix at 2.5g m^{-2}. Developments can be seen in Figure 5.23 and 5.24.

Data were collected onsite by project students in summer 2011, encompassing soil chemical analysis and plant community analysis. The site was intended as a long-term experimental facility, but was ultimately scheduled for redevelopment in 2013, which led to the eventual clearance and demolition of the plots. One of the aims of this site was to attempt to quantify the potential for inorganic C storage at a 'typical' urban redevelopment site: to investigate the significance of carbonate formation and allow the potential of other similar sites to be estimated.

Figure 5.23 a and b – Construction of the Carbon Capture Gardens, carbon capture gardens in progress

Table 5.6 – Carbon capture gardens cell layout and treatment schematic

E	**F**	**A**	**D**	**B**	**C**	**F**	**E**	**B**	**D**	**C**	**A**
B	**F**	**E**	**C**	**A**	**D**	**A**	**D**	**B**	**C**	**F**	**E**

A Compost + Buddleia + Wildflower
B Compost + Birch + Wildflower
C Compost + Wildflower
D No Compost + Buddleia + Wildflower
E No Compost + Wildflower
F No Treatment

Soils were hand sampled to 20cm on the plots and air-dried. Organic and inorganic carbon analysis was carried out with the use of a Leco total carbon determinator and acid digestion respectively. As in previous chapters, samples were analysed for bulk carbonate by acid digestion using an Eikjelkamp Calcimeter (methodology detailed in methods section of Appendix A), which had been calibrated immediately prior to analysis, to BS 7755-3.10:1995 ISO 10693:1995. Samples were reacted with 0.4M HCl and $CaCO_3$ content inferred from volumetric measurement of CO_2 gas evolved

Plant cover and species were assessed through the use of species count and ground cover methods (as % cover), undertaken with the use of a 2 x 2m quadrat.

Results and discussion

Studies carried out by Matt Buxton (MSc student in Environmental Consultancy) in summer 2011 found that there was little observable difference in $CaCO_3$ concentration between the treatments applied to the plots. One-way Analysis of Variance (ANOVA) was used to determine the significance of variations observed between the plots. Treatments E, F and D had the highest three mean $CaCO_3$ contents respectively (28.94%, 25.1%, 20.76%), while treatments C, B and A had the lowest three respectively (11.11%, 12.64%, 16.04%). This may be in large part a dilution effect from admixing of compost to the plots. A significant improvement in biodiversity was noted, with species establishing in all plots, with higher density in those with compost, but more evidence of weed species which had encroached from other parts of the site. In August, treatment A yielded the highest mean cover (39.25%), followed by B and C. Treatment F yielded the lowest cover (1.313%).

Through the data collected, limited conclusions could be drawn regarding the efficacy of the Carbon Capture Gardens with respect to soil carbon sequestration. Variation in carbonate content between the plots was not significant after 7 months of cell development, however this may not have been the case after longer periods of maturation. Vegetation cover showed significant variation, however this was in part due to the promotion of plant growth in compost over un-improved construction and demolition waste, and weeds propagated from other parts of the site presented a large proportion of the vegetation cover noted on the composted plots.

Summary

The coupled plant−soil system naturally removes CO_2 from the atmosphere, and in so doing carbon is transferred to the soil. Manning et al (2013a) note that one approach to integrating vegetation in to soils designed for mineral carbon capture (and organic carbon capture) to remove atmospheric CO_2 could be analogous to the use of constructed wetlands to clean up contaminated waters. Careful design of “carbon capture gardens” has the potential to provide a number of ecosystem services, including carbon sequestration, water management, nutrient cycling, biodiversity and social / cultural services provided by open green spaces.

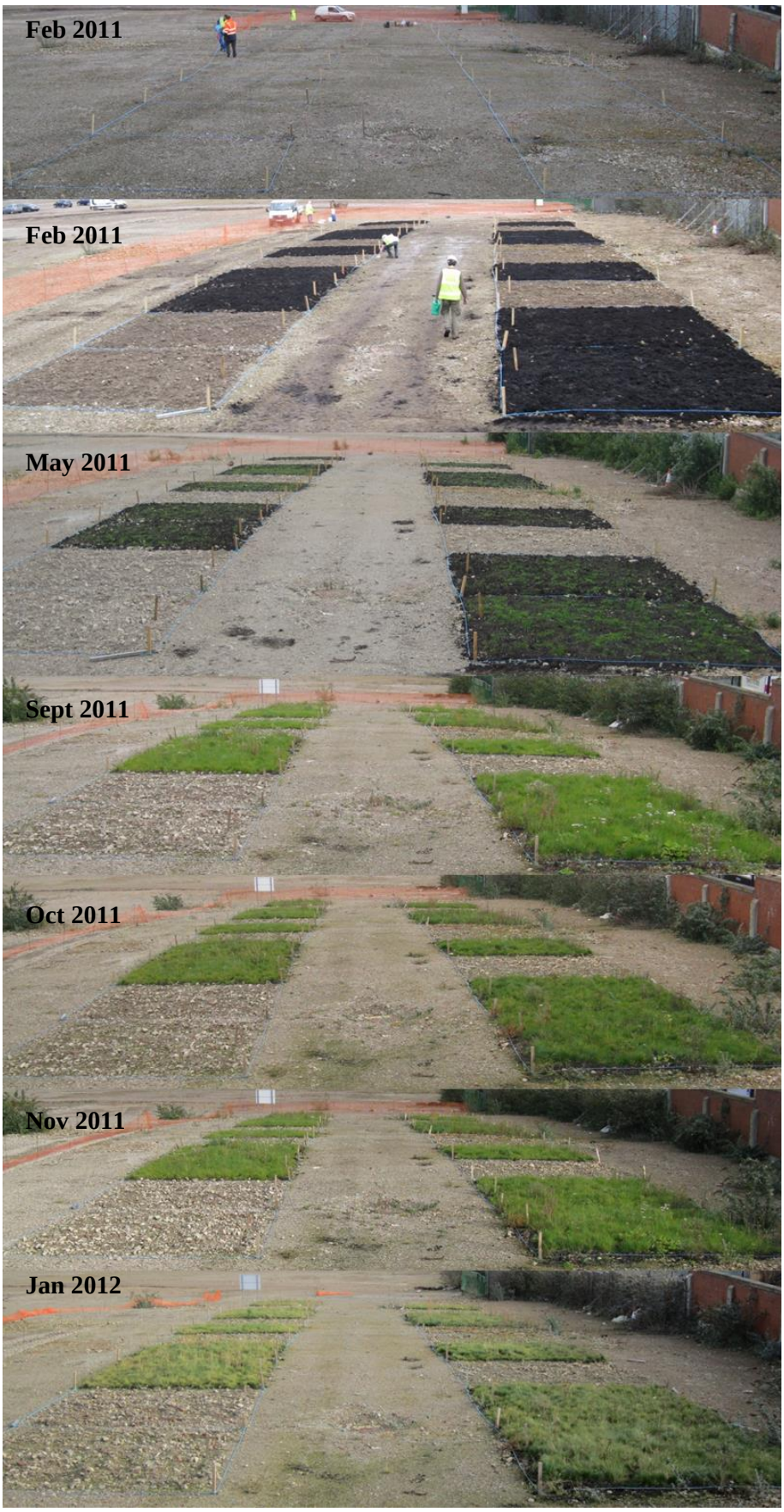

Figure 5.24 –Time lapse photography of vegetation growth at the carbon capture gardens between construction and August 2012 (Photos courtesy of Dr Elisa Lopez-Capel)

5.5 Quantification of capture and capture potential

One of the challenges in engineering sites for carbon capture is quantifying the carbon capture potential of the processes occurring on measurable spatial and temporal and scales. As discussed in Chapter 2, the overall potential of materials suitable for carbonation can be estimated by simply knowing their bulk chemistry, and inferring carbon capture potential from the concentration of leachable divalent cations.

In the field this is more complex, as due to some of the factors explored in Chapters 3-5 this full potential is not always reached, or may only be partially exploited by the time at which a site is investigated. In order to quantify the carbon capture potential of field sites and large-scale engineering systems a methodology for addressing this had to be developed. This exploited multiple lines of evidence including carbonate content, bulk chemistry (determined by XRF or similar) and an assessment of the ratio of lithogenic to hydroxylated carbonate present (determined by IRMS and end-member analysis).

The Science Central site, described in Chapter 4, can be used as an example of how this process might be carried out. Research at the large urban brownfield site 'Science Central' in Newcastle upon Tyne demonstrated capture and storage of significant quantities of CO_2 as secondary carbonate minerals over short timescales. Published data of an initial survey carried out in September 2010 (Washbourne et al., 2012) demonstrated $CaCO_3$ wt % in soils onsite of 22.15 ± 6.86, with hydroxylation carbonate representing 39.4±8.8%. XRF and IRMS analysis was carried out on the samples and used to determine the bulk chemistry of the material on site and stable isotope values of C and O in carbonates to indicate the likely partitioning between lithogenic and pedogenic carbonate.

Table 5.7 summarises the storage of inorganic C as carbonate on the Science Central site, presenting carbonation figures based upon the measured contemporary divalent cation (Ca, Mg) contents calculated from XRF analysis (shown in Chapter 4) and known carbonate contents measured by acid digestion (shown in Chapter 4). As in Washbourne et al. (2012), both datasets were converted to molar notation then end member analysis (Figure 5.25) was used to estimate the molar proportions of Ca and Mg in lithogenic and hydroxylation carbonate respectively (partitioning the overall carbonate content in to lithogenic and hydroxylation, and assigning cations to each assuming stoichiometric reaction to form carbonate minerals). Any residual mass of

divalent cations not incorporated in carbonates was assumed to be representative of the residual carbon capture potential of the site. Details of these calculations can be seen in Appendix D.

Table 5.7 - Summary of site data to estimate carbon capture potential assuming reaction of material to full depth (2010)

	Description	**% of material**	**Mol kg^{-1}**	**$kgCO_2$ t^{-1}***
1	Total inorganic carbon – from acid digestion	**2.74 ± 0.85**	**2.28**	
2	Carbonate-C derived from lithogenic sources (old) – from isotopic end-member analysis	**60.61 ± 8.83**	**1.43**	
3	Carbonate-C derived from high pH solution (new) – from isotopic end-member analysis	**39.39 ± 8.83**	**0.85**	
4	Total calcium (CaO)	**13.68 ± 2.84**	**2.44**	
5	Total magnesium (MgO)	**1.85 ± 1.01**	**0.46**	
6	Total cations (4+5)		**2.91**	
7	Total carbon capture potential (6 – 2)		**1.47**	**64.8**
8	Residual carbon capture potential (7 - 3)		**0.62 (41.6%)**	**27.3**
9	Already exploited carbon capture potential (7-8) or (3)		**0.85 (58.4%)**	**37.4**
*assumes 1 Mt of material				

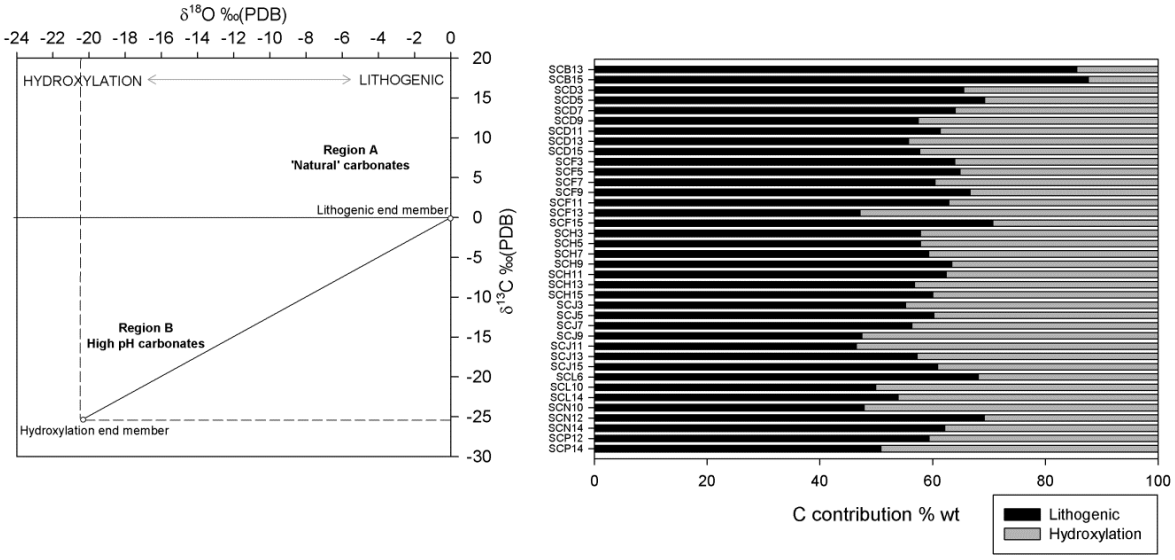

Figure 5.25 – Illustration of 'mixing line' method by which proportional contribution of different carbonate formation pathways is calculated from IRMS data, and proportion of 'hydroxylated' carbonate present (2010)

Science Central is covered by approximately 1 million tonnes of demolition material (Norwest Holst, October 2005 Project No. F15481A). Based on XRF and stable

isotopes of C and O, it is likely that the initial material onsite possessed an overall carbon capture potential of 64,804 t CO_2. The current concentration of divalent cations (Ca and Mg) at the site not currently bound in carbonates suggest approximately 58.36% of this potential has already been exploited, capturing 37,463 t CO_2, leaving a remaining sequestration potential of 27,341 t CO_2. This quantity is significant within the scope of a development project of this type, as it presents a potential for offsetting C produced during production of the original construction materials and can be considered as an on-going offset by the site developers if the sequestration reaction is promoted in areas of exposed soil or managed vegetation.

The carbon capture potential of any site of this type depends upon the quantity of material present, the quantity of material which is composed of Ca/Mg-silicate minerals and the depth to which carbonation reactions are able to occur. The rate at which carbonation occurs is determined by the supply of cations from weathering and by CO_2 supply that forms carbonate in solution. One of the major challenges is constraining the depth to which carbonation naturally occurs, or can occur in engineered settings. Sampling depth was restricted by the presence of concealed structures during trial pit operations, therefore the calculations in Table 5.7 present an idealised carbon capture potential, assuming full carbonation of materials throughout their full depth profile.

The economic value of urban soils as carbon capture devices is discussed further in Chapter 6.

Summary

- Quantification of the potential for inorganic C storage at a ‘typical’ urban redevelopment site is complex to reconstruct, even when site geochemistry is accurately mapped over time. Further constraining of these parameters is required to investigate the significance of carbonate formation and allow the potential of other similar sites to be estimated

5.6 Summary

This chapter presents data from engineered systems where MCCS is occurring without significant energy input. Flow-through weathering experiments demonstrated that in smaller systems $CaCO_3$ formation shows little variation with depth or treatment regime over the short-term and that a significant proportion of calcium (Ca) leaching occurs within the first 1-24 hrs of the study. This suggests that progressively carbonating *in situ* layers of material, or similar low-impact engineering interventions have significant potential for encouraging MCCS. In these systems pH appeared to be buffered at ~11.6 for fresh slag and at ~9.1 for weathered slag. This was also observed at field scale through the analysis of leachate sampling data from a large silicate waste landfill site, which identified two pH 'populations', near-neutral possibly moderated by the dissolution of minerals such as portlandite and high-pH potentially buffered by the presence of calcite. Modelling indicated the widespread precipitation of calcium carbonate throughout the landfill environment.

In identifying other passive interventions which may increase MCCS, a short term field-study suggested that "carbon capture gardens", using silicate wastes in engineered, vegetated landscaping, could provide a number of useful ecosystem services. This presents one possible framing for the implementation of soil engineering for carbon capture at the scale of a single development site.

Quantifying carbon capture even at a single field site is a complex process. The approach shown in section 5.5 used multiple lines of geochemical evidence to quantify the potential for inorganic C storage at a 'typical' urban redevelopment site. A 10ha site is predicted to have possessed an initial overall carbon capture potential of 64,804 t CO_2, a large quantity at the scale of a single development project.

The following chapter draws together the findings presented to this point in the broader context of real-world systems, assessing how the technical aspects of MCCS at field-scale are likely to be influenced by economic and policy factors.

CHAPTER 6 - Economic and policy implications of mineral carbon capture in soils

The technical factors surrounding mineral carbon capture in soils, discussed in the preceding chapters, are considered in this chapter together with their economic and policy implications. Technical factors govern the rate and capacity of the process, which are critical in determining the likelihood of a potentially useful technology being implemented based upon net costs and benefits. Existing policies have the potential to promote or discourage implementation based upon technical, environmental or social incentives or penalties (all of which may have at least a partial economic basis) applied to the materials, processes or products.

Physical and chemical properties of materials which might be used in engineering soils for carbon capture through mineral sequestration has been broadly discussed in Chapters 2-4; following on from Chapter 5 this chapter considers the technical aspects of treating, transporting, emplacing and managing these materials and the sites on which they are used. These management aspects all have tangible economic implications, which are briefly considered to contextualise the cost of implementation.

To explore the possible applications of the experimental work and field studies presented in the preceding chapters, and to relate this work more directly to real world settings, this chapter directly links the proposed benefits of carbon capture and storage in soil settings with the technical and legislative issues which would surround its implementation. Proposals are also offered, framing the ways in which existing policy could be applied to this technology and how new legislation might be formed to favour, or discourage, its implementation.

Chapter Summary:

Contemporary economic and legislative aspects of the MCCS process in soils are framed in the context of lifecycle assessment, current economics and legislation.

- Current advantages – reuse of ‘wastes’, ecosystem service provision (carbon capture, biodiversity), low cost of intervention, potential for economic incentive
- Current disadvantages – competition for use of materials in other settings, issues with waste transportation regulations, lack of economic incentive

6.1 Technical / Economic factors

Factors affecting the implementation of mineral carbon capture in soils include all the ways in which materials are handled between their source and final application, encompassing extraction or collection, treatment methods, transport and any *in situ* processes linked to emplacement or on-going management of the materials to encourage carbonation.

All of these factors have the potential to alter the amount of energy and associated material inputs that the mineral carbon capture process requires. The minimisation of these factors is a significant means of improving the efficiency (technical and economic) of the process, therefore consideration is given throughout this work to the compromises which may need to be taken into account in any one of these parameters to ensure the success of the process overall.

6.1.1 Technical opportunities and barriers to implementation

Table 6.1 summarises a number of considerations which may impact upon the technical feasibility of mineral carbon capture, from acquisition of materials to treatment and management of residual products. This demonstrates a simplified summary of some of the possible material and energy inputs at each stage of the process. Each of the factors listed is generalised and may comprise a number of embodied processes.

While the focus of this work remains on the feasibility of implementing mineral carbon capture and storage in passive settings, the following sections contain information on both reactor-based and passive treatments. Mineral carbonation in a reactor setting is, in a number of ways, a more developed area of technology than passive carbonation with a large amount of small-scale and theoretical work carried out to date. Most studies devoted to this topic have concluded that without further economic incentive in place most reactor-based mechanisms are too costly to run at commercial scale (Huijgen et al., 2007) (summarised later in this chapter). Estimated process steps, energy and economic costs of this technique are used as a comparison to the passive methodology in order to determine where savings and compromises can be made.

Table 6.1 - Summary of technical factors in the mineral carbon capture process

Extraction	Extraction of silicate material from its original source: quarried materials from mineral deposits, artificial silicates from industrial process waste streams, stockpiles, waste transfer stations or demolition sites	Blasting Quarrying plant (fixed / mechanical) Quarrying plant (vehicular)
Transport	Movement of material around extraction site, from extraction site to treatment points and offsite to ultimate site of use	Vehicles, conveyer belts and other necessary infrastructure (rail, road etc.)
Crushing and pre-treatment	Crushing of materials, either as part of a larger industrial process (e.g. crushing of quarried rock for aggregate) or intentionally to encourage carbonation reactions. Includes unintentional production of fines at each processing stage which may be suitable for carbonation	Crushing and screening
Additional treatment	Further processing of the material as part of a larger industrial process (e.g. washing or weathering)	Crushing and screening
Reactor treatment	Treatment of materials in a process-based reactor	Heating and high pressure conditions
Transport of products	Transport of products from reactor away from the reactor site for further use or disposal	Vehicles and necessary infrastructure (rail, road etc.)
In situ treatment	Treatment of materials in a passive setting	
Management of *in situ* carbonation	Processes required to maximise the potential of passive, in situ carbonation processes	Vehicles and necessary infrastructure (rail, road etc.). Site construction.

Tables 6.2 and 6.3 detail some of the process-based considerations which also have the potential to affect the feasibility of these techniques. From these summaries it can be seen that the most cost-effective processes require the greatest quantity of carbonation for the least intervention at each process stage. Crushing, pre-treatment and transport of materials are all energy expensive processes, as is the provision of the reactor vessels with elevated pressure and temperature conditions required by reactor-based mineral carbon capture projects.

While particle size has an impact on carbonation, the reactive surface area of the mineral grains is the main determiner. For passive *in situ* carbonation, the need to grind materials to a very fine state is reduced due to increased residence time of the material, however this is a requirement for reactor-based processes due to the necessarily rapid rate of turnover required in these processes. Renforth (2012) estimates the energy required to prepare materials for effective mineral sequestration (extraction, crushing,

screening and grinding) is likely to be between 10 and 316 kWh t^{-1}. Penner et al. (2004) estimate that parasitic energy losses for ultrafine grinding may be in excess of 50% of the total plant energy when applied in a reactor setting. A number of suitable materials are available as fine particles as the unintentional by-product of processing steps, such as secondary aggregate production from C&D waste and crushed aggregate production from steel slag, reducing the need for specific processing.

Table 6.2 - Conceptual summary of mineral carbonation strategies adapted from Renforth (2011 thesis, adapted)

Above ground natural silicate carbonation					
Extraction, through blasting and mechanical impact	Primary / secondary / tertiary crushing Carbonated overburden disposed	Carbonation in a reactor at elevated temperature and CO_2 partial pressure	Carbonated material sold as secondary aggregate or used in the quarry	Fines transported to local farmland and spread on land	Material worked into soils to promote the formation of pedogenic carbonates
Carbonation of C&D waste					
C&D waste sorted onsite to separate cement based material	Primary / secondary / tertiary crushing	Transported to a carbonation reactor	Carbonated material sold as secondary aggregate or spread on demolition site	Fines transported to local construction site and used as made ground to promote the formation of pedogenic carbonates	
Underground carbonation of natural silicates, artificial heaps and landfill cells					
CO_2 piped / transported from point sources	CO_2 stored / pressurised	CO_2 injected in to existing spoil heaps	CO_2 injected into existing (using directional drilling) or engineered landfill cell		

Table 6.3 - Schematic of crushing methods: from Renforth (thesis) adapted from Guimaraes et al. (2007)

Blasting from the working face	Primary crushing	Screening	Secondary crushing	Screening	Settling pond
20% fines	3-5% fines		30-40% fines		Fines

These tables highlight the need to understand, through experimental work, where trade-offs can best be made in order to ensure the efficiency of the process whilst reducing energy intensity. For example, investigating the variation in rate of carbonation between crushed and uncrushed materials (as carried out in previous chapters) in different environments allows the estimation of an acceptable limit for crushing at which the

carbonation reaction still proceeds rapidly without the investment of large quantities of energy.

When considering the areas highlighted in the tables above, *in situ* carbonation has an inherent energy and material benefit over carbonation in a reactor. *In situ* mineral sequestration requires minimal mechanical intervention or management, but compromises the rate at which reactions occur and the extent to which these can be controlled and monitored. Nonetheless it has an economic benefit, in comparison to engineered mineral carbonation processes, of eliminating a significant number of treatment and transport stages which contribute additional cost.

One of the most effective ways to assess the relative benefits of the two types of mineral carbon capture is to carry out a life cycle assessment (LCA), to determine the long-term viability of the processes, and the time over which we would expect the processes to act in order to be fit for purpose. An LCA can be thought of as charting the "evolution of a building or product back into its natural constituents" (Kosmatka and Wilson, 2011) through material sourcing, construction, use, and end of life. A life cycle assessment would normally take in to account the service life of the material in construction and operation (in the case of C&D waste and steel slag) as well as its production and fate (Figure 6.1). In this instance it is assumed that the materials studied have similar impacts in these respects, therefore only the differences in process elements related to carbon capture and storage are reported. ISO Standard 14044 is a point of reference which provides guidance on conducting a full LCA (ISO 2006).

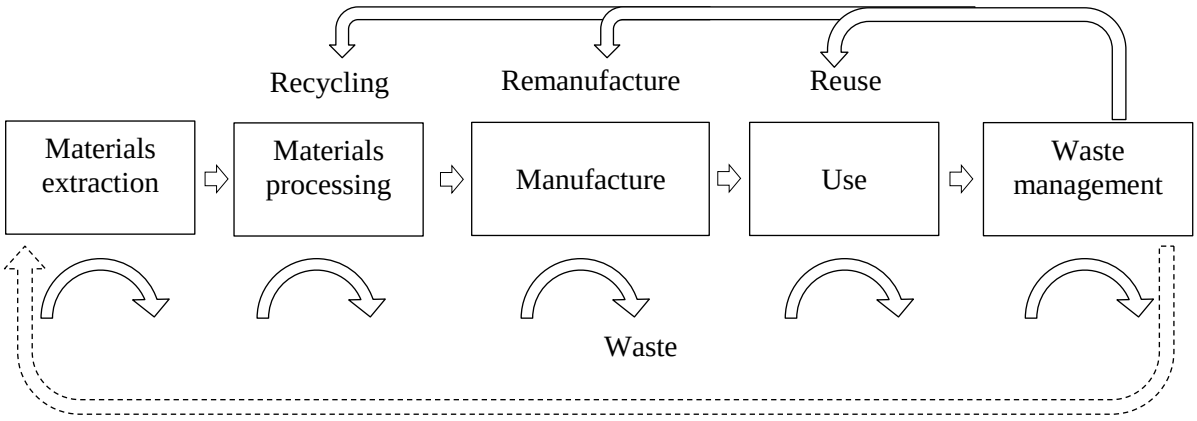

'Closing loop' through effective waste management and carbon sequestration

Figure 6.1 – Generic product life cycle (Portland Cement Association)

In Huntzinger 2006 (thesis), and Huntzinger et al., 2008 a life cycle assessment was carried out to determine the overall feasibility of using cement kiln dust (CKD) to sequester CO_2, as a comparison method with other possible manufacturing processes and end-use routes for the material. Assessing processing, transport and environmental impact at each stage Huntziger et al (2008) found that utilization of CKD for sequestration appeared to offer a means to reduce carbon emissions and produced a reduction in the environmental impact score of approximately 5% over traditional Portland cement.

The parameters assessed by the life cycle assessment model used (Huntzinger et al, 2009) were:

- Energy and heat
- Material
- Sequestration potential
- Transport, processing and final use
- Environmental impact categories including leaching and metal content

A full LCA could categorise the impacts over a materials life in to impact categories such as land use, resource use, climate change and health effects (ISO 14040:2006 Environmental Management - LCA principles and framework, ISO 14044:2006 Environmental Management - LCA requirements and guidelines). Table 6.4 summarises the ways in which the parameters listed above are likely to influence the feasibility of passive carbon capture and storage processes. Reactor-based carbonation is listed alongside for comparison at each stage.

A full life cycle assessment of the mineral carbon capture process is not included, as many assessments already exist for the separate components of the process (Huntzinger, 2008; Chen et al., 2011; Khoo et al. 2011) and an exhaustive analysis is beyond the scope of this report. Figure 6.2 illustrates the basic information required to carry out a life cycle assessment to compare passive and reactor-based mineral carbon capture. The points where the two processes differ most are the additional energy inputs for crushing, reactor construction and operation, transport and disposal of waste products, and additional associated CO_2 emissions for reactor based approaches. Whilst the passive system has fewer environmental and energy penalties, it must be noted from Table 6.4 that compromises are likely to be made regarding the rate of reaction and potential for re-use of any useful products.

Table 6.4 – Life cycle parameters likely to influence the feasibility of carbon capture and storage processes

	In situ carbonation (soils)	**Reactor carbonation**
Preparation	Crushing may be intentionally applied or occur as part of other treatment processes such as aggregate production	Crushing and screening to small particle size necessary for most reactor-based processes
Transport	Transportation from production site Transportation to crushing facility Transportation to field site	Transportation from production site Transportation to crushing facility Transportation between reactor stages Transportation of reacted product
Pre-treatment	N/A	A variety of possible processes including pre-leaching of the reactive cations
Treatment Capacity Rate	 Fixed by the amount of available materials, estimated to be 192-333 Mt C a^{-1} (for artificial silicates. Natural silicates >10,000 Gt) Days - Years	 Fixed by the amount of available materials, estimated to be 192-333 Mt C a^{-1} (for artificial silicates. Natural silicates >10,000 Gt). Reactors are likely to require more specific feedstock than *in situ* carbonation Minutes - Hours
Post-treatment	N/A unless re-excavated	Recovery from reactor Utilisation of products where appropriate (from aggregates to high purity minerals depending on the process)

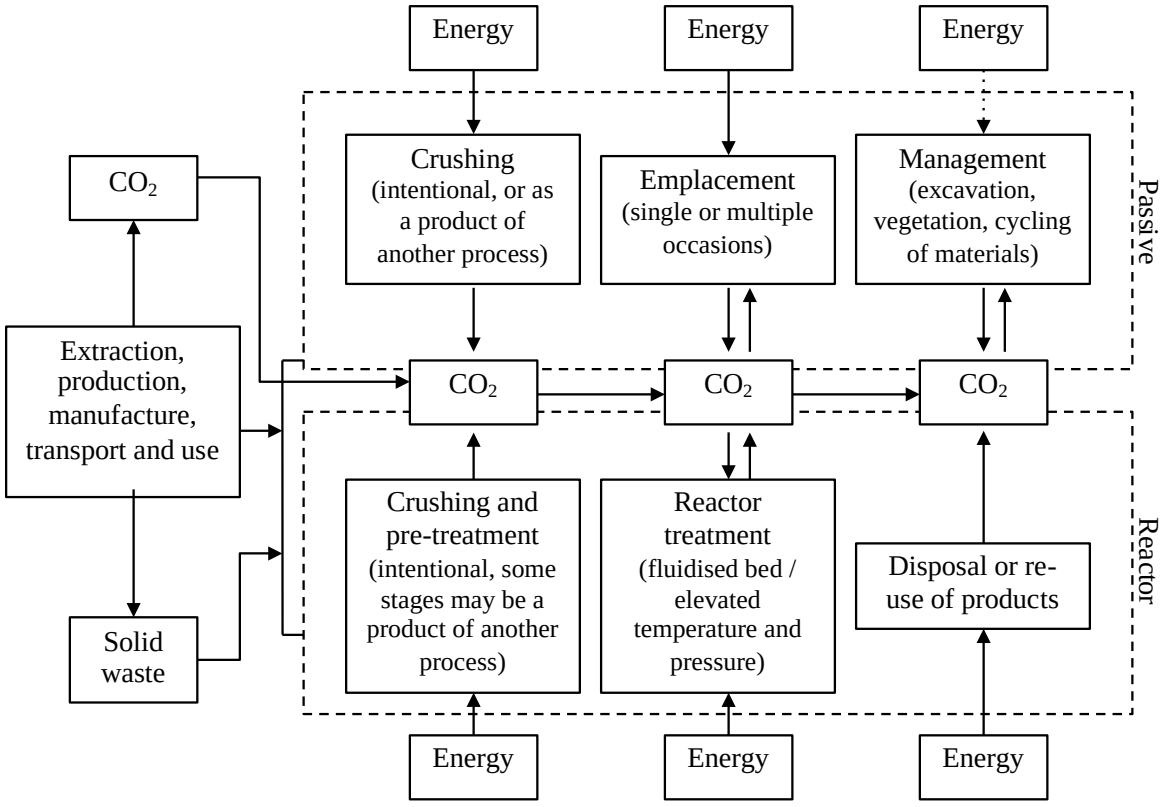

Figure 6.2 – A comparative LCA of mineral carbon capture and storage in passive and reactor settings

Renforth (2012) states that the energy costs of enhanced weathering may be 880-4249 kWh tCO_2^{-1} (net CO_2 draw-down, which accounts for emissions during production) for passive *in situ* weathering of basic and ultrabasic rocks in the UK. This may vary significantly with the use of artificial silicates. Operational costs are estimated at £59-438 tCO_2^{-1}. Crushing and material transport are noted as the most energy intensive steps in the process, accounting for 77–94% of the energy requirements collectively. The highest estimates for reactor based approaches taken from the literature (Table 6.5) are up to 2300 kWh tCO_2^{-1} with operational costs of £5-130 tCO_2^{-1} ($8-210 tCO_2^{-1}). A large amount of variability remains in predicting the actual costs of these processes, and it can be seen that the estimated operational costs for passive and reactor-based processes show significant overlap.

6.1.2 Cost of the process: carbon price / incentives required

Collective net reduction in emissions may be achieved through the treatment of suitable materials for carbonation. Many sources claim that mineral carbon capture processes could have a large impact on reducing global emissions and be theoretically implemented to capture 0.1–1 Mt CO_2 a^{-1} in the UK via carbonation of mineral wastes alone (Sanna et al., 2012). Aside from available cation content, no compositional factors significantly hinder the quantitative ability of suitable waste to sequester CO_2. The theoretical limits offered take into account not only the total potential of the materials, but factors such as the likely availability of sites at which these technologies could be implemented.

A major influence on the implementation of any process is economics; if the process promises an economic benefit, or at least offers the avoidance of an economic penalty, this acts as a strong incentive for its implementation. There are various ways in which this incentive may occur, which are discussed further in the following sections, with a focus on legislation. One of the ways in which this can be achieved is through the assignment of a 'carbon cost'. This cost takes in to account the potentially damaging effects of CO_2 emission, and assigns an appropriate price penalty to emitters. Schemes such as the European Union Emissions Trading Markets (EU ETS, 2003 (Directive 2003/87/EC)) have been in place for a number of years, apply this approach for certain technologies and industries and will be discussed further in following sections.

Sanna et al (2012) note that many contemporary mineral carbon capture schemes present high energy requirements and high costs compared to geological storage (one of

the most widely implemented carbon capture technologies at the current time).These potential limitations do not directly apply to passive *in situ* storage processes. If the cost of a mineral carbon capture process is greater than the value of the carbon sequestered then the process will have a net operational cost, and unless otherwise incentivised is not likely to be adopted. Table 6.5 presents a summary of the current estimated costs for a number of mineral carbon capture processes. This shows that different processes have highly variable associated costs. Assuming the current EU ETS trading cost of £8-£12/tCO_2, if able to be suitably accredited, the use of trickle bed systems (Stolaroff et al., 2005), part way between passive *in situ* and reactor based carbonation, would fall within the economically feasible zone. The other processes listed all require a significantly higher carbon cost before they could be viewed as economically viable in their current form.

Other factors also contribute to determining the economic feasibility of these processes, including incentives for recycling or re-use of industrial waste materials which may avoid current economic penalties associated with disposal to landfill. Carbonation may also act to physically or chemically stabilise the treated materials, reducing their environmental impact or increasing their value as useable products.

Table 6.5 – Suggested costs of a selection of MCCS processes

Process type	**Source**	**Cost (estimated)**
Concrete waste and steel slag and buffer solutions in spray trickle bed systems (able to sequester 50% of the CO_2)	Sanna et al 2012 Stolaroff 2005	\$8/tCO_2
Cement waste at 30 bar and 50 °C	Sanna et al 2012 Iizuka 2004	\$22.6/tCO_2 (excluding capital costs)
Weak acid extraction processes (laboratory scale)	Sanna et al 2012 Kakizawa 2001	\$27/tCO_2
Carbonation using serpentine, high pressure and temperature various conditions	Khoo et al 2011	\$105.6/tCO_2 to \$127.2/tCO_2
Direct high pressure and temperature mineral carbonation	Sanna et al 2012 Gerdemann 2007	\$64/tCO_2 to \$210/tCO_2 (from 430 kW h/tCO_2 to 2300 kW h/tCO_2)

In the case of *in situ* passive soil carbon sequestration, as materials are not intended to be ultimately recovered after reaction, a large element of the value is in the provision of a carbon capture and storage mechanism. While the avoidance of penalties for sending material to landfill, implementation of effective recycling schemes, and credit for improving ecosystem services of managed sites may apply, for the process to be

successfully implemented at larger scale on economic terms a value must be assigned to the carbon captured, and environmental benefits, and be capable of validation.

As discussed in Chapter 5, even single development sites are able to provide a significant carbon capture and storage function. At the Science Central site, Newcastle upon Tyne, in 2010 around 37,463 t CO_2 had been bound in carbonates leaving a remaining sequestration potential of 27,341 t CO_2 (Washbourne et al., 2012). This quantity is significant within the scope of a development project of this type, as it presents a potential for offsetting carbon produced during production of the original construction materials and can be considered as an on-going offset by the site developers if the sequestration reaction is promoted in areas of exposed soil or managed vegetation on sites of this type.

The value of urban soils as carbon capture devices depends heavily upon the level of intervention and management required to optimise this function, which is assumed in this case to be minimal, and the inherent 'value' of the carbon they remove from the atmosphere. Mineral carbonation techniques have not yet been granted status as a valid carbon mitigation technology by the EU ETS. Theoretically assuming that this may occur, and applying the current CO_2 trading cost of £8-£12/tCO_2, the current value of CO_2 sequestration at the Science Central site in 2010 was £518,432 – £777,647 or £51,843 – £77,765 ha^{-1}.

For industries producing wastes suitable for use in this process there is significant scope for economic gain if a carbon price were attached to technologies in this way. The Carbon Trust (2011) notes that the iron and steel industry contributes around 6% of all anthropogenic global CO_2, a figure which could be partially offset by effective re-use of the industry wastes; iron and steel slag. Approximately 400 million tonnes of slag are produced every year (GlobalSlag.com, 2008), with the global total for iron slag accounting for 260 to 310 million tons, and steel slag around 130 to 210 million tonnes (USGS, Mineral Commodity Summary 2012). Similarly, other industries producing the materials noted in Chapter 2 could address a portion of their environmental impact through the implementation of mineral carbon capture in their wastes.

It is important to note mineral sequestration in wastes is not able to capture more CO_2 than was originally emitted in the production of the waste material. This idea of 'closing the loop' on these processes by capturing their emission using their own wastes raises a

number of interesting points relating to the attribution of emission penalties versus capture incentives.

One of the more philosophical aspects regarding the economic and legislative validity of carbon capture and storage via atmospheric sequestration, and the economics of this process, relates to the ‘ownership’ of the original emissions. Whilst the geochemical balance of an open sink for carbon capture can be accurately modelled, further work would need to be directed towards calculation of the industry mass-balance. If a company were to privately invest in a scheme of this type, it is likely that assurances would need to be made that the emissions off-set balanced closely with the company needs – there is the potential for ‘over-efficient’ atmospheric capture projects to be seen as undesirably providing offset above and beyond the necessary capacity. This extends to the perception of carbon capture technologies in global carbon emission reduction strategy, discussed in the following section.

6.2 Legislative factors

Legislative factors related to mineral carbon capture come in a number of forms, with practical legislation relating to the materials and processes used, and wider environmental legislation relating to the local and global-scale application and actions of the technologies. In terms of the wider environmental legislation, *in situ* passive mineral carbon capture using industrial wastes has the potential to interact with guidance on carbon emissions at the global scale, and contaminated land (including development and remediation), mineral resources and waste at the local scale.

The first two of these factors, carbon emissions and contaminated land, could be considered as examples of 'pollution' controlled by legislation. Huntzinger (2006 (PhD thesis)) discussed pollution as a complex issue, an 'externality' the impacts of which are seen as a by-product of the consumption or production of goods with associated transactional costs and third-party impacts. Pollution is the unwanted result of a process or action which has the potential to cause harm to sensitive receptors such as living organisms. In the case of contaminated land, there are many examples of contemporary legislation and existing control or regulatory measures. In many cases pollution of land is identifiable, quantifiable, and easy to attribute to a particular source. Contaminated land legislation within the UK (The Contaminated Land (England) Regulations 2006) is based on site-by-site guidance pertaining to the concentration at which particular pollutants present a risk (potential to cause harm) to sensitive receptors. This guidance is flexible, taking into account the sources, pathways and possible receptors of pollution in order to assess contaminated sites (Environment Agency, 2009), and to provide regulatory guidance for contemporary polluters. Contaminated land penalties tend to be based on the 'polluter pays' principle, where polluting actions attributed to individuals and companies must be 'repaid' in suitable remediation measures by these bodies, except under exceptional circumstances (HMRC, accessed 2013).

Legislation for pollution through carbon emissions is more complex. While large emitters are currently obliged to carry out a regular inventory of their emissions (Companies Act 2006 (Strategic Report and Directors' Report) Regulations 2013), as a pollutant in the atmosphere carbon is more difficult to trace and attribute than pollutants on land. Legislation for carbon pollution has a much shorter history than contaminated land legislation, but in many ways follows precedents set by early developments in environmental legislation such as the UK Clean Air Act (1956). This trailblazing

environmental act set out guidance to reduce air pollution by regulating the burning of smoke-producing fuels, and ordered the relocation of emitters away from sensitive populations. Most carbon emission control policies set out to reduce the impact of large industrial emitters through economic penalties, though consideration is now being given to the ways in which other measures could be effective in emissions control.

6.2.1 Carbon emissions

As a major global influence on the success of mineral carbon capture schemes, it is important to understand the feasibility of carbon emission control policies in their broader setting, as these play such a critical part in dictating the adoption of mineral carbon capture. Ultimately this understanding links to many of the aspects discussed in Chapter 2, tied to basic questions relating to the nature of climate change; quantification and attribution of causes to demonstrate what its impacts are symptomatic of, and decision-making as to where changes need to take place in order to address it.

Emissions caps are applied through a number of regulatory mechanisms to large emitters of CO_2. These caps are not static, but in most cases become stricter with the progress of time, in the presumption that many industries have the inherent ability to reduce their carbon intensity through gradual improvements in process technology. There is a theoretical limit for the emissions reduction of all industries, and emissions caps are generally designed to bring all industries under their remit as close as feasibly possible to this limit.

EU ETS (EU ETS, 2005) and other similar trading schemes, and related proposals, are often referred to as ‘cap and trade’ schemes. These schemes combine the practise of applying emissions caps with the potential for participating bodies to trade any ‘spare’ allowances they have available to them or purchase any they require to meet their capped targets. Many of these schemes have planned in their initial phase to over-allocate emissions caps or provide them at an artificially low cost, in order to incentivise early participation (EU ETS, 2013). Participating bodies that have not reached their cap by the end of the trading period are able to trade these allowances in in a number of ways. These schemes also allow bodies that have exceeded their cap to purchase additional units, at an economic penalty, to cover their deficit.

In a number of cases it has been deemed that the efficiency of ‘command and control’ directly from government on carbon pollution is not the most environmentally effective

approach (Ellerman, 2003). A 'market-based' approach like the trading schemes broadly outlined helps to separate legislative and economic interests. Both of these approaches require, directly or indirectly, the application of a 'cost of carbon'. This has proven a difficult element to agree, with DEFRA (2002) estimating a value of £70/tonne CO_2 with a large range of variability within estimates (upper value of £140/tC and a lower value of £35/tC). The EU ETS scheme consistently places the value at <£20/tonne CO_2, and the current (2013) value of CO_2 in UK environmental legislation is £9-20/tonne CO_2 (DECC 2011). It is possible that if the polluting effect of CO_2 is undervalued it becomes difficult to economically incentivise the trading schemes and actions to mitigate its emission.

The UKs current stance on carbon emission management follows a period of legislative development on greenhouse gas emission reduction. A GHG emission reduction target was agreed by the EU in 2008 of 20 percent by 2020, relative to 1990 (UK Climate Change Act 2008), supported by the EU Emissions Trading System (EU ETS, 2003) covering the power sector and heavy industry (traded sectors). The traded sector (around 40 percent of emissions) is covered by the EU ETS. The non-traded sector (around 60 percent of emissions) is covered by a number of other policy measures. The EU ETS Phases 1 and 2 (2005-2012) carried financial penalties for non-compliance.

Legislation in the UK does not currently incentivise carbon capture through mineral sequestration as a means of carbon emission reduction. While a number of structures are in place which could allow this to be introduced (inclusion in carbon credits schemes, incentives for sustainable engineering), the issues of attribution and quantification would need to be resolved in order for this to be strongly considered.

Table 6.6 summarises a number of the EU and UK policies with the potential to affect approaches to greenhouse gas emission mitigation.

Table 6.6 – Summary of EU and UK greenhouse gas emission reduction policies

Sector	**Policy**
Cross-cutting economic incentives	EU Emissions Trading System Climate change levy (energy tax)
Industry	Climate change agreements Inclusion in CCS competition
Transport	EU new car and van emission targets Renewable transport fuel obligation Plug-in car grant Plugged-in Places program
Waste	EU Landfill Directive Landfill tax

6.2.2 Contaminated land

With respect to the application of *in situ* mineral carbon capture techniques, the most appropriate contaminated land legislation relates to the contaminant potential of materials introduced to the soil system. Many industrial waste materials contain elevated levels of potential contaminants including heavy metals and organic chemicals. An assessment would need to be made of this potential on a site by site basis, with a detailed knowledge of the composition of the materials emplaced.

A number of studies have shown that carbonation reactions taking place in industrial wastes like those discussed have the potential to immobilise potentially harmful pollutants in stable mineral phases (Fernández Bertos et al., 2004). Further work is needed to address this *in situ*, however it is possible that even where materials present a possible pollution risk, the geochemical development of the site may render this insignificant due to the immobilising effect produced by the formation of secondary minerals including carbonates.

6.2.3 Mineral resources

A large amount of legislation related to the exploitation of mineral resources exists in the UK (National Planning Policy Framework (NPPF), published in 2012). This legislation regulates the quantity of primary resources exploited and determines the manner in which secondary resources are utilised. This study has focussed on the use of waste materials for mineral carbon capture, therefore the legislation relating to their use is taken from that applied to secondary / recycled minerals rather than primary resources.

Legislation in place in the UK (Aggregates Levy, 2002) currently incentivises the use of secondary materials in favour of primary resources, which has increased the value of secondary aggregates for construction purposes. In some contexts this may act in conflict with mineral carbon capture schemes, if the value of the suitable Ca/Mg-rich waste as a secondary resource (especially as a secondary aggregate) is significantly greater than its value as a material for carbon emission reduction.

6.2.4 Waste

Waste legislation in the UK has undergone a series of recent developments (The Waste (England and Wales) (Amendment) Regulations, 2012; EU Waste Framework Directive, 2008), which have the potential to act both positively and

negatively in the implementation of *in situ* mineral carbon capture. Significant effort has been placed on the development of legislation which reduces the amount of waste to landfill, by incentivising re-use and recycling of materials wherever this is possible (WRAP, 2001). Charges have been introduced to discourage the disposal of materials which could be diverted to further use, including many of the industrial wastes suitable for carbon capture, incentivising the development of alternative applications.

Changes in codes of practise for remediation and development of sites has the potential to affect the way in which 'waste' materials, especially construction and demolition waste are able to be transported and re-used between sites (Contaminated Land: Applications in Real Environments (CL:AIRE), 1999). This may limit the transport and application of materials from their source to possible field sites, or require the need for specific allowances to be made.

A useful way of combining these legislative ideas on large and local scales, mentioned briefly in earlier chapters, is through an ecosystem services approach. The goal of two EPSRC-funded Impact Award projects carried out on Science Central, Newcastle upon Tyne, was to encourage the concept of designing a carbon capture function into urban soils as an additional ecosystem service with a tangible value. One of the main issues identified through stakeholder engagement activities carried out during these projects was the implications of current legislation and its combined environmental context. On these site-specific scales it was considered that existing legislation had the potential to impact the approach positively or negatively depending upon a number of physical and temporal factors, the most pertinent examples summarised in Table 6.7.

Whilst this list is far from exhaustive, Table 6.7 highlights the types of legislative issues presented by the development of a mineral carbon capture site. It reinforces the need to approach every site differently and supports the notion that, as with many environmental interventions and remediation approaches, carbon capture projects are not equally suited to every site. A preliminary assessment should be undertaken to determine whether materials suitable for carbon capture, once identified, can be utilised without significant additional costs for remediation or transport, before being placed in a setting where carbon capture processes are able to occur without negative environmental impact.

Table 6.7 – Summary of UK legislation with possible impacts upon the implementation of passive mineral carbon capture and storage with artificial silicate minerals

Legislation	**Impact on adoption of UCC**	
	+	-
CL:AIRE (CL:AIRE, 1999) Code of practise for land development and remediation: definition of waste	Provides stringent guidelines within which waste materials can be reused	May limit transport and re-use of UCC materials if deemed to be wastes, especially if offsite
BREEAM (BREEAM, 2013) Standard for best practice in sustainable building design, construction and operation	Incentivises improving the environmental quality, ecology and sustainability of developments	
National planning policy framework (CLG, 2012) Guidance for sustainable development in planning, building and the environment	Incentivises protecting our built environment, improving biodiversity, minimising waste and pollution, mitigating climate change	
CLR 11 Contaminated Land Model (EA, 2004)) Procedures for the Management of Land Contamination	Provides stringent guidelines within which potentially contaminated sites can be redeveloped	May limit re-use of UCC materials if deemed to pose a contamination risk
EU Waste Framework Directive (EU, 2008) Managing waste to reduce the potential for it to pollute surface water, groundwater, soil, air, and also contribute to climate change	Assists in defining wastes and 'end-of-waste' specifications. Providing environmental protection and ensuring that wastes have environmental and economic benefit	May complicate classification of onsite materials as wastes, limiting their future usage
Soils Framework Directive (provisional) (EU, 2006) Framework to protect European soils, while at the same time ensuring their sustainable use	May improve protection afforded to soil systems, raising awareness of functions, providing guidance and legislation for sustainable environmental management	
Aggregates levy (HMRC, 2002) Waste and Resources Action Programme (WRAP) tax on primary aggregates		Penalises use of primary aggregates making secondary alternatives more attractive
Landfill tax (HMRC, 1996)	Discourages disposal of waste materials to landfill	Many wastes suitable for UCC are classified under the lower rate of landfill tax, reducing penalties
SUDS (DEFRA, 2011)	Promotes construction of naturalistic urban drainage systems: may act as a complimentary technology	
EU ETS (EU, 2003)	Provides an legal and economic structure by which carbon capture projects may receive economic credit	Does not currently accredit soil carbon capture methods

In summary, contemporary legislation has the potential to play a pivotal role in determining the wider implementation of carbon capture through carbonation of waste. Incentives for increasing the sustainability of developments, promoting reuse of waste, raising awareness of soil functions and integrating green space may have positive implications. Many of the current planning and waste directives have the potential to limit the approach on sites with complex development histories and high potential for contamination, however in these cases carbon capture could be integrated as part of a site remediation strategy at little or no additional cost.

Legislative factors to be considered in a carbon capture development include:

- Type and quantity of material used (or to be imported) and its waste classification
- Material history and potential for contamination
- Potential for transfer of material between sites and associated cost
- Applicability of the carbon capture project to subsequent site development (e.g. is it a standalone project, or will it be integrated in to a wider project plan. Over what timescale will it be implemented.)
- Environmental, economic and social contribution of carbon capture sites to the planned development
- Potential for integration within multiple schemes
- BS 6031:2009 Code of practice for earthworks contains a proviso for 'carbon critical design'. However, the associated carbon calculator (available from the Environment Agency website) accounts for the emissions from material production and transport, and does not account for changes in carbon due to soil modification.

6.2.5 Proposals and policies

As discussed in the preceding section there are a number of existing precedents for economic and policy conditions surrounding the topic of *in situ* mineral carbon capture, but no specific guidance on the technology itself. International policies relating to carbon emission mitigation do not currently take in to account the impact of this form of sequestration, but discussions surrounding these policies do go some way to attempting to address the way in which diffuse capture technologies could contribute to addressing the problem (FAO, 2013; FAO, 2000).

Carbon pollution in the atmosphere impacts upon a ‘common pool resource’ in the global commons, therefore the solution is the proportional responsibly of all who have contributed. Global hesitancy in the application of strong emissions legislation relates to a number of issues, not least the political controversy of limited or unilateral application of climate regulation, due to perceived loss in economic market competitiveness this would incur. Voluntary enactment of climate regulation by a small number of nations is seen as potentially damaging to their social and economic wellbeing, and would require a willingness to impose policies which are not within the short-term interest of policy makers. There are also significant issues of attribution, determining the individual responsibility of emitters to undo their share of the damage caused, which in some cases may have a complex legacy of many decades.

Potential impacts of proposed legislation such as the UK Climate Change Act, which has set ambitious targets for emissions reduction (80% against a 1990 baseline by 2050) may be to incentivise the adoption of additional emissions reduction technologies in order to ensure that targets are suitably met. The timescale of environmental issues acting alongside the timescales of politics can often be difficult to resolve, but in these pieces of legislation long-term goals have been set and provide the basis for development of long-term management techniques.

6.3 Summary

In summary, the preceding section recounts some of the legislative and economic issues surrounding the development of a carbon capture site using waste materials. In this case, a theoretical site based in the UK using construction and demolition waste or steel slag as the carbon capture substrates is described.

Construction and demolition waste and steel slag do not currently receive carbon credits for their sequestration properties (*in situ* or in carbonation reactors). If a carbon price could be applied to these properties, the economic incentive would depend strongly upon the cost of carbon.

- Assuming an average capture potential of C&D waste = 65kg t^{-1} CO_2 (Washbourne et al, 2012) and a value of carbon around £8-12 t^{-1} CO_2 (EU ETS) the potential carbon capture value = £5.20-7.80 t^{-1}. Whilst this is around the same as the current aggregate sales price, it is assumed that carbon capture value is gross value, whilst only a proportion of the aggregate value reflects profit, making these closely comparable.

Recent changes in waste legislation mean that construction and demolition waste and steel slag are now economically valuable secondary aggregates. The use of secondary aggregates in development projects is incentivised by waste legislation and the aggregates levy.

- In many instances, C&D waste, steel slag and other materials suitable for carbon can also be utilised as secondary aggregates. The current sales price of crushed concrete as a secondary aggregate is around £6-10 t^{-1} (depending on technical specifications met), around the same price as primary aggregates (Personal communication with industry stakeholders 2012).

Construction applications and use as carbon capture materials are not mutually exclusive and should not necessarily be in direct competition. Mineral carbon capture projects are particularly suited to the use of material unsuitable as aggregate, especially fines. In certain construction applications mineral carbon capture processes may still be able to occur

- At present mineral carbon capture is not accredited under the EU Emissions Trading Scheme (EU ETS, 2003), therefore no direct economic credit is available for the

carbon captured by a MCCS site. The development of peripheral environmental legislation such as the Soils Framework Directive may assist in promoting the importance of soils as carbon sinks, allowing a system of accreditation to be formed. The carbon capture potential of these sites could be on an economically significant scale.

Full economic assessment of a carbon capture project is more complex than the statements above; however it is useful to address some of the basic costs and benefits and determine how these may compliment or compete against one another. Benefits which are not intrinsically economic may be especially motivating in some development settings. Examples for carbon capture sites include: reuse of 'waste' for aesthetic redevelopment of brownfield sites, improved ecosystem services and environmental resilience and provision of temporary or permanent green space in urban areas for social use

CHAPTER 7 – Discussion

This study investigated the proposition that artificial minerals could be effectively used for carbon capture and storage in the ambient soil environments. MCCS, through the weathering of suitable materials and precipitation of secondary, soil-formed (pedogenic) carbonate minerals, is a process which occurs naturally in a number of global soil systems and appears to persist in many anthropogenic soil environments.

The work in Chapters 3-5 is presented systematically at increasing scale, with batch weathering experiments assisting in setting the parameters for a predictive model of the weathering of each material presented, column / flow-through weathering experiments investigating these properties at a larger scale and in a dynamic system, and field investigation validating the initial predictions and demonstrating the presence of additional factors for consideration for field-scale implementation. Referring to the original aims of this thesis (Chapter 1) a conceptual model can be assembled to summarise the contribution of the work to filling the perceived knowledge gaps. The legislative and policy setting is summarised, with technical data shaping its scope.

Chapter summary:

- Conceptual model for MCCS in soils
    - Weathering rates
    - Geochemical markers
    - Engineered soils / engineered sites
    - Engineering potential
    - Quantification
- Policy

7.1 Conceptual model

The conceptual model presented in Figure 7.1 illustrates information critical to the effective implementation of MCCS in soil settings, visualising how the main areas investigated by the technical work in this thesis fit in to understanding the overall process. These topics are grouped in to sections 7.1.1 – 7.1.5 and 7.2 of this Chapter: weathering rates, geochemical markers, engineered sites, engineering potential, quantification and policy.

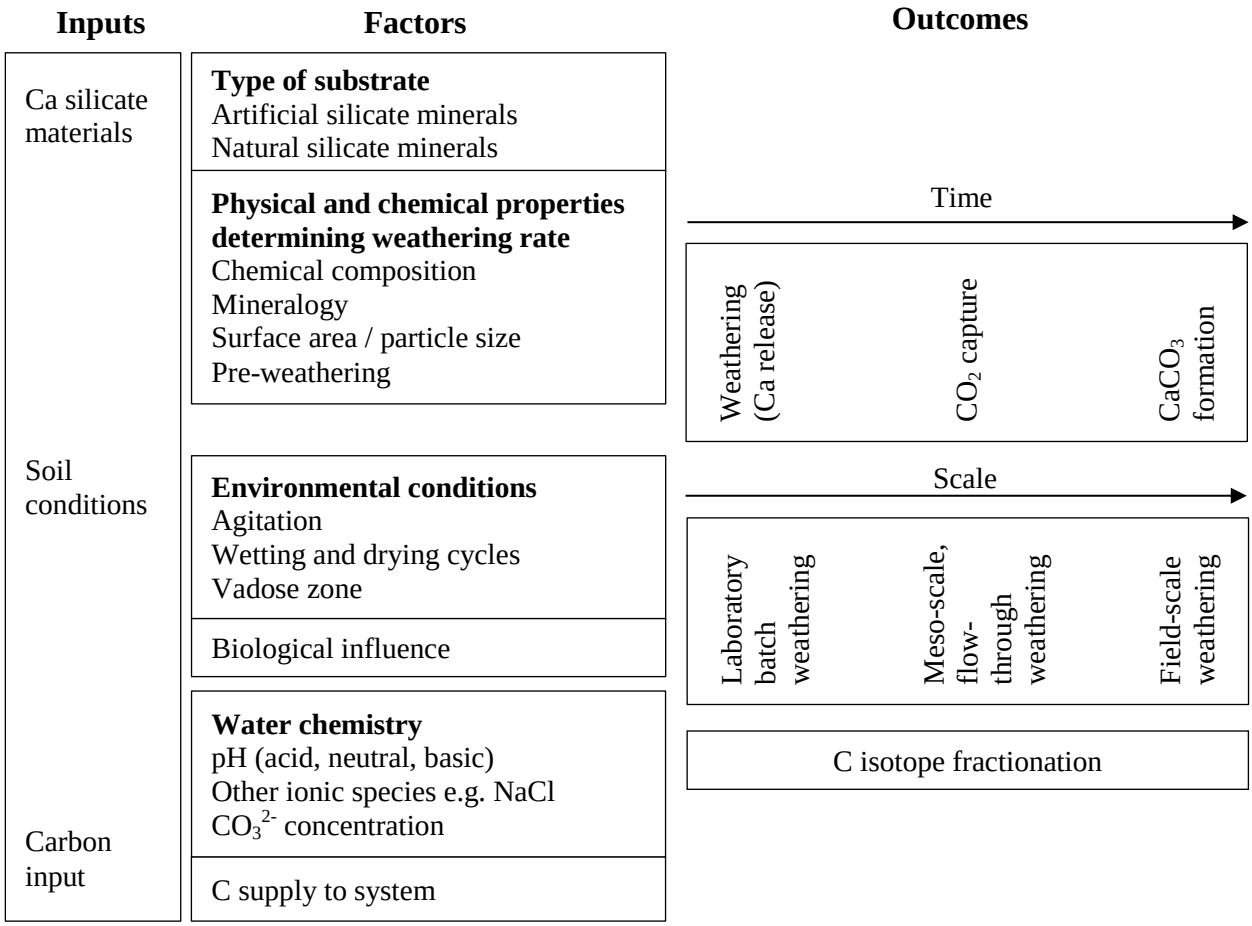

Figure 7.1 – Conceptual model of MCCS considering areas where the technical work contained in this thesis has the potential to contribute knowledge

7.1.1 Weathering rates

Weathering rates were determined for a number of calcium rich materials (Chapter 3), illustrating the variation between batch weathering, pH controlled weathering and *in situ* weathering rates over known time periods for a suite of materials. Weathering experiments on natural and artificial silicate minerals were in all cases found to be comparable to, or more rapid than, previously reported weathering rates for similar silicate minerals, with implications for the rapid rate at which MCCS could progress under ambient conditions.

The rate of carbon capture on sites where artificial silicate materials had already been emplaced was analysed in spatial detail, and over a known period of time, in order to estimate field-scale weathering rates. Yarborough Landfill, Scunthorpe and Science Central, Newcastle upon Tyne provided complimentary study sites. Field sites contained in this work were found to capture C at a rate of up to 18 kg CO_2 Mg^{-1} a^{-1}. Scaling from lab to field-scale had an impact on weathering rates of the selected materials, however this was not as marked as was the case in previous studies (from

Hartmann et al., 2013; White and Brantley, 1995) which may be due to the comparatively rapid overall weathering rates of the materials studied. Figure 7.2 compares the weathering rates derived for these materials under different conditions.

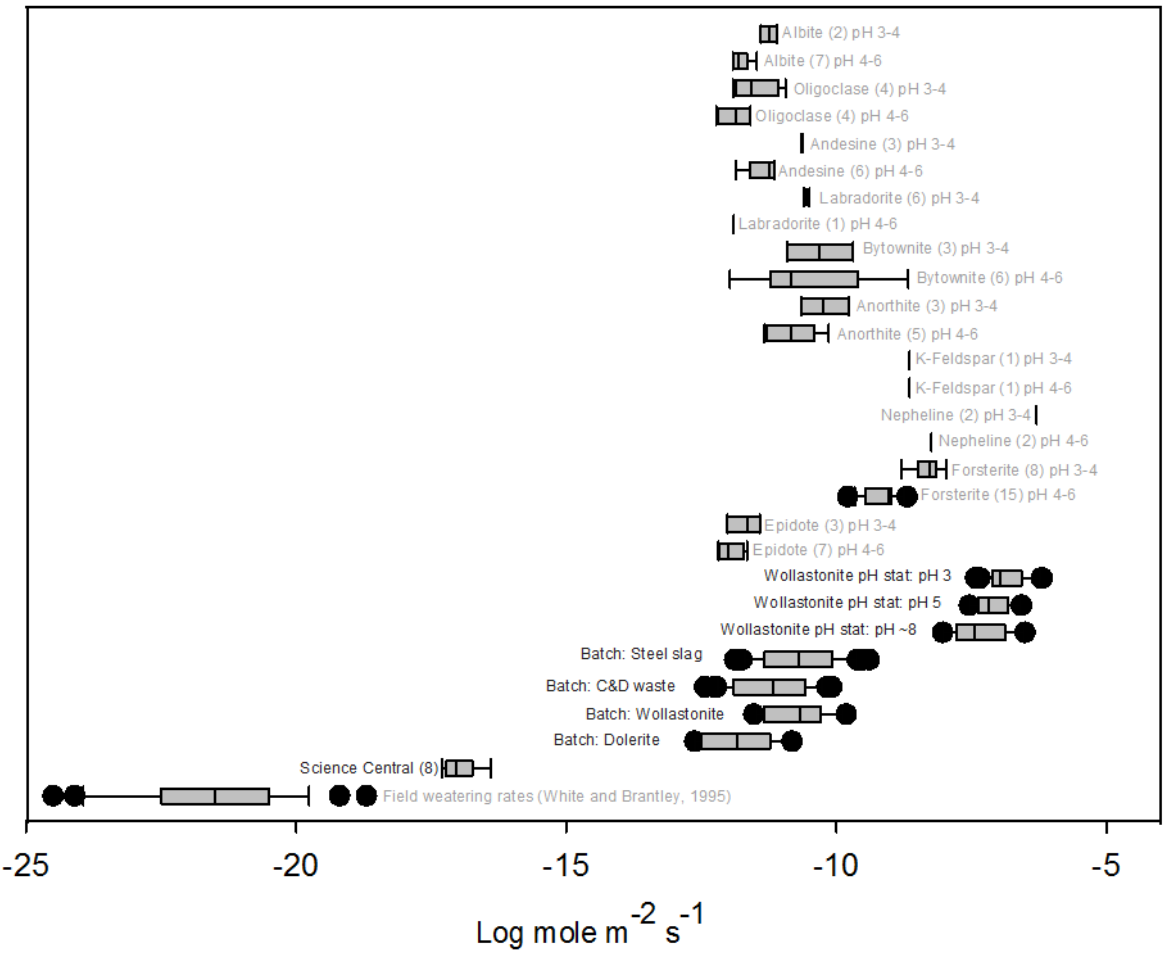

Figure 7.2 – Comparative weathering rates of materials reported in Chapters 3 and 5 (legend in black indicates studies contained in this thesis)

7.1.2 Geochemical markers

IRMS

Through application and adaptation of a previously published method (Renforth et al, 2009) samples analysed were found to contain carbonate C sequestered from atmospheric CO_2. Very negative values for $\delta^{13}C$ observed are characteristic of carbonate formed in high-pH environments and through diffusion of atmospheric CO_2. These data indicate a strong atmospheric influence on the provenance of stable isotopes in the carbonates analysed. Some materials showed evidence of higher depletion in $\delta^{13}C$ with increasing age: stockpiled steel slag at Tata Scunthorpe 16 days = -17.73‰, 89 days = -19.54‰, 991 days = -20.45‰. These findings reinforce the value of stable isotope

analysis in determining the provenance of C and O in pedogenic carbonates, and for estimating proportional contribution of different carbonate formation routes.

Radiocarbon (^{14}C)

Radiocarbon (^{14}C) analysis also supported the conclusion that high levels of atmospheric C are included in the pedogenic carbonates analysed during this thesis, by illustrating that a significant proportion of the C present in carbonates analysed from Science Central soil samples is 'modern'. 80.73 ± 0.37 % of the carbonate in a sample with a $\delta^{13}C$ value of -14.0 ± 0.5‰ was found to be 'modern'; recently formed through a non-lithogenic route. ^{14}C analysis could also be a useful method for determining C provenance in pedogenic carbonates.

7.1.3 Engineered soils / engineered sites

Meso-scale investigations of weathering behaviour (flow-through column experiments) illustrated that $CaCO_3$ formation showed little variation with depth / distance from fluid inlets and outlets over an 8-56 day time period and that a significant proportion of calcium (Ca) leaching occurred within the early stages of the study. In the case of steel slag it is likely that some of this rapid early leaching is indicative of the weathering of free lime (CaO) in the material, with subsequent release of Ca dependent upon slower weathering steps for minerals such as portlandite and calcium silicates. Figure 7.3 illustrates the rate of Ca leaching as a possible composite of a number of weathering reactions. This reconstruction is speculative, but based on the leaching curves determined in Chapters 3 and 5.

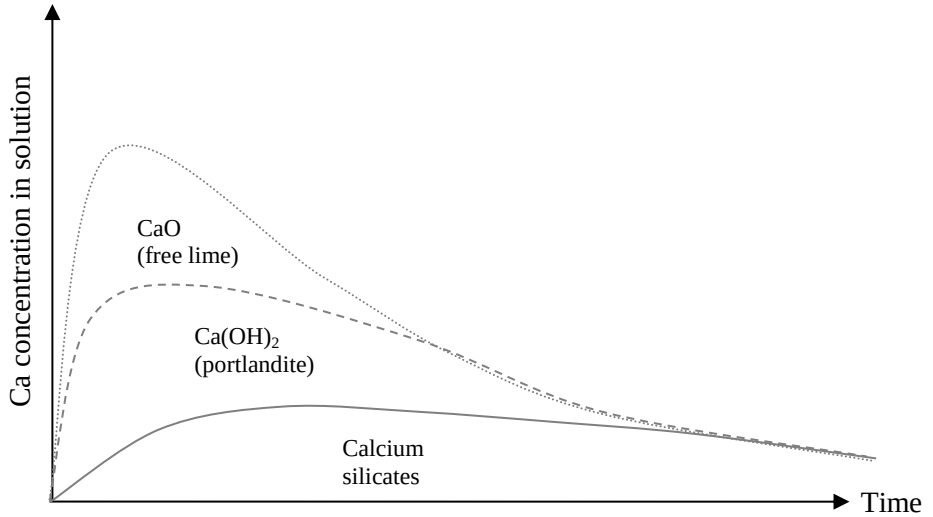

Figure 7.3 – Visualising the rate of weathering as the possible composite weathering rates of a variety of mineral phases over time (see Figure 5.6, Chapter 5)

System pH appeared to be buffered ~11.6 for fresh slag, by portlandite dissolution, and at ~9.1 for weathered slag, by persistence of calcium carbonate, illustrating the complexity of these geochemical systems, and challenges for monitoring real-world sites engineered for the purpose of MCCS.

Analysis of geochemical data from an engineered waste landfill containing artificial silicate minerals, and analysis of variation in pH and EC, showed that a large amount of variation occurred across the site, but that single sampling points showed relatively small variations in both parameters over time. This illustrates the value of implementing long-term monitoring in these settings to spatially assess and quantify MCCS.

7.1.4 Engineering potential

Determining the engineering potential for inorganic C storage at a 'typical' urban redevelopment site is complex when looked at in retrospect. Few of the tested physical parameters considered in this thesis had a large effect on weathering rates, although the physical parameters of the materials themselves (surface area, particle size) did. The effects of changes in chemical parameters were of varying magnitude, with the addition of bicarbonate ions and variations in solution chemistry having little effect, but the modification of pH using strong acids or addition of carbon dioxide producing a more marked response. Further constraint of these parameters is required to investigate their significance for carbonate formation and allow a methodology for effective soil engineering to be developed.

The development of 'Carbon Capture Gardens', intentionally vegetated plots, on sites where silicate wastes had been emplaced was shown to be feasible with respect to experimental design and plant growth, but insufficient data are available at this stage to draw any detailed conclusions from this work. An intervention like the test pads illustrated in Figures 7.4 and 7.5 could be used to investigate *in situ* field behaviour of materials under long-term monitoring, and determine the effects of admixing additional wastes / high organic C materials and introducing vegetation cover. Test pads would be intended to provide a large-scale example of carbonation in a field context, but be designed to present the potential for on-going observation and monitoring throughout their research use, with integrated measures to allow ease of access for observation and monitoring.

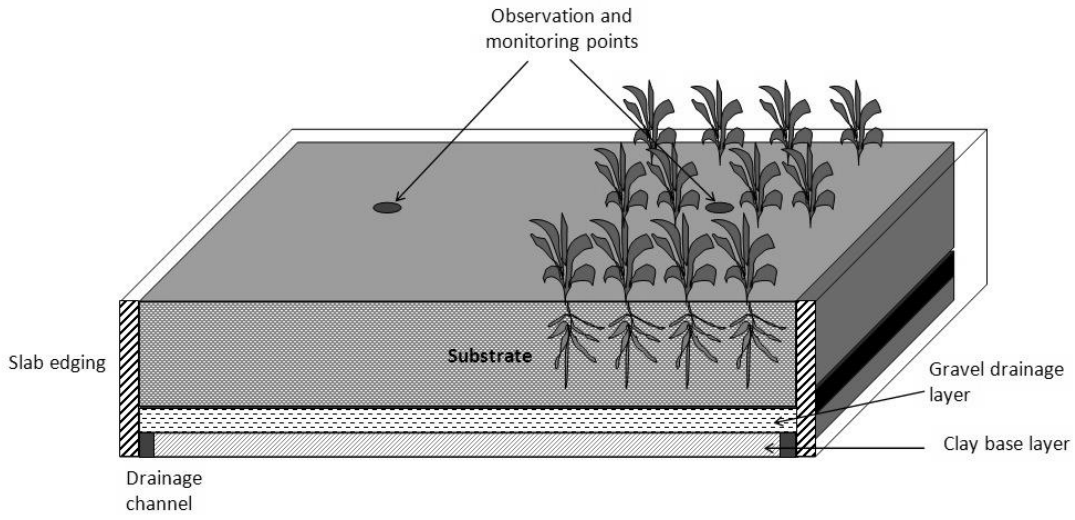

Figure 7.4 –Test pad proposal, side elevation and aerial projection (retaining sections shown in section in upper image)

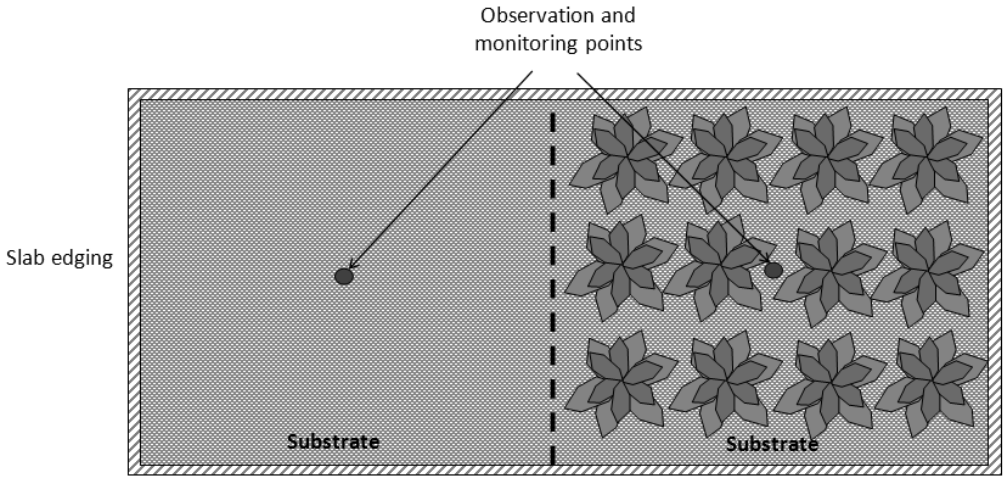

Figure 7.5 –Test pad proposal, side elevation and aerial projection (retaining sections shown in section in upper image)

7.1.5 Quantification

Overview

Quantification of the potential for inorganic C storage is complex to reconstruct and in this work many lines of evidence were ultimately used to quantify carbon capture parameters. The field-scale efficacy of carbon capture using industrial residues was quantified using carbonate content, XRF (total oxides) and IRMS with additional information from ^{14}C dating.

Many artificial and 'waste' silicate materials have the appropriate composition to act as substrates for mineral carbon capture and storage. The overall carbon capture potential

of the materials included in this study (C&D waste, iron and steel slag) is 109-236 MtC a^{-1}. Globally, waste silicate minerals have the potential to capture 192-333 MtC a^{-1}, representing 2.0-3.7% of global emissions (Renforth et al., 2010). Studying how artificial and waste silicate minerals can be used in soil engineering for carbon capture provides an insight into the possible use of natural silicate minerals, which have a much larger carbon capture potential, for the same purpose.

Local potential of sites

Individual field sites are able to provide cumulative contributions to MCCS. There is a significant presence of calcium carbonate in many anthropogenic soils, including those which form the study sites in this thesis, which has formed over a relatively short time period with no obvious C contribution other than from atmospheric sources. This is encouraging in the assessment of these materials with respect to their use in carbon sink engineering, especially considering the lack of special engineering measures to promote MCCS in these settings.

The C&D waste soils at Science Central were found to potentially capture 18 kg $CO_2\ Mg^{-1}\ a^{-1}$. The developments in MCCS seen over an 18 month period at the Newcastle Science Central site reiterate the need for long term (5-10 years) investigation of carbon dynamics in artificial soils at field scale.

Many anthropogenic soils suitable for MCCS are associated with urban areas and these findings contribute strongly towards the contemporary urban planning concept of city as a force for good (Beck et al., 2010), highlighting the capacity for engineering to restore and maintain ecosystem services in the urban setting while providing wider environmental benefits. Urban soil engineering is an important on-going focus for contemporary regeneration and development, with the potential to be coupled with aspects of green infrastructure in long-term projects, or even short term, temporary uses of vacant urban land (Taylor, 2008).

7.2 Policy

The efficacy and capacity of carbon capture using industrial residues was considered at commercial scales and in current legislative settings assessing the different economic and legal aspects of their use in MCCS.

The critical interface that soils occupy in the global carbon cycle is not necessarily currently reflected in legislation and MCCS in soils is not currently recognised as an accredited carbon mitigation technology. If a carbon price could be applied to this carbon capture property the economic incentive for implementation would depend strongly upon the cost of carbon. Currently changes in the economic value of the study materials in other settings (such as secondary aggregates) is likely to strongly affect the way in which MCCS would be approached.

Full feasibility assessment of a contemporary MCCS project is more complex than can be gleaned from the information presented above; however this work has contributed to determining the technical aspects of the process under ambient conditions and at field scale, and some effort has been made to identify the costs and benefits involved in the utilisation of MCCS in soil settings as a real-world technology.

The studies contained in this thesis add to a growing body of evidence for the formation of carbonate minerals in soil settings where Ca/Mg-rich silicate minerals occur. They also support the idea that engineered soils could be effectively utilised for carbon sequestration over feasible timescales with minimal intervention. Including a carbon capture function in soil management, and undertaking the design of appropriate engineered infrastructure, could add environmental value to a variety of field settings with little additional energy input.

CHAPTER 8 – Conclusions and future work

Chapter Summary:

- Conclusions
- Future work
    - Technical (laboratory-scale)
    - Technical (field-scale)
    - Technical (overarching)
    - Economic and legislative

8.1 Conclusions

Climate change is a pressing scientific and societal issue, with consequences for the maintenance of a stable global environment and significant implications for policymaking and economic development. Currently global anthropogenic emissions account for approximately ~8,900 Mt C a^{-1} (EIA, 2011). The UK Government is committed to reducing carbon emissions by 80% in 2050 (compared to a 1990 baseline) and soils have a role to play, acting as sinks for carbon. It is proposed that soil engineering measures could harness the high C turnover of the global pedologic system to develop an efficient method of enhanced weathering. The atmosphere-soil carbon flux equates to approximately 120,000 Mt C a^{-1} (Manning, 2008); soil carbon therefore acts as a significant buffer reservoir for atmospheric carbon dioxide.

High Ca and Mg silicate materials can be used to sequester CO_2 from the atmosphere. Artificial silicates have the potential to collectively capture 190-332 Mt C a^{-1} through MCCS, representing 2.0-3.7% of total global C emissions, while natural silicates present a potential MCCS store many orders of magnitude greater. Many anthropogenic soils are known to contain substantial quantities of Ca and Mg-rich silicate minerals derived from industrial and demolition activity (including iron and steel slag, cement and concrete). =

Batch weathering experiments on natural and artificial silicate minerals were in all cases found to be comparable to, or more rapid than, previously reported weathering rates for similar silicate minerals. Steel slag was shown to weather at a $\log_{10}$ rate of -9.39 to -

11.88 mol Ca m^{-2} sec^{-1} in laboratory settings and -7.11 to -7.56 mol Ca m^{-2} sec^{-1} under ambient environmental conditions in the field over 975 days. This is exceptionally rapid, demonstrating the potential for MCCS to occur over short time periods under certain field conditions. A summary of the determined rates is shown in Table 8.1.

Table 8.1 – Comparative weathering rates of materials reported in Chapters 3 and 5

	Weathering rate (log mol Ca m^{-2} sec^{-1})	**Estimation method**
Steel slag	Batch -9.39 to -11.88 Column -8.44 to -10.90 Field -7.11 to -7.56	Leaching of Ca Leaching of Ca Formation of $CaCO_3$
C&D waste	Batch -10.10 to -12.40	Leaching of Ca
Wollastonite	Batch -9.82 to -11.53 pH stat -6.19 to -8.03	Leaching of Ca Leaching of Ca
Dolerite	Batch -10.82 to -12.62	Leaching of Ca

Analysis of samples from selected silicate waste-covered field sites illustrated mean soil carbonate values of 21.8 ± 4.7% wt in 2010 and 41.16 ± 9.89 wt % in 2012 (Science Central) and 27.61 % wt (Yarborough landfill), demonstrating that a significant quantity of soil carbonate forms and persists in these environments. Stable isotope data ($\delta^{13}C$, $\delta^{18}O$) confirm that up to 81% of C in these pedogenic carbonates is atmospherically derived. ^{14}C data also support this notion by illustrating that a significant proportion of the C present in carbonates analysed is 'modern'. C&D waste soils (Science Central) were shown to have the potential to capture 18 $kgCO_2$ Mg^{-1} a^{-1}.

Flow-through weathering experiments at meso-scale show that a significant proportion of calcium (Ca) leaching occurs within the first 1-24 hrs. pH appeared to be buffered in the weathering systems at ~11.6 for fresh slag, by portlandite dissolution, and at ~9.1 for weathered slag, by persistence of carbonate with implications for the development of these systems in engineered field settings. The log_{10} values for Ca leaching vary from -8.44 to -10.90 $mol^{-1}sec^{-1}cm^{-2}$ in fresh slag (#3 C4) and weathered slag (#1 C3) respectively, within the range of laboratory figures determined elsewhere in this study (Table 8.1), suggesting that steel slag weathers rapidly under ambient environmental conditions.

Geochemical monitoring data from a large field site were analysed using SOLMINEQ 88 (Kharaka, Yousif K., USGS 1989) and illustrated the complexity in predicting saturation of carbonate minerals in waters across an engineered study site.

Quantification of the potential for inorganic C storage at a 'typical' urban redevelopment site is complex to reconstruct, and multi-experiment data were used to quantify carbon capture parameters for the Science Central site. In 2010 the 10 ha site was found to have a 'carbon capture potential' of 64,804 t CO_2 with analysis suggesting that 58.36% of this potential had already been exploited, capturing 37,463 t CO_2, leaving a remaining sequestration potential of 27,341 t CO_2. Nominally applying the current CO_2 trading cost of £8-£12/tCO_2, the value of CO_2 sequestration at the Science Central site in 2010 was £518,432 – £777,647 or £51,843 – £77,765 ha^{-1}.

Laboratory and field-scale studies have shown that carbonation reactions occur readily in artificial silicate minerals under ambient environmental conditions, providing a carbon capture function. This thesis illustrates the potential for anthropogenic soils to provide carbon sequestration as a prominent ecosystem service. Preliminary studies showed that the development of 'Carbon Capture Gardens', intentionally vegetated plots on sites where silicate wastes had been emplaced, was feasible, but insufficient data were available to draw any detailed conclusions from this work. As urban areas grow in magnitude and complexity a deep understanding of the environment which supports them becomes critical to ensuring sustainable growth and maintenance of ecosystem services. It also supports the utilisation of materials considered to be anthropogenic 'wastes' in helping to develop and support environmental management, providing an important route for re-use.

The studies contained in this thesis add to a growing body of evidence for the formation of carbonate minerals in soil settings where Ca/Mg-bearing silicate minerals occur. They also support the idea that engineered soils could be effectively utilised for carbon sequestration. Including a carbon capture function in soil management, and design of appropriate engineered infrastructure, can add environmental value with little additional energy input. Ultimately if soil carbonates are included in emissions offsetting schemes, alongside management of soil organic carbon, this technology has potential to provide carbon capture credentials to sites and to be included in development projects.

The next stage in the research into MCCS in soils is ultimately to demonstrate optimised carbon capture processes in soils specifically designed for this purpose. Further work is required to determine the potential for accelerating passive C capture by anthropogenically influenced soils in a synergistic system of planning and green

infrastructure development. On-going work should focus on a long-term (5-10 years) investigation of carbon dynamics in artificial soils at field scale. Additional research is also required to establish appropriate practises for promoting carbon accumulation in soils, both organic and inorganic, and a life cycle analysis is needed to evaluate the long-term suitability and value of these materials as a carbon capture technology.

8.2 Future work

Considering the parameters shown in the conceptual model in Chapter 7, Figure 7.1, a range of work with the potential to support or build upon the technical findings of this report is outlined below. This is divided in to four topical areas: technical (laboratory-scale), technical (field-scale), technical (overarching), economic and legislative.

8.2.1 Technical (laboratory-scale)

Environmentally realistic conditions

The laboratory experiments presented in Chapters 3 and 5 aimed to reproduce conditions experienced in natural weathering settings, however a number of factors were unaccounted for or only briefly covered, including a broad spectrum of water geochemistry and long-term changes in any of these parameters. It would be useful to carry out long-term batch experiments on the materials studied in Chapter 3 under a broader range of conditions.

Multi-phase single mineral studies

Many mineral dissolution studies are reported in the academic literature. It would be useful to compile these in to a catalogue which could be used in order to support the study of multi-phase reactions. The effect of interactions with other materials during the weathering process was not investigated in depth within the data presented in this thesis. Dissolution rates for the chemically simple silicate wollastonite are included, and other mineral weathering experiments could be carried out to allow predictions to be made of the processes and outcomes of multi-phase reactions.

8.2.2 Technical (field-scale)

Rigorous control

The field sites presented in this study do not provide a fully comprehensive control from which to start monitoring. It would be useful to carry out a similar survey on a site which has been chemically characterised from emplaced of the material onwards. It would be of interest to observe carbonate formation at field sites in different climatic regions.

Longitudinal studies

The data presented for the Science Central and Yarborough Landfill sites in Chapter 4 covers periods of 18 months and 1 year respectively. It would be useful for studies to be carried out on field sites over much longer periods to assess the formation rate and stability of carbonate minerals formed.

Carbon capture gardens

A brief summary of the work carried out on the Carbon Capture Gardens site, presented in Chapter 5, provides a useful basis for on-going work in this area. The interactions with other soil materials and biological actors is poorly constrained for the MCCS reactions, therefore the construction of field sites would be beneficial in determining this further.

8.2.3 Technical (overarching)

Isotope studies

IRMS has been shown to be useful tool in determining the provenance of C in carbonates and illustrating variations over time where fresh carbonate is being formed. Further work may include studies in controlled settings (possibly with labelled CO_2) to better constrain the organic and inorganic interactions in these systems and determine the consequences for the resultant isotope signatures. ^{14}C dating was used on a limited number of samples to illustrate its potential to confirm the presence of 'modern' (Appendix C) carbon in carbonates. A larger study would be useful in determining the efficacy of this approach.

Ecosystem services

MCCS provides carbon sequestration as an ecosystem service. As noted in Chapter 4, the process has the potential to provide a number of other services, especially when integrated in to a setting with soil organic matter, vegetation etc. It would be useful to

implement a long-term field study to focus on the potential for additional ecosystem services such as nutrient cycling to be affected by MCCS.

Whole-system modelling

Once more data are available for the interaction of environmental parameters with the MCCS processes, model parameters could be more reliably used to determine the most effective means of engineering soils for carbon capture. Model parameters could be defined as:

Carbonate precipitation as a function of silicate weathering in soils

- Bulk density, porosity and void ratio
- PSD, permeability and surface area
- Carbon dioxide in solution
- Carbonate precipitation
- Solution composition

Other factors

- Climatic conditions
- Duration of weathering
- Presence of soil organic matter
- Vegetation type and cover

8.2.4 Economic and legislative

Lifecycle analysis

A full lifecycle analysis of the materials and processes involved in MCCS should be carried out in order to better constrain the benefits of the process in the context of mineral production and eventual fate. Much of the current work focuses only on the relative benefits to the environment once the material has been produced.

Cost-benefits of process

A full cost-benefit analysis of the process could be carried out, in comparison to the alternative options for re-use and disposal. One of the main issues preventing the implementation of MCCS in soils is relative value of the materials in other settings,

such as secondary aggregates, when compared to their value in carbon capture leading to their diversion to other markets.

Policy – stakeholder engagement, especially with policymakers

A small amount of stakeholder engagement was carried out at Newcastle University over the period of this project (supported by two EPSRC Impact Award grants) of which the author was a part. It would be useful to foster and maintain engagement on the topic of MCCS in soil systems with relevant stakeholders in industry and policy in order to understand contemporary opportunities and risks and to allow useful co-production of research outputs.

REFERENCES

American Geophysical Union (2013) *Climate change position statement: Human-induced climate change requires urgent action.* AGU

American Geophysical Union (2009) *Geoengineering position statement: Geoengineering solutions to climate change require enhanced research, consideration of societal impacts, and Policy Development*. AGU

Andrews J.E. (2006) Palaeoclimatic records from stable isotopes in riverine tufas: Synthesis and review. *Earth-Science Reviews*, 75, p. 85-104.

Andrews, J.E., Gare, S.G., Dennis, P.F. (1997) Unusual isotopic phenomena in welsh quarry water and carbonate crusts. *Terra Nova*, 9, p. 67-70.

Arrhenius, S. (1897) On the influence of carbonic acid in the air upon the temperature of the earth. *Publications of the Astronomical Society of the Pacific.* 9 (54) 14.

Arrhenius, S. (1896) On the influence of carbonic acid in the air upon the temperature of the ground. *Philosophical Magazine and Journal of Science* Series 5, 41, p. 237-276.

Anand, R.R., Phang, C., Wildman, J.E., & Lintern, M.J. (1997) Genesis of some calcretes in the southern Yilgarn Craton, Western Australia: Implications for mineral exploration. *Australian Journal of Earth Sciences: An International Geoscience Journal of the Geological Society of Australia*, 44 (1)

Beck, M.B., Jiang, F., Shi, F., Villarroel Walker, R., Osidele, O.O., Demir, I., Lin, Z., Hall, J.W. (2010) Re-engineering cities as forces for good in the environment. Proceedings of the Institution of Civil Engineers, *Journal of Engineering Sustainability*, 16, p. 31-46.

Berner, R.A., and Kothavala, Z. (2001) Geocarb III: A revised model of atmospheric CO_2 over Phanerozoic time. *American Journal of Science*, 301 (2) p. 182-204

Berner, R.A. (1994) GEOCARB II: A revised model for atmospheric CO_2 over Phanerozoic time, *American Journal of Science*, 294 (1) p. 56-91

Berner R.A. (1991) A model for atmospheric CO_2 over Phanerozoic time, *American Journal of Science,* 291 (4) p. 339-376

Berner, R.A. and Lasaga, A.C. (1989) Modelling the geochemical carbon cycle. *Scientific American,* 260 p.74-81.

Berner, R.A., Lasaga, A.C., Garrels, R.M. (1983) The carbonate-silicate geochemical cycle and its effect on atmospheric carbon dioxide over the past 100 million years. *American Journal of Scienc*e 283 p. 641-683

Boguckyj, A.B., Lanczont, M., Lacka, B., Madeyska, T., Zawidzki, P. (2006) Stable isotopic composition of carbonates in Quaternary sediments of the Skala Podil'ska sequence (Ukraine). *Quaternary International*, 152-153, p. 3-13.

Bolin, B. (editor) (1979) *The global carbon cycle*. Chichester ; New York

Brady, P.V. and Walther, J.V. (1989) Controls on silicate dissolution rates in neutral and basic pH solutions at 25°C. *Geochimica et Cosmochimica Acta*. 53 (11) p. 2823–2830

BREEAM (Accessed 2013) Standards for best practice in sustainable building design, construction and operation http://www.breeam.org/podpage.jsp?id=362

British Geological Survey (2012) *United Kingdom Minerals Yearbook*. BGS Minerals and waste programme. Open report OR/13/024

British Standards Institution (2009) BS 6031:2009 Code of practice for earthworks

British Standards Institution (1995) BS 7755-3.10:1995 ISO 10693:1995 Soil quality. Chemical methods. Determination of carbonate content. Volumetric method

British Standards Institution (1990) BS 1377-2:1990 Methods of test for soils for civil engineering purposes. Classification tests

British Standards Institution (2004) BS EN ISO 14688:2:2004 Geotechnical investigation and testing. Identification and classification of soil. Principles for a classification

Busenberg, E. and Clemency, C.V., (1976) The dissolution kinetics of feldspars at 25°C and 1 atm CO_2 partial pressure. *Geochimica et Cosmochimica Acta* 40 (1) p. 41–49

Butt, D.P., Lackner, K.S., Wendt, C.H., Park, Y.S., Benjamin, A., Harradine, D.M., Holesinger, T., Rising, M., Nomura, K. (1997). A method for permanent disposal of CO_2 in solid form. *Global Warming International Conference*. Columbia University, NY.

Callendar, G.S. (1938) The artificial production of carbon dioxide and its influence on temperature. *Quarterly Journal of the Royal Meteorological Society* 64(275) p. 223-240.

Carbon Trust (2011) *International carbon flows: Steel*

Chen, B., Yang, J., Ouyang, Z. (2011) Life Cycle Assessment of Internal Recycling Options of Steel Slag in Chinese Iron and Steel Industry. *International Journal of Iron and Steel Research*, 18 (7) p. 33-40

Chen, J.J., Thomas, J.J., Taylor, H.F., Jennings, H.M. (2004) Solubility and structure of calcium silicate hydrate. *Cement and Concrete Research*, *34* (9) p. 1499-1519

Chiquet, A., Michard, A., Nahon, D., Hamelin, B. (1999) Atmospheric input vs in situ weathering in the genesis of calcretes: an Sr isotope study at Gálvez (Central Spain). *Geochimica et Cosmochimica Acta*, 63 (3–4) p. 311–323

Chou, L. and Wollast, R. (1984) Study of the weathering of albite at room temperature and pressure with a fluidized bed reactor. *Geochimica et Cosmochimica Acta* 48 (11) p. 2205-2217

CL:AIRE (1999) *Contaminated land application in real environments*.

CLG (2012) *National Planning Policy Framework (NPPF).*

Craul, P.J., (1992) *Urban Soil in Landscape Design*, John Wiley & Sons Inc.

Curtis, C.D. (1976) Stability of minerals in surface weathering reactions: a general thermochemical approach. *Earth surface processes*, 1 p. 63-70

Darling, W.G., Bath, A.H., Talbot, J.C. (2003) The O and H stable isotope composition of freshwaters in the British Isles. 2. Surface waters and groundwater. *Hydrology and Earth System Sciences*, (7) p. 183-195.

Dart, R.C., Barovich, K.M., Chittleborough, D.J., Hill, S.M. (2007) Calcium in regolith carbonates of central and southern Australia: its source and implications for the global carbon cycle. *Palaeogeography, Palaeoclimatology, Palaeoecology*, 249 p. 322-334.

DECC (2013) https://www.gov.uk/government/policies/increasing-the-use-of-low-carbon-technologies/supporting-pages/carbon-capture-and-storage-ccs (Accessed 2013)

DECC (2012) *CCS Commercialisation competition* https://www.gov.uk/uk-carbon-capture-and-storage-government-funding-and-support#ccs-commercialisation-competition (Accessed 2013)

DECC (2011) *Update short term traded carbon values for UK public policy appraisal*

DEFRA (2011) *National Standards for sustainable drainage systems: Designing, constructing, operating and maintaining drainage for surface runoff*

DEFRA (2009) *Safeguarding our Soils: A Strategy for England.* Department for Environment, Food and Rural Affairs. London. 2009. Unique Identifier: PB13297.

DEFRA (Clarkson, R. and Deyes, K.) (2002) *Estimating the Social Cost of Carbon Emissions.* Government Economic Service Working Paper 140

Dietzel, M., Usdowski, E., Hoefs, J. (1992) Chemical and $^{13}C/^{12}C$- and $^{18}O/^{16}O$-isotope evolution of alkaline drainage waters and the precipitation of calcite. *Applied Geochemistry,* 7 p. 177-184.

Doney, S.C., Fabry, V.J., Feely, R.A., and Kleypas, J.A. (2009) Ocean Acidification: The Other CO_2 Problem. *Annual Review of Marine Science*, 1 p. 169–92

Drever, J.I. and Stillings, L.L. (1989) The role of organic acids in mineral weathering. *Colloids and Surfaces A: Physicochemical and Engineering Aspects*. 120 (1–3) p. 167–181

Durand, N., Gunnell, Y., Curmi, P., Ahmad, S.M., (2007) Pedogenic carbonates on Precambrian silicate rocks in South India: Origin and paleoclimatic significance. *Quarternary International*, 162-163, p.35-49.

Durand, N., Gunnell, Y., Curmi, P., Ahmad, S.M. (2006) Pathways of calcrete development on weathered silicate rocks in Tamil Nadu, India: Mineralogy, chemistry and paleoenvironmental implications. *Sedimentary Geology* 192, p. 1-18.

Effland, W.R and Pouyat, R.V. (1997) The genesis, classification, and mapping of soils in urban areas. *Urban Ecosystems*, 1 p. 217-228.

EIA (2011) *Annual energy outlook 2011.* U.S. Energy Information Administration

Ellerman, A.D. (2003) Are cap-and-trade programs more environmentally effective than conventional regulation? *MIT Center for Energy and Environment Research*

Environment Agency (Accessed 2013) *Carbon calculator for construction activities.* http://www.environment-agency.gov.uk/business/sectors/136252.aspx

Environment Agency (2009) *Updated technical background to the CLEA model Science report: SC050021/SR3.* Environment Agency

Environment Agency (2007) *Waste protocols project - Blast Furnace Slag*. Environment Agency.

Environment Agency (2004) CLR 11 Contaminated Land Model Procedures for the Management of Land Contamination

Ettler, V., Zelena, O., Mihaljevic, M., Sebek, O., Strnad, L., Coufal, P., Bezdicka, P., (2006). Removal of trace elements from landfill leachate by calcite precipitation. *Journal of Geochemical Exploration,* 88 p. 28-31.

EU (2013) EU Emissions Trading Scheme factsheet http://ec.europa.eu/clima/publications/docs/factsheet_ets_en.pdf

EU (2008) Directive 2008/98/EC on waste (Waste Framework Directive)

EU (2006) EU Soils Framework Directive. Proposal for a Soil Framework Directive (COM(2006) 232) Establishing a framework for the protection of soil and amending directive 2004/35/EC.

EU (2005) EU Emissions Trading Scheme launch

EU (2003) European Union Emissions Trading Markets (EU ETS) Directive (2003/87/EC)

EU (2000) ECCP (European Climate Change Programme I) 2001-2004

EU (2000) ECCP (European Climate Change Programme II) from 2005

EU (1999) EU Landfill Directive (EEC/1999/31/EC)

FAO (Accessed 2013) Land resources: Soil carbon sequestration http://www.fao.org/nr/land/sustainable-land-management/soil-carbon-sequestration/en/

FAO (2000) World Soil Resources Reports. Carbon sequestration options under the clean development mechanism to address land degradation

Fernández Bertos, M., Simons, S.J.R, Hills, C.D. Carey, P.J. (2004) A review of accelerated carbonation technology in the treatment of cement-based materials and sequestration of CO_2. *Journal of Hazardous Materials B*, 112 p. 193–205

Fournet, J., (1833) Mémoire sur la décomposition des minérais d'origine igneé, et leur conversion en kaolin. *Annales de chimie et de physique*. 55 p. 225–256

Fredericci, C., Zanotto, E.D., Ziemath, E.C. (2000) Crystallization mechanism and properties of a blast furnace slag glass. *Journal of Non-Crystalline Solids, 273* (1) p. 64-75.

Garlick, G.D. (1969) The stable isotopes of oxygen. *Handbook of geochemistry*. Springer-Verlag Berlin

Geerlings, J.J.C., and Wesker, E. (2006). *European Patent No. EP 1554031*. Process for removal and capture of carbon dioxide from flue gases Munich, Germany: European Patent Office.

Gérard, F., Ranger, J., Ménétrier, C., Bonnaud, P. (2003) Silicate weathering mechanisms determined using soil solutions held at high matric potential. *Chemical Geology*, 202 (3–4) p. 443–460

Gerdemann, S.J., O'Connor, W.K., Dahlin, D.C., Penner, L.R., & Rush, H. (2007). Ex situ aqueous mineral carbonation. *Environmental Science & Technology, 41* (7) p. 2587-2593.

GlobalSlag.com (2013) Knowledge base http://www.globalslag.com/knowledge-base (Accessed 2013)

Goldich, 1938 A study in rock weathering. *The Journal of Geology*, 46 (1) p. 17-58

Google Maps (Accessed 2010) Google maps image (Scunthorpe, UK)

Goudie, A.S. (1983) Calcrete. In: Goudie, A. S. & Pye, K. (Eds), *Chemical Sediments and Geomorphology*, p. 93–131. London: Academic Press.

Guimaraes, M.S., Valdes, J.R., Palomino, A.M., Santamarina, J.C. (2007) Aggregate production: Fines generation during rock crushing. *International Journal of Mineral Processing*, 81 (4) p. 237-247.

The Guardian (UK) (2009) Budget 2009: Darling promises 34% emissions cuts with world's first binding carbon budgets http://www.theguardian.com/environment/2009/apr/22/carbon-emissions-budget-20091 (Accessed 2013)

Gunning, P.J., Hills, C.D., Carey, P.J. (2010) Accelerated carbonation treatment of industrial wastes. *Waste Management*, 30 p. 1081-1090.

Hamilton, J.P., Pantano, C.G., Brantley, S.L. (2000) Dissolution of albite glass and crystal. *Geochimica et Cosmochimica Acta*, *64* (15) p.2603-2615.

Harrison, A.L., Power, I.M., Dipple, G.M. (2013) Accelerated carbonation of brucite in mine tailings for carbon sequestration. *Environmental Science and Technology*, *47*(1), 126-134.

Hartmann, J., West, J., Renforth, P., Köhler, P., De La Rocha, C.L., Wolf-Gladrow, D. A., Dürr, H. Scheffran, J. (2013) Enhanced chemical weathering as a geoengineering strategy to reduce atmospheric carbon dioxide, a nutrient source and to mitigate ocean acidification. *Reviews of Geophysics.*

HMRC (Accessed 2013) L*and remediation relief: exclusions: polluter pays* http://www.hmrc.gov.uk/manuals/cirdmanual/cird60120.htm

HMRC (2002) *Aggregates Levy.*

HMRC (1996) *Landfill Tax.*

Hoeffs, J. (1997) *Stable Isotope Geochemistry 4th Edition*, Springer-Verlag (Berlin)

Holdren Jr, G. R. and Speyer, P. M. (1987) Reaction rate-surface area relationships during the early stages of weathering. II. Data on eight additional feldspars. *Geochimica et Cosmochimica Acta* 51 (9) p. 2311-2318.

Huang, W.H. and Keller, W.D. (1972) Organic acids as agents of chemical weathering of silicate minerals. *Nature physical science* 239 p. 149-151

Huijgen, W.J.J, Comans, R.N.J., Witkamp, G-J. (2007) Cost evaluation of CO2 sequestration by aqueous mineral carbonation. *Energy Conversion and Management* 48 p. 1923–1935.

Huijgen, W.J.J., Comans, R.N.J. (2006) Carbonation of steel slag for CO_2 sequestration: leaching of products and reaction mechanisms. *Environmental Science and Technology,* 40 p. 2790-2796.

Huijgen, W.J.J., Witkamp, G-J., Comans, R.N.J. (2005) Mineral CO_2 sequestration by steel slag carbonation. *Environmental Science and Technology*, 39 p. 9676-9682.

Huntzinger, D.N., Gierke, J.S., Kawatra, S.K., Eisele, T.C., Sutter, L.L. (2009) Carbon dioxide sequestration in cement kiln dust through mineral carbonation. *Environmental Science & Technology,* 43 p. 1986-1992.

Huntzinger, D.N. (2006) *Carbon dioxide sequestration in cement kiln dust through mineral carbonation*. PhD thesis. Michigan Technological University

IEA (2012) International Energy Agency 2012 Report

Iizuka, A., Fujii, M., Yamasaki, A., Yanagisawa, Y. (2004) Development of a new CO_2 sequestration process utilizing the carbonation of waste cement. *Industrial & Engineering Chemistry Research*, 43(24) p.7880-7887.

IPCC (2013) [Stocker, T.F., Qin, D., Plattner, G.-K., Tignor, M., Allen, S.K., Boschung, J., Nauels, A., Xia, Y., Bex, V., Midgley, P.M. (eds.)]. *Climate Change 2013: The Physical Science Basis*. Contribution of Working Group I to the Fifth Assessment Report of the Intergovernmental Panel on Climate Change Cambridge University Press

IPCC (2007) [Solomon, S., Qin, D., Manning, M., Chen, Z., Marquis, M., Averyt, K.B., Tignor, M., Miller, H.L. (eds.)] (2007). *Climate Change 2007: The Physical Science Basis* Contribution of Working Group I to the Fourth Assessment Report of the Intergovernmental Panel on Climate Change.

IPCC (2005) [Metz, B., Davidson, O., de Coninck, H., Loos, M., Meyer, L. (eds)] *IPCC Special Report on Carbon dioxide Capture and Storage*. New York, Intergovernmental Panel on Climate Change.

IPCC (2001) [Houghton, J.T., Ding, Y., Griggs, D.J., Noguer, M., van der Linden, P.J., Dai, X., Maskell, K., Johnson, C.A. (eds.)]. *Climate Change 2001: The Physical Science Basis* Contribution of Working Group I to the Third Assessment Report of the Intergovernmental Panel on Climate Change.

IPCC (2001) [Metz, B., Davidson, O., Swart, R., Pan, J., (eds.)] *Climate change 2001: mitigation*, contribution of Working Group III to the third assessment report of the Intergovernmental Panel on Climate Change.

IPCC (2000) *IPCC Emissions Scenarios.* A special report of working group III of the Intergovernmental Panel on Climate Change

IPCC (1997a) [Houghton, J.T., Meria Filho, L.G., Lim, B., Treanton, K., Mamaty, I. ,Bonduki, Y., Griggs, D.J., Callender B.A. (eds.)]. *Revised 1996 IPCC Guidelines for National Greenhouse Gas Inventories Reporting Instructions (Volume 1).* Intergovernmental Panel on Climate Change.

IPCC (1997b) [Houghton, J.T., Meria Filho, L.G., Lim, B., Treanton, K., Mamaty, I. ,Bonduki, Y., Griggs, D.J., Callender B.A. (eds.)]. *Revised 1996 IPCC Guidelines for National Greenhouse Gas Inventories Workbook (Volume 2).* Intergovernmental Panel on Climate Change.

IPCC (1997c) [Houghton, J.T., Meria Filho, L.G., Lim, B., Treanton, K., Mamaty, I. ,Bonduki, Y., Griggs, D.J., Callender B.A. (eds.)]. *Revised 1996 IPCC Guidelines for National Greenhouse Gas Inventories Reference Manual (Volume 3).* Intergovernmental Panel on Climate Change.

IPCC (1995) *Climate Change: Impacts, Adaptations and Mitigation of Climate Change.* Scientific-Technical Analyses 1996.

IPCC (1990) [J.T. Houghton, G.J. Jenkins and J.J. Ephraums (eds.)]. *Climate Change: The IPCC Scientific Assessment Report,* prepared for Intergovernmental Panel on Climate Change by Working Group I. Cambridge University Press

ISO 14040:2006 Environmental Management – Lifecycle assessment principles and framework

ISO 14044:2006 Environmental Management - Lifecycle assessment requirements and guidelines

Jenny, H. (1980) *The Soil Resource: origin and behaviour,* Springer, New York. ISBN: 038790453X.

Jones, D.L., Dennis, P.G., Owen, A.G., & van Hees, P.A.W. (2003) Organic acid behavior in soils – misconceptions and knowledge gaps. *Plant and Soil,* 248 p. 31–41

Kakizawa, M., Yamasaki, A., Yanagisawa, Y. (2001) A new CO_2 disposal process via artificial weathering of calcium silicate accelerated by acetic acid. Energy 26 (4) p. 341-354.

Kalin, R.M., Dardis, G., Lowndes, J. (1997) Secondary carbonates in the antrim basalts: geochemical weathering at 35KyBP. *Geofluids II Conference Extended Abstract*, Belfast; Queen's University Belfast.

Kaye, J.P., McCulley, R.L., Burke, I.C. (2005) Carbon fluxes, nitrogen cycling, and soil microbial communities in adjacent urban, native and agricultural ecosystems. *Global Change Biology*, 11 p. 575-587.

Kharaka, Y.K, Gunter, W.D., Aggarwal, P.K., Perkins, E.H., DeBraal, J.D. (1989) SOLMINEQ-88: A Computer Program for Geochemical Modelling of Water-Rock Interactions. Menlo Park, CA, USGS.

Khoo, H.H., Bu, J., Wong, R.L., Kuan, S.Y., Sharratt, P.N. (2011) Carbon capture and utilization: Preliminary life cycle CO_2, energy, and cost results of potential mineral carbonation. *Energy Procedia 10th International Conference on Greenhouse Gas Control Technologies*. Volume 4, Pages 2494–2501

Keeling, C.D. and Whorf, T.P. (and Carbon Dioxide Research Group) (2004) Atmospheric CO_2 concentrations (ppmv) derived from in situ air samples collected at Mauna Loa Observatory, Hawaii. Scripps Institution of Oceanography, University of California, La Jolla, California.

Keith, D., Ha-Duong, M., Stolaroff, J.K. (2006) Climate strategy with CO_2 capture from the air. *Climatic Change*. 74 (1-3) p. 17-45

Kelemen, P.B., Matter, J., Streit, E.E., Rudge, J.F., Curry, W.B., & Blusztajn, J. (2011) Rates and mechanisms of mineral carbonation in peridotite: natural processes and recipes for enhanced, in situ CO_2 capture and storage. *Annual Review of Earth and Planetary Sciences*, 39 p. 545-576.

Knauss, K.G. and Wolery, T.J. (1988) The dissolution kinetics of quartz as a function of pH and time at 70°C. *Geochimica et Cosmochimica Acta* 52 (1) p. 43-53.

Knauth, L.P., Brilli, M., Klonowski, S., (2003) Isotope Geochemistry of Caliche Developed on Basalt. *Geochimica et Cosmochimica Acta*, 67 (2) p. 185-195.

Kosmatka, S.H. and Wilson, M.L. (2011) LCA – excerpt from: *Portland Cement Association. Design and Control of Concrete Mixtures, 15th edition.* Item Code: EB001.15

Kovda, I., Mora, C.I., Wilding, L.P., (2006) Stable Isotope Composition of Pedogenic Carbonates and Soil Organic Matter in a Temperate Climate Vertisol with Gilgai, Southern Russia. *Geoderma* 136 p. 423-435.

Krishnamurthy, R.V., Schmitt, D., Atekwana, E.A., Baskaran, M. (2003) Isotopic Investigations of Carbonate Growth on Concrete Structures. *Applied Geochemistry*, 18 p. 435-444.

Kump, L.R., Kasting, J.F., Crane, R.G. (2004) *The Earth System.* Upper Saddle River, New Jersey, Pearson Prentice Hall.

Łącka, B., Łanczont, M., Komar, M., Madeyska, T. (2008) Stable isotope composition of carbonates in loess at the Carpathian margin (SE Poland). *Studia Quaternaria*, 25 p. 3-21.

Lackner, K.S. (2003) A guide to CO_2 sequestration. *Science*, 300 p. 1677-1678.

Lackner, K.S., Butt, D.P., Wendt, C.H. (1997) Progress on binding CO_2 in mineral substrates. *Energy Conversion And Management*, 38 p. 259-264.

Lackner, K.S., Wendt, C.H., Butt, D.P., Joyce, E.L., Sharp, D.H., (1995) Carbon Dioxide Disposal in Carbonate Minerals. *Energy*, 20 p. 1153-1170.

Lal, R. (2004) Soil carbon sequestration to mitigate climate change. *Geoderma*, 123 p. 1 – 22.

Lasaga, A.C., Soler, J.M., Ganor, J., Burch, T.E. Nagy, K.L. (1994) Chemical weathering rate laws and global geochemical cycles. *Geochimica et Cosmochimica Acta*, *58* (10) p. 2361-2386.

Lasaga, A.C., Berner, R.A. and Garrels, R.M. (1985) An improved geochemical model of atmospheric CO_2 fluctuations over the past 100 million years. *Geophysical Monograph Series*, 32 p. 397-411.

Lavorel, S., McIntyre, S., Landsberg, J. and Forbes, T.D.A. (1997) Plant functional classifications: from general groups to specific groups based on response to disturbance. *Trends in Ecology & Evolution*, 12 (12) p. 474-478.

Lee, A.R. (1974) *Blast furnace and Steel Slag: Production, Properties and Uses.* London, Edward Arnold.

Lehmann, A. and Stahr, K. (2007) Nature and significance of anthropogenic urban soils. *Journal of Soils and Sediments*, 7 p. 247-260.

Limbachiya, M.C., Marrocchino, E., Koulouris, A. (2007) Chemical–mineralogical characterisation of coarse recycled concrete aggregate. Waste Management, 27 (2) p. 201-208.

Lin, H., Fujii, T., Takisawa, R., Takahashi, T., Hashida, T. (2008) Experimental evaluation of interactions in supercritical CO_2/water/rock minerals system under geologic CO_2 sequestration conditions. *Journal of Materials Science*, 43 (7) p. 2307-2315.

Lorenz, K., Lal, R. (2009) Biogeochemical C and N cycles in urban soils. *Environment International*, 35 p. 1-8.

Lothenbach, B., Matschei, T., Möschner, G., Glasser, F.P. (2008) Thermodynamic modelling of the effect of temperature on the hydration and porosity of Portland cement. *Cement and Concrete Research*, 38 (1) p. 1-18.

Lovelock, J.E., & Watson, A.J. (1982) The regulation of carbon dioxide and climate: Gaia or geochemistry. *Planetary and Space Science*, *30* (8) p. 795-802.

Macleod, G., Fallick, A.E., Hall, A.J. (1991) The mechanism of carbonate growth on concrete structures, as elucidated by carbon and oxygen isotope analyses. *Chemical Geology*, 86 p. 335-343.

Mahieux, P.Y., Aubert, J.E., Escadeillas, G. (2009) Utilization of weathered basic oxygen furnace slag in the production of hydraulic road binders. *Construction and Building Materials*, 23 (2) p. 742-747.

Manning, D.A.C., Renforth, P. (2013a) Passive sequestration of atmospheric CO2 through coupled plant-mineral reactions in urban soils. *Environmental Science and Technology*, 47 (1) p. 135-141.

Manning, D.A.C., Renforth, P., Lopez-Capel, E., Robertson, S., Ghazireh, N. (2013b) Carbonate precipitation in artificial soils produced from basaltic quarry fines and composts: an opportunity for passive carbon sequestration. *International Journal of Greenhouse Gas Control*, 17 p. 309-317.

Manning, D.A.C. (2008) Biological enhancement of soil carbonate precipitation: passive removal of atmospheric CO_2. *Mineralogical Magazine*, Mineralogical Society 72 p. 639-649.

Manning, D.A.C. (2001) Calcite precipitation in landfills: an essential product of waste stabilisation. *Mineralogical magazine*, Mineralogical Society. 65 p. 603-610.

Marchetti, C., (1976) *On Geoengineering and the CO_2 problem*. Research Memorandum RM-76-17. International Institute for Applied Systems Analysis, Vienna

Mast, A.M., and Drever, J.I. (1987) The effect of oxalate on the dissolution rates of oligoclase and tremolite. *Geochimica et Cosmochimica Acta*, 51 (9) p. 2559-2568.

Matschei, T., Lothenbach, B., Glasser, F.P. (2007) Thermodynamic properties of Portland cement hydrates in the system $CaO–Al_2O_3–SiO_2–CaSO_4–CaCO_3–H_2O$. *Cement and Concrete Research*, 37 (10) p. 1379-1410.

Mayes, W.M., Younger, P.L., Aumônier, J. (2008) Hydrogeochemistry of alkaline steel slag leachates in the U.K. *Water Air and Soil Pollution,* 195 p. 35-50.

Met Office (Accessed 2013) Historic station data (Durham) http://www.metoffice.gov.uk/climate/uk/stationdata/durhamdata.txt

Met Office (Accessed 2013) Historic station data (Sheffield) http://www.metoffice.gov.uk/climate/uk/stationdata/sheffielddata.txt

Mikhailova, E.A., Post, C.J., Magrini-Bair, K., Castle, J.W, (2006) Pedogenic carbonate concretions in the Russian chernozem. *Soil Science,* 171 (12) p. 981-991.

Morales-Flórez, V., Santos, A., Lemus, A., Esquivias, L. (2011) Artificial weathering pools of calcium-rich industrial waste for CO_2 sequestration. *Chemical Engineering Journal*, 166 p. 132-137.

Mumm, A.S. and Reith, F., (2007) Biomediation of calcrete at the gold anomaly of the Barns prospect, Gawler Craton, South Australia. *Journal of Geochemical Exploration,* 92 p. 13-33.

Nettleton, W.D. (1991) Occurrence, characteristics, and genesis of carbonate, gypsum, and silica accumulations in soils. *Soil Science Society of America*. Issue 26 of SSSA special publication. ISBN: 0891187944

Nier, A.O. (1950) A redetermination of the relative abundances of the isotopes of carbon, nitrogen, oxygen, argon, and potassium. *Physical Review*, 77 (6) p. 789.

Norwest Holst Soil Engineers Ltd.. Report on a Ground Investigation at the Former Tyne Brewery, Newcastle upon Tyne, Sites 1 and 2. October 2005: Project Number F15481A.

Norwest Holst Soil Engineers Ltd.. Report on a Ground Investigation at the Former Tyne Brewery, Newcastle upon Tyne, Site 3. July 2009: Project Number F15481B.

Nugent, M.A., Brantley, S.L., Pantano, C.G., Maurice, P.A. (1998) The influence of natural mineral coatings on feldspar weathering. *Nature*, 395 p. 588-591

Oelkers E.H. (2001) An experimental study of forsterite dissolution as a function of temperature, and aqueous Mg and Si concentration. *Chemical Geology*, 175 p. 485–494.

Olajire, A.A. (2013) A review of mineral carbonation technology in sequestration of CO_2. *Journal of Petroleum Science and Engineering*, 109 p. 364-392.

Oxburgh, R., Drever, J.I., Sun, Y.T. (1994) Mechanism of plagioclase dissolution in acid solution at 25 C. *Geochimica et Cosmochimica Acta*, 58 (2) p. 661-669.

Palandri, J.L. and Kharaka, Y.K. (2004) *A compilation of rate parameters of water-mineral interaction kinetics for application to geochemical modeling* (No. OPEN-FILE-2004-1068). Geological Survey Menlo Park Ca.

Pao, H.T., and Tsai, C.M. (2010) CO_2 emissions, energy consumption and economic growth in BRIC countries. *Energy Policy*, 38 (12) p. 7850-7860.

Paustian, K., Six, J., Elliott, E.T., Hunt, H.W. (2000) Management options for reducing CO_2 emissions from agricultural soils. *Biogeochemistry*, 48 (1) p. 147-163.

Penner, L., O'Connor, W.K., Dahlin, D.C., Gerdemann, S., Rush, G.E. (2004) Mineral carbonation: energy costs of pre-treatment options and insights gained from flow loop reaction studies. In *Proceedings of the 3rd Annual Conference on Carbon Capture and Sequestration. Washington, DC CD-ROM.*

Personal communication (2012) EPSRC Impact Award meeting 2012 secondary aggregate price

Poh, H.Y., Ghataora, G.S., Ghazireh, N. (2006) Soil stabilization using basic oxygen steel slag fines. *Journal of Materials in Civil Engineering*, 18 (2) p. 229-240.

Pokrovsky, O. S. and Schott, J. (2000) Kinetics and mechanism of forsterite dissolution at 25°C and pH from 1 to 12. *Geochimica et Cosmochimica Acta*, 64 (19) p. 3313-3325.

Pouyat, R.V., Yesilonis, I.D., Nowak, D.J. (2006) Carbon Storage by Urban Soils in the United States. *Journal of Environmental Quality*, 35 p. 1566-1575.

Power, I., Wilson, S., Small, D., Dipple, G., Wan, W., Southam, G. (2011) Microbially mediated mineral carbonation: Roles of phototrophy and heterotrophy. *Environmental Science & Technology*, 45 (20) p. 9061-9068.

Power, I., Wilson, S., Thom, J., Dipple, G., Gabites, J., Southam, G. (2009) The hydromagnesite playas of Atlin, British Columbia, Canada: A biogeochemical model for CO_2 sequestration, *Chemical Geology*, 260 (3-4) p. 286-300.

Powers, T.C. (1958) Structure and physical properties of hardened Portland cement paste. *Journal of the American Ceramic Society*, 41 (1) p. 1-6.

Proctor, D.M., Fehling, K.A., Shay, E.C., Wittenborn, J.L., Green, J.J., Avent, C., Bigham, R.D., Connolly, M., Lee, B.T., Shepker, O., Zak, M.A. (2000) Physical and chemical characteristics of Blast Furnace, Basic Oxygen Furnace, and Electric Arc Furnace steel industry slags. *Environmental Science and Technology*, 34 (8) p. 1576–1582.

Quade, J., Chivas, A.R., McCulloch, M.T., (1995). Strontium and Carbon Isotope Tracers and the Origins of Soil Carbonate in South Australia and Victoria. *Palaeogeography, Palaeoclimatology, Palaeoecology*, 113 p. 103-117.

Rawlins, B.G., Henrys, P., Breward, N., Robinson, D.A., Keith, A.M., Garcia-Bajo, M. (2011) The importance of inorganic carbon in soil carbon databases and stock estimates: a case study from England. *Soil Use and Management*, 27 p. 312-320.

Rawlins, C.H. (2008) *Geological Sequestration of Carbon Dioxide by Hydrous Carbonate Formation in Steel Making Slag.* PhD Thesis. Missouri University of Science and Technology.

Rawlins, C.H., Peaslee, K.D., Richards, V. (2008) Feasibility of processing steelmaking slag for carbon dioxide sequestration and metal recovery. *Iron & Steel Technology* AIST 5 p. 164-174

Reddy, K.J., Gloss, S.P., Wang, L. (1994) Reaction of CO_2 with Alkaline Solid Wastes to Reduce Contaminant Mobility. *Water Research,* 28 (6) p. 1377-1382.

Renforth, P. (2012) The potential of enhanced weathering in the UK. *International Journal of Greenhouse Gas Control*, 10 p. 1-15.

Renforth, P., Edmondson, J., Leake, J.R., Gaston, K.J., Manning, D.A.C. (2011a) Designing a carbon capture function into urban soils, *Proceedings of the Institution of Civil Engineers: Urban Design and Planning*, 164 p. 121-128.

Renforth P., Manning, D.A.C. (2011b) Laboratory carbonation of artificial silicate gels enhanced by citrate: Implications for engineered pedogenic carbonate formation. *International Journal of Greenhouse Gas Control*, 5 p. 1578-1586

Renforth, P., Washbourne, C-L., Taylder, J., Manning, D.A.C. (2011c) Silicate production and availability for mineral carbonation. *Environmental Science and Technology*, 45 p. 2035-2041.

Renforth, P. (2011) *Mineral carbonation in soils engineering the soil carbon sink*. PhD thesis. Newcastle University.

Renforth, P., Manning, D.A.C., Lopez-Capel, E. (2009) Carbonate precipitation in artificial soils as a sink for atmospheric carbon dioxide. *Applied Geochemistry*, 24: 1757-1764

Rimstidt J.D. and Barnes H.L. (1980) The kinetics of silica-water reactions. *Geochimica et Cosmochimica Acta*, 44 p. 1683-1699.

Robie, R.A. and Hemingway, B.S. (1995) Thermodynamic properties of minerals and related substances at 298.15 K and 1 bar (10^5 Pascals) pressure and at higher temperatures. *US Geological. Survey Bulletin*, 2131, p. 461-461

Rodgers, W.B. and Rodgers, R.E. (1848) On the decomposition and partial solution of minerals and rocks by pure water and water charged with carbonic acid. *American Journal of Science*, 5 p. 401-405.

Rosenbaum, M.S., McMillan, A.A., Powell, J.H., Cooper, A.H., Culshaw, M.G., Northmore, K.J. (2003) Classification of artificial (man-made) ground. *Engineering Geology*, 69 p. 399-409.

Royal Society (2009) *Geoengineering the climate: science, governance and uncertainty* RS Policy document 10/09

Royer, D.L. (1999) Depth to pedogenic carbonate horizon as a paleoprecipitation indicator? *Geology*, 27 (12) p. 1123-1126.

Ruddiman, W.F. (2005) How did humans first alter global climate? *Scientific American,* 292 (3) p. 46-53.

Ruddiman, W.F. (2003) The anthropogenic greenhouse era began thousands of years ago. *Climatic Change*, 61 p. 261–293.

Ryskov, Y.G., Demkin, V.A., Oleynik, S.A., Ryskove, E.A. (2008) Dynamics of pedogenic carbonate for the last 5000 years and its role as a buffer reservoir for atmospheric carbon dioxide in soils of Russia " *Global and Planetary Change,* 61 p. 63-69.

Salomons, W., Mook, W.G., (1976) Isotope geochemistry of carbonate dissolution and reprecipitation in soils. *Soil Science*, 122 (1) p. 15-24.

Sanna, A., Dri, M., Hall, M.R., & Maroto-Valer, M. (2012) Waste materials for carbon capture and storage by mineralisation (CCSM)–A UK perspective. *Applied Energy*.

Scharenbroch, B.C., Lloyd, J.E., Johnson-Maynard, J.L.. (2005) Distinguishing urban soils with physical, chemical, and biological properties. *Pedobiologia*, 49 p. 283-296.

Schlesinger, W.H. (1982) Carbon storage in the caliche of arid soils: A case study from Arizona. *Soil Science,* 247-255.

Schuiling, R., Wilson, S., Power, I. (2011) Enhanced silicate weathering is not limited by silicic acid saturation, *Proceedings Of The National Academy Of Sciences Of The United States Of America*, 108 (12) p. E41.

Schuiling, R.D., Krijgsman, P. (2006) Enhanced weathering; an effective and cheap tool to sequester CO_2. *Climatic Change*, 74 p. 349-354.

Seifritz, W. (1990) CO_2 disposal by means of silicates. *Nature,* 345 p. 486.

Shen, H. and Forssberg, E. (2003) An overview of recovery of metals from slags. *Waste Management*, 23 (10) p. 933-949.

Shibata, S.N., Tanaka, T., Yamamoto, K. (2006) Crystal structure control of the dissolution of rare earth elements in water-mineral interactions. *Geochemical Journal,* 40 (5) p.437-446.

Siegel, D.I. and Pfannkuch, H.O. (1984) Silicate mineral dissolution at pH 4 and near standard temperature and pressure. *Geochimica et Cosmochimica Acta,* 48 (1) p. 197-201.

Sinha, R., Tandon, S.K., Sanyal, P., Gibling, M.R., Stuben, D., Berner, Z., Ghazanfari, P. (2006) Calcretes from a Late Quaternary interfluve in the Ganga Plains, India: Carbonate types and isotopic systems in a monsoonal setting. *Palaeogeography, Palaeoclimatology, Palaeoecology,* 242 p. 214-239.

Smith, P., (2004) Carbon sequestration in croplands: the potential in Europe and the global context. *European Journal of Agronomy,* 20 p. 229-236.

Smith, P., Powlson, D., Glendinning, M., Smith, J. (1997) Potential for carbon sequestration in European soils: preliminary estimates for five scenarios using results from long-term experiments. *Global Change Biology*, p. 67-79.

Sohi, S.P., Mahieu, N., Arah, J.R.M., Powlson, D.S., Madari, B., Gaunt, J.L. (2001) A procedure for isolating soil organic matter fractions suitable for modeling. *Soil Science Society of America Journal*, 65 p.1121-1128.

Statoil (Accessed 2013) CO_2 Capture and storage: Sleipner West http://www.statoil.com/en/technologyinnovation/newenergy/co2management/pages/sleipnervest.aspx

Statoil (Accessed 2013) Statoil operated fields in Norway: The Sleipner area. UtsiraBasin http://www.statoil.com/en/ouroperations/explorationprod/ncs/sleipner/pages/default.aspx

Stolaroff, J.K., Lowry, G.V., Keith, D.W. (2005) Using CaO-and MgO-rich industrial waste streams for carbon sequestration. *Energy Conversion and Management*, 46 (5) p. 687-699.

Stern, N. (2007) *Stern Review: The Economics of Climate Change*. HM Treasury, London

Sundquist, E.T. and Broecker, W.S. (1985) *The carbon cycle and atmospheric CO2: Natural variations Archean to present* (Vol. 32, pp. 1-627). American Geophysical Union.

Swart, P.K., Lohmann, K.C., McKenzie, J., Savin, S. (1993) *Climate change in continental isotopic records* (Vol. 78, pp. 1-374). American Geophysical Union.

Taylor, A.S., Blum, J.D., & Lasaga, A.C. (2000) The dependence of labradorite dissolution and Sr isotope release rates on solution saturation state. *Geochimica et Cosmochimica Acta*, *64* (14) p. 2389-2400.

Taylor, D. (CABE) (2008) *Public space lessons Land in limbo: making the best use of vacant urban spaces CABE Space 2008*. PDF Retrieved from http://www.cabe.org.uk/publications/land-in-limbo.

Terraconsult Factual Report on 2004/2005 Ground Investigation April 2005

Thom, J.G.M., Dipple, G.M., Power, I.M., Harrison, A.L. (2013) Chrysotile dissolution rates: Implications for carbon sequestration. *Applied Geochemistry*, 35 p. 244-254.

Tossavainen, M., Engstrom, F., Yang, Q., Menad, N., Lidstrom Larsson, M., Bjorkman, B. (2007) Characteristics of steel slag under different cooling conditions. *Waste management*, *27*(10), 1335-1344.

UK Parliament (2013) Companies Act 2006 (Strategic Report and Directors' Report) Regulations 2013

UK Parliament. (2012) The Waste (England and Wales)(Amendment) Regulations 2012

UK Parliament (2008) Climate Change Act 2008

UK Parliament (2006) The Contaminated Land (England) Regulations 2006

UKCCSC (Accessed 2013) The UK Carbon Capture and Storage Research Centre http://www.ukccsrc.ac.uk/

UKCIP (Accessed 2013) (United Kingdom Climate Impacts Programme) (2002) http://www.ukcip.org.uk/

UN (2009) World Urbanization Prospects: The 2009 Revision, United Nations Department of Economic and Social Affairs Population Division.

UNFCCC (2013) COP19 http://unfccc.int/2860.php#decisions (Accessed 2013)

UNFCCC (1997) Kyoto Protocol to the United Nations Framework Convention on Climate Change adopted at COP3 in Kyoto, Japan, on 11 December 1997

UNFCCC (Accessed 2013) United Nations Framework Convention on Climate Change 1992 http://unfccc.int/

Urey, H.C. (1952) On the early chemical history of the earth and the origin of life. *Proceedings of the National Academy of Sciences of the United States of America*, 38 (4) p. 351.

Usdowski, E. and Hoefs, J. (1986) $^{13}C/^{12}C$ partitioning and kinetics of CO_2 absorption by hydroxide buffer solutions. *Earth and Planetary Science Letters*, 80 (1–2) p. 130-134.

USGS (2012) *Mineral Commodity Summary 2012*

USGS (2011) *Mineral Commodity Summary 2011*

USGS (2010) *Mineral Commodity Summary 2010*

USGS (2009) *Mineral Commodity Summary 2009*

USGS (2008) *Mineral Commodity Summary 2008*

van Breemen, N., Finlay, R., Lundström, U., Jongmans, A.G., Giesler, R., Olsson, M. (2000) Mycorrhizal weathering: A true case of mineral plant nutrition? *Biogeochemistry*, *49* (1) p. 53-67.

van den Berg, G.A., Loch, J.P.G. (2000) Decalcification of soils subject to periodic waterlogging. *European Journal of Soil Science* 51 (1) p. 27–33

van Hees, P.A., Jones, D.L., Godbold, D.L. (2002) Biodegradation of low molecular weight organic acids in coniferous forest podzolic soils. *Soil Biology and Biochemistry*, 34 (9) p. 1261-1272.

van Oss, H. and Padovani, A.C. (2002) Cement manufacture and the environment. *Journal of Industrial Ecology*, 6 (1) p. 89-106.

van Zomeren, A., Van der Laan, S.R., Kobesen, H., Huijgen, W.J., Comans, R.N. (2011) Changes in mineralogical and leaching properties of converter steel slag resulting from accelerated carbonation at low CO_2 pressure. *Waste Management,* 31 (11) p. 2236–2244

Velbel, M.A. (1993) Constancy of silicate-mineral weathering-rate ratios between natural and experimental weathering: Implications for hydrologic control of differences in absolute rates. *Chemical Geology*, 105 (1) p. 89-99.

Wang, Y., Li, Y., Ye, X., Chu, Y., Wang, X. (2010) Profile storage of organic/inorganic carbon in soil: From forest to desert, *Science of The Total Environment*, 408 (8) p. 1925-1931.

Washbourne, C-L., Renforth, P., Manning, D.A.C. (2012) Investigating carbonate formation in urban soils as a method for atmospheric carbon capture and storage. *Science of the total environment,* 431 p. 166-175.

Washbourne, C-L. (2009) *Ground Engineering using 'waste' materials*. MSc thesis. Newcastle University

Welch, S.A., & Ullman, W.J. (1996) Feldspar dissolution in acidic and organic solutions: Compositional and pH dependence of dissolution rate. *Geochimica et Cosmochimica Acta*, 60 (16) p. 2939-2948.

Welch, S.A., & Ullman, W.J. (1993). The effect of organic acids on plagioclase dissolution rates and stoichiometry. *Geochimica et Cosmochimica Acta*, 57 (12) p. 2725-2736.

White, A.F., & Brantley, S.L. (2003) The effect of time on the weathering of silicate minerals: why do weathering rates differ in the laboratory and field? Controls on Chemical Weathering. *Chemical Geology,* 202 (3–4) 30 p. 479–506

White, A.F. (2003) Natural weathering rates of silicate minerals. *Treatise on Geochemistry,* 5 p. 133-168.

White, A.F., Blum, A.E., Schulz, M.S., Bullen, T.D., Harden, J.W., & Peterson, M.L. (1996) Chemical weathering rates of a soil chronosequence on granitic alluvium: I. Quantification of mineralogical and surface area changes and calculation of primary silicate reaction rates. *Geochimica et Cosmochimica Acta*, 60 (14) p. 2533-2550.

White, A.F., & Brantley, S.L. (1995) *Chemical Weathering Rates of Silicate Minerals*. Mineralogical Society of America

Wilson, S., Dipple, G., Power, I., Fallon, S., Southam, G., Barker, S. (2011) Subarctic weathering of mineral wastes provides a sink for atmospheric CO_2, *Environmental Science & Technology*, 45 (18) p. 7727-7736.

Wilson, S., Barker, S., Dipple, G., Atudorel, V. (2010) Isotopic disequilibrium during uptake of atmospheric CO_2 into mine process waters: Implications for CO_2 sequestration, *Environmental Science & Technology*, 44 (24) p. 9522-9529.

Wilson, S.A., Dipple, G.M., Power, I.M., & Thom, J.M. Anderson., R.G., Raudsepp, M., Gabites, J.E. and Southam, G. (2009) Carbon dioxide fixation within mine waste of ultramafic-hosted ore deposits: Examples from the Clinton Creek and Cassiarchrysotile deposits, Canada. *Economic Geology*, 104 p. 95-112.

Worrell, E., Price, L., Martin, N., Hendriks, C., Meida, L.O. (2001) Carbon dioxide emissions from the global cement industry 1. *Annual Review of Energy and the Environment*, 26 (1) p. 303-329.

WRAP (2001) Waste and Resources Action Programme (WRAP) http://www.wrap.org.uk/ (Accessed 2013)

Wright, V.P., & Tucker, M.E. (eds.). (1991). *Calcretes (Vol. 2).* Wiley-Blackwell.

Yaalon, D.H., Yaron, B. (1966) Framework for man-made soil changes-an outline of metapedogenesis. *Soil Science,* 102 p. 272-277.

APPENDICES

APPENDIX A – ANALYTICAL METHODS

A.1 Atomic absorption spectroscopy (AAS)

Principle of method

Analysis of a range of metals in solution was carried out using AAS analysis at Newcastle University. Samples were passed through a flame atomiser, using a lamp and detector to quantify the presence of Ca, Mg, Fe, Na and K by determining the absorbance value through the flame.

Apparatus

Varian SpectrAA 400 atomic absorption spectrometer
Acetylene bottle with connectors
Volumetric flasks
Sterilin sample containers (20ml)
Pipettes and pipette tips (1ml and 5ml)

Reagents

Lanthanum chloride
Deionised water venting bottle
Concentration stock solutions for standards

Sample preparation

Samples were filtered prior to analysis using 0.2µm syringe filters and acidified to <pH 3 with concentrated nitric acid

Quality control

Apparatus was frequently calibrated using standards, freshly made from 1000 mg l^{-1} stock solutions. For Ca these standards ranged from 0 mg l^{-1} to 25mg l^{-1}, setting these values as the accurate detection range. (Stock solutions were also spiked with lanthanum chloride prior to use)

Procedure

All samples were diluted in volumetric flasks to within the calibration range

All samples were spiked with 0.1 % lanthanum chloride (which acts as an accelerant)

Samples were run through the AAS apparatus in an air-acetylene mix using a pre-determined computer programme which set flow rates and other experimental parameters for the material of interest

Between sample runs the apparatus was flushed with dilute nitric acid solution to avoid carry-over between samples.

Repeatability

Triplicate determinations were carried out every 5 samples.

A.2 BET surface analysis (University of Reading)

Principle of method

BET analysis investigates the specific surface area of materials by the adsorption of nitrogen as a function of pressure, with respect to parameters determined by Brunauer et al (1938). The technique assessed the external area and internal pore area of samples to derive a value for total specific surface area.

Apparatus

Micromeritics Gemini 2370 Surface Area Analyser

Sample preparation

Samples supplied moist or agglomerate require a pre-treatment. Prior to analysis these samples are dried at 35C in order to remove moisture without altering the physical propriety of the material. The dried material obtained was then gently press in order to disperse the agglomerate particles.

Procedure

The Gemini surface area analyser uses a flowing gas technique in which the analysis gas flows into a tube containing the sample and into a balance tube, at the same time. The internal volume and the temperature surrounding both tubes are maintained at identical conditions. The only difference is the presence of the sample in the sample tube.

The Gemini requires only pure nitrogen as the analysis gas, even for low surface area samples. Helium is used for free space measurement to determine any slight differences in volume between the balance tube and the sample tube. From this information, the Gemini automatically compensates for these small differences in calculating analysis results.

Samples must be free of moisture and other contaminants before analysis. This is achieved by use of a degassing machine, the Micromeritics FlowPrep 060, in which the

sample is maintained overnight at a pre-set temperature (usually 60°C) in a flow of nitrogen.

The sample and balance tubes are immersed in a single liquid nitrogen bath which maintains isothermal conditions for both tubes.

The analysis gas is then delivered to the sample tube by a servo valve mechanism. The delivery rate of analysis gas flow into the balance tube is controlled by another servo valve connected to a differential pressure transducer.

This differential pressure transducer measures the pressure imbalance between the sample and balance tubes, which is caused by the adsorption of the analysis gas onto the sample.

As the sample adsorbs analysis gas, the pressure drops in the sample tube. The servo valve continuously restores the pressure balance between the two tubes by admitting more gas into the sample tube.

The end result is that the Gemini maintains a constant pressure of analysis gas over the sample while varying the rate of analysis gas delivery to exactly match the rate at which the sample can adsorb the gas.

Calculation

Typically, five data points are collected and a BET (Brunauer et al, 1938) transformation is calculated for each point as follows:

$$B_I = \frac{Prel_I}{(1.0 - Prel_I)(Nads_I)}$$

where B_I = units of g/cm^3

$Prel_I$ = relative pressure adsorbed after equilibrating I^{th} dose (cm^3 STP)

$Nads_I$ = amount of gas

A least-squares fit is performed on the (B_I, $Prel_I$) designated pairs where B is the dependent variable and $Prel_I$ is the independent variable. The following are calculated: slope, y-intercept, error of the slope, error of the y-intercept, and the correlation coefficient. Using the results of these calculations, the BET surface area (in units of m^2/g) can be obtained:

$$SA_{BET} = \frac{(CSA)(6.023 \times 10^{23})}{(22414\,cm^3\ STP)(10^{18}\,nm^2/m^2)(S + Y_{INT})}$$

where CSA = analysis gas cross-sectional area (nm^2)

S = slope (g/cm^3 STP)

Y_{INT} = y-intercept (g/cm^3 STP)

References

Brunauer, S., Emmett, P.H. and Teller, E. (1938) *J. Am. Chem. Soc.* ***60***, 309

A.3 Calcimeter analysis: carbonate

Principle of method

Approximately 0.5g-1.0g of sample was added to a conical flask and acidified with 4.0 M hydrochloric acid. The CO_2 evolved was measured using a burette, and converted to a value for carbonate content based on calibrated values using reagent grade calcium carbonate.

Apparatus

Eijkelkamp calcimeter
Proprietary calcimeter reagent tubes
Conical flasks (150ml)
Plastic tongs
20ml Measuring cylinder
Deionised water bottle
Pipette (10ml) and pipette filler
Balance, readable to ± 0.0001 g, Mettler AE 163, calibrated

Reagents

Calcium carbonate (powder: reagent grade)
4.0 M Hydrochloric acid

Sample preparation

Soil samples were prepared by hand crushing, with the use of a pestle and mortar Samples were sieved to a maximum particle size of 2mm. Samples were returned to dry, labelled containers

Quality control

Analyse a portion of Inorganic Laboratory Reference Soil

Procedure

Calcimeter equipment was calibrated with the use of two suites of blanks and two suites of control samples, both containing the same known volume of water (20ml):

Blanks: Burette readings starting at 20ml and 80ml marks respectively, reacting with 7ml of hydrochloric acid

Controls: Containing a known mass of calcium carbonate, 0.2g and 0.4g, reacting with 7ml of hydrochloric acid.

Approximately 1g of sample were weighed in to a weighing boat (or ≤0.5g if the sample is expected to be very high in carbonate)

The sample was poured in to a clean conical flask, and mixed with 20ml of de-ionised water

7ml of 4mol/l hydrochloric acid was measured in to a reaction vessel, which was lowered in to the conical flask with the use of tweezers, taking care to avoid premature mixing of solutions

With the measuring burette taps open, the bungs connected to the inlet tubes of the calcimeter were wetted and fitted securely to the necks of the conical flasks

The measuring burette was set to a value of 3ml, and the taps set to the closed 'measuring' position.

In turn, each flask was tipped and agitated so that hydrochloric acid from the reaction vessel entered the soil sample solution.

The buffer vessel was moved down the slider in response to any gas emitted, so that the water level in the measuring burette and the top of the buffer vessel did not differ by more than 3ml at any point

Readings were taken from the burette at 10 minutes, 20 minute and 30 minutes from the initiation of the reaction

All waste solutions were disposed to a designated waste bottle. Equipment was cleaned using de-ionised water and dried in heated drying cabinets.

Sample data was analysed to determine the presence of calcium carbonate as a percentage of the bulk weight of each sample

Repeatability

Reproducibility was determined experimentally by the analysis of repeat samples (usually one for every 5 analysed), in order to assess the homogeneity of the sample

Equipment error was calculated by the comparison of blank calibration runs

References

BS 7755-3.10:1995 ISO 10693:1995: Soil quality. Chemical methods: Determination of carbonate content. Volumetric method

A.4 Electrical conductivity

Principle of method

Electrical conductivity (EC) of solutions (as a proxy for the concentration of dissolved salts and other species) was carried out using a calibrated EC meter.

Apparatus

VWR International EC300 Conductivity meter
Deionised water venting bottle

Reagents

Standards (210 and 670 μS)

Quality control

Analysis was carried out in duplicate on all samples.

Procedure

Conductivity meter was rinsed with deionised water and dried

The meter was introduced to the solution bottle and gently agitated

Once the meter reading had stabilised it was recorded and the process repeated for all other samples.

A.5 Environmental scanning electron microscopy

Principle of method

Thin sections prepared from steel slag were analysed for surface and structural features using an environmental scanning electron microscope at Newcastle University.

Apparatus

FEI/Phillips XL-30 field emission environmental scanning electron microscope

Sample preparation

24 x 48 mm polished thin sections were prepared at Edinburgh University.

Procedure

The microscope was operated at room temperature, under a low vacuum,

Characteristic X-ray spectra were determined using X-ray photoelectron spectroscopy.

A.6 Isotope ratio mass spectrometry (Iso-Analytical)

Principle of method

Gas evolved from acid digestion of carbonates in soil samples analysed for stable isotope values for C and O by Europa Scientific 20-20 continuous-flow isotope ratio mass spectrometer (IRMS) (Iso-Analytical, Cheshire UK)

Apparatus

Europa Scientific 20-20 continuous-flow isotope ratio mass spectrometer

Reagents

Phosphoric acid.

The phosphoric acid used for digestion had been prepared for isotopic analysis in accordance with Coplen *et al.* (1983) Nature, **302**, 236-238, was injected through the septum into the vials.

Sample preparation

Use air-dried soil, crushed to pass through a 63 μm sieve.

Quality control

The reference material used during analysis was IA-R022 (Iso-Analytical working standard calcium carbonate, $\delta^{13}C_{V\text{-}PDB}$ = -28.63 ‰ and $\delta^{18}O_{V\text{-}PDB}$ = -22.69 ‰). IA-R022, NBS-18 (carbonatite, $\delta^{13}C_{V\text{-}PDB}$ = -5.01 ‰ and $\delta^{18}O_{V\text{-}PDB}$ = -23.2 ‰) and NBS-19 (limestone, $\delta^{13}C_{V\text{-}PDB}$ = +1.95 ‰ and $\delta^{18}O_{V\text{-}PDB}$ = -2.2 ‰) were run as quality control check samples during analysis of your samples.

NBS-18 and NBS-19 are inter-laboratory comparison standard distributed by the International Atomic Energy Agency (IAEA). IA-R022 has been calibrated against and is traceable to NBS-18 and NBS-19.

Procedure

Samples were weighed into clean Exetainer™ tubes and the tubes placed in a drying oven for 24 hours to remove moisture. Once the samples were dry, septum caps were fitted to the tubes. The tubes were then flushed with 99.995 % helium. Then phosphoric acid was injected to the samples and they were allowed to react in the acid overnight to allow conversion to CO_2.

The CO_2 gas liberated from samples was then analysed by Continuous Flow-Isotope Ratio Mass Spectrometry (CF-IRMS). Carbon dioxide was sampled from the Exetainer™ tubes into a continuously flowing He stream using a double holed needle.

The CO_2 was resolved on a packed column gas chromatograph and the resultant chromatographic peak carried forward into the ion source of a Europa Scientific 20-20 IRMS where it is ionised and accelerated. Gas species of different mass are separated in a magnetic field then simultaneously measured using a Faraday cup collector array to measure the isotopomers of CO_2 at m/z 44, 45, and 46.

Repeatability

Repeat analyses were run in duplicate every 5-10 samples

References

Coplen *et al.* (1983) Nature, **302**, 236-238,

A.7 Isotope ratio mass spectrometry (University of Oxford)

Principle of method

Gas evolved from acid digestion of carbonates in soil samples analysed using a Delta V Advantage isotope mass spectrometer fitted with a Kiel IV carbonate device and a Gas Bench II

The relative $^{18}O/^{16}O$ values ($\delta^{18}O$) and 13C/12C values ($\delta^{13}C$) of carbonate are expressed in per mil relative to

Apparatus

Delta V Advantage isotope mass spectrometer fitted with a Kiel IV carbonate device and a Gas Bench II

Reagents

Phosphoric acid.

Sample preparation

Use air-dried soil, crushed to pass through a 63 μm sieve.

Quality control

External error (0.08permil, n = 62) is calculated from repeat measurements of NBS-18 and NBS-19. We assume that the phosphoric acid–carbonate fractionation is the same for NBS-19 and our calcite samples (Coplen, 1996).

Procedure

The Kiel device converted the carbonates to CO_2 with 100% H_3PO_4 (McCrea, 1950).

The CO_2 gas liberated from samples was then analysed by Isotope Ratio Mass Spectrometry

Repeatability

Repeat analyses were run in duplicate every 5-10 samples

References

McCrea, J. M. (1950). On the isotopic chemistry of carbonates and a paleotemperature scale. *The Journal of Chemical Physics*, *18*, 849.

Coplen, T. B. (1996). New guidelines for reporting stable hydrogen, carbon, and oxygen isotope-ratio data. *Geochimica et Cosmochimica Acta*, *60*, 3359-3360.

A.8 Optical light microscopy

Principle of method

Thin sections prepared from steel slag were analysed using an optical petrographic microscope at Newcastle University to determine structure and mineralogy

Apparatus

Phillips optical petrographic microscope

Sample preparation

24 x 48 mm polished thin sections were prepared at Edinburgh University.

Procedure

Polished thin sections were observed in normal and plane polarised light conditions to investigate their structure and mineralogy.

A.9 Soil analysis - determination of pH-H_2O

Principle of method

5 mL soil was shaken with 25 mL water for 15 minutes. The soil-water suspension was then left to equilibrate for between 2 and 24 hours. The pH-H_2O of the suspension was measured using a pH electrode and meter, which have been calibrated using standard buffer solutions.

Apparatus

Sample bottles were rinsed several times with deionised water and dried, before use.

5 mL scoop
Spatula
60 mL, wide mouth, polypropylene bottles
30 mL, bottle top dispenser, set to deliver 25 mL
Orbital shaker, IKA KS 500
Timer, calibrated, Fisherbrand serial no. 61573216
pH meter, Jenway 3020, calibrated as described in Method I002
pH electrode, VWR 662-1761, combination with BNC connector
Temperature probe

Reagents

Water, 15MΩ.cm
Sample preparation

Air-dried soil, crushed to pass through a 2 mm sieve.

Quality control

Analyse a portion of Inorganic Laboratory Reference Soil.

Procedure

The scoop was filled with sample.

Excess sample was removed by scraping the spatula across the top of the scoop.

Soil was transferred into a 60 mL bottle.

25 mL of deionised water was added and the bottle was stoppered.

The bottle was placed in a horizontal position on the orbital shaker.

The shaker speed was set at 275 ± 10 revs per minute and the shaker started and allowed to run for 15 minutes.

Bottles were removed from the shaker and allowed to stand for at least 2 hours, but not longer than 24 hours, before measuring the pH-H_2O.

The pH meter and electrode were calibrated using buffer solutions at pH 4, 7 and 10.

The pH-H_2O of the reference soils was measured, and checked to ensure it was within the limits stated.

Sample suspensions were shaken thoroughly before pH-H_2O.measurement and the pH measured in the settling suspension.

Readings were allowed to stabilise and recorded to two decimal places.

The pH electrode was rinsed thoroughly with deionised water and dried prior to each new analysis.

Calibration of the pH meter was checked after every 10 samples.

Repeatability

The results of duplicate determinations should be within the limits stated below.

pH range	Acceptable variation
$pH \leq 7.00$	0.15
$7.00 < pH < 7.50$	0.20
$7.50 \leq pH \leq 8.00$	0.30
$pH > 8.00$	0.40

References

BS7755, Section 3.2, 1995; ISO 10390, 1994; Soil Quality, Part 3, Chemical Methods, Section 3.2, Determination of pH.

A.10 Thermogravimetric - differential scanning calorimetry – quadrupole mass spectrometry

Principle of method

Samples were analysed using thermogravimetry and differential scanning calorimetry, combined with mass spectrometry of the gas evolved during thermal decomposition to determine mass change and presence of indicative species.

Apparatus

Netzsch Jupiter STA449C TG-DSC system connected to a Netzsch Aeolos 403C QMS
Pestle and mortar
Alumina crucible
Balance, readable to ± 0.1 mg, calibrated

Sample preparation

Samples were ground to a fine powder using an agate pestle and mortar (or passed through a 63µm sieve).

Procedure

A subsample (ca. 75mg) was accurately weighed into an alumina crucible and analysed using a Netzsch Jupiter STA449C TG-DSC (thermogravimetry-differential scanning calorimetry) system connected to a Netzsch Aeolos 403C quadrupole mass spectrometer (QMS) for the mass spectral analysis of evolved gas.

Samples were heated from 30°C to 1000°C at a rate of 10°C min^{-1} in an atmosphere of 80% He + 20% O_2 (purge gas, flow rate 30 ml min^{-1}). The protective gas was helium (flow rate 30 ml min^{-1}). Adapter heads and transfer lines were heated at 150°C and 300°C, respectively.

TG and DSC data were acquired and processed using the Netzsch TA4 Proteus Analysis software.

The QMS was operated in full scan mode over the range m/z 10-300, and mass spectrometric data were acquired and processed using Quadstar 422 IPI software.

Quantitative data for the abundance of selected ions in the evolved gas during heating was converted to ASCII format and subsequently into Excel.

A.11 Total carbon analysis: Leco

Principle of method

Approximately 0.1 g sample was ignited in a stream of oxygen, oxidising carbon to carbon dioxide, and sulphur to sulphur dioxide. The CO_2 and SO_2 produced were quantified by infra-red detection, using a Leco Carbon/Sulphur Analyser, previously calibrated with a standard reference soil, of known carbon and sulphur concentration.

Apparatus

Crucibles, Leco part no. 528-018
Crucible tray
Crucible tongs
Balance, readable to ± 0.0001 g, Mettler AE 163, calibrated
Aluminium foil

Reagents

Iron chip accelerator, Leco part no. 501-077
Lecocell II accelerator, Leco part no. 763-266

Sample preparation

Use air-dried soil, crushed to pass through a 0.5 mm sieve.

Quality control

Analyse a portion of Inorganic Laboratory Reference Soil No. 1.

Procedure

At least 2 replicate determinations should be performed.

The sample should be thoroughly mixed by shaking the sample container for 5 minutes, and then left to settle for 2 minutes.

A crucible was placed onto the balance pan.

Tare was pressed, to set the display to zero.

Approximately 0.1 g of sample was weighed into the crucible.

The weight of sample was recorded to the nearest 0.1 mg.

The crucible was placed on the crucible tray.

The position number of the crucible on the tray was recorded.

To prevent contamination of the samples, the tray was covered with aluminium foil.

The Leco CS244 Carbon/Sulphur Analyser was calibrated, using a Carbon/Sulphur standard soil, using a minimum of 5 standards.

A scoopful of both accelerators was added to the crucibles.

The total carbon and sulphur content of the reference soil was measured

The carbon/sulphur readings were checked, to ensure they were within the tolerances stated for the reference soil.

The total carbon and sulphur content of the samples was measured.

A Carbon/Sulphur standard soil was analysed after every 5 samples.

The carbon/sulphur readings were checked to ensure they were within the tolerances stated for the Carbon/Sulphur standard soil.

Calculation

Carbon/sulphur content was calculated to an oven dry basis:

$$\text{Total carbon/sulphur, \%} = \frac{C}{D}$$

where

C is the measured Carbon/Sulphur concentration

D is the dry matter factor, determined as described in Method S002.

Repeatability

The results of duplicate determinations should be within the limits stated overleaf.

Carbon content %		Acceptable variation
Greater than	Up to and including	
0.0	0.25	0.025 % absolute
0.25	7.50	10% relative
7.50		0.75 % absolute

References

BS7755, Section 3.8, 1995; ISO 10694, 1995; Soil Quality, Part 3, Chemical Methods, Section 3.8, Determination of organic carbon and total carbon after dry combustion (elementary analysis)

A.12 Total carbon analysis solutions: total carbon analyser

Principle of method

Total and inorganic carbon in solution were measured separately. Total carbon was analysed by injecting an aliquot of sample in to a furnace which converts all carbon in the sample to carbon dioxide to be quantified by an infra-red detector. Inorganic Carbon (IC) was measured using interactions with an acidic medium to produce carbon dioxide for detection.

Apparatus

Shimadzu TOC 5050A Total Carbon Analyser
Square glass vials (5ml)

Reagents

Deionised water
Standards (inorganic: 2.5ppm, organic 25ppm)

Sample preparation

All samples were filtered using a 0.2μm cellulose nitrate filter.

Quality control

Standards were run around the expected analytical range of the samples. Blanks are run to detect any carry-over of samples.

Procedure

Samples were decanted in to labelled glass vials
Vials were loaded in to auto-sampler apparatus
Auto-analysis run was carried out

Repeatability

1 sample in 5 run in duplicate.

A.13 Total organic carbon analysis (removal of carbonates): Leco

Principle of method

Approximately 0.1 g of sample, in a porous crucible, was treated with sufficient hydrochloric acid, 4 mol/L, to remove carbonates. After the acid had drained from the crucible, the crucible and sample were dried overnight at 65°C. The organic carbon was determined.

Apparatus

Filtering/porous crucibles, Sci-Lab part no. AR8028
Crucible tray(s)
Crucible tongs
Balance, readable to ± 0.1 mg, calibrated
Pipette, 10 mL graduated in 0.1 mL divisions
Laboratory Oven No. 2, set at 65°C ± 5°C
Aluminium foil

Reagents

Hydrochloric acid, 4.0 mol/L

Sample preparation

Use air-dried soil, crushed to pass through a 0.5 mm sieve.

Quality control

Analyse a portion of Inorganic Laboratory Reference Soil No. S003.
Use approximately 0.1 g for analysis

Procedure

Carry out a method blank determination.

A crucible was placed onto the balance pan.

Tare was pressed, to set the display to zero.

Approximately 0.1 g of sample was weighed into the crucible.

The weight of sample was recorded to the nearest 0.1 mg.

The crucible was placed on the crucible tray.

The position number of the crucible on the tray was recorded.

Steps 1 to 6 were repeated for each sample.

For the Method Blank determination, an empty crucible was placed on the crucible tray.

The position number of the crucible on the tray was recorded.

The weight of "Method Blank" was recorded as 0.1000 g.

The crucibles were removed from the tray and placed in the well of a fume cupboard.

1.0 mL of hydrochloric acid 4.0 mol/L was added to each crucible.

Acid was allowed to drain from the crucible for a minimum of 4 hours.

The crucibles were placed on the crucible tray, making sure that they were in their original positions.

The crucible tray was placed in the oven at 65°C and left for 16-24 hours

The crucible tray was removed from the oven.

To prevent contamination or loss of sample, the crucible tray was covered with aluminium foil until the samples are analysed. The crucibles were allowed to cool.

The Leco CS244 Carbon/Sulphur Analyser was calibrated using a minimum of 5 standards.

The organic carbon content of Reference Soil No. S003 was measured and recorded

The organic carbon content of the method blank was measured and recorded

Checks were made to ensure that the organic carbon value of Reference Soil No.S003 were within the limits stated.

Calculation

The organic carbon content is calculated as follows:

$$\text{Organic Carbon, \%} = C_s - C_{bl}$$

where
C_s is the measured carbon percentage of the sample
C_{bl} is the measured carbon percentage of the blank

To calculate the organic carbon content to an oven dry basis:

$$\text{Organic Carbon, \%} = \frac{C_s - C_{bl}}{D}$$

Where: D is the dry matter factor, determined as described in Method S002.

Repeatability

The results of duplicate determinations should be within the limits stated below.

Carbon content %		Acceptable variation
Greater than	Up to and including	
0.0	0.25	0.025 % absolute
0.25	7.50	10% relative
7.50		0.75 % absolute

References

BS7755, Section 3.8, 1995; ISO 10694, 1995; Soil Quality, Part 3, Chemical Methods, Section 3.8, Determination of organic carbon and total carbon after dry combustion (elementary analysis)

Leco Corporation, Instruction Manual CS 244

Method I003 - Instrument Operation – Calibration of Leco CS244 Carbon - Sulphur Analyser

Method I004 - Instrument Operation – Operation of Leco CS244 Carbon - Sulphur Analyser

A.14 X-ray diffraction (XRD)

Principle of method

XRD analysis was conducted at Newcastle University. A multipurpose diffractometer was used to identify likely mineral phases present in samples.

Apparatus

PANalytical X'Pert Pro Multipurpose Diffractometer

Sample preparation

Samples were air-dried and crushed to pass through a 63 μm sieve.

Procedure

XRD analysis was carried using a PANalytical X'Pert Pro Multipurpose Diffractometer fitted with an X'Celerator and a secondary monochromator, operating with a Cu anode at 40 kV and 40 mA. Spectra were acquired for Cu Kα (λ = 1.54180 Å) or Cu Kα1 (λ = 1.54060 Å) radiation over 2-70°2θ with a nominal step size of 0.0167°2θ and time per step of 100 or 150 seconds. Scans were carried out in continuous mode using the X'Celerator RTMS detector.

Data were analyses using proprietary software, including PANalytical X'Pert Data Viewer

A.15 X-ray fluorescence (XRF)

Principle of method

XRF analysis was conducted at the University of Leicester, Department of Geology using a PANalytical Axios Advanced XRF spectrometer. Samples were reported as total oxides, to illustrate their relative chemical compositions.

Apparatus

PANalytical Axios Advanced XRF spectrometer

Sample preparation

Samples were air-dried and crushed to pass through a 63 μm sieve.

Quality control

The XRF machine was calibrated using a range of certified standards, including British Chemical Standards (BCS) BCS375 (sodium feldspar), BCS376 (potassium feldspar) and BCS372/1 (hydrated cement).

Procedure

Powdered samples were mixed with 1:5 ratio of flux (80% lithium metaborate, 20% lithium tetraborate).

The samples and flux were ignited at 1100 °C and cast into fused beads.

Fused beads were run through XRF, data was collected and received in report format.

Repeatability

Duplicate determinations were carried out every 5-10 samples

APPENDIX B – ADDITIONAL DATA: CHAPTER 3

B.1 Batch weathering

Table B.1 - Batch setup matrix

Ref	Material	Particle Size	Approx. starting concentration (mg l^{-1})	Conditions
B1A	Steel slag	<63µm	100	Low conc.
B1B	Steel slag	<63µm	1000	-
B1C	Wollastonite	<63µm	100	Low conc.
B1D	C&D waste	<63µm	100	Low conc.
B1E	Dolerite	<63µm	100	Low conc.
B2A	Steel slag	<2mm	1000	Particle size
B2B	C&D	<2mm	1000	Particle size
B3A	C&D	<63µm	1000	Addition of carbonate (Evian)
B3B	Steel slag	<63µm	1000	Addition of carbonate (Evian)
B4A	Steel slag	<63µm	1000	Agitation
B4B	C&D	<63µm	1000	Agitation

Table B.2 - Batch sampling schedule

	Time (hours)										
	1	**2**	**3**	**4**	**5**	**12**	**24**	**48**	**72**	**96**	**144**
B1A	✓	✓	✓	✓	✓	✓	✓	✓	✓	✓	✓
B1B	✓	✓	✓	✓	✓	✓	✓	✓	✓	✓	✓
B1C	✓	✓	✓	✓	✓	✓	✓	✓	✓	✓	✓
B1D	✓	✓	✓	✓	✓	✓	✓	✓	✓	✓	✓
B1E	✓	✓	✓	✓	✓	✓	✓	✓	✓	✓	✓
B2A	✓	✓	✓	✓	✓	✓	✓	✓	✓	✓	✓
B2B	✓	✓	✓	✓	✓	✓	✓	✓	✓	✓	✓
B3A	✓	✓	✓	✓	✓	✓	✓	✓	✓	✓	✓
B3B	✓	✓	✓	✓	✓	✓	✓	✓	✓	✓	✓
B4A	✓	✓	✓	✓	✓	✓	✓	✓	✓	✓	✓
B4B	✓	✓	✓	✓	✓	✓	✓	✓	✓	✓	✓

Table B.3 - Batch data B1A

Elapsed (sec)	**Starting mass (mg)**	**Ca (mg l^{-1})**	**Rate (mol Ca m^{-2} sec^{-1})**
3600	2.8	9.47	-9.39
7200	2.0	10.18	-9.52
10800	2.5	9.82	-9.81
14400	2.1	10.00	-9.85
18000	2.2	11.24	-9.91
43200	2.1	12.09	-10.24
86400	2.2	15.33	-10.46
172800	2.7	17.30	-10.80
259200	2.5	19.34	-10.89
345600	2.0	18.55	-10.94
518400	2.7	25.74	-11.10

Table B.4 - Batch data B1B

Elapsed (sec)	**Starting mass (mg)**	**Ca (mg l^{-1})**	**Rate (mol Ca m^{-2} sec^{-1})**
3600	19.9	40.80	-9.61
7200	20.2	43.00	-9.90
10800	21.4	47.10	-10.06
14400	19.8	44.40	-10.17
18000	21.3	50.80	-10.24
43200	19.9	48.80	-10.61
86400	21.3	51.50	-10.92
172800	20.3	52.50	-11.19
259200	20.9	58.80	-11.33
345600	20.2	65.80	-11.39
518400	20.5	61.40	-11.61

Table B.5 - Batch data B1C

Elapsed (sec)	**Starting mass (mg)**	**Ca (mg l^{-1})**	**Rate (mol Ca m^{-2} sec^{-1})**
3600	2.4	1.16	-9.82
7200	2.1	0.99	-10.13
10800	2.8	1.40	-10.28
14400	2.3	1.33	-10.34
18000	2.3	1.36	-10.43
43200	2.1	1.74	-10.66
86400	2.4	2.38	-10.89
172800	2.1	2.06	-11.19
259200	2.6	2.76	-11.33
345600	2.2	3.05	-11.34
518400	2.8	3.80	-11.53

Table B.6 - Batch data B1D

Elapsed (sec)	**Starting mass (mg)**	**Ca (mg l^{-1})**	**Rate (mol Ca m^{-2} sec^{-1})**
3600	2.0	6.11	-10.09
7200	2.4	6.30	-10.45
10800	2.0	6.56	-10.53
14400	2.5	6.62	-10.75
18000	2.6	6.28	-10.89
43200	2.0	6.15	-11.16
86400	2.6	6.95	-11.53
172800	2.4	7.78	-11.74
259200	2.6	7.80	-11.95
345600	2.2	6.91	-12.06
518400	2.9	8.44	-12.27

Table B.7 - Batch data B1E

Elapsed (sec)	**Starting mass (mg)**	**Ca (mg l^{-1})**	**Rate (mol Ca m^{-2} sec^{-1})**
3600	2.2	0.62	-10.82
7200	2.6	0.84	-11.07
10800	2.3	0.76	-11.23
14400	2.6	0.84	-11.37
18000	2.4	0.72	-11.50
43200	2.4	0.80	-11.83
86400	2.1	0.80	-12.07
172800	2.8	1.00	-12.40
259200	2.2	0.91	-12.51
345600	2.1	1.05	-12.56
518400	2.6	1.66	-12.62

Table B.8 - Batch data B2A

Elapsed (sec)	**Starting mass (mg)**	**Ca (mg l^{-1})**	**Rate (mol Ca m^{-2} sec^{-1})**
3600	21.5	1.32	-
7200	19.8	0.66	-
10800	19.4	1.80	-
14400	20.4	1.12	-
18000	25.1	3.27	-
43200	23.5	2.07	-
86400	21.2	8.38	-
172800	20.6	6.40	-
259200	24.2	8.89	-
345600	21.1	7.38	-
518400	23.2	87.90	-

Table B.9 - Batch data B2B

Elapsed (sec)	**Starting mass (mg)**	**Ca (mg l^{-1})**	**Rate (mol Ca m^{-2} sec^{-1})**
3600	24.0	1.79	-
7200	20.6	1.38	-
10800	19.9	1.50	-
14400	21.7	1.54	-
18000	21.2	1.82	-
43200	21.4	1.60	-
86400	19.9	3.26	-
172800	21.7	3.26	-
259200	22.1	4.82	-
345600	23.0	4.26	-
518400	21.6	4.14	-

Table B.10 - Batch data B3A

Elapsed (sec)	**Starting mass (mg)**	**Ca (mg l^{-1})**	**Rate (mol Ca m^{-2} sec^{-1})**
3600	22.9	56.80	-10.18
7200	21.3	60.60	-10.42
10800	21.3	55.50	-10.63
14400	20.2	56.10	-10.73
18000	21.3	52.90	-10.88
43200	21.3	48.50	-11.29
86400	22.4	44.40	-11.66
172800	22.5	43.00	-11.97
259200	22.5	44.30	-12.14
345600	20.6	44.80	-12.22
518400	21.0	41.30	-12.44

Table B.11 - Batch data B3B

Elapsed (sec)	**Starting mass (mg)**	**Ca (mg l^{-1})**	**Rate (mol Ca m^{-2} sec^{-1})**
3600	21.2	48.30	-9.57
7200	20.4	24.28	-10.15
10800	21.2	19.94	-10.43
14400	22.0	15.79	-10.67
18000	20.0	13.86	-10.78
43200	20.8	13.28	-11.20
86400	21.5	15.17	-11.45
172800	21.5	20.15	-11.63
259200	21.4	22.99	-11.75
345600	20.5	21.54	-11.88
518400	22.7	37.30	-11.87

Table B.12 - Batch data B4A

Elapsed (sec)	**Starting mass (mg)**	**Ca (mg l^{-1})**	**Rate (mol Ca m^{-2} sec^{-1})**
3600	22.0	40.20	-9.66
7200	21.6	39.80	-9.96
10800	22.4	41.20	-10.14
14400	20.3	38.10	-10.25
18000	20.6	39.10	-10.34
43200	22.1	43.90	-10.70
86400	21.1	41.10	-11.01
172800	21.9	41.80	-11.32
259200	22.3	43.50	-11.49
345600	21.4	41.50	-11.62
518400	22.2	42.50	-11.80

Table B.13 - Batch data B4B

Elapsed (sec)	**Starting mass (mg)**	**Ca (mg l^{-1})**	**Rate (mol Ca m^{-2} sec^{-1})**
3600	21.4	60.00	-10.12
7200	22.7	68.50	-10.39
10800	22.1	71.90	-10.54
14400	20.4	73.60	-10.62
18000	21.2	75.70	-10.72
43200	20.3	82.70	-11.04
86400	20.0	92.10	-11.29
172800	22.2	101.20	-11.59
259200	20.2	103.20	-11.72
345600	21.2	105.90	-11.86
518400	21.3	110.50	-12.02

Batch data: additional graphs

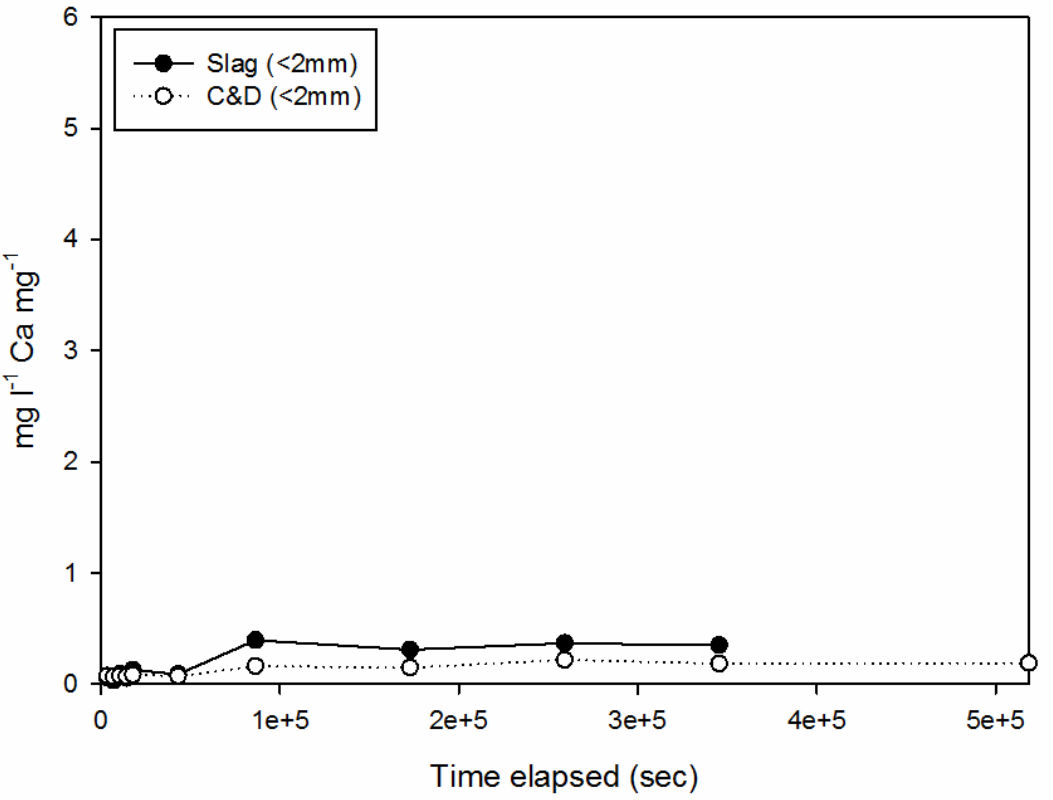

Figure B.1 - Batch 2 AAS data

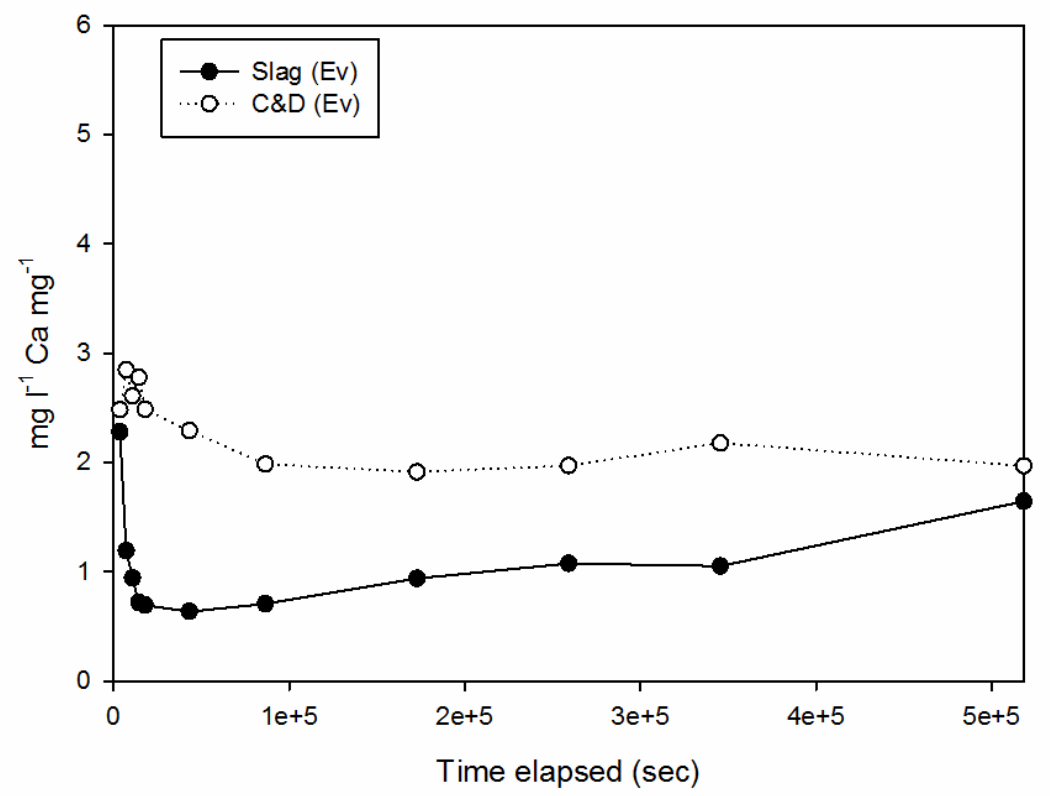

Figure B.2 - Batch 3 AAS data

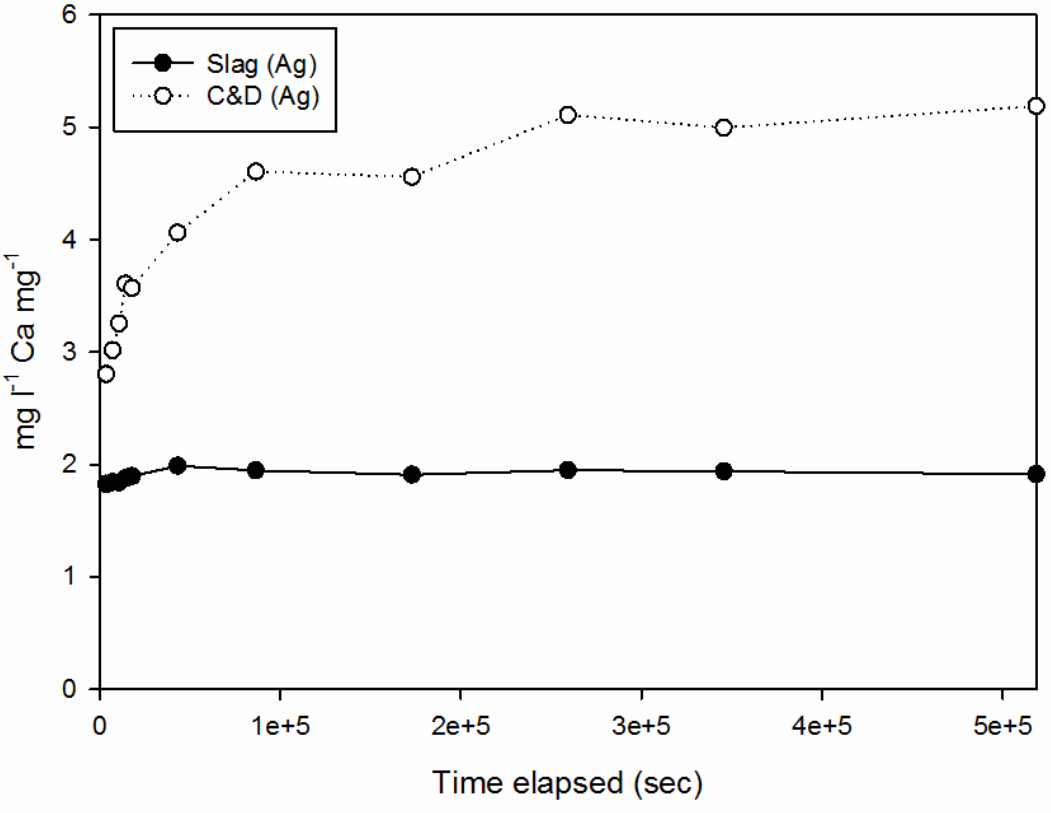

Figure B.3 - Batch 4 AAS data

B.2 pH stat

Table B.14 - pH stat matrix setup

Material	Reagent	Initial mass (g)	pH
Wollastonite 90	HCl (Analar Normapur)	1.4993	3
Wollastonite 90	HCl (Analar Normapur)	0.1490	3
Wollastonite 90	HCl (Analar Normapur)	0.1500	5
Wollastonite 90	HCl (Analar Normapur)	0.1518	8

Table B.15 - pH stat data B1

Elapsed (sec)	Ca (mg l^{-1})	Rate (mol Ca m^{-2} sec^{-1})
600	16.40	-6.19
1200	18.40	-6.44
1800	20.70	-6.56
3600	25.90	-6.77
7200	35.50	-6.93
10800	51.10	-6.95
14400	62.40	-6.99
18000	70.30	-7.03
25200	88.05	-7.08

Table B.16 - pH stat data B2

Elapsed (sec)	Ca (mg l^{-1})	Rate (mol Ca m^{-2} sec^{-1})
600	1.58	-6.20
1200	1.70	-6.47
1800	1.90	-6.60
3600	2.50	-6.78
7200	3.25	-6.97
14400	5.30	-7.05
21600	7.00	-7.11
28800	8.50	-7.15
43200	10.88	-7.22
86400	16.55	-7.34
172800	27.45	-7.42

Table B.17 - pH stat data B3

Elapsed (sec)	**Ca (mg l^{-1})**	**Rate (mol Ca m^{-2} sec^{-1})**
600	0.68	-6.57
1200	0.90	-6.75
1800	1.10	-6.84
3600	1.65	-6.96
7200	2.13	-7.15
14400	3.60	-7.23
28800	6.60	-7.26
43200	8.25	-7.34
90000	13.48	-7.45
172800	21.15	-7.54

Table B.18 - pH stat data B4

Elapsed (sec)	**Ca (mg l^{-1})**	**Rate (mol Ca m^{-2} sec^{-1})**
600	0.80	-6.50
1200	0.85	-6.78
1800	0.95	-6.91
3600	1.20	-7.11
7200	1.40	-7.34
14400	1.80	-7.53
21600	2.30	-7.60
48600	3.65	-7.75
86400	5.08	-7.86
172800	6.90	-8.03

Table B.19 – Reaction rate calculations

K is the equilibrium value or the maximum value that the curve rises to.
To obtain a value adjust K to give the value of R2 in the graph closest to 1.000

	time (mins)	time (hours)	K (mg/l)	c/K	1-c/K	time (seconds)	ln(1-c/K)	SLOPE (-N)	R2
		k	197			25200			
pH 3									
Mass									
0.15g	10	0.17	1.58	0.04	0.97	600.00	-0.04	-5.2E-07	0.997
Surface area	20	0.33	1.70	0.04	0.96	1200.00	-0.04		
0.1055m^2	30	0.50	1.90	0.04	0.96	1800.00	-0.04		
	60	1.00	2.50	0.06	0.94	3600.00	-0.06		
	120	2.00	3.25	0.07	0.93	7200.00	-0.07		
	240	4.00	5.30	0.12	0.88	14400.00	-0.13		
	360	6.00	7.00	0.16	0.84	21600.00	-0.17		
	480	8.00	8.50	0.19	0.81	28800.00	-0.21		
	720	12.00	10.88	0.24	0.76	43200.00	-0.28		
	1440	24.00	16.55	0.37	0.63	86400.00	-0.46		
	2880	48.00	27.45	0.61	0.39	172800.00	-0.94		
		k	45.00						
pH 5									
Mass	10	0.17	0.68	0.02	0.98	600.00	-0.02	-6.1E-07	0.998
0.15g	20	0.33	0.90	0.03	0.97	1200.00	-0.03		
Surface area	30	0.50	1.10	0.03	0.97	1800.00	-0.03		
0.1062m^2	60	1.00	1.65	0.05	0.95	3600.00	-0.05		
	120	2.00	2.13	0.07	0.93	7200.00	-0.07		
	240	4.00	3.60	0.11	0.89	14400.00	-0.12		
	480	8.00	6.60	0.21	0.79	28800.00	-0.23		
	720	12.00	8.25	0.26	0.74	43200.00	-0.30		
	1500	25.00	13.48	0.42	0.58	90000.00	-0.55		
	2880	48.00	21.15	0.66	0.34	172800.00	-1.08		
		k	32.00						
pH 8									
Mass	10	0.17	0.80	0.10	0.90	600.00	-0.11	-1.08E-06	0.999
0.15g	20	0.33	0.85	0.11	0.89	1200.00	-0.11		
Surface area	30	0.50	0.95	0.12	0.88	1800.00	-0.13		
0.1075m^2	60	1.00	1.20	0.15	0.85	3600.00	-0.16		
	120	2.00	1.40	0.18	0.83	7200.00	-0.19		
	240	4.00	1.80	0.23	0.78	14400.00	-0.25		
	360	6.00	2.30	0.29	0.71	21600.00	-0.34		
	810	13.50	3.65	0.46	0.54	48600.00	-0.61		
	1440	24.00	5.08	0.63	0.37	86400.00	-1.01		
	2880	48.00	6.90	0.86	0.14	172800.00	-1.98		
		k	8						

Wollastonite			
	pH	equilibrium value, K	rate, N x10^{-7} s^{-1}
	3	45	0.520
	5	32	0.610
	8	8	1.080

B.3 Stockpile analysis

Table B.20 - Stockpile sample log

Sample Ref.	Description	Production Date	Age (Days)
YAR/TAR/1	6/10 Slag 3 Months	01/03/10	89
YAR/TAR/2	6/10 Slag 3 Months	01/03/10	89
YAR/TAR/3	6/10 Slag Fresh	15/05/10	16
YAR/TAR/4	6/10 Slag Fresh	15/05/10	16
YAR/TAR/5	6/10 Slag 12 Months	29/04/09	395
YAR/TAR/6	6/10 Slag 12 Months	29/04/09	395
YAR/TAR/7	6/10 Slag 6 Months	27/10/09	214
YAR/TAR/8	6/10 Slag 6 Months	27/10/09	214
YAR/TAR/9	6/10 Slag Oldest	10/09/07	991
YAR/TAR/10	6/10 Slag Oldest	10/09/07	991

Table B.21 - Stockpile data: Acid digestion data

Sample Ref.	Age (Days)	% wt $CaCO_3$
YAR/TAR/1	89	14.70
YAR/TAR/2	89	16.96
YAR/TAR/3	16	6.35
YAR/TAR/4	16	7.35
YAR/TAR/5	395	10.60
YAR/TAR/6	395	10.60
YAR/TAR/7	214	11.90
YAR/TAR/8	214	9.09
YAR/TAR/9	991	15.11
YAR/TAR/10	991	12.89

Table B.22 - Stockpile data: pH data

Sample Ref.	Age (Days)	pH
YAR/TAR/1	89	12.64
YAR/TAR/2	89	12.63
YAR/TAR/3	16	12.63
YAR/TAR/4	16	12.62
YAR/TAR/5	395	12.57
YAR/TAR/6	395	12.56
YAR/TAR/7	214	12.54
YAR/TAR/8	214	12.53
YAR/TAR/9	991	12.46
YAR/TAR/10	991	12.48

Table B.23 - Stockpile data: summary of reported samples

Sample Ref.	**Age (Days)**	**pH**	**% wt CaCO3**
YAR/TAR/4	16	12.62	7.35
YAR/TAR/2	89	12.63	16.96
YAR/TAR/9	991	12.46	15.11

Table B.24 - Stockpile data: IRMS

	Mean $\delta^{13}C_{V\text{-}PDB}$ (‰)	**Mean $\delta^{18}O_{V\text{-}PDB}$ (‰)**
YAR/TAR/4	-17.73	-12.91
YAR/TAR/2	-19.54	-13.12
YAR/TAR/9	-20.45	-12.25

APPENDIX C – ADDITIONAL DATA: CHAPTER 4

C.1 Yarborough landfill

Figure C.1 – Excavation of YAR/TP3

Figure C.2 – Exposed sampling profile of YAR/TP4 and later profile

Table C.1 - Excavation data: Yarborough landfill 2010

Sample Ref.	**Date Collected**	**Depth**	**% wt $CaCO_3$**	**$\delta^{13}C$ (‰ V-PDB)**
YAR/TP4/75	04/06/10	75	8.70	-15.81
YAR/TP4/45	04/06/10	45	8.10	-16.18
YAR/TP4/15	04/06/10	15	8.97	-15.91
YAR/TP4/SUR	04/06/10	0	27.45	-17.18
YAR/TP3/95	04/06/10	95	16.38	-16.40
YAR/TP3/65	04/06/10	65	10.35	-16.22
YAR/TP3/35	04/06/10	35	8.57	-15.90
YAR/TP3/SUR	04/06/10	0	13.33	-14.93
YAR/TP3/CONC	04/06/10	30-35	27.10	-18.68

Table C.2 - Excavation data: Yarborough landfill 2012

Sample Ref.	**Date Collected**	**Depth**	**% wt $CaCO_3$**	**$\delta^{13}C$ (‰ V-PDB)**
Carb Clay L2	21/02/12	2.50	6.24	-
Carb L2 # 1	21/02/12	2.50	8.60	-
Carb L2 # 2	21/02/12	2.50	25.57	-
Carb Slag 0.5m	21/02/12	0.50	25.65	-
0.5m Block	21/02/12	0.50	6.44	-
0.5m Block	21/02/12	0.50	10.48	-

Figure 7 Chapter 3 – ESEM point analysis

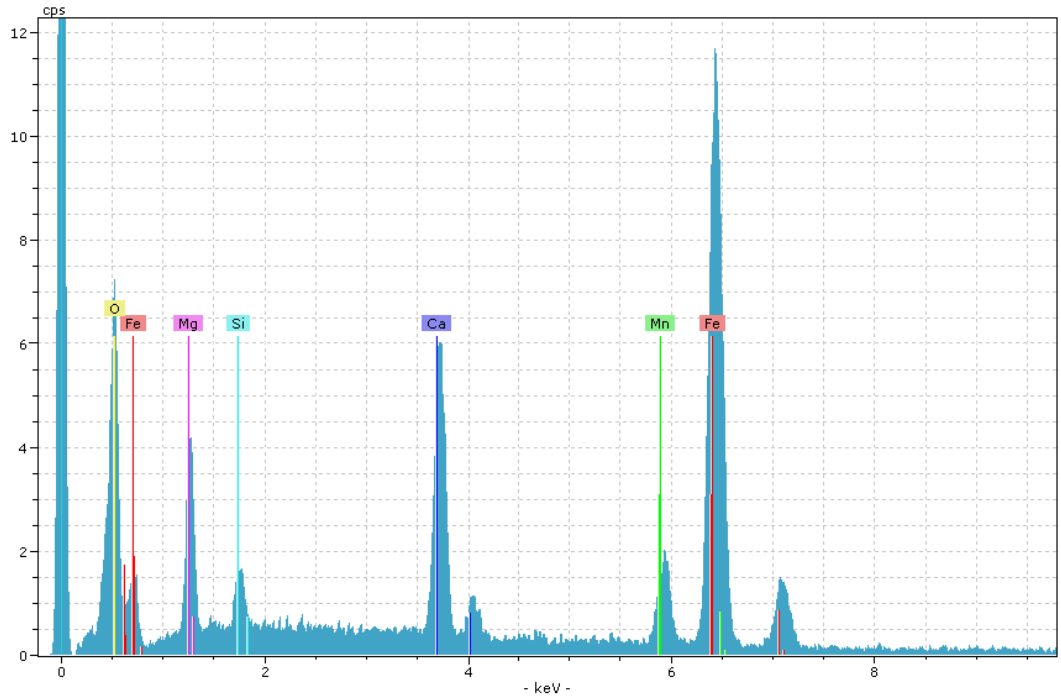

Figure C.3 - TP30-50 point 0

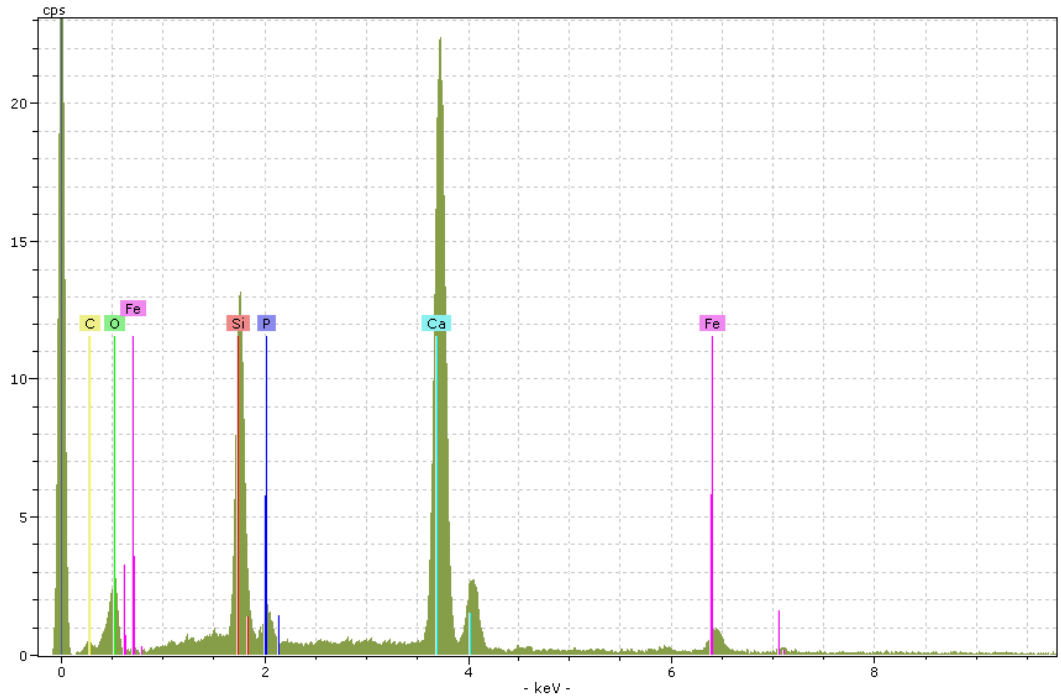

Figure C.4 - TP30-50 point 1

Figure C.5 – Slag blocks prior to suspension in leachate wells

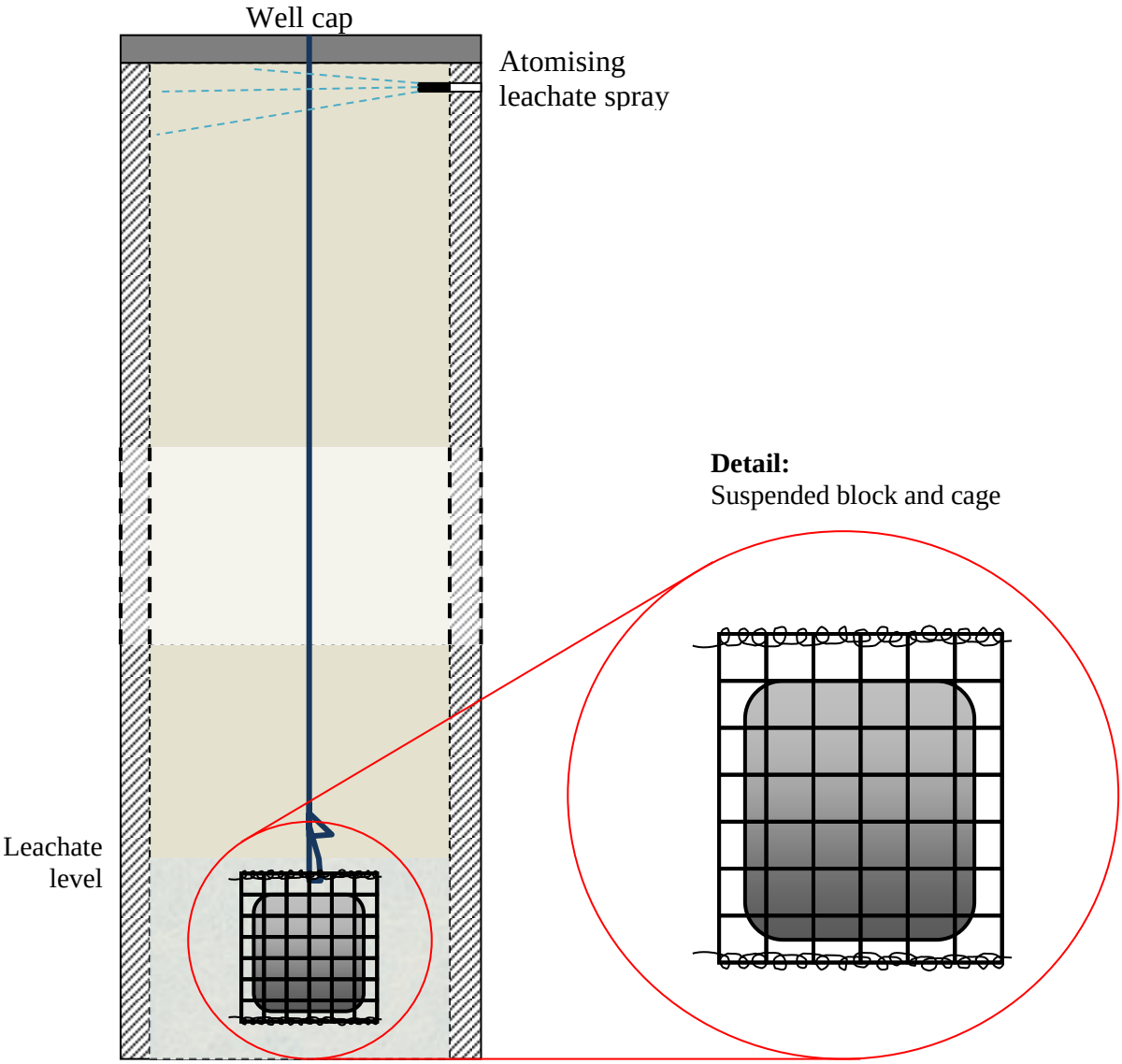

Figure C.6 –Diagram of suspended slag block in leachate analysis well. (Most of the leachate wells in the newer part of the Yarborough site receive an influx of leachate as a spray from the surface, where water management techniques require lagoons and temporary pools to be drained to the wells – this is not intended as an additional piece of experimental equipment)

Table C.3 - Science Central field data 2010

ID	Easting (m)	Northing (m)		$\%CaCO_3$	%TOC	%TIC	%CaO	%MgO	$\%Fe_2O_3$	$\delta^{13}C$ (‰)	$\delta^{18}O$ (‰)
B12	423921.43	564286.96		23.03	1.32	2.76					
B13	423921.43	564266.96		44.38	1.02	5.33	22.03	6.17	3.55	-3.65	-8.10
B14	423921.43	564246.96		42.95	0.99	5.15					
B15	423921.43	564226.96		50.17	0.27	6.02	22.01	5.25	3.24	-3.13	-8.69
C3	423941.43	564466.96		26.21	1.72	3.15					
C4	423941.43	564446.96		27.27	1.54	3.27					
C5	423941.43	564426.96		24.14	2.03	2.90					
C6	423941.43	564406.96		25.08	1.60	3.01					
C7	423941.43	564386.96		26.73	1.59	3.21					
C8	423941.43	564366.96		25.46	1.59	3.05					
C9	423941.43	564346.96		22.75	2.00	2.73					
C10	423941.43	564326.96		26.39	1.49	3.17					
C11	423941.43	564306.96		25.67	1.40	3.08					
C12	423941.43	564286.96		25.54	1.52	3.06					
C13	423941.43	564266.96		22.04	0.93	2.64					
C14	423941.43	564246.96		20.47	1.12	2.46					
C15	423941.43	564226.96		32.02	1.22	3.84					
D3	423961.43	564466.96		23.92	1.27	2.87	13.90	2.09	3.85	-8.72	-10.46
D4	423961.43	564446.96		19.36	1.37	2.32					
D5	423961.43	564426.96		32.12	1.27	3.85	17.93	2.08	3.50	-7.79	-11.18
D6	423961.43	564406.96		25.64	1.51	3.08					
D7	423961.43	564386.96		21.06	1.77	2.53	13.06	2.05	4.06	-9.11	-9.40
D8	423961.43	564366.96		26.67	1.71	3.20					
D9	423961.43	564346.96		19.15	2.88	2.30	11.45	1.53	4.13	-10.78	-10.62

ID	Easting (m)	Northing (m)		%$CaCO_3$	%TOC	%TIC	%CaO	%MgO	%Fe_2O_3	$\delta^{13}C$ (‰)	$\delta^{18}O$ (‰)
D10	423961.43	564326.96		25.72	1.68	3.09					
D11	423961.43	564306.96		21.87	2.15	2.62	13.21	1.90	4.12	-9.78	-9.79
D12	423961.43	564286.96		30.50	1.76	3.66					
D13	423961.43	564266.96		24.46	1.74	2.94	14.04	1.54	3.83	-11.20	-11.93
D14	423961.43	564246.96		20.32	0.87	2.44					
D15	423961.43	564226.96		21.98	1.99	2.64	13.34	1.97	3.57	-10.70	-10.77
E3	423981.43	564466.96		25.47	1.64	3.06					
E4	423981.43	564446.96		27.57	1.98	3.31					
E5	423981.43	564426.96		28.98	1.50	3.48					
E6	423981.43	564406.96		26.61	1.61	3.19					
E7	423981.43	564386.96		19.80	1.64	2.38					
E8	423981.43	564366.96		20.84	2.33	2.50					
E9	423981.43	564346.96		23.29	2.06	2.79					
E10	423981.43	564326.96		18.88	2.67	2.27					
E11	423981.43	564306.96		20.35	1.34	2.44					
E12	423981.43	564286.96		26.45	1.62	3.17					
E13	423981.43	564266.96		20.46	1.46	2.45					
E14	423981.43	564246.96		22.98	2.04	2.76					
E15	423981.43	564226.96		28.02	1.32	3.36					
F3	424001.43	564466.96		22.91	1.41	2.75	13.93	1.57	3.83	-9.12	-10.46
F4	424001.43	564446.96		24.79	1.38	2.98					
F5	424001.43	564426.96		20.30	2.33	2.44	16.76	2.00	3.70	-8.89	-10.19
F6	424001.43	564406.96		24.92	1.59	2.99					
F7	424001.43	564386.96		21.67	1.52	2.60	13.39	1.65	3.88	-10.01	-11.39
F8	424001.43	564366.96		29.24	1.82	3.51					

ID	Easting (m)	Northing (m)		%$CaCO_3$	%TOC	%TIC	%CaO	%MgO	%Fe_2O_3	$\delta^{13}C$ (‰)	$\delta^{18}O$ (‰)
F9	424001.43	564346.96		30.07	1.72	3.61	15.83	2.24	4.08	-8.44	-10.09
F10	424001.43	564326.96		27.96	1.45	3.36					
F11	424001.43	564306.96		27.46	1.55	3.30	15.91	2.09	3.51	-9.39	-10.78
F12	424001.43	564286.96		27.52	1.78	3.30					
F13	424001.43	564266.96		24.06	1.34	2.89	14.60	1.88	3.69	-13.38	-11.61
F14	424001.43	564246.96		25.91	3.26	3.11					
F15	424001.43	564226.96		26.17	2.26	3.14	13.65	2.47	3.83	-7.42	-10.07
G3	424021.43	564466.96		21.06	1.60	2.53					
G4	424021.43	564446.96		25.08	1.47	3.01					
G5	424021.43	564426.96		23.07	2.06	2.77					
G6	424021.43	564406.96		19.96	1.72	2.40					
G7	424021.43	564386.96		22.24	1.84	2.67					
G8	424021.43	564366.96		27.21	1.66	3.27					
G9	424021.43	564346.96		28.34	1.48	3.40					
G10	424021.43	564326.96		26.52	1.72	3.18					
G11	424021.43	564306.96		23.07	1.31	2.77					
G12	424021.43	564286.96		25.59	1.37	3.07					
G13	424021.43	564266.96		24.12	1.40	2.89					
G14	424021.43	564246.96		32.58	1.50	3.91					
G15	424021.43	564226.96		29.59	1.48	3.55					
H3	424041.43	564466.96		21.70	1.44	2.60	14.35	1.29	3.85	-10.66	-10.98
H4	424041.43	564446.96		25.37	1.58	3.04					
H5	424041.43	564426.96		21.08	2.08	2.53	12.42	1.39	3.55	-10.67	-11.79
H6	424041.43	564406.96		16.89	2.42	2.03					
H7	424041.43	564386.96		21.08	2.01	2.53	13.43	1.62	3.83	-10.30	-11.15

ID	Easting (m)	Northing (m)		$\%CaCO_3$	%TOC	%TIC	%CaO	%MgO	$\%Fe_2O_3$	$\delta^{13}C$ (‰)	$\delta^{18}O$ (‰)
H8	424041.43	564366.96		25.11	1.64	3.01					
H9	424041.43	564346.96		25.72	1.89	3.09	16.49	1.86	3.65	-9.26	-9.53
H10	424041.43	564326.96		24.77	1.48	2.97					
H11	424041.43	564306.96		25.63	1.61	3.08	16.59	2.00	3.61	-9.51	-10.42
H12	424041.43	564286.96		27.45	1.40	3.29					
H13	424041.43	564266.96		21.06	3.20	2.53	12.78	1.48	3.45	-10.93	-10.66
H14	424041.43	564246.96		17.27	1.21	2.07					
H15	424041.43	564226.96		18.57	1.21	2.23	11.78	1.70	3.43	-10.12	-10.83
I3	424061.43	564466.96		20.53	1.62	2.46					
I4	424061.43	564446.96		18.10	2.19	2.17					
I5	424061.43	564426.96		17.18	2.11	2.06					
I6	424061.43	564406.96		22.27	1.69	2.67					
I7	424061.43	564386.96		17.54	1.96	2.10					
I8	424061.43	564366.96		20.04	1.81	2.40					
I9	424061.43	564346.96		23.07	1.45	2.77					
I10	424061.43	564326.96		29.00	1.78	3.48					
I11	424061.43	564306.96		25.21	1.50	3.02					
I12	424061.43	564286.96		19.09	1.63	2.29					
I13	424061.43	564266.96		20.59	1.18	2.47					
I14	424061.43	564246.96		19.07	1.07	2.29					
I15	424061.43	564226.96		22.77	1.05	2.73					
J3	424081.43	564466.96		19.71	1.90	2.37	12.87	1.15	4.08	-11.34	-10.74
J4	424081.43	564446.96		24.98	1.45	3.00					
J5	424081.43	564426.96		22.38	1.81	2.69	13.76	1.62	4.10	-10.06	-11.51
J6	424081.43	564406.96		19.00	1.71	2.28					

ID	Easting (m)	Northing (m)		$\%CaCO_3$	%TOC	%TIC	%CaO	%MgO	$\%Fe_2O_3$	$\delta^{13}C$ (‰)	$\delta^{18}O$ (‰)
J7	424081.43	564386.96		19.80	1.88	2.38	12.56	1.57	3.98	-11.05	-11.10
J8	424081.43	564366.96		17.42	1.66	2.09					
J9	424081.43	564346.96		17.19	1.87	2.06	11.05	1.13	4.11	-13.29	-10.86
J10	424081.43	564326.96		21.79	1.64	2.61					
J11	424081.43	564306.96		17.07	1.61	2.05	10.90	0.92	4.22	-13.55	-11.43
J12	424081.43	564286.96		17.78	2.17	2.13					
J13	424081.43	564266.96		21.91	1.42	2.63	12.39	1.78	3.73	-10.81	-11.27
J14	424081.43	564246.96		22.08	1.37	2.65					
J15	424081.43	564226.96		21.63	1.52	2.60	12.77	1.70	3.50	-9.89	-11.08
K4	424101.43	564446.96		22.65	1.93	2.72					
K5	424101.43	564426.96		20.37	1.82	2.44					
K6	424101.43	564406.96		19.01	1.71	2.28					
K7	424101.43	564386.96		10.51	2.73	1.26					
K10	424101.43	564326.96		19.01	1.72	2.28					
K11	424101.43	564306.96		16.43	1.86	1.97					
K12	424101.43	564286.96		14.75	1.61	1.77					
K13	424101.43	564266.96		22.64	1.93	2.72					
K14	424101.43	564246.96		5.27	4.30	0.63					
K15	424101.43	564226.96		17.31	3.26	2.08					
L6	424121.43	564406.96		18.43	1.48	2.21	12.53	1.81	3.96	-8.07	-10.18
L10	424121.43	564326.96		17.35	1.64	2.08	10.85	0.95	4.04	-12.68	-11.88
L14	424121.43	564246.96		15.14	2.33	1.82				-11.67	-10.96
L15	424121.43	564226.96		13.85	2.32	1.66	9.09	1.05	4.15		
M10	424141.43	564326.96		15.63	1.77	1.88					
M14	424141.43	564246.96		25.19	1.69	3.02					

ID	Easting (m)	Northing (m)		%$CaCO_3$	%TOC	%TIC	%CaO	%MgO	%Fe_2O_3	$\delta^{13}C$ (‰)	$\delta^{18}O$ (‰)
M15	424141.43	564226.96		10.42	5.67	1.25					
N10	424161.43	564326.96		16.36	3.17	1.96	10.51	0.91	4.06	-13.19	-11.64
N12	424161.43	564286.96		22.76	1.78	2.73	13.51	1.93	3.85	-7.81	-10.05
N13	424161.43	564266.96		15.43	2.43	1.85					
N14	424161.43	564246.96		18.99	2.75	2.28	12.39	1.58	4.04	-9.58	-11.36
N15	424161.43	564226.96		7.34	1.88	0.88					
O12	424181.43	564286.96		17.61	2.18	2.11					
O13	424181.43	564266.96		14.17	2.67	1.70					
O14	424181.43	564246.96		10.91	3.23	1.31					
P12	424201.43	564286.96		12.00	1.69	1.44	8.01	1.23	4.28	-10.29	-9.83
P13	424201.43	564266.96		17.35		2.08					
P14	424201.43	564246.96		21.88	2.37	2.63	13.95	1.04	4.33	-12.43	-11.41
Q13	424221.43	564266.96		18.61	2.28	2.23					

Table C.4 - Science Central field data 2012

ID	Easting (m)	Northing (m)		$\%CaCO_3$	%TOC	%TIC	%CaO	%MgO	$\%Fe_2O_3$	$\delta^{13}C$ (‰)	$\delta^{18}O$ (‰)
B12	423921.43	564286.96		44.69	2.33	4.98					
B14	423921.43	564246.96		61.35	1.92	7.09	26.70	6.76	3.77	-6.53	-10.02
E3	423981.43	564466.96		38.50	6.39	4.33					
E4	423981.43	564446.96		41.08	7.15	5.05					
E6	423981.43	564406.96		52.17	2.30	5.51	23.62	3.55	3.86	-13.06	-12.79
E8	423981.43	564366.96		45.67	2.55	4.37					
E10	423981.43	564326.96		44.88	2.09	5.40					
E12	423981.43	564286.96		41.54	2.41	5.07					
E14	423981.43	564246.96		31.78	5.09	3.39					
H3	424041.43	564466.96		35.07	2.89	3.72	20.18	1.81	4.85	-13.35	-12.72
H4	424041.43	564446.96		33.21	1.97	3.89					
H6	424041.43	564406.96		37.10	7.47	4.37					
H8	424041.43	564366.96		43.73	2.09	4.94					
H10	424041.43	564326.96		43.14	2.16	4.59					
H12	424041.43	564286.96		49.49	1.80	5.51					
H14	424041.43	564246.96		38.95	2.00	4.17					
K6	424101.43	564406.96		33.23	2.75	3.92					
K10	424101.43	564326.96		36.73	2.66	4.03	19.32	1.43	5.02	-13.95	-12.67
K12	424101.43	564286.96		27.51	3.26	3.15					
K14	424101.43	564246.96		32.35	2.34	3.47					
N10	424161.43	564326.96		39.58	2.29	4.29	21.84	1.45	4.76	-14.01	-13.26
N12	424161.43	564286.96		26.46	3.34	3.02	19.28	1.32	5.15	-14.57	-12.57
N14	424161.43	564246.96		28.71	3.06	3.21	16.58	2.16	5.02	-12.72	-13.84

Table C.5 - Science Central: Rate calculations (surface areas are assumed iteratively in order to test sensitivity to change in this parameter)

1	$m^2 g^{-1}$	0.5	$m^2 g^{-1}$	1.5	$m^2 g^{-1}$	2	$m^2 g^{-1}$	2.5	$m^2 g^{-1}$
10000	$cm^2 g^{-1}$	5000	$cm^2 g^{-1}$	15000	$cm^2 g^{-1}$	20000	$cm^2 g^{-1}$	25000	$cm^2 g^{-1}$
1E+16	cm^2	5E+15	cm^2	1.5E+16	cm^2	2E+16	cm^2	2.5E+16	cm^2
2E-13	mol cm^2 sec^{-1}	4E-13	mol cm^2 sec^{-1}	1.3E-13	mol cm^2 sec^{-1}	1E-13	mol cm^2 sec^{-1}	8E-14	mol cm^2 sec^{-1}
-16.70	log mol m^2 sec^{-1}	-16.40	log mol m^2 sec^{-1}	-16.87	log mol m^2 sec^{-1}	-17.00	log mol m^2 sec^{-1}	-17.10	log mol m^2 sec^{-1}

3	$m^2 g^{-1}$	3.5	$m^2 g^{-1}$	4	$m^2 g^{-1}$
30000	$cm^2 g^{-1}$	35000	$cm^2 g^{-1}$	40000	$cm^2 g^{-1}$
3E+16	cm^2	3.5E+16	cm^2	4E+16	cm^2
6.67E-14	mol cm^2 sec^{-1}	5.72E-14	mol cm^2 sec^{-1}	5E-14	mol cm^2 sec^{-1}
-17.18	log mol m^2 sec^{-1}	-17.24	log mol m^2 sec^{-1}	-17.30	log mol m^2 sec^{-1}

1000000	t material onsite
1.00E+12	g material onsite
200000	t Si change 2010-12
2.00E+11	g Si change 2010-12
9.33E+10	mol Si
46656000	seconds elapsed
2000.45725	mol s^{-1}
1	$m^2 g^{-1}$
10000	$cm^2 g^{-1}$
1.00E+16	cm^2
2.00E-13	mol cm^{-2} sec^{-1}
-12.698871	log mol cm^{-2} sec^{-1}

C.2.1 ^{14}C Data Report

Pre-treatment

An aliquot of air-dried, homogenised material from each sample was placed in a Polaron K1050X Plasma Reactor and subjected to low-temperature ashing in an oxygen plasma to remove organic (i.e. non-carbonate) carbon. Low-temperature oxygen plasma ashing is a surface-active technique that employs oxygen gas excited by a radio frequency generator to oxidize organic material without raising the sample temperature beyond c.150˚C. Ashing was performed until a constant sample weight was achieved (46 hours).

The ashed samples were then hydrolysed to CO_2 using 85% Ortho-phosphoric acid (H_3PO_4) in small hydrolysis vessels. The evolved sample CO_2 was cryogenically purified.

Measurement

$\delta^{13}C$ values were obtained for the samples for normalization of measured sample $^{14}C/^{13}C$ ratios to values corresponding to $\delta^{13}C$ = -25‰ prior to calculation of ^{14}C ages (Stuiver and Polach, 1977; Donhaue et al., 1990).

An aliquot of the purified sample CO_2 (as described above) was converted to graphite by the method of Slota et al. (1987) for ^{14}C measurement by Accelerator Mass Spectrometry. Sample $^{14}C/^{13}C$ ratios were measured with carbon in the +1 charge state on the SUERC SSAMS at 245 keV.

Results

Table C.6 - ^{14}C data

Material ID code	**Estimated Age**	**off-line d13C and error**	**^{14}C Age yrs BP ± 1 sigma error**	**Percent Modern Carbon ± 1 sigma error**
SC-B15-2010	Low expected atm CO_2	-1.9 ± 0.5	9509 ± 35	30.39 ± 0.14
SC-J11-2010	High expected atm CO_2	-14.0 ± 0.5	1661 ± 35	80.73 ± 0.37

References

Donahue, D.J., Linick, T.W., Jull, A.J.T. 1990. Radiocarbon 32, 135-142.

Slota, P.J., Jull, A.J.T., Linick, T.W., Toolin, L.J. 1987. Preparation of small samples for ^{14}C accelerator targets by catalytic reduction of CO. Radiocarbon 29, 303-306.

Stuiver, M., Polach, H.A. 1977. Discussion: Reporting of ^{14}C data. Radiocarbon 19, 355-363.

APPENDIX D – ADDITIONAL DATA: CHAPTER 5

D.1 Flow-through weathering

Table D.1 - Flow through weathering: Schedule and details

Run #	Column	Slag	Duration	Conditions
1	1	6/10 Fresh YAR/TAR/3	8 days	Distilled water
1	2	6/10 Fresh YAR/TAR/3	8 days	Evian water (high bicarbonate content)
1	3	6/10 Weathered YAR/TAR/10	8 days	Distilled water
2	1	6/10 Fresh YAR/TAR/3	21 days	Deionised water
2	2	6/10 Fresh YAR/TAR/3	21 days	Deionised water Vadose zone to 200mm from surface of slag-packed column
2	3	6/10 Fresh YAR/TAR/3	21 days	Deionised water Wetting-drying cycles: column fully drained every 7 days, dried for 24 hours and refilled with fresh leachate solution
2	4	6/10 Fresh YAR/TAR/3	21 days	Deionised water Periodic mobilisation of materials fully drained every 7 days, inverted 4-5 times and refilled with fresh leachate solution
3	3	6/10 Fresh YAR/TAR/3	56 days	Deionised water
3	4	6/10 Fresh YAR/TAR/3	56 days	Simulated groundwater (NaCl)
4	1	6/10 Fresh YAR/TAR/3	21 days	CO_2 supply

Table D.2 - Flow through weathering: Sampling schedule

		Time elapsed (mins)			Time elapsed (mins)
pH, Cond., Metals, TC		0	pH, Cond., Metals, TC	**Day 24**	32400
pH, Cond., Metals		10	pH, Cond., Metals	**Day 25**	33840
pH, Cond., Metals		30	pH, Cond., Metals	**Day 26**	35280
pH, Cond., Metals	**Day 1**	60	pH, Cond., Metals	**Day 27**	36720
pH, Cond., Metals		120	pH, Cond., Metals, TC	**Day 28**	38160
pH, Cond., Metals		240	pH, Cond., Metals	**Day 29**	39600
pH, Cond., Metals		480	pH, Cond., Metals	**Day 30**	41040
pH, Cond., Metals		960	pH, Cond., Metals	**Day 31**	42480
pH, Cond., Metals, TC	**Day 2**	1440	pH, Cond., Metals, TC	**Day 32**	43920
pH, Cond., Metals		1920	pH, Cond., Metals	**Day 33**	45360
pH, Cond., Metals		2400	pH, Cond., Metals	**Day 34**	46800
pH, Cond., Metals, TC	**Day 3**	2880	pH, Cond., Metals	**Day 35**	48240
pH, Cond., Metals		3600	pH, Cond., Metals, TC	**Day 36**	49680
pH, Cond., Metals, TC	**Day 4**	4320	pH, Cond., Metals	**Day 37**	51120
pH, Cond., Metals, TC	**Day 5**	5760	pH, Cond., Metals	**Day 38**	52560
pH, Cond., Metals, TC	**Day 6**	7200	pH, Cond., Metals	**Day 39**	54000
pH, Cond., Metals, TC	**Day 7**	8640	pH, Cond., Metals, TC	**Day 40**	55440
pH, Cond., Metals	**Day 8**	10080	pH, Cond., Metals	**Day 41**	56880
pH, Cond., Metals, TC	**Day 9**	11520	pH, Cond., Metals	**Day 42**	58320
pH, Cond., Metals	**Day 10**	12960	pH, Cond., Metals	**Day 43**	59760
pH, Cond., Metals, TC	**Day 11**	14400	pH, Cond., Metals, TC	**Day 44**	61200
pH, Cond., Metals	**Day 12**	15840	pH, Cond., Metals	**Day 45**	62640
pH, Cond., Metals, TC	**Day 13**	17280	pH, Cond., Metals	**Day 46**	64080
pH, Cond., Metals	**Day 14**	18720	pH, Cond., Metals	**Day 47**	65520
pH, Cond., Metals, TC	**Day 15**	20160	pH, Cond., Metals, TC	**Day 48**	66960
pH, Cond., Metals	**Day 16**	21600	pH, Cond., Metals	**Day 49**	68400
pH, Cond., Metals, TC	**Day 17**	23040	pH, Cond., Metals	**Day 50**	69840
pH, Cond., Metals	**Day 18**	24480	pH, Cond., Metals	**Day 51**	71280
pH, Cond., Metals, TC	**Day 19**	25920	pH, Cond., Metals, TC	**Day 52**	72720
pH, Cond., Metals	**Day 20**	27360	pH, Cond., Metals	**Day 53**	74160
pH, Cond., Metals, TC	**Day 21**	28800	pH, Cond., Metals	**Day 54**	75600
pH, Cond., Metals	**Day 22**	29520	pH, Cond., Metals	**Day 55**	77040
pH, Cond., Metals	**Day 23**	30960	pH, Cond., Metals, TC	**Day 56**	78480

Flow through weathering: Sampling data

Table D.3 - Flow-through weathering Run 1 Column 1

Elapsed (mins)	**pH**	**EC mS cm^{-1}**	**Ca mg/L**	**Mg mg/L**
0	11.6	1.223	279.75	2.72
10	11.59	0.996	240.50	9.40
30	11.69	1.333	309.50	7.23
60	11.85	1.915	431.75	4.25
120	11.86	2.292	530.75	3.09
240	11.9	2.558	586.25	1.61
360	11.8	2.579	481.00	0.00
840	11.77	2.637	653.25	1.75
1320	11.29	2.589	616.25	1.62
1800	11.66	2.534	609.75	1.30
2280	11.87	2.452	616.00	1.16
2760	11.58	2.37	558.50	0.93
3240	11.71	2.307	564.50	1.98
3720	11.56	2.17	501.75	0.84
4440	11.74	1.847	471.50	0.59
5160	11.63	1.824	449.00	0.61
6600	11.7	1.464	233.00	0.19
8040	11.36	1.304	392.75	0.52
12360	11.24	0.975	328.00	2.04

$CaCO_3$ wt % (Start) 1.65
$CaCO_3$ wt % (End) 2.98
$CaCO_3$ wt % (Difference) 1.32

Table D.4 - Flow-through weathering Run 1 Column 2

Elapsed (mins)	**pH**	**EC mS cm^{-1}**	**Ca mg/L**	**Mg mg/L**
0	11.76	1.677	377.25	0.48
10	11.64	1.043	235.5	0.92
30	11.73	1.49	342.25	0.38
60	11.89	2.03	467.25	0.43
120	11.86	2.365	551.75	0.15
240	11.89	2.444	568	0.27
360	11.85	2.477	560.5	0.09
840	11.66	2.335	563.5	0.13
1320	11.34	2.283	535.5	0.40
1800	11.55	2.305	557.75	0.18
2280	11.75	2.067	532.75	0.25
2760	11.58	2.191	524.25	0.26
3240	11.31	2.118	510.75	0.09
3720	11.45	2.091	485.25	0.15
4440	11.68	1.88	515.75	0.56
5160	11.64	1.849	491.5	0.13
6600	11.65	1.594	354.75	0.19
8040	11.44	1.555	506.75	0.14
12360	11.4	1.346	400.25	0.20

$CaCO_3$ wt % (Start) 1.65
$CaCO_3$ wt % (End) 3.55
$CaCO_3$ wt % (Difference) 1.89

Table D.5 - Flow-through weathering Run 1 Column 3

Elapsed (mins)	**pH**	**EC mS cm^{-1}**	**Ca mg/L**	**Mg mg/L**
0	9.2	0.0455	20.51	1.56
10	9.04	0.0711	30.55	
30	9.08	0.0678	24.79	3.02
60	9.2	0.0683	17.92	2.71
120	9.16	0.0655	15.92	2.62
240	9.17	0.0584	12.89	2.27
360	9.14	0.0545	11.68	2.17
840	9.11	0.0498	12.13	1.85
1320	9.21	0.054	13.61	1.95
1800	9.13	0.0476	11.98	1.63
2280	9.22	0.0464	12.71	1.68
2760	9.04	0.046	12.53	1.62
3240	9.01	0.0381	10.47	1.12
3720	8.94	0.0368	10.53	1.05
4440	8.94	0.0334	10.96	0.97
5160	8.95	0.0038	10.47	1.01
6600	9.03	0.0292	12.69	0.66
8040	8.95	0.0377	11.11	0.70
12360	9.12	0.0383	12.02	0.84

$CaCO_3$ wt % (Start) 7.04
$CaCO_3$ wt % (End) 7.56
$CaCO_3$ wt % (Difference) 0.52

Table D.6 - Flow-through weathering Run 2 Column 1

Elapsed (mins)	**pH**	**EC mS cm^{-1}**	**Ca mg/L**
0	11.56	2.306	354.5
10	11.47	1.991	343.8
30	11.56	2.354	405.3
60	11.58	2.591	442.0
120	11.59	2.702	463.0
240	11.68	2.776	475.8
360	11.78	2.814	488.3
840	11.82	2.708	458.3
1320	11.92	2.525	446.3
1800	11.58	2.375	427.8
2280	11.80	2.351	410.5
2760	11.70	2.197	389.8
3240	11.59	2.028	364.5
3960	11.68	1.953	343.8
4680	11.46	1.790	320.5
5400	11.47	1.740	296.5
6120	11.38	1.582	280.5
6840	11.27	1.537	265.0
8280	11.23	1.588	277.3
9720	11.45	1.558	274.0
11160	11.33	1.484	244.8
12600	11.35	1.546	245.8
14040	11.37	1.460	212.5
15480	11.28	1.359	209.8
16920	11.29	1.332	202.8
18360	11.28	1.401	190.3
19800	11.34	1.242	183.0
21240	11.32	1.165	174.8
22680	11.34	1.124	159.8
24120	11.36	1.127	158.3
25560	11.25	1.071	150.3
27000	11.30	1.069	146.8
28440	11.28	0.999	147.3

$CaCO_3$ wt % (End) 3.29

Table D.7 - Flow-through weathering Run 2 Column 2

Elapsed (mins)	**pH**	**EC mS cm^{-1}**	**Ca mg/L**
0	11.47	1.749	257.8
10	11.51	1.971	327.5
30	11.59	2.459	403.5
60	11.60	2.598	415.0
120	11.59	2.744	453.3
240	11.65	2.735	435.0
360	11.88	2.776	415.8
840	11.84	2.525	396.0
1320	11.86	2.359	366.3
1800	11.59	2.134	344.5
2280	11.73	2.015	337.8
2760	11.55	1.747	313.5
3240	11.48	1.623	288.8
3960	11.51	1.454	252.3
4680	11.28	1.322	230.0
5400	11.30	1.253	207.8
6120	11.21	1.107	191.5
6840	11.14	1.047	174.5
8280	11.11	1.115	192.3
9720	11.28	1.077	181.0
11160	11.31	1.074	173.0
12600	11.20	1.032	171.8
14040	11.28	1.007	149.0
15480	11.07	0.914	142.8
16920	11.10	0.935	140.3
18360	11.13	0.969	130.3
19800	11.12	0.859	123.8
21240	11.08	0.814	117.3
22680	11.15	0.754	109.0
24120	11.13	0.730	103.5
25560	11.06	0.724	100.3
27000	11.13	0.688	98.8
28440	11.02	0.662	98.3

$CaCO_3$ wt % (End) 3.37

Table D.8 - Flow-through weathering Run 2 Column 3

Elapsed (mins)	**pH**	**EC mS cm^{-1}**	**Ca mg/L**
0	11.73	1.537	289.5
10	11.78	2.106	382.5
30	11.82	2.395	435.3
60	11.91	2.731	474.8
120	11.73	2.708	536.3
240	11.77	2.776	539.5
360	11.71	2.764	536.3
840	11.80	2.743	537.3
1320	11.63	2.530	511.8
1800	11.80	2.364	491.5
2280	11.61	2.324	465.8
2760	11.63	2.345	426.5
3240	11.46	2.151	418.3
3960	11.43	2.050	405.8
4680	11.32	1.917	365.0
5400	11.29	1.864	333.0
6120	11.49	1.848	364.3
6840	11.21	1.899	339.3
8280	11.39	1.727	317.0
9720	11.53	1.970	305.8
11160	11.30	1.924	293.5
12600	11.52	1.707	264.0
14040	11.18	1.587	244.8
15480	11.25	1.570	238.5
16920	11.23	1.525	222.3
18360	11.24	1.431	212.5
19800	11.21	1.370	205.3
21240	11.34	1.214	193.8
22680	11.30	1.253	182.5
24120	11.20	1.207	174.8
25560	11.30	1.138	164.3
27000	11.17	1.111	159.8
28440	11.30	1.085	167.3

$CaCO_3$ wt % (End) 3.49

Table D.9 - Flow-through weathering Run 2 Column 4

Elapsed (mins)	**pH**	**EC mS cm^{-1}**	**Ca mg/L**
0	11.59		
10	11.60	0.765	171.0
30	11.60	0.735	167.8
60	11.71	0.873	155.3
120	11.73	2.143	176.0
240	11.78	2.713	516.5
360	11.76	2.704	620.0
840	11.78	2.560	548.8
1320	11.59	2.343	531.0
1800	11.86	2.231	516.5
2280	11.51	2.150	520.8
2760	11.61	2.151	491.8
3240	11.41	1.965	486.8
3960	11.37	1.957	469.5
4680	11.32	1.782	429.0
5400	11.31	1.691	414.5
6120	11.42	1.663	379.5
6840	11.21	1.781	390.8
8280	11.35	1.625	395.5
9720			365.8
11160	11.31	1.764	
12600	11.53	1.698	360.5
14040	11.16	1.443	309.0
15480	11.37	1.324	291.5
16920	11.15	1.325	278.5
18360	11.19	1.314	264.8
19800			
21240	11.36	1.272	249.8
22680	11.30	1.262	251.8
24120	11.17	1.165	226.8
25560	11.27	1.152	194.0
27000	11.15	1.031	189.8
28440	11.26	0.982	175.8

$CaCO_3$ wt % (End) 3.12

Table D.10 - Flow-through weathering Run 3 Column 3

Elapsed (mins)	**pH**	**EC mS cm^{-1}**	**Ca mg/L**
0	11.44	1.839	543.5
10	11.59	1.870	482.5
30	11.69	2.120	553.0
60	11.74	2.542	582.0
120	11.83	2.733	638.3
240	11.82	2.574	624.8
480	11.79	2.817	634.6
960	11.61	2.879	731.5
1440	11.68	2.772	648.5
1920	11.62	2.827	638.0
2400	11.60	2.647	609.0
2880	11.64	2.428	619.3
3600	11.56	2.787	610.8
4320	11.69	2.732	611.5
5760	11.73	2.726	601.3
7200	11.65	2.402	572.5
8640	11.61	2.328	564.3
10080	11.61	2.198	527.3
11520	11.56	1.931	496.3
12960	11.41	1.872	470.5
14400	11.44	1.847	526.1
15840	11.38	1.721	415.5
18720	11.34	1.562	364.5
20160	11.44	1.329	319.8
21600	11.27	1.392	308.0
23040	11.22	1.360	293.5
24480	11.48	1.764	395.0
25920	11.45	1.411	297.0
27360	11.15	1.216	267.0
28800	11.24	1.157	265.8
30240	11.13	1.066	234.2
31680	11.11	1.006	213.5
33120	11.24	1.010	204.4
34560	11.26	0.953	201.7
36000	11.26	0.942	180.3
37440	11.06	0.846	186.3
38880	11.32	0.857	185.8
40320	11.00	0.823	184.7
41760	10.97	0.818	182.2
44640	11.05	0.720	207.1
47520	11.01	0.683	139.1
50400	10.76	0.667	142.4
53280	10.98	0.652	137.2

Elapsed (mins)	**pH**	**EC mS cm^{-1}**	**Ca mg/L**
56160	10.89	0.665	132.9
59040	10.76	0.580	122.9
61920	10.70	0.508	123.6
64800	10.72	0.516	120.9
67680	10.71	0.449	105.1
70560	10.56	0.459	108.9
73440	10.70	0.432	105.3
76320	10.67	0.422	76.5

$CaCO_3$ wt % (End) 3.81

Table D.11 - Flow-through weathering Run 3 Column 4

Elapsed (mins)	**pH**	**EC mS cm^{-1}**	**Ca mg/L**
0	11.62	2.880	498.0
10	11.69	2.986	470.0
30	11.69	2.876	503.0
60	11.73	2.910	520.0
120	11.86	3.443	692.0
240	11.88	3.553	706.5
480	11.86	3.825	689.0
960	11.81	3.721	887.5
1440	11.73	3.576	705.5
1920	11.77	3.577	701.5
2400	11.76	3.472	716.5
2880	11.78	3.296	653.0
3600	11.68	3.375	656.5
4320	11.80	3.435	591.0
5760	11.82	3.316	568.3
7200	11.73	3.165	538.5
8640	11.60	2.945	512.0
10080	11.73	2.832	465.0
11520	11.63	2.779	422.8
12960	11.56	2.448	396.0
14400	11.68	2.516	401.8
15840	11.53	2.354	339.8
18720	11.45	2.269	306.3
20160	11.62	2.197	285.8
21600	11.49	2.192	269.0
23040	11.47	2.076	261.5
24480	11.51	2.029	237.3
25920	11.56	2.029	233.8
27360	11.46	1.983	228.8
28800	11.39	1.931	220.5
30240	11.41	1.908	220.3
31680	11.38	1.915	221.5
33120	11.49	1.806	205.0
34560	11.58	1.813	207.5
36000	11.50	1.796	196.8
37440	11.36	1.702	177.0
38880	11.46	1.703	177.3
40320	11.32	1.651	174.0
41760	11.25	1.726	173.0
44640	11.37	1.694	191.8
47520	11.25	1.579	151.8
50400	11.17	1.528	142.8
53280	11.23	1.542	140.3

Elapsed (mins)	**pH**	**EC mS cm^{-1}**	**Ca mg/L**
56160	11.27	1.538	140.8
59040	11.14	1.484	132.0
61920	11.12	1.482	122.0
64800	11.19	1.471	120.8
67680	11.11	1.362	101.3
70560	11.15	1.420	115.3
73440	11.08	1.382	104.8
76320	11.15	1.347	73.3

$CaCO_3$ wt % (End) 3.86

Table D.12 - Flow-through weathering Run 4 Column 1

Elapsed (mins)	**pH**	**EC mS cm^{-1}**	**Ca mg/L**
0	10.37	2.343	70.3
10	10.33	0.3361	82.1
30	10.37	0.4406	110.2
60	10.55	0.579	141.5
120	10.8	0.794	203.9
240	10.76	0.707	163.6
480	11.26	0.788	180.0
960	10.48	0.2189	121.7
1440	9.16	0.1257	79.1
1920	7.33	0.2108	84.4
2400	6.93	0.938	61.0
2880	6.66	1.162	650.0
3600	7.03	1.181	648.5
4320	6.99	1.167	615.5
5760	6.83	1.209	624.5
7200	6.59	1.034	544.0
8640	6.7	0.997	541.0
10080	6.77	0.947	528.0
11520	6.46	0.991	513.5
12960	6.57	0.88	451.0
14400	7.03	0.8	421.0
15840	7.03	0.765	404.5
17280	6.73	0.752	374.5
18720	6.93	0.754	371.5
20160	6.37	0.755	377.5
21600	6.07	0.904	499.0
23040	6.74	0.675	338.0
24480	6.9	0.661	110.9
25920	6.81	0.678	112.1
27360	6.93	0.596	93.5

$CaCO_3$ wt % (End) 2.90

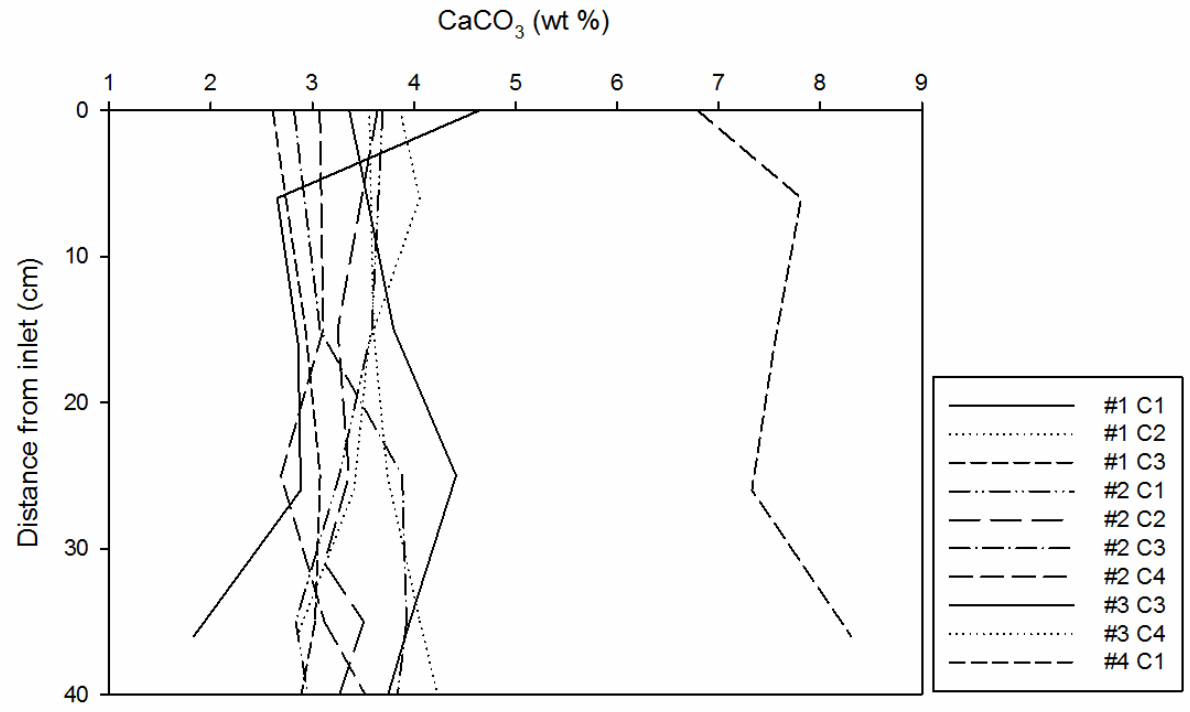

Figure D.1 - $CaCO_3$ formation vs distance from inlet

Table D.13 - Flow-through weathering: IRMS

Sample	corrected $\delta^{13}C$	corrected $\delta^{18}O$
YAR/TAR 3	-14.986	-10.542
#1 C1 L INLET	-13.729	-9.276
#1 C1 L 80-100	-14.172	-10.099
#1 C2 L INLET	-15.167	-10.566
#1 C2 L 80-100	-15.211	-11.079
#1 C3 L INLET	-19.186	-11.485
#1 C3 L 80-100	-20.691	-11.620
#2 C1 UL SS 6/10 1	-16.468	-11.983
#2 C1 L 0-5	-15.679	-13.015
#2 C1 L 450	-17.071	-12.134
#2 C2 VADOSE	-13.608	-9.125
#2 C3 UL SS 6/10 2	-13.779	-9.065
#2 C3 L 0-5	-16.445	-13.252
#2 C3 L 450	-15.377	-12.870
#3 C1 UL	-15.828	-13.891
#3 C3 UL	-15.885	-14.663
#3 C4 UL	-15.943	-14.876
#3 C1 L 0-5	-28.552	-17.422
#3 C1 L 410	-27.293	-13.338
#3 C3 L 0-5	-15.566	-14.449
#3 C3 L 450	-17.577	-15.318
#3 C4 L 0-5	-15.310	-14.884
#3 C4 L 440	-17.400	-15.967

D.2 Yarborough landfill leachate monitoring

Table D.14 – Yarborough sample reference points

Sample Reference	Analysis Reference	Type
1	YO401	Groundwater
2	YO402	Groundwater
3	YO403	Groundwater
4	YO404 / 5	Groundwater
5	YO405	Groundwater
6	YO406	Groundwater
7	YO407	Groundwater
8	YO408A	Groundwater
9	YO409	Groundwater
10	YO409A	Groundwater
11	YO410C	Groundwater
12	YO413A	Groundwater
13	YO415	Groundwater
14	YO417	Groundwater
15	YSW1	Surface
16	YSW2	Surface
17	YSW3	Surface
18	YSW4	Surface
19	YSW5	Surface
20	YSW6	Surface

Table D.15 - Saturation indices March 2005

Sample	**Calcite SI**	**$FeCO_3$ SI**	**$MnCO_3$ SI**	**pH**	**Carbonate estimated from**
YO401	0.471	0.785	-	7.70	Alkalinity
YO403	0.658	1.973	0.784	8.30	Alkalinity
YO404/5	0.604	1.956	0.776	8.20	Alkalinity
YO408A	2.414	0.891	2.294	11.10	Alkalinity
YO409	0.062	0.359	-	7.70	Alkalinity
YO409A	0.351	1.583	0.228	6.90	Alkalinity
YO410C	1.019	0.293	0.698	7.60	Alkalinity
YO413A	2.639	-	2.491	12.90	Alkalinity
YO415/15	0.33	0.85	-	7.50	Alkalinity
YO415/16	0.065	-	0.141	7.30	Alkalinity
YSW1	0.341	-	-	8.00	Alkalinity
YSW2	0.531	-	-	7.80	Alkalinity
YSW3	0.056	-	-	7.60	Alkalinity
YSW4	1.191	2.014	1.55	10.20	Alkalinity
YSW6	0.989	0.672	0.276	8.50	Alkalinity

Table D.16 - Saturation indices April 2005

Sample	**Calcite SI**	**$FeCO_3$ SI**	**$MnCO_3$ SI**	**pH**	**Carbonate estimated from**
YO401	0.164	-	-	7.40	Alkalinity
YO403	-	0.116	-	8.50	Alkalinity
YO405	0.391	-	-	7.00	Alkalinity
YO407	0.407	0.307	0.40	7.50	Alkalinity
YO408A	2.659	-	1.574	11.60	Alkalinity
YO413A	2.553	-	2.172	12.90	Alkalinity
YO415	0.795	0.302	0.151	7.40	Alkalinity
YO417	0.706	1.03	0.349	7.10	Alkalinity
YSW1	0.432	-	-	7.50	Alkalinity
YSW2	0.007	-	-	7.40	Alkalinity
YSW4	0.77	1.765	0.871	9.70	Alkalinity
YSW5	0.185	-	-	8.90	Alkalinity

Table D.17 - Saturation indices May 2006

Sample	**Calcite SI**	**$FeCO_3$ SI**	**$MnCO_3$ SI**	**pH**	**Carbonate estimated from**
CW501	1.544	0.28	0.305	11.90	Alkalinity
CW502	1.105	1.359	0.476	7.60	Alkalinity
CW503	1.077	1.891	0.309	7.70	Alkalinity
CW505	1.013	2.014	1.263	7.40	Alkalinity
CW506	1.498	2.518	0.812	8.00	Alkalinity
CW507A	1.138	2.241	0.945	7.10	Alkalinity
CW508	0.613	1.514	0.3	7.70	Alkalinity
CW509	0.26	1.028	0.429	7.20	Alkalinity
CW510	0.196	0.365	-	8.20	Alkalinity
CW511	0.901	1.388	0.389	7.40	Alkalinity
CW512	1.287	2.001	0.941	8.40	Alkalinity
CW513	1.051	2.177	0.774	7.20	Alkalinity
CW514	0.878	1.684	0.849	7.30	Alkalinity
CW515	0.712	0.707	0.273	7.80	Alkalinity
CW516	0.916	1.988	0.947	7.10	Alkalinity
CW518	0.975	1.696	0.585	7.30	Alkalinity
CSW1	1.314	-	-	8.30	Alkalinity
CSW2	1.477	0.561	0.805	8.50	Alkalinity
CSW3	0.648	0.201	0.596	8.20	Alkalinity
CSW4	1.444	-	-	8.40	Alkalinity
YO401	1.142	-	-	8.30	Alkalinity
YO402	1.416	3.282	1.668	8.00	Alkalinity
YO403	0.421	1.312	-	8.80	Alkalinity
YO404	1.085	1.623	0.094	8.00	Alkalinity
YO405	1.165	2.307	0.772	7.60	Alkalinity
YO406	1.17	2.409	0.927	7.70	Alkalinity
YO407	1.49	3.031	1.668	8.20	Alkalinity
YO408A	2.682	-	1.169	12.60	Alkalinity
YO409	0.144	0.398	-	8.30	Alkalinity
YO409A	1.327	2.128	1.02	7.60	Alkalinity
YO410C	1.3	1.722	1.22	7.60	Alkalinity
YO413A	2.049	-	-	13.9	Alkalinity
YSW1	0.865	-	-	8.50	Alkalinity
YSW2	1.278	0.267	0.343	8.40	Alkalinity
YSW3	1.312	0.28	0.265	8.40	Alkalinity
YSW4	0.907	1.496	0.456	9.10	Alkalinity
YSW5	1.099	0.24	-	9.50	Alkalinity
YSW6	1.544	0.28	0.305	9.40	Alkalinity

Table D.18 - Met Office rainfall data (Scunthorpe, 2008-2013)

Year	Month	Rainfall (mm)
2008	Jan	154.0
	Feb	48.7
	Mar	98.8
	Apr	79.2
	May	43.5
	Jun	56.7
	Jul	108.7
	Aug	82.6
	Sep	92.4
	Oct	93.2
	Nov	60.0
	Dec	52.8
2009	Jan	47.0
	Feb	39.6
	Mar	44.2
	Apr	51.0
	May	81.7
	Jun	168.2
	Jul	113.4
	Aug	46.4
	Sep	26.8
	Oct	50.0
	Nov	161.6
	Dec	66.1
2010	Jan	48.6
	Feb	53.6
	Mar	56.4
	Apr	24.8
	May	21.2
	Jun	41.2
	Jul	68.3
	Aug	39.6
	Sep	67.8
	Oct	65.4
	Nov	112.7
	Dec	18.8
2011	Jan	49.6
	Feb	104.2
	Mar	12.4
	Apr	11.2
	May	40.2
	Jun	47.8
	Jul	18.0

	Aug	42.0
	Sep	27.8
	Oct	57.2
	Nov	37.4
	Dec	124.6
2012	Jan	87.6
	Feb	26.2
	Mar	32.6
	Apr	180.6
	May	48.0
	Jun	166.6
	Jul	107.2
	Aug	99.2
	Sep	90.6
	Oct	61.2
	Nov	110.6
	Dec	136.0
2013	Jan	81.5
	Feb	63.4
	Mar	63.4
	Apr	9.2
	May	84.2
	Jun	37.8

Table D.19 - Science Central: Quantification calculations for carbon capture potential

	Calcimeter	Leco	From XRF		From IRMS										
ID	**%$CaCO_3$**	**%TIC**	**%CaO**	**%MgO**	**% Lith**	**% Hydrox**	**Mol Ca/kg**	**Mol Mg/kg**	**Total Ca / Mg**	**Mol C/kg**	**Mol lithC/kg**	**Mol HydC/kg**	**Total Potential**	**Residual Potential**	**Res as %**
B13	44.38	5.33	22.03	6.17	85.59	14.41	3.93	1.54	5.48	4.44	3.80	0.64	1.68	1.04	61.86
B15	50.17	6.02	22.01	5.25	87.61	12.39	3.93	1.31	5.24	5.02	4.40	0.62	0.85	0.23	26.64
D3	23.92	2.87	13.90	2.09	65.51	34.49	2.48	0.52	3.00	2.39	1.57	0.82	1.44	0.61	42.59
D5	32.12	3.85	17.93	2.08	69.23	30.77	3.20	0.52	3.72	3.21	2.22	0.99	1.50	0.51	34.00
D7	21.06	2.53	13.06	2.05	64.00	36.00	2.33	0.51	2.84	2.11	1.35	0.76	1.50	0.74	49.30
D9	19.15	2.30	11.45	1.53	57.41	42.59	2.04	0.38	2.43	1.92	1.10	0.82	1.33	0.51	38.54
D11	21.87	2.62	13.21	1.90	61.33	38.67	2.36	0.47	2.83	2.19	1.34	0.85	1.49	0.65	43.32
D13	24.46	2.94	14.04	1.54	55.73	44.27	2.51	0.39	2.89	2.45	1.36	1.08	1.53	0.45	29.23
D15	21.98	2.64	13.34	1.97	57.69	42.31	2.38	0.49	2.87	2.20	1.27	0.93	1.61	0.68	42.08
F3	22.91	2.75	13.93	1.57	63.96	36.04	2.49	0.39	2.88	2.29	1.47	0.83	1.42	0.59	41.65
F5	20.30	2.44	16.76	2.00	64.88	35.12	2.99	0.50	3.49	2.03	1.32	0.71	2.18	1.46	67.22
F7	21.67	2.60	13.39	1.65	60.45	39.55	2.39	0.41	2.80	2.17	1.31	0.86	1.49	0.64	42.66
F9	30.07	3.61	15.83	2.24	66.62	33.38	2.83	0.56	3.39	3.01	2.00	1.00	1.38	0.38	27.49
F11	27.46	3.30	15.91	2.09	62.89	37.11	2.84	0.52	3.36	2.75	1.73	1.02	1.64	0.62	37.75
F13	24.06	2.89	14.60	1.88	47.13	52.87	2.61	0.47	3.08	2.41	1.13	1.27	1.94	0.67	34.52
F15	26.17	3.14	13.65	2.47	70.68	29.32	2.44	0.62	3.06	2.62	1.85	0.77	1.21	0.44	36.38
H3	21.70	2.60	14.35	1.29	57.86	42.14	2.56	0.32	2.89	2.17	1.26	0.91	1.63	0.72	43.91
H5	21.08	2.53	12.42	1.39	57.84	42.16	2.22	0.35	2.57	2.11	1.22	0.89	1.35	0.46	33.97
H7	21.08	2.53	13.43	1.62	59.30	40.70	2.40	0.41	2.80	2.11	1.25	0.86	1.55	0.70	44.79
H9	25.72	3.09	16.49	1.86	63.38	36.62	2.94	0.47	3.41	2.57	1.63	0.94	1.78	0.84	47.09
H11	25.63	3.08	16.59	2.00	62.41	37.59	2.96	0.50	3.46	2.56	1.60	0.96	1.86	0.90	48.27
H13	21.06	2.53	12.78	1.48	56.78	43.22	2.28	0.37	2.65	2.11	1.20	0.91	1.46	0.55	37.55
H15	18.57	2.23	11.78	1.70	59.99	40.01	2.10	0.42	2.53	1.86	1.11	0.74	1.41	0.67	47.43
J3	19.71	2.37	12.87	1.15	55.18	44.82	2.30	0.29	2.59	1.97	1.09	0.88	1.50	0.62	41.05
J5	22.38	2.69	13.76	1.62	60.25	39.75	2.46	0.41	2.86	2.24	1.35	0.89	1.51	0.62	41.22
J7	19.80	2.38	12.56	1.57	56.31	43.69	2.24	0.39	2.64	1.98	1.12	0.87	1.52	0.66	43.09
J9	17.19	2.06	11.05	1.13	47.49	52.51	1.97	0.28	2.25	1.72	0.82	0.90	1.44	0.54	37.26
J11	17.07	2.05	10.90	0.92	46.44	53.56	1.95	0.23	2.18	1.71	0.79	0.91	1.38	0.47	33.93
J13	21.91	2.63	12.39	1.78	57.29	42.71	2.21	0.44	2.66	2.19	1.26	0.94	1.40	0.47	33.19
J15	21.63	2.60	12.77	1.70	60.90	39.10	2.28	0.42	2.70	2.16	1.32	0.85	1.39	0.54	39.06
L6	18.43	2.21	12.53	1.81	68.12	31.88	2.24	0.45	2.69	1.84	1.26	0.59	1.43	0.85	59.04
L10	17.35	2.08	10.85	0.95	49.88	50.12	1.94	0.24	2.17	1.74	0.87	0.87	1.31	0.44	33.56

ID	%$CaCO_3$	%TIC	%CaO	%MgO	% Lith	% Hydrox	Mol Ca/kg	Mol Mg/kg	Total Ca / Mg	Mol C/kg	Mol lithC/kg	Mol HydC/kg	Total Potential	Residual Potential	Res as %		
L15	13.85	1.66	9.09	1.05	53.86	46.14	1.62	0.26	1.89	1.39	0.75	0.64	1.14	0.50	43.92		
N10	16.36	1.96	10.51	0.91	47.86	52.14	1.88	0.23	2.10	1.64	0.78	0.85	1.32	0.47	35.42		
N12	22.76	2.73	13.51	1.93	69.14	30.86	2.41	0.48	2.90	2.28	1.57	0.70	1.32	0.62	46.91		
N14	18.99	2.28	12.39	1.58	62.12	37.88	2.21	0.39	2.61	1.90	1.18	0.72	1.43	0.71	49.57		
P12	12.00	1.44	8.01	1.23	59.34	40.66	1.43	0.31	1.74	1.20	0.71	0.49	1.03	0.54	52.41		
P14	21.88	2.63	13.95	1.04	50.87	49.13	2.49	0.26	2.75	2.19	1.11	1.08	1.64	0.56	34.39		
		2.74	13.68	1.85	60.61	39.39	2.44	0.46	2.91	2.28	1.43	0.85	1.47	0.62	41.64		
		0.85	2.84	1.01	8.83	8.83	0.51	0.25	0.73	0.71	0.72	0.15					
								Assumed quantity of material onsite					1000000	tonnes			
													1.47E+09	**mol**	**64803.96**	**tonnesCO_2**	**Total**
													6.21E+08	**mol**	**27340.52**	**tonnesCO_2**	**Used**
															37463.44	**tonnesCO_2**	**Available**

APPENDIX E – FORMULAE

Chapter 1

Equation 1.1:

$$(Ca, Mg)SiO_3 + CO_2 + 2H_2O \rightarrow (Ca, Mg)CO_3 + H_4SiO_4$$

Chapter 2

Equation 2.1:

$$CO_2 + CaSiO_3 = CaCO_3 + SiO_2$$

Equation 2.2:

$$CaCO_3 + CO_2 + H_2O = Ca^{2+} + 2HCO_3^-$$

Chapter 3

Equation 3.1 (adapted from White et al 2003):

$$R = \frac{Q}{St}$$

Where R (mol Ca m^{-2} s^{-1}) is the weathering rate of a silicate mineral with respect to Ca, where Q (mol) is the moles of Ca in solution, S (m^2) is the surface area and t (s) is time elapsed in seconds.

Equation 3.2:

$$\text{Plot of } \left(1 - \frac{c}{K}\right) vs. t \text{ to find slope = -N}$$

$$N = ka(K - c)$$

(Where N = rate of dissolution (m s^{-1}), c = observed concentration at time t (mol m^{-3}), K = equilibrium concentration (mol m^{-3}), a = area (m^2) and k = the coefficient of mass transfer of the dissolving material in to solution (m/s))

Equation(s) 3.3a, b, c, d:

$$CO_{2\,(aq)} + H_2O = H_2CO_3$$

$$H_2CO_3 = H^+ + HCO_3^-$$

$$HCO_3^- = H^+ + CO_3^{2-}$$

$$Ca^{2+} + CO_3^{2-} = CaCO_3$$

Equation 3.4:

$$\mathrm{Ca(OH)_2 + CO_2 \leftrightarrow Ca^{2+} + 2OH^- + CO_{2\,(aq)} \leftrightarrow CaCO_3 + H_2O}$$

Chapter 4

Equation 4.1:

$$(Ca, Mg)SiO_3 + CO_2 + 2H_2O \rightarrow (Ca, Mg)CO_3 + H_4SiO_4$$